UNIVERSITY OF LIVERPOOL

The role of HRS phosphorylation in endosomal trafficking and signalling

Douglas Grimes

Thesis submitted in accordance with the requirements of the University of Liverpool for the Degree of Doctor in Philosophy

May 2019

The role of HRS phosphorylation in endosomal trafficking and signalling

Douglas Grimes

Abstract

Hepatocyte growth factor receptor substrate (HRS) is a component of the ESCRT-0 complex. It is involved in the sorting of ubiquitylated receptors into the lumen of multivesicular bodies (MVBs), thus targeting them for lysosomal degradation. HRS is highly phosphorylated in response to stimulation by various growth factors, but despite this, the functional role of its phosphorylation is still contentious. Preliminary data from our laboratory suggested that HRS may also act as a signalling adaptor, involved in the crosstalk between receptor tyrosine kinases (RTKs) and G protein couple receptors (GPCRs). In order to investigate this hypothesis, I first examined the EGF dependent interactors of HRS by mass spectrometry. I then developed tools for the measurement of endosomal cAMP production and PKA signalling.

My data suggests that HRS interacts with the E3 ligase deltex3-like (DTX3L) in an EGF dependent manner. Although an association between these proteins has previously been made, its EGF dependence is novel. DTX3L has previously been shown to modulate the recruitment of HRS to endosomes in response to stimulation of the G-protein coupled receptor CXCR4. This new finding offers a theoretical means through which different receptor classes could crosstalk and elicit an integrated signalling response.

I further show that GFP-HRS is recruited directly to newly formed vesicles containing EGF and its receptor. Recruitment of HRS to endosomes/vesicles in response to TGFα, but not EGF, is partly dependent on phospho-tyrosine residues Y329 and Y334. Furthermore, HRS has recently been implicated in the recruitment of the recycling complex WASH to endosomes. This, combined with the previous observation, suggests that phosphorylation of these two sites may be involved in receptor recycling.

Overall, my thesis generates new tools for the study of HRS function and for the analysis of endosomal signalling. I provide evidence for the role of HRS in RTK and GPCR crosstalk alongside providing insights into the mechanisms governing recruitment of HRS.

Table of Contents

List of Figures

List of tables

Abbreviations

7TM	7 Transmembrane
ABD	Actin-binding domain
AC	Adenylate cyclase
ACN	Acetonitrile
ACTL8	Actin-like protein 8
AD	Alzheimers disease
AF555	AlexaFluor555
AIP4	Atrophin-1 interacting protein 4
AKAR	A-kinase activity reporter
AMSH	Associated molecule with the SH3 domain of STAM
APEX	Ascorbte peroxidase
APF-1	ATP-dependent proteolysis factor-1
Atg	Autophagy related genes
ATP	Adenosine triphosphate
BAR	Bin amphiphysin-Rvs
BLOC-1	Biogenesis of lysosomal-related organelles complex1
BMP	Bone morphogenetic protein
BP	Biotin phenol
BSA	Bovine serum albumin
cAMP	Cyclic adenosine monophosphate
Cbl	Casitas B-lineage Lymphoma
CBM	Clathrin binding domain
CCC	CCDC22, CCDC93, and COMMD
CFP	Cyan fluorescent protein
CHMP	Charged multivesicular body protein
CIMPR	Cation independent mannose 6-phosphate receptor
CLN5	Ceroid-lipofuscinosis neuronal protein 5
CME	Clathrin-mediated endocytosis
CPS	Carboxypeptidase S

CPY	Carboxypeptidase Y
CSC	Cargo selective complex
CURL	Compartment for uncoupling receptor from ligand
CXCL12	C-X-C motif chemokine 12
CXCR4	Chemokine receptor 4
DAB	3,3'-Diaminobenzidine
DAPI	4',6-Diamidino-2-phenylindole
DEPTOR	DEP domain-containing mTOR-interacting protein
DMEM	Dulbecco's modified eagle's medium
DNA	Deoxyribonucleic acid
dNTPs	Deoxyribonucleotide triphosphate
DRD1	Dopamine Receptor D1
DSCR3	Down syndrome critical region gene 3
DTT	Dithiothreitol
DTX3L	Deltex-3-like
DUB	Deubiquitylase
EAP	ELL-associated proteins
EEA1	Early endosome antigen 1
EGF	Epidermal growth factor
EGFR	Epidermal growth factor receptor
EM	Electron microscopy
Eps15	Epidermal growth factor receptor substrate 15
ER	Endoplasmic reticulum
ESCRT	Endosomal sorting complex required for transport
EV71	Enterovirus 71
FBS	Fetal bovine serum
FDA	Food and drug administration
FDR	False discovery rate
FF	FENS-FYVE
FGF	Fibroblast growth factor
FGFR	Fibroblast growth factor receptor
FHA1	Forkhead associated domain 1

FRAP	Fluorescence recovery after photobleaching
FRET	Fluorescence resonance energy transfer
FRT	Flippase recognition target
Fsk	Forskolin
FYVE	Fab1, YOTB, Vac1, EEA1
Gag	Group-specific antigen
GAP	GTPase-activating proteins
GDP	Guanosine diphosphate
GFP	Green fluorescent protein
GGA	Golgi-localised, γ-adaptin ear homology domain
GLUE	GRAM-like ubiquitin binding in EAP45
GPCR	G-protein coupled receptor
GPI	Glucose-6-phosphate isomerase
GRK2	G Protein-Coupled Receptor Kinase 2
GS	Goat serum
GTP	Guanosine-5'-triphosphate
HB-EGF	Heparin-binding EGF
Hbp	HRS binding partner
HBSS	Hank's balanced salt solution
HECT	Homologous to the E6-AP carboxyl terminus
HEK	Human embryonic kidney cells
HEPES	4-2-Hydroxyethyl-1-piperazineethanesulfonic acid
HGF	Hepatocyte growth factor
Hh	Hedgehog
HIV	Human immunodeficiency virus
HPLC	High-performance liquid chromatography
HRS	Hepatocyte growth factor receptor substrate
IAA	Iodoacetamide
IBMX	3-isobutyl-1-methylxanthine
ICUE	Indicator of cAMP using Epac
IDR	Intrinsically disordered regions
IF	Immunofluorescence

IGF-1	Insulin-like growth factor-1
IL2	Interleukin receptor 2
ILV	Intraluminal vesicles
IP	Immunoprecipitation
IPTG	Isopropyl bet-D-1-thiogalactopyrnoside
IRS1	Insulin receptor substrate 1
Iso	Isoproterenol
ITAM	Immunoreceptor tyrosine-based activation motif
JAK	Janus kinase
KD	Knockdown
LC	Liquid chromotography
LDL	Low-density lipoprotein
LPA	Lysophosphatic acid
MAGE-L2	Melanoma-associated antigen family member L2
MAPK	Mitogen-activated protein kinase
MEM	Minimum essential medium
MHC	Major histocompatibility complex
MPI	Mammalian protease inhibitor
MS	Mass spectrometry
MT1-MMP	Membrane type I-matrix metalloproteinase
mTORC	Mammalian target of rapamycin
MVB	Multivesicular body
NEAA	Non-essential amino acids
NES	Nuclear export sequence
NGF	Nerve growth factor
NP-40	Nonidet P-40
NPF	Nucleation-promoting factor
NZF	Npl4 zinc finger
ORF	Open reading frame
PAS	Pre-autophagosomal structure
PBS	Phosphate-buffered saline
PCR	Polymerase chain reaction

PDGF	Platelet-derived growth factor
PDGFR	Platelet-derived growth factor receptor
PFA	Paraformaldehyde
PI-3-K	Phosphoinositide 3-kinase
PIKfyve	Phosphoinositide kinase, FYVE-type zinc finger containing
PKA	Protein kinase A
PKM2	Pyruvate kinase isozymes M2
PM	Plasma membrane
PMSF	Phenylmethylsulfonyl fluoride
PSME1	Proteasome Activator Subunit 1
PTB	Phospho-tyrosine binding domain
PtdIns(3)*P*	Phosphatidylinositol 3-phosphate
PTH	Parathyroid hormone
PTM	Post translational modification
PTP	pProtein tyrosine phosphatase
PTSD	Post-traumatic stress disorder
PX	Phox homology
PY	Phospho-tyrosine
RA	Ras associated
RanBP	Ran binding protein
RBR	RING between RING
RE	Restriction endonuclease
RING	Really interesting new gene
RIOK2	RIO Kinase 2
RNA	Ribonucleic acid
RPL	Ribosomal protein L
RTK	Receptor tyrosine kinase
S1P1R	Sphingosine-1-phosphate receptor 1
SDM	Site-directed mutagenesis
SDS-PAGE	Sodium dodecyl sulphate polyacrylamide gel electrophoresis
SEM	Standard error of the mean
SH2	Src homology 2

SH3	Src homology 3
Shc	SH2 domain containing
SILAC	Stable isotope-labelling by amino acids in the cell culture
SMCs	Smooth muscle cells
Smo	Smoothened
Snx	Sorting nexin
Sos	Son of sevenless
STAM	Signal transducing adaptor molecule
TBC1D5	TBC1 Domain Family Member 5
TBS	Tris-buffered saline
TEM	Transmission electron microscope
TGFα	Transforming growth factor α
TKD	Tyrosine kinase domain
TLR7	Toll-like receptor 7
TMPS	Triple membrane passing signalling
Trf	Transferrin
TRIM27	Tripartite Motif-Containing Protein 27
TrkA	Tropomyosin receptor kinase A
Trolox	6-hydroxy-2,5,7,8-tetramethylchroman-2-carboxylic acid
TSG101	Tumor susceptibility gene 101
TSH	Thyroid-stimulating hormone
UA	Uranyl acetate
Ub	Ubiquitin
UBA1	Ubiquitin-like modifier-activating enzyme 1
UBD	Ubiquitin-binding domain
UEV	Ubiquitin E2 variant
UIM	Ubiquitin interacting motif
USP	Ubiquitin-specific protease
UV	Ultraviolet
V2R	Vasopressin receptor 2
VEGF	Vascular endothelial growth factor
VEGFR	Vascular endothelial growth factor receptor

VHS	VPS27, HRS and STAM
VPS	Vacuolar protein sorting
WASH	WAS Protein Family Homolog
WASP	Wiskott-Aldrich syndrome protein
WAVE	WASP-family verprolin-homologous protein
Wnt	Wingless/Int
WT	Wild type
Y2H	Yeast two hybrid
YFP	Yellow fluorescent protein
Znf	Zinc finger
βARK	β-adrenergic receptor kinase

Acknowledgements

I would like to dedicate this thesis to my family. In particular to my late mother, who sadly passed away in June 2010 after a short fight with cancer. I still miss you to this day. I will always remember your support and advice which have helped to guide me through my younger years and continues to guide me through life now. To my father, you have always backed me throughout my entire life, for which I am eternally grateful. Your support has helped give me the confidence to believe in myself. To my brother who has been a great friend over the last few years and helped to keep me sane.

To my beautiful wife, Lauren. I cannot begin to express how grateful I am for you. I would never have been able to complete this PhD without your incredible love and support. You have gotten me through the toughest points over the last few years and I am where I am today because of you. You inspire me to be the best I can possibly be. Whatever happens next, I know I will be happy as long as I have you by my side.

I would also like to thank all of my supervisors Michael Clague, Sylvie Urbé and Tobias Zech for their support and guidance over the last 4 years. Thank you for sharing your knowledge and experience, which has allowed me to become a better scientist as a result.

I would like to express gratitude to Emma Rusilowicz-Jones, Alice Howarth, Fiona Hood, Ewan Macdonald and Stephanie Mo for their amazing help with certain aspects of my PhD. I would also like to thank in no particular order, Eri Bertsoulaki, Jane Jardine, Hannah Elcocks, Andreas Kalinos, Claire Heride, Anne Clancy, Elena Marcasa, Yvonne Tang, Vicky Smith, Lisa Mullee, Aitor Martinez-Zarate, Leila Rochin, Svetlana Telnova, Leah Wilson, Yasmina Sahraoui, Adam Linley, Hannah Warren, Zohra Butt, Dan Newman, Tom Waring, Louise Brown, Arnauld Selvais, Alison Beckett and Lucy Isherwood for making the 4th and 5th floors such an enjoyable place to work. I am grateful to have met each and every one of you.

Publications

Manuscripts

'HRS-WASH axis governs actin-mediated endosomal recycling and cell invasion.'

J Cell Biol, 2018

'A *Caenorhabditis elegans* assay of seizure-like activity optimised for identifying antiepileptic drugs and their mechanisms of action.'

J Neurosci Methods, 2018

Conferences

5th International Meeting on Anchored cAMP Signaling Pathways poster presentation. 'Development of endosomal sensors for the investigation of cAMP signalling and endosomal trafficking.'

Conference abstract:

'Sorting of receptors at the endosome has been proposed to play a role in modulating signalling through controlling the balance between receptor cycling and degradation. More recently the concept of specific receptor signalling outputs associated with passage through the endosomal pathway has been established. Proof of principle was provided by studies of receptor tyrosine kinases, with the best characterised example being the EGFR. However, this concept may transfer to GPCRs and associated cAMP signalling. Current models suggest a second wave of activation occurs at endosomal membranes, leading to prolonged cAMP signals and downstream effects on endosomal acidification mediated by PKA. Furthermore, localised generation of the cAMP dictates signalling outcomes. Hitherto, studies have used global measurements

of cAMP but there is an unmet need for direct visualisation of cAMP generation at endosomes. We are developing endosomal localised reporters for cAMP generation and PKA activation and will provide details of their characterisation to date. The ultimate goal is to combine these with defined perturbations of endosomal trafficking allowing for an increase the granularity of our understanding of these effects.

Important for ushering a receptor through to degradation, is its internalisation into the endosomal lumen and formation of MVB's. A process which is controlled by the ESCRT machinery. Later on, trafficking was shown to regulate signal transduction by having distinct signalling outcomes from the plasma membrane, as opposed to the signalling outcomes from the endosome. An aim for the lab is to determine whether the ESCRT machinery is involved in this phenomena by acting as a signalling platform. Here we describe the development and characterisation of endosomally localised biosensors for the cAMP pathway. Through this we aim to further the field by directly visualising and measuring cAMP produced at the endosomes and begin to dissect the mechanisms involved in governing endosomal cAMP, and GPCR, signalling.'

Chapter one: Introduction

1.1. Endocytic pathway overview

The endocytic pathway is a series of morphologically distinct compartments that allow cells to deal with internalised material. The steps within this pathway are involved in many cellular processes such as, protein degradation, regulation of receptor signalling and the immune system. The physical properties of each compartment, along with a complex array of regulating proteins, allow for the correct sorting and trafficking of any internalised cargoes. Disruption to the organisation of endocytic compartments has been implicated in diseases ranging from cancer to various forms of dementia.

1.1.1. Endocytosis

Endocytosis is the cellular process by which extracellular material is taken into the cell. There are many types of endocytosis that can broadly be categorised into macro- or micro-endocytosis. Macro-endocytosis describes the process of how the cell intakes large quantities of extracellular material, whether it be by macropinocytosis or phagocytosis used by cells of the immune system to ingest pathogens. This type of endocytosis is often referred to as cell eating or drinking. Micro-endocytosis, as the name suggests, is a much smaller scale form of internalisation, typically smaller than 200nm (Kumari, Mg et al. 2010). Micro-endocytosis can first be categorised by whether it takes place in lipid raft or non-lipid raft domains (El-Sayed and Harashima 2013). Outside of lipid rafts, Clathrin-mediated endocytosis (CME) is the primary form of micro-endocytosis and the most widely researched endocytic pathway. Endocytosis occurring within lipid raft domains can be further defined by the associated molecules involved. These are: Caveolae-mediated, Flotillin-dependent, GRAF1-dependent, ArF6-dependent and RhoA-dependent endocytosis (El-Sayed and Harashima 2013). These mechanisms of endocytosis are generally less selective than CME. GRAF1-dependent endocytosis has been proposed to be responsible for the uptake of larger proteins (Bhagatji, Leventis et al. 2009).

Evidence for endocytosis dates back to the 19th century, when it was observed that cells could internalise litmus paper into acidic compartments (Roth 2006). In the 1930's macrophages were imaged internalising extracellular fluid, estimating that a macrophage could internalise the equivalent of a third of its own cell volume per hour. Then, in 1964, Roth and Porter imaged the sequence of events that lead to the formation of endocytic vesicles in *Aedes aegypti* oocytes by electron microscopy, describing invagination of the membrane, formation of coated pits and the subsequent pinching off of the endocytic vesicle (Roth and Porter 1964). A few years later, the molecular coat on internalised vesicles was described as a regular cage-like structure (Kanaseki and Kadota 1969). The major component of this coat was identified as clathrin in 1975 (Pearse 1975, Pearse 1976). Around the same time, work by Anderson, Brown and Goldstein, described the ligand-induced internalisation of the low-density lipoprotein (LDL) receptor. They discovered a mutation in the LDL receptor that prevented it from clustering within coated pits, effectively linking the binding of a ligand to the assembly of clathrin coated pits (Anderson, Brown et al. 1977, Anderson, Goldstein et al. 1977, Goldstein, Anderson et al. 1979). A process that is now known as receptor-mediated endocytosis. Later this form of endocytosis was shown to induce receptor internalisation with stimulation of insulin, EGF and α2-macroglobin (Maxfield, Schlessinger et al. 1978).

Despite the cave-like morphology of caveolae first being described in 1953 by George Palade, it wasn't until 1992 that caveolin was identified as the coat component of these structures (Kurzchalia, Dupree et al. 1992, Rothberg, Heuser et al. 1992). This form of endocytosis is less well understood than clathrin-mediated endocytosis.

1.1.2. Endosomes

Endosomes are a complex series of endocytic compartments involved in the sorting, recycling and degradation of internalised material and trans-membrane proteins. They can be categorised into various subtypes, based on their morphology, function and associated proteins and phospholipid species. These subtypes are: the early

endosome, also referred to as sorting endosomes, the recycling endosome and the late endosomes, also known as multivesicular bodies (MVBs) (Figure 1.1).

1.1.3. Early endosomes

During the 1970's, extensive research went in to the study of endocytosis, but the destination of internalised vesicles was unclear (Roth 2006). Roth and Porter suggested that small vesicles fuse to form larger vesicles, based on the observation of different sized yolk filled vesicles in their experiments. In 1980, studies into the endocytosis of viruses provided an insight into the fate of endocytic vesicles (Helenius, Kartenbeck et al. 1980). Viruses were bound to cells at low temperatures to prevent their internalisation. The cells were fixed after being warmed for varying amounts of time. Initially, single virions are observed in small, coated vesicles. After a few more minutes, multiple virions are found within larger, uncoated vesicles, and at later time points in MVBs and lysosomes. A few years later in 1983, Geuze et al. would use a double labelling immunogold combined with cryoEM to show that the asialoglycoprotein receptor and its ligand were trafficked to a distinctive organelle (Geuze, Slot et al. 1983). Here the ligand would accumulate in the organelles lumen, with the receptor concentrated in tubular extensions. They named this organelle CURL (compartment of uncoupling receptor from ligand). This organelle is now known as the sorting endosome.

The sorting endosome is the first organelle to receive endocytosed material. From here, this material is then sorted for either degradation or recycling. The morphology of this organelle greatly aids in this function. It is estimated that approximately 60-70% of the luminal volume is in the vesicular body and the tubular extensions account for 50-80% of its surface area (Mukherjee, Ghosh et al. 1997). This morphology encourages the recycling of receptors and the degradation of ligands (Dunn, McGraw et al. 1989). Receptors and transmembrane proteins are directed towards degradation by being sequestered into intraluminal vesicles (ILVs) of the maturing endosome, whereas, those designated for recycling are either trafficked directly back to the plasma membrane or towards the tubular network of the recycling endosome.

1.1.4. Late endosomes/MVBs

Multivesicular bodies were discovered in the 1950's by electron microscopy (EM), due to their distinctive morphology (Sotelo and Porter 1959). MVBs contain small intraluminal vesicles which form from the limiting membrane of the maturing endosome. Studies from Stanley Cohen and colleagues in the late 1970's followed ferritin-conjugated EGF which had been internalised. They show that this tagged EGF passes through MVBs en route to the lysosome (Gorden, Carpentier et al. 1978, Haigler, McKanna et al. 1979). In the following decade it was shown that the EGFR was sorted with EGF into the lumen of MVBs (Miller, Beardmore et al. 1986). It was not clear, however, if material sorted for degradation at the sorting endosome was subsequently trafficked to MVBs or sorting endosomes matured into MVBs over time. This question was answered in 1992 by Dunn et al. who provided evidence for the maturation of sorting endosomes (Dunn and Maxfield 1992).

MVBs are formed through the loss of material destined for recycling and the accumulation of material designated for degradation (Katzmann, Odorizzi et al. 2002). This material is internalised into the endosomal lumen to form ILVs, a process which is controlled by the ESCRT machinery (described in section 1.2.6). MVBs were shown to fuse directly with lysosomes in 1996 (Futter, Pearse et al. 1996). By the end of the decade, it was known that segregation of active receptors into ILVs was important for the down regulation of receptor signalling by removing the active kinase domain away from the cytosol (Ceresa and Schmid 2000). Disruption to the components involved in this process can lead to tumourgenesis (Di Fiore and Gill 1999).

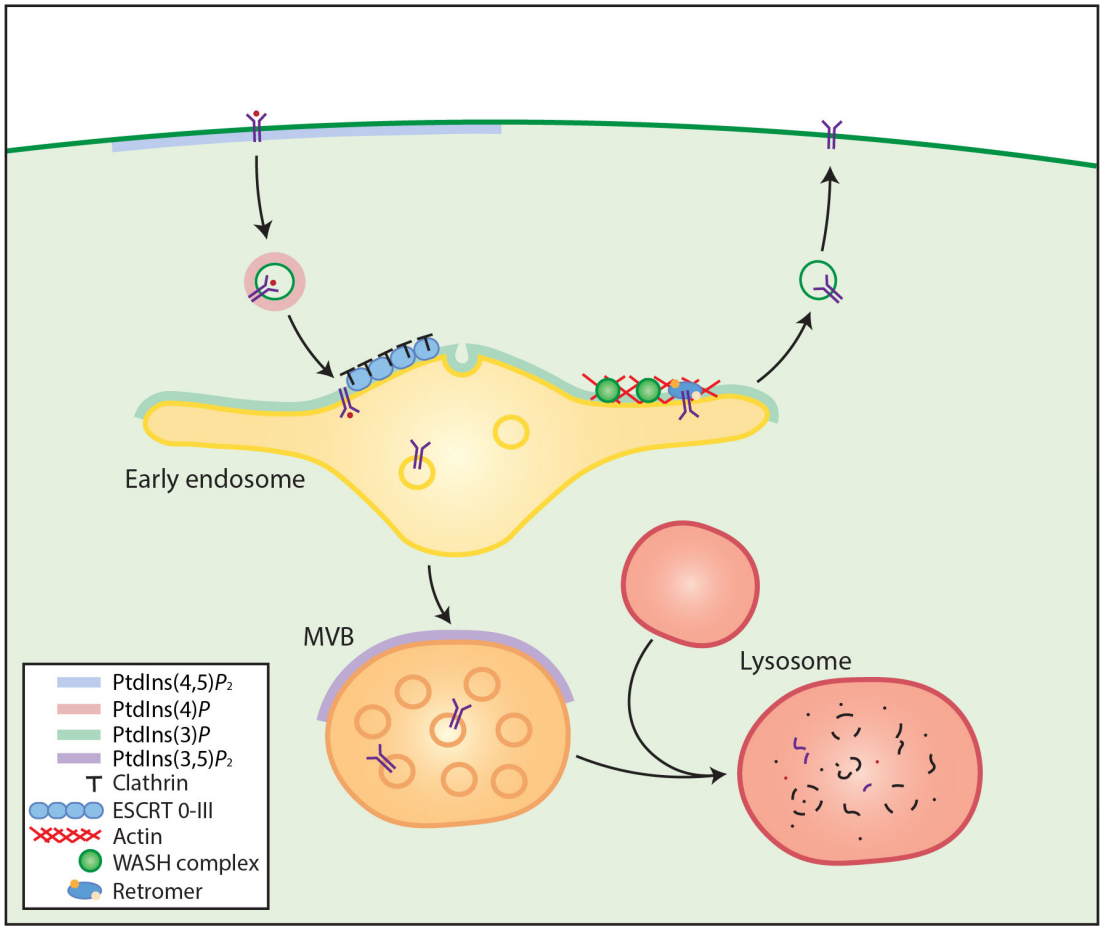

Figure 1.1 Simplified overview of the endocytic pathway. Once bound to its ligand, a receptor is internalised into the cell, forming a vesicle. The vesicle then traffics to the early endosome for further sorting. From here, the receptor can be recycled back to plasma membrane via actin rich domains, a process primarily mediated by the retromer and WASH complex. Alternatively, the receptor can be sorted for degradation through interaction with the ESCRT machinery, leading to internalisation into the lumen of the endosome and the formation of the multivesicular body (MVB). The MVB then fuses with a lysosome, leading to the degradation of its contents by digestive enzymes. Phosphotidylinositide lipids are responsible for the identification of each of the Endo-membranes.

1.1.5. Markers of endocytic membranes

The different endocytic compartments can be identified morphologically by EM. The resolution of light microscopy is generally not high enough to identify their distinct morphological features (Ullrich, Reinsch et al. 1996). It is therefore necessary to use markers to identify the different classes of endosomes. This can be achieved by using the specific proteins or lipid species associated with each compartment.

Markers of the early endosome include: PtdIns(3)*P*, VPS34, Rab5, Rab4 and EEA1. Rab5 is a small GTPase that mediates the fusion of endocytic vesicles with the early endosome (Gorvel, Chavrier et al. 1991, Bucci, Parton et al. 1992). Rab5 is responsible for the recruitment of the class III PI-3 kinase, VPS34 (Christoforidis, Miaczynska et al. 1999). VPS34 generates PtdIns(3)*P* on early endosomes. PtdIns(3)*P* is an important lipid species, as it is responsible for the recruitment and localisations of FYVE (Fab1, YOTB, Vac1 and EEA1) domain containing proteins to early endosomes (Gillooly, Simonsen et al. 2001). The most widely used protein marker of early endosomes is the Rab5 effector, EEA1. EEA1 is recruited to early endosomes by the dual interaction with Rab5 and with PtdIns(3)*P* though its FYVE domain (Mu, Callaghan et al. 1995, Stenmark, Aasland et al. 1996).

In conjunction with Rab5, Rab4 and Rab21 are also present on early endosomes (van der Sluijs, Hull et al. 1991, Simpson, Griffiths et al. 2004). Rab4 is responsible for the trafficking of material from the early endosome to the recycling endosome (van der Sluijs, Hull et al. 1992). Rab4 is also present on this compartment, but the predominant Rab species on the recycling endosome is Rab11 (Ullrich, Reinsch et al. 1996). The function of Rab21 is less well understood but has been shown to be involved in the endosomal sorting of integrins (Pellinen, Arjonen et al. 2006, Pellinen, Tuomi et al. 2008).

Specific markers of the MVB/late endosome are difficult to come by as many of the components of MVBs are also present at other endocytic compartments (Hanson and Cashikar 2012). Lamp1 and Lamp2 can both be observed on late endosomes, but are also markers of the lysosome (Carlsson, Roth et al. 1988). These proteins can be used as markers for the late endosome when used in conjunction with the mannose 6-phosphate receptor (CIMPR). This receptor ferries proteins between the Golgi complex and endosomes, but is not present on lysosomes (Geuze, Slot et al. 1985). The co-occurrence of these two markers can effectively define late endosomes.
As the endosome matures, PIKFyve is recruited via interaction with PtdIns(3)*P* and its FYVE domain (Sbrissa, Ikonomov et al. 2002). PIKFyve is responsible for the generation of PtdIns(3,5)P_2 from PtdIns(3)*P* (Sbrissa, Ikonomov et al. 1999). Despite PtdIns(3)*P* still

being present on late endosomes in small amounts, PtdIns(3,5)P_2 is the predominant PtdIns lipid species present on MVBs. Similarly, small amounts of Rab5 are still present on late endosomes, but due to the decreasing levels of PtdIns(3)*P*, the levels of Rab5 also decrease as the endosome matures (Woodman and Futter 2008). Rab5 is subsequently replaced by Rab7, the major Rab species of MVBs, in a process known as the Rab5-to-Rab7 conversion (Rink, Ghigo et al. 2005).

1.2. Degradation

The 1930's work by Schoenheimer described the dynamic nature of proteins through the study of rats fed with stable isotope-labelled amino acids (Schoenheimer, Ratner et al. 1939). Now, we know that there are three main modes of degradation present within cells. These degradation pathways are associated with the lysosome, autophagosome, and the proteasome. The small 8.5kDa protein, ubiquitin, is involved in all three of these pathways (Clague and Urbe 2010).

1.2.1. Discovery of the Lysosome

The first of these pathways to be discovered was the lysosome in the 1950's by Christian de Duve (de Duve 2005). Initially interested in carbohydrate metabolism and insulin response (de Duve 2004), de Duve applied centrifugation techniques, which had recently been developed by Albert Claude (Claude 1946), in order to study the distribution of the enzyme; acid phosphatase (Appelmans, Wattiaux et al. 1955). The enzyme was distributed jointly across a primarily mitochondrial fraction and a lighter fraction consisting of smaller granules termed microsomes. By adjusting the centrifugation protocol, they were able to separate an additional fraction, which contained the acid phosphatase within it, instead of the enzyme being spread amongst the microsome and mitochondrial fractions. De Duve subsequently searched for other enzymes that might be concentrated with this fraction. His group found a collection of four more hydrolases that also had an acid optimum pH and all acted on very different targets (De Duve, Pressman et al. 1955). This gave rise to the notion that the

particles isolated within this fraction functioned as digestive compartments. The term 'lysosome' was subsequently given to these particles from the Greek words 'lysis', meaning digestive, and 'soma', meaning body. Soon after lysosomes were visualised via EM, first in purified lysosomal fractions and then in sections of liver tissue (Novikoff, Beaufay et al. 1956).

1.2.2. Discovery of autophagy

Further EM studies would later give rise to the second degradative pathway known as autophagy, or 'self-eating'. EM studies of mouse kidney tubule cells would show the presence of an unusual vacuole that often times contains cellular components such as mitochondria (Novikoff, Beaufay et al. 1956, Clark 1957). Similarly, acid-phosphatase positive compartments had also been identified to contain mitochondria. These compartments could be induced by stimulation with glucagon and along with careful EM the sequential formation of the pre-autophagosomal structure (PAS) was elucidated by Arstila and Trump (Ashford and Porter 1962, Arstila and Trump 1968). This pathway is initiated by the formation of a small membrane 'sac'. This membrane sac then extends to form a C-shaped membrane that begins to engulf a portion of the cytosol. The membrane continues to extend until the two ends fuse together, forming a double membraned organelle called the autophagosome, which at this point is devoid of hydrolytic enzymes. The autophagosome then fuses with the lysosome forming the single-membraned structure called the autophagolysosome. The inner-membrane of the autophagosome, along with the luminal contents, is thus degraded by the hydrolytic enzymes present within the lysosome.

Despite the term 'autophagy' being coined in 1963, the proteins responsible for autophagy were not identified until the 1990's (Ohsumi 2014). A genetic Yeast screen by Yoshinori Ohsumi would determine a series of genes involved in the process of autophagy. Now termed autophagy-related (Atg) genes, almost all of the proteins/genes identified were completely uncharacterised (Tsukada and Ohsumi 1993, Nakatogawa, Suzuki et al. 2009).

1.2.3. Discovery of the proteasome and the ubiquitin system

Either by endocytosis or via the autophagosome, the lysosome was believed to be the primary site for degradation. However, these methods of degradation couldn't easily explain the varying half-life or the energy requirement for degradation of intracellular proteins (Ciechanover 2005). Furthermore, Studies into haemoglobinopathies found that reticulocytes, which do not contain lysosomes, are able to rapidly degrade abnormal haemoglobin (Rabinovitz and Fisher 1964). Disruption of lysosomal degradation by treatment with chloroquine effectively abolishes degradation of extracellular proteins, but had no effect on the degradation of short-lived intracellular proteins (Poole, Ohkuma et al. 1977). It was not until 1977, more than two decades after the initial identification of the lysosome, that an ATP-dependent protein degradation pathway separate from the lysosome was discovered (Etlinger and Goldberg 1977). This work was carried out in Reticulocyte lysates and in an attempt to identify the components of the new degradative system led to the identification of ATP-dependent proteolysis factor-1 (APF-1), an 8,500Da peptide that is covalently attached to target substrates via an isopeptide bond (Ciechanover, Hod et al. 1978). Around the same time, ubiquitin was characterised as a post-translational modification of the side chain of lysine residues on Histone 2A (Goldknopf and Busch 1977). The characteristics of the bond between ubiquitin and Histone 2A shared remarkable similarities to that of APF-1, as well as being the same size, and after a series of experiments the two proteins were shown to be one of the same (Wilkinson, Urban et al. 1980).

Soon after the rest of the components of the ubiquitin conjugating pathway were deciphered. The pathway consists of a cascade of three enzymes leading to the addition of ubiquitin to the target substrate (Hershko, Heller et al. 1983). The first class of enzymes in this cascade is the ubiquitin-activating enzyme (E1), followed by the ubiquitin-carrier protein (E2) and finally the ubiquitin-protein ligase (E3). The E1 enzyme binds to free ubiquitin. The ubiquitin is then passed from the E1 to an E2 enzyme. From here, the ubiquitin molecule is either ligated directly to the substrate with the help of an E3 ligase, as seen with the RING class of E3 ligases, or the ubiquitin

molecule is accepted by the E3 prior to being ligated to the target substrate, as seen with HECT E3 ligases (Figure 1.2). There is also another class of E3 ligases called RING between RING (RBR) that contains RING domains but function more similarly to the HECT class of E3 ligases. Today there are over a 1000 components of the ubiquitin system, falling into these three categories of enzymes and along with a class of enzymes responsible for the cleavage of ubiquitin called deubiquitylating enzymes (DUBs). The protease complex responsible for the degradation of proteins targeted by ubiquitin was identified as the 26S proteasome complex in 1988, providing the final piece to the ubiquitin-proteosome degradation system (Arrigo, Tanaka et al. 1988).

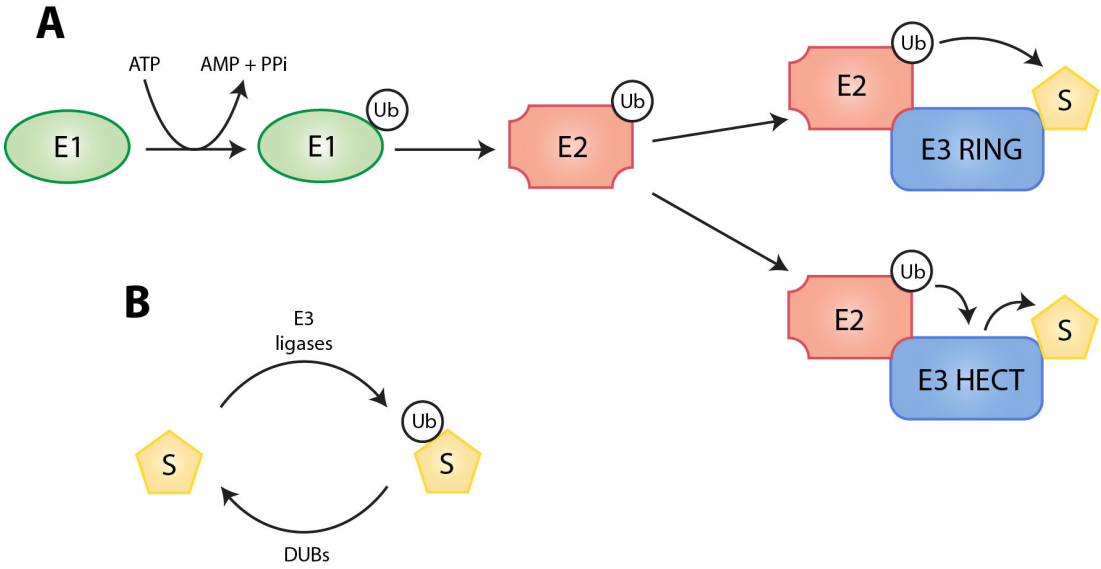

Figure 1.2 Ubiquitin ligase cascade. An E1 enzyme will bind ubiquitin through a thioester bond, requiring ATP hydrolysis in order to do so. The E1 enzyme will then pass the ubiquitin on to an E2 enzyme. The E2 enzyme will then interact with an E3 ligase in order to the attach the ubiquitin to the side chain of lysine on the substrate protein. Depending on the type of E3 ligase, this is done either by attaching the ubiquitin directly to the substrate from the E2, or by passing the ubiquitin onto the E3 and then again to the substrate. Opposing the action of the E3 ligases, are a family of enzymes called deubiquitinating enzymes (DUBs).

1.2.4. Ubiquitin as a signal for lysosomal degradation

For the next decade after the discovery of the proteasome, it was believed that ubiquitin was primarily the signal for degradation via the proteasome. In 1998, the first example from a study showed that ubiquitin is also responsible for targeting

transmembrane proteins to be degraded via the lysosome. The yeast G-protein coupled receptor (GPCR), Ste2, activates the mitogen-activated protein (MAP) kinase pathway in response to stimulation with a peptide hormone, α-factor (Terrell, Shih et al. 1998). This receptor is sorted into the lumen of MVBs en-route to vacuole degradation; however, mutation of the lysine residues within its cytoplasmic domain prevents the down regulation of this receptor. Further evidence that ubiquitin can target proteins for lysosomal degradation came when ubiquitin was fused to a stable plasma membrane ATPase, resulting in its internalisation and degradation (Shih, Sloper-Mould et al. 2000).

The role ubiquitin plays in targeting proteins to lysosomal degradation is a little less straightforward (Katzmann, Odorizzi et al. 2002). The ubiquitin-ATPase chimera mentioned above suggests that ubiquitin acts as a signal for internalisation. This idea is supported by a reduced uptake of the Ste2 lysine mutant. For other proteins however, internalisation is not affected by defects in their ubiquitylation. Ste6 and Fur4, for example, accumulate in pre-vacuolar compartments instead of being degraded by the vacuole (Dupre and Haguenauer-Tsapis 2001, Losko, Kopp et al. 2001). These examples clearly show a role for ubiquitin as being important for sorting after internalisation.

In mammalian cells, the chemokine receptor, CXCR4, is still internalised but no longer degraded when its lysine residues are mutated and it cannot be ubiquitylated anymore (Marchese and Benovic 2001). The EGFR is ubiquitylated by the E3 ligase, Cbl (Joazeiro, Wing et al. 1999, Yokouchi, Kondo et al. 1999). Mutations to Cbl don't prevent the internalisation of the receptor but do prevent it from being degraded by the lysosome (Levkowitz, Waterman et al. 1999, Waterman, Levkowitz et al. 1999). Conversely, overexpression of wild type Cbl leads to increased EGFR degradation (Thien, Walker et al. 2001). The viral oncogene, v-Cbl, displays a dominant negative effect over wild type Cbl by competing for EGFR binding, but is unable to add ubiquitin, preventing the receptor from being sorted towards the lysosome for degradation. This leads to sustained EGFR activation and tumour formation (Blake, Shapiro et al. 1991).

1.2.5. Ubiquitin-binding domains

Much like the phosphorylation of tyrosine, serine and threonine residues provides a new binding site on proteins, the addition of ubiquitin to substrates also provides a new site that other proteins can interact with. In order to interact with ubiquitin, proteins need a ubiquitin-binding domain (UBD). There are many different UBDs, which have different affinities for either mono- or poly-ubiquitin chains, and even for different chain links, providing context specific ubiquitin binding (Hicke, Schubert et al. 2005, Dikic, Wakatsuki et al. 2009). The first UBD to be identified was the ubiquitin interacting motif (UIM) of the proteasome subunit, S5A (Young, Deveraux et al. 1998). The sequence of this motif was subsequently used in a bioinformatics search to identify other ubiquitin binding proteins (Hofmann and Falquet 2001). Yeast two hybrid (Y2H) experiments using ubiquitin as bait, along with further bioinformatics analysis of ubiquitylating and deubiquitylating enzyme sequences, would lead to the identification of even more UBDs (Hofmann and Bucher 1996, Shih, Prag et al. 2003). A summary of UBDs is shown in table 1.1.

UBDs can be found on many endosomal proteins. Since ubiquitin is a signal for lysosomal degradation, components of the endosomal sorting machinery require the ability to recognise and interact with ubiquitylated cargo (Katzmann, Babst et al. 2001). This allows for the efficient sorting of proteins destined for degradation.

Ubiquitin binding domain	Class	Example protein	Refs
CUE	α-Helix	Vps9	(Prag, Misra et al. 2003)
dUIM	α-Helix	HRS	(Hirano, Kawasaki et al. 2006)
GAT	α-Helix	GGA3, TOM1	(Akutsu, Kawasaki et al. 2005)
GLUE	PH domain	EAP45	(Slagsvold, Aasland et al. 2005)
IUIM	α-Helix	RABEX5	(Lee, Tsai et al. 2006)
Jab1/MPN	Other	Prp8	(Bellare, Small et al. 2008)
NZF	Zinc Finger (ZnF)	Vps36	(Alam, Sun et al. 2004)
PAZ	Zinc Finger (ZnF)	USP5	(Reyes-Turcu, Horton et al. 2006)
PFU	Other	Doa1	(Fu, Zhou et al. 2009)
PRU	PH domain	RPN13	(Schreiner, Chen et al. 2008)
SH3	Other	Sla1	(Stamenova, French et al. 2007)
UBA	α-Helix	NBR1	(Kirkin, Lamark et al. 2009)
UBAN	α-Helix	NEMO	(Rahighi, Ikeda et al. 2009)
UBC	Ubc-like domain	UBCH5	(Brzovic, Lissounov et al. 2006)
UBM	α-Helix	Polymerase iota	(Bienko, Green et al. 2005)
UBZ	Zinc Finger (ZnF)	Polymerase-h	(Bienko, Green et al. 2005)
UEV	Ubc-like domain	TSG101	(Sundquist, Schubert et al. 2004)
UIM	α-Helix	S5a/Rpn10, STAM	(Terrell, Shih et al. 1998)
VHS	α-Helix	STAM, HRS	(Mizuno, Kawahata et al. 2003)
ZnF A20	Zinc Finger (ZnF)	RABEX5	(Penengo, Mapelli et al. 2006)

Table 1.1 List of the different ubiquitin-binding domains that have been identified.

1.2.6. The ESCRT machinery

At its core, the ESCRT (endosomal sorting complex required for transport) machinery is comprised of four complexes (ESCRT 0-III, table 1.2) that recognise cargo and create membrane curvature (Henne, Buchkovich et al. 2011). They are vital for the formation of MVBs, appropriate trafficking of membrane proteins to the lysosome and attenuation of receptor signalling like growth factor signalling pathways (Figure 1.3). Due to this, dysfunction of the ESCRT complexes can lead various diseases such as cancer and dementia (Li and Cohen 1996, Saksena and Emr 2009).

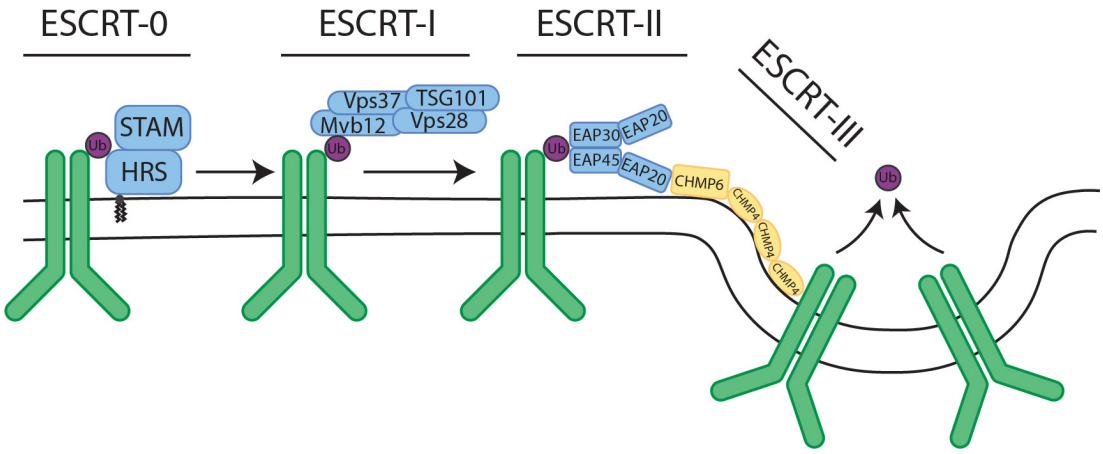

Figure 1.3 Overview of the ESCRT machinery. Ubiquitylated receptors at the endosome are recognised by the ESCRT-0 complex comprised of HRS and STAM. As this complex can bind to multiple ubiquitin molecules, it corrals receptors into clathrin coated microdomains before passing the receptor on to the ESCRT-I complex. This in turn passes the receptors on the ESCRT-II, which also recruits ESCRT-III. The ESCRT-III complex is responsible for the invagination of the endosomal membrane, by forming long chains of Snf7, which form coiled structures. This coiled structure also acts like a 'fence', preventing the receptors from escaping. Deubiquitinating enzymes (DUBs) also act to remove the ubiquitin from the receptors to be used again.

The components of the ESCRT machinery were initially identified in *Saccharomyces cerevisiae* yeast in a large genetic screen that looked for mis-trafficking of the vacuolar glycol protein CPY, and later for morphological defects in the yeast vacuole (Rothman and Stevens 1986, Banta, Robinson et al. 1988, Robinson, Klionsky et al. 1988). Genes identified in the screens are now known as Vacuolar protein sorting (Vps) mutants. These Vps mutants can be further characterised in to classes depending on the morphological defect. All components of the ESCRT machinery are classified as 'Class E' Vps mutants, which are defined by enlarged endosomes (Raymond, Howald-Stevenson et al. 1992). Membrane proteins were shown to traffic to the vacuole via MVBs through studies with carboxypeptidase S (CPS) (Odorizzi, Babst et al. 1998, Reggiori and Pelham 2001). Further studies with a chimera protein of CPS and His3 would establish that the enlarged endosomes seen in class E mutants is due to defective sorting into the endosomal lumen (Odorizzi, Katzmann et al. 2003, Katzmann, Sarkar et al. 2004).

Complex	Yeast protein name	Metazoan protein name
ESCRT-0	Vps27	HRS
	Hse1	STAM
ESCRT-I	Vps23	TSG101
	Vps28	VPS28
	Vps37	VPS37
	Mvb12	MVB12
ESCRT-II	Vps22	EAP30
	Vps36	EAP45
	Vps25	EAP20
ESCRT-III	Vps2	CHMP2
	Vps20	CHMP6
	Vps24	CHMP3
	Snf7	CHMP4
	Vps60	CHMP5
	Did2	CHMP7

Table 1.2 Yeast and mammalian homologues of the ESCRT machinery

As well as being involved in MVB formation, ESCRT proteins has also been associated with various other cellular processes. These include: cell abscission, viral budding, exosome secretion and nuclear envelope reformation (Garrus, von Schwedler et al. 2001, Carlton and Martin-Serrano 2007, Nabhan, Hu et al. 2012, Olmos, Hodgson et al. 2015). Much of the more recent research looking at ESCRT function is examining the alternate functions of these complexes (Campsteijn, Vietri et al. 2016).

1.2.7. ESCRT-I

ESCRT-I was the first complex to be described in the early 2000's (Katzmann, Babst et al. 2001). The complex consists of TSG101, Vps28, Vps37 and hMvb12 being identified as a subunit a few years later (Bishop and Woodman 2001, Bache, Slagsvold et al. 2004, Chu, Sun et al. 2006). ESCRT-I interacts with membranes only by weak

electrostatic interactions (Kostelansky, Schluter et al. 2007) but requires interactions with ESCRT-0 for recruitment to endosomal membranes (Bache, Brech et al. 2003, Lu, Hope et al. 2003). From its crystal structure, we can see that this complex is an elongated heterotetramer, with coiled-coil body and a globular head (Kostelansky, Sun et al. 2006). ESCRT-I interacts with both ESCRT-0 and ESCRT-II at opposite ends of its structure with cargo recognition occurring through a UEV domain on TSG101 and a UBD on Mvb12. The UEV domain of TSG101 is also responsible for interacting with a P(S/T)AP-like motif on HRS of ESCRT-0 (Katzmann, Stefan et al. 2003), an interaction that is mimicked by HIV Gag proteins (Pornillos, Higginson et al. 2003).

1.2.8. ESCRT-II

ESCRT-II, along with ESCRT-III, was described a few years after ESCRT-I. It forms a Y shaped heterotetramer comprised of EAP30, EAP45 and two EAP20's (Babst, Katzmann et al. 2002, Langelier, von Schwedler et al. 2006). EAP30 and EAP45 form the base while the two EAP20's form the arms of the Y structure (Hierro, Sun et al. 2004, Teo, Perisic et al. 2004). ESCRT-II binds to Vps28 of ESCRT-I via a GLUE domain on EAP45 (Gill, Teo et al. 2007). In yeast VPS36 (EAP45), the GLUE domain contains two NZF domains, which are responsible for its interaction with ESCRT-I (Teo, Gill et al. 2006). The GLUE domain of mammalian EAP45, however, doesn't contain these NZF domains, but is still able to interact with ESCRT-I. The GLUE domain is also responsible for binding to PtdIns(3)*P* with high affinity (Slagsvold, Aasland et al. 2005). The two EAP20 arms are responsible for binding to Vps20 (CHMP6) of the next ESCRT complex, ESCRT-III.

1.2.9. ESCRT-III

ESCRT-III is the final ESCRT complex recruited to the endosomal membrane and is the complex responsible for causing membrane curvature and the eventual formation of the ILV (Henne, Buchkovich et al. 2011). It consists of CHMP2, CHMP3, CHMP4 and CHMP6 in mammalian cells but due to the fact that this complex is unstable in the

cytosol it is difficult to crystallise (Babst, Katzmann et al. 2002). Further to this, ESCRT-III monomers do not localise to the endosome by themselves (Zamborlini, Usami et al. 2006, Shim, Kimpler et al. 2007). Recruitment of ECRT-III occurs when EAP20 subunit from ESCRT-II binds to CHMP6 (Teo, Perisic et al. 2004). CHMP6 then recruits CHMP4, which forms long polymer chains (Teis, Saksena et al. 2008, Saksena, Wahlman et al. 2009). These chains are then capped by CHMP3 and the final subunit, CHMP2, is also recruited. CHMP4 chains can also recruit various accessory proteins as well as DUBs to remove the ubiquitin chains from the cargo targeted for degradation, in order to preserve the ubiquitin pool within the cell (Luhtala and Odorizzi 2004, Schmidt and Teis 2012).

1.2.10. ESCRT-0

The last complex to be described as an ESCRT complex was ESCRT-0. This complex, consisting of Hepatocyte growth factor receptor substrate (HRS) and Signal transducing adaptor molecule (STAM), had already been identified prior to being described as an ESCRT complex and was already known as a class E Vps mutant (Asao, Sasaki et al. 1997, Bache, Raiborg et al. 2003). They became associated with the rest of the ESCRT machinery through studies looking into viral budding of HIV (Clague and Urbe 2003). HIV hijacks the ESCRT machinery in order to bud out of T cells at the plasma membrane (Pornillos, Garrus et al. 2002). Viral Gag proteins bind to TSG101 of the ESCRT-I complex, leading to the recruitment of the rest of the machinery (Garrus, von Schwedler et al. 2001). Studies showed that this was through a P(S/T)AP motif on the viral proteins (Pornillos, Alam et al. 2002). Analysis of the human genome would reveal the same motif on HRS (Pornillos, Higginson et al. 2003). The ESCRT-0 complex is the first point of contact a ubiquitylated receptor will have with the ESCRT machinery and is essential for the initiation of the ESCRT pathway at endosomes and the formation of MVBs. ESCRT-0 is also required for MVB formation in *Drosophila melanogaster*, mice and yeast, indicating that its role is conserved among different species (Raymond, Howald-Stevenson et al. 1992, Komada and Soriano 1999, Lloyd, Atkinson et al. 2002). The primary role of this complex is thought to be to corral ubiquitylated receptors in order for them to subsequently be internalised into an ILV

(Urbé, Sachse et al. 2003). This is achieved by the multiple domains capable of binding to ubiquitin on both STAM and HRS (Raiborg and Stenmark 2002).

1.2.11. HRS

HRS is an 86kDa protein initially identified as a substrate for hepatocyte growth factor (HGF) receptor (Komada and Kitamura 1995). HRS is recruited to endosomal membranes via its FYVE domain, which interacts with PtdIns(3)*P* (Gaullier, Simonsen et al. 1998, Raiborg, Bremnes et al. 2001*)*. HRS also contains a double sided ubiquitin interacting motif (UIM), as well as a VHS domain that is also capable of binding to ubiquitin, Golgi-localised, γ-adaptin ear homology domain (GGA) proteins interact with ubiquitin via VHS domains (Bilodeau, Urbanowski et al. 2002). Though these domains only weakly bind to ubiquitin, they allow HRS to gather the ubiquitylated receptors in clathrin coated regions on endosomes (Raiborg, Bache et al. 2002). Clathrin is recruited to endosomes via the C-terminal of HRS (Raiborg, Gronvold Bache et al. 2001). Interestingly, though HRS is required for proper sorting and trafficking to the lysosome, over-expression of HRS leads to a dominant negative effect, disrupting correct sorting for receptors (Chin, Raynor et al. 2001, Urbé, Sachse et al. 2003).

As mentioned above, HRS was first identified as a substrate for the HGF receptor, c-Met. When stimulating cells with HGF and blotting for phospho-tyrosine, apart from the receptor itself, HRS is the most intense band identified. The same can be seen with other growth factors and cytokines (Komada and Kitamura 1995). When stimulating with EGF, ESCRT-0 subunits are highly phosphorylated (Bache, Raiborg et al. 2002), and this is blocked with the inhibition of endocytosis (Urbé, Mills et al. 2000). If HRS is so highly phosphorylated by these growth factors, the question arises as to what the purpose of this phosphorylation is. It has been suggested that phosphorylation alters the membrane binding dynamics of HRS. When stimulated with a growth factor, phosphorylated HRS is predominantly present in the cytosol, despite the fact that endocytosis of growth factor receptors to the endosome is required for this phosphorylation in the first place (Urbé, Mills et al. 2000). It could be that phosphorylation of HRS leads to it dropping off the endosome and allowing the

ubiquitylated cargo to be passed off to the other ESCRT complexes. This also fits with the observation that HRS over-expression inhibits protein trafficking.

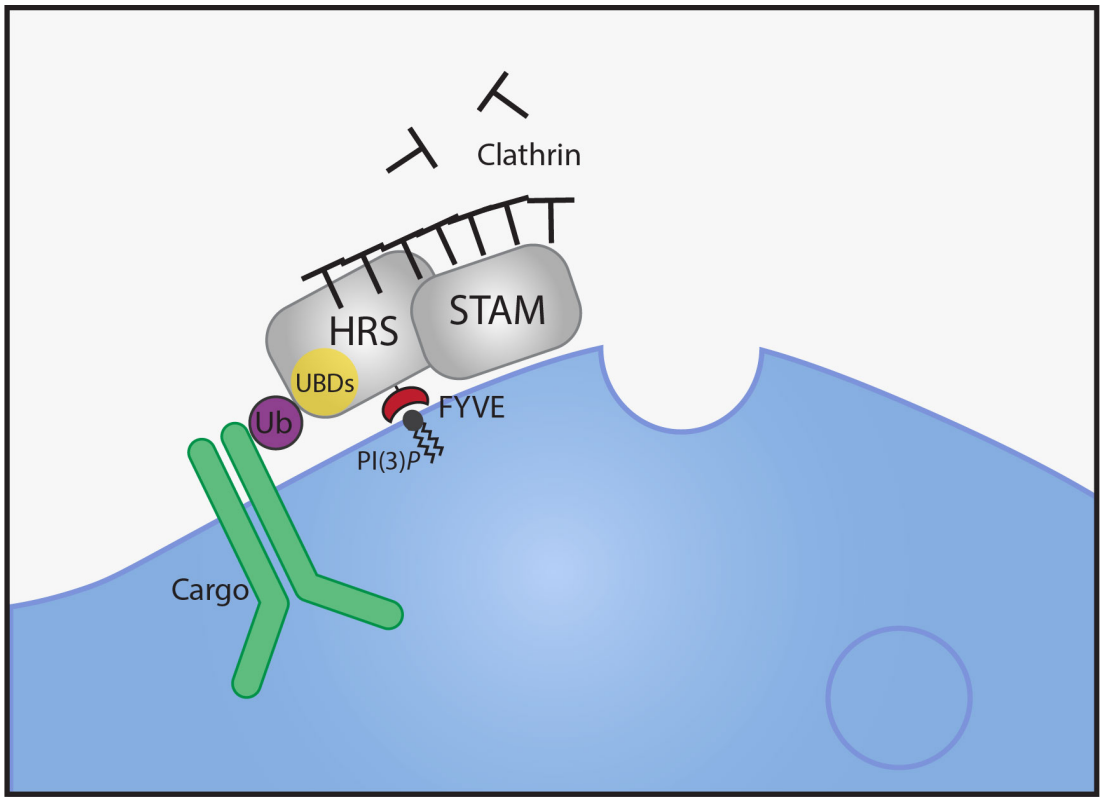

Figure 1.4 Schematic diagram of HRS at endosomes. HRS is recruited to early endosomes through the interaction between its FYVE domain and PtdIns(3)*P*, where it forms the ESCRT-0 complex with STAM. HRS can interact with ubiquitylated receptor via its multiple ubiquitin binding domains (UBDs). HRS recruits Clathrin to endosomes, forming discreet clathrin microdomains.

Despite this, however, when examining the various phosphorylation sites available on HRS, we can see that many of these phosphorylation sites exist outside the functional domains of HRS (Figure 1.5), and that many of these sites have been more highly observed than those sites found within the functional domains (Urbé, Sachse et al. 2003). Furthermore, different growth factors induce different phosphorylation profiles on HRS and STAM (Row, Clague et al. 2005).

1.2.12. HRS and disease

HRS is a critical component of the machinery involved in the trafficking and sorting of many receptors and cell surface proteins. It is therefore understandable that disruption to which will lead to serious consequences for the cell and its intercellular function.

Since it is known that the function of HRS as part of the ESCRT machinery is to aid in sorting ubiquitylated receptors into newly forming ILVs, thus targeting cargo for lysosomal degradation, it comes as no surprise that HRS has been shown to be involved in the down regulation of EGFR signalling (Lloyd, Atkinson et al. 2002). Overexpression of HRS paradoxically displays a dominant negative effect over EGFR trafficking and accumulation in the early endosome (Chin, Raynor et al. 2001). A study from Scoles et al. however showed that ectopic expression of HRS in rat schwannoma cells led to a reduction of EGFR abundance, contrary to preceding studies on the issue (Scoles, Qin et al. 2005). The authors suggest a cell type-specific effect of HRS on EGFR trafficking. This idea is strengthened by a study published a couple of years later, which suggests that knockdown of HRS led to an inhibition of proliferation and malignancy (Toyoshima, Tanaka et al. 2007). This was due to improper degradation of E-cadherin, resulting in sequestering of beta-catenin in the cytoplasm and preventing it from entering the nucleus to exhibit its mitogenic effects. A study into the kinome of liver cancers with beta-catenin mutations showed that these cells also relied on HRS (Canal, Anthony et al. 2015). Silencing of HRS resulted in inhibition to cell growth. HRS has also shown to be involved in the entry of Kaposi's Sarcoma-associated herpes virus into the cell by macropinocytosis (Veettil, Kumar et al. 2016).

Classification of HRS as a component of the ESCRT machinery came about through studies examining the outward budding of HIV. Subsequent studies have demonstrated the involvement of HRS in the normal functioning of the immune system. In 2011, HRS was shown to actually inhibit HIV-1 virion production (Ding, Su et al. 2011). This effect is mediated through its interaction with citron kinase via its FYVE domain. Depletion of HRS led to increased virion production. Sorting of the

interleukin receptor (IL2) has also been shown to be mediated by HRS, in a manner that is independent of its ubiquitin binding (Yamashita, Kojima et al. 2008). A study from Nagata et al. in 2014 provided evidence for the importance of HRS in the development of peripheral B lymphocytes and in the T-cell dependent production of antibodies (Nagata, Murata et al. 2014). In patients infected with Enterovirus 71 (EV71), it was found that HRS had been upregulated and is an important regulatory of Toll-like receptor 7 (TLR7). HRS recruits TLR7 to endosomes in order to facilitate activation of NF-κB signalling pathways (Luo, Ge et al. 2017).

A growing body of evidence is emerging implicating HRS in neurodegenerative disease and the regular functioning of neurons. Neurons rely heavily on the endocytic system and disruption to degradative processes can lead to the accumulation of protein aggregates, ultimately leading to the loss of neurons and neurodegenerative disease. Conditional knockdown of HRS in the central nervous system of hrs(flox/flox);Synl-Cre mice led to the accumulation of ubiquitylated proteins and loss of hippocampal CA3 pyramidal neurons (Tamai, Toyoshima et al. 2008). HRS was further shown to be important for the normal recycling of full length TrkB receptor, another interaction not dependent on the UIM of HRS (Huang, Zhao et al. 2009). In 2016, loss of HRS was shown to lead to the disruption of the autophagic degradation of disease-related proteins, such as Huntingtin. This leads to ER-stress and both apoptosis and necrotopic cell death in hippocampal neuronal cells (Oshima, Hasegawa et al. 2016). Watson et al. showed that neuronal deficits in teetering mice were a result of spontaneous mutation to HRS. They show that HRS plays a role in the maintenance of synaptic transmission and that the expression of HRS in the nervous systems is developmentally regulated (Watson, Bhattacharyya et al. 2015). Further examples demonstrating the importance of HRS in development highlight the role it plays in developmental signalling pathways. Miura et al. show HRS is important for Bone morphogenetic proteins (BMP) signal transduction, by localising TAK1 to early endosomes, leading to its activation and phosphorylation (Miura and Mishina 2011). Additionally, as well as BMP signalling, HRS was also implicated in Hedgehog (Hh) signalling via interactions with cell surface protein Smoothened (Smo). Loss of HRS led to accumulation of Smo

in endosomes and enhancement of the wing defect caused by the dominant-negative Smo mutation (Fan, Jiang et al. 2013).

A study from Hasseine et al. in 2007 suggests that HRS plays a protective role in diabetic retinopathies, by preventing the degradation of the VEGF insulin receptors (Hasseine, Murdaca et al. 2007). The authors come to this conclusion by introducing ectopic expression of HRS in HEK293 cells, which leads to increased levels of the two receptors. However, this effect is more like due to the dominant-negative effects of HRS overexpression. Another study from 2012 shows that HRS, but not other ESCRT proteins, is required for the transport of cholesterol from endosomes to the ER (Du, Kazim et al. 2012). HRS depletions has also been shown to decrease contractility in smooth muscle cells (SMCs) leading to oesophagus dilation (Chen, Hou et al. 2015). This study also showed that SMCs exhibited an excessive production of cytokines and chemokines. More recently, HRS was identified in an epigenetic meta-analysis of studies on post-traumatic stress disorder (PTSD). Methylation of HRS was significantly associated with those suffering from PTSD (Uddin, Ratanatharathorn et al. 2018).

1.2.13. STAM

STAM is a 70kDa protein and was initially identified in 1996 as a downstream effector of JAK tyrosine kinases (Takeshita, Arita et al. 1996). This interaction is mediated by the immunoreceptor tyrosine-based activation motif (ITAM) on STAM, which serves as a docking site for Src homology 2 (SH2) domain-containing proteins. STAM is thus, phosphorylated by JAK kinases in response to cytokine receptor stimulation (Takeshita, Arita et al. 1997). Due to its role in cytokine signalling, STAM was expected to be an essential gene in lymphocyte development, however this was not the case (Yamada, Takeshita et al. 2001).

STAM became associated with endocytic trafficking when a second STAM gene, STAM2/HRS-binding-partner (Hbp), was identified and shown to interact with HRS via coiled-coil regions in both proteins (Asao, Sasaki et al. 1997, Takata, Kato et al. 2000). The role of STAM in endocytic trafficking was corroborated by sub cellular localization

on endosomes (Lohi and Lehto 2001). Further to this, STAM contains a VHS domain and a UIM domain, which allows STAM to interact with ubiquitylated receptors (Bache, Raiborg et al. 2003). STAM also contains an Src homology 3 (SH3) domain, which allows it to recruit the deubiquitylases USP8 and AMSH to endosomes (Tanaka, Kaneko et al. 1999, Kato, Miyazawa et al. 2000). They also interact with later ESCRT complexes in order to deubiquitylate proteins, which have been targeted for degradation (McCullough, Row et al. 2006). This serves to maintain the pool of ubiquitin within the cell.

It has also been suggested that STAM may be responsible for the dissociation of the ESCRT-0 complex from endosomal membranes. Over-expression of STAM leads to a diffuse distribution of HRS (Kojima, Amano et al. 2014). This is believed to aid in the function of ESCRT-0 by allowing the complex to pass ubiquitylated cargo on to the subsequent ESCRT complexes.

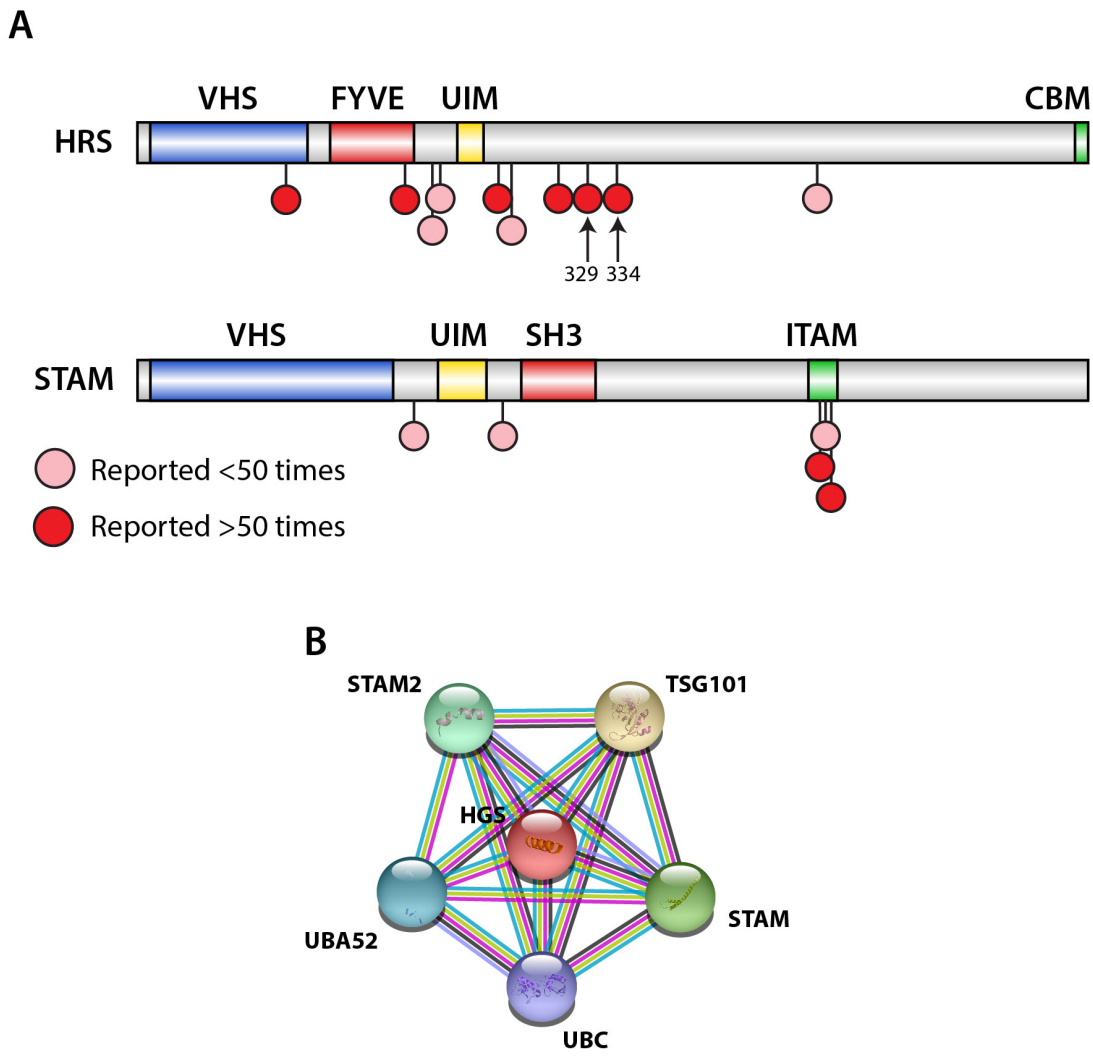

Figure 1.5 Schematic of the functional domains, phosphorylation sites and binding partners of HRS and STAM. (A) The functional domains and phosphorylation sites of HRS and STAM. Both HRS and STAM are highly phosphorylated in response to growth factor stimulation. Shown are commonly seen tyrosine phosphorylation sites. Sites indicated in red have been seen more than 50 times by high throughput mass spectrometry, whereas sites indicated in pink have been seen fewer than 50 times. (Data obtained through phosphosite). Tyrosine residues 329 and 334 have been highlighted due to the fact that they are of high interest in this thesis. **(B)** A network of the known interactors of HRS according to the STRING database.

1.3. Recycling

Recycling of internalised cell surface proteins is important to maintain the cellular pool. When the sorting endosome was first described, termed CURL (compartment for uncoupling receptor from ligand), it was believed that recycling predominantly

occurred by a bulk flow mechanism. This was driven by the morphology of the sorting endosome, with the majority of the compartments membrane existing in the tubular regions, encouraging transmembrane proteins to be recycled. As with degradation and the ESCRT machinery, there is a collection of complexes that are involved in the efficient sorting of recycling proteins (Figure 1.6).

1.3.1. The Retromer

Initially identified in yeast, the retromer complex is a highly conserved complex and an integral component of the endosomal recycling machinery (Seaman 2012). The complex is comprised of 5 proteins, Vps35p, Vps29p, Vps26p, Vps5p and Vps17p (Horazdovsky, Davies et al. 1997, Seaman, Marcusson et al. 1997). The retromer mediates many elements of transport from the endosome and is implicated in many important biological processes, such as Wnt signalling, iron transport, cell polarity, direct mediation of GPCR signalling, as well as retrieval to the Golgi and recycling to the plasma membrane of various receptors and membrane associated proteins e.g. the cation independent mannose 6-phosphate receptor (CIMPR), Sortilin and Amyloid precursor protein (APP) (Arighi, Hartnell et al. 2004, Seaman 2004, Nielsen, Gustafsen et al. 2007, Eaton 2008, Tabuchi, Yanatori et al. 2010, Fjorback, Seaman et al. 2012). Defects in the retromer are implicated in some cases of Alzheimer disease (AD) (Small, Kent et al. 2005).

When first discovered in yeast, the retromer was described as a pentamer. However, opinion over the years has shifted to view the complex more as two sub-complexes that transiently interact with each other. Particularly when you consider that the traditional pentamer is not as stable in mammalian cells as was seen in yeast (Swarbrick, Shaw et al. 2011). The retromer can therefore be divided into a cargo selective trimer consisting of Vps35p, Vps29p and Vps26p; and a dimer made from the dimerization of the Sorting nexin (Snx) family members, Vps5p and VPS17p (Horazdovsky, Davies et al. 1997, Nothwehr and Hindes 1997). These proteins are often described as Snx-BAR proteins to differentiate them from other Snx family members, due to the inclusion of a Bin Amphiphysin-Rvs (BAR) domain in their C-

terminus. In mammalian cells, Snx1 and Snx2 are orthologues of Vps5p with Snx5 and Snx6 being orthologues of Vps17p (Wassmer, Attar et al. 2007). From here on out these proteins will be referred to by their mammalian names (table 1.3).

Yeast protein name	Metazoan protein name
Vps35p	VPS35
Vps29p	VPS29
Vps26p	VPS26
Vps5p	Snx1 Snx2
Vps17p	Snx5 Snx6

Table 1.3 Yeast and mammalian homologues of the Retromer complex

Recruitment of the Snx-BAR dimers to membranes occurs through their Phox homology (PX) domains, common amongst the Snx family of proteins (Cozier, Carlton et al. 2002). The PX domains of the Snx-BAR proteins bind with high affinity to PtdIns(3)*P* (Yu and Lemmon 2001) present on early endosomes and do not rely on the cargo selective complex (CSC) for recruitment (Arighi, Hartnell et al. 2004). The CSC trimer is recruited to endosomes however, via its interaction with the GTPase Rab7a (Rojas, van Vlijmen et al. 2008, Seaman, Harbour et al. 2009). This interaction was first shown in amoeba (Nakada-Tsukui, Saito-Nakano et al. 2005). Interestingly, the retromer CSC requires both Snx3 and Rab7a for efficient recruitment to endosomes, suggesting that the recruitment of the whole complex is temporally controlled and occurs during the Rab5/7 switch of the maturing endosome (Harterink, Port et al. 2011). Further regulation of the retromer CSC is also evident from the fact that Rab7a is also present on lysosomes but the CSC is not. Moreover, proteins implicated in the regulation of Rab7a activity will also be indirectly involved in the regulation of retromer CSC recruitment. TBC1D5, a Rab-GAP that can displace the CSC from endosomes if overexpressed (Seaman, Harbour et al. 2009). Whereas, mutations in CLN5 can lead to a reduction in Rab7a activity and the degradation of proteins

normally transported out of the endosomal compartments, such as sortilin and CIMPR (Mamo, Jules et al. 2012).

More recently, evidence has emerged that suggests a redundancy in the roles of the retromer with other endosomal sorting components. Firstly, it isn't clear how the retromer CSC recognises cargo or how the retromer can distinguish between which proteins are to be trafficked to the Golgi and which are to be trafficked to the plasma membrane (Seaman 2012). Some studies in yeast suggest that Vps35 can directly bind to cargo, such as Vps10p (Nothwehr, Ha et al. 2000, Arighi, Hartnell et al. 2004), while others have suggested Vps26 may be responsible due to the fact that it has a similar structure to that of β-arrestin and can recognise the cytoplasmic tail of SorL1/SorLA (Shi, Rojas et al. 2006). Furthermore, CIMPR requires Vps26a for appropriate endosomal sorting, but does not require Vps26b (Bugarcic, Zhe et al. 2011). In conjunction with this, although early studies indicated that cargo sorting by the retromer required both the CSC timer and the Snx-BAR dimer, instances where this rule does not apply have begun to be reported. For example, the P2Y1 receptor requires the Snx-BAR dimer for correct sorting, and not the retromer CSC (Nisar, Kelly et al. 2010). The opposite observation was shown with Wntless/MIG-14 trafficking in *C. elegans*, where Snx1 and the Snx-BAR component of the retromer was not required for Wntless/MIG-14 retrieval (Harterink, Port et al. 2011, Zhang, Wu et al. 2011).

In 2017, a second complex, which is functionally similar to the retromer, was discovered and named retriever (McNally, Faulkner et al. 2017). This study investigated the retromer independent recycling of integrin α5β1, which is mediated by the cargo adaptor Snx17 (Steinberg, Heesom et al. 2012). Two GFP-tagged Snx17 proteins were generated with GFP tagged to either the N-terminus or the C-terminus. When GFP is tagged to the C-terminus, Snx17 is unable to rescue α5β1 recycling after Snx17 knockdown. These two fusion proteins were used as bait to identify candidates responsible for the recycling of the integrin. This identified many components of the CCC complex, along with C16orf62, DSCR3 and Vps29. The complex produced from C16orf62, DSCR3 and Vps29 form a structurally similar complex to that of the retromer

(Gershlick and Lucas 2017), which was shown to mediate the recycling of over 120 cell surface proteins (McNally, Faulkner et al. 2017).

1.3.2. The WASH complex

Endosomal sorting of proteins and endosomal maturation both require localised actin polymerisation (Ohashi, Tanabe et al. 2011)(Figure 1.6). Generation of branch actin filaments involves the Arp2/3 complex, which acts as a nucleation point for actin polymerisation (Machesky, Atkinson et al. 1994, Rotty, Wu et al. 2013). Activation of this complex, however, requires the activity of a nucleation-promoting factor (NPF) (Higgs and Pollard 1999). The major actin NPF at endosomes is Wash1, a member of the Wiskott-Aldrich syndrome protein (WASP) family of actin NPFs (Derivery, Sousa et al. 2009).

Wash1 is a component of the WASH complex, which was identified through affinity isolation of Wash1 (Derivery, Sousa et al. 2009). This complex consists of 5 proteins, the interactions between which were resolved using biochemical and yeast two hybrid techniques (Jia, Gomez et al. 2010, Harbour, Breusegem et al. 2012). These proteins are: Wash1, Strumpellin, Fam21, CCDC53 and KIAA1033/SWIP (hereafter referred to as KIAA1033). Knockdown of any of these components leads to complex instability and degradation of the other subunits. The WASH complex is ubiquitously expressed and evolutionarily conserved (Derivery and Gautreau 2010). It also shares functional and structural analogy with the WAVE complex, which mediates actin polymerisation at the leading edge of migrating cells (Jia, Gomez et al. 2010).

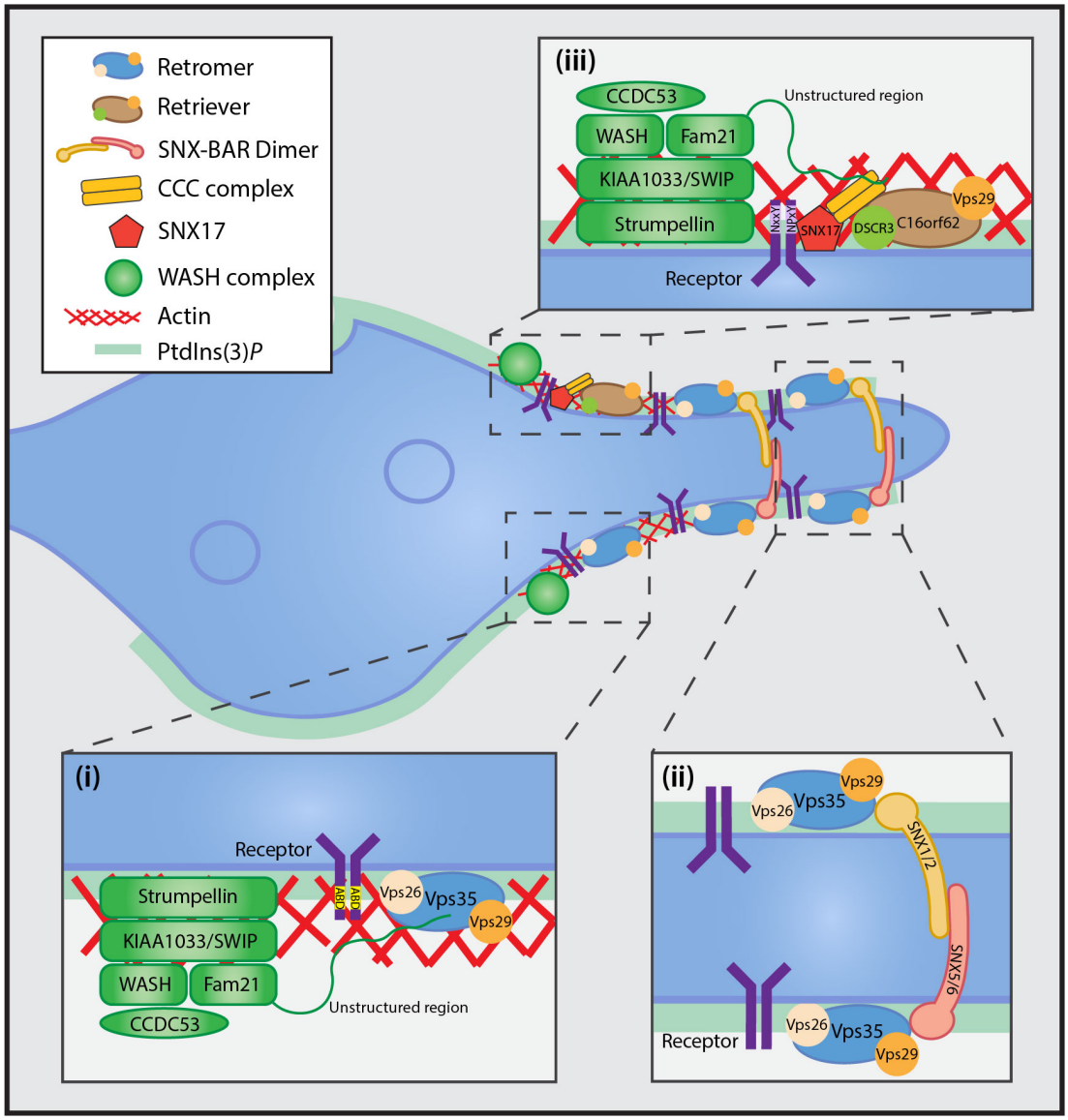

Figure 1.6 Overview of the complexes involved in recycling from sorting endosomes. Recycling of receptors occurs at tubular regions of sorting endosomes. **(i)** The WASH complex is recruited to endosomes in part by its interaction with the retromer complex. Wash is responsible for generating actin rich microdomains at endosomes. These domains help to sort actin-binding domain (ABD) containing proteins for recycling. **(ii)** The retromer CSC is comprised of VPS26, VPS35 and VPS29. This complex interacts with Snx-BAR dimers formed from the dimerization of Snx1 or Snx2 with Snx5 or Snx6. **(iii)** The retriever complex is structurally similar to the retromer complex and mediates the recycling of cargo dependent on Snx17. It is comprised of C16orf62, DSCR3 and VPS29.

Recruitment of the WASH complex to endosomes is mediated through an interaction with the retromer CSC, since RNAi silencing of the CSC leads to disassociation of the WASH complex from endosomal membranes, but not to other endosomal proteins such as Snx1 and EEA1 (Harbour, Breusegem et al. 2010). This interaction occurs via

the unstructured tail of Fam21. Fam21 contains a globular head, which is responsible for its interactions with Wash1 and KIAA1033, and an unstructured tail. The unstructured tail alone is enough to localise Fam21 to membranes. The tail contains multiple Leu-Phe and acidic residue repeated motifs (LFa motifs) (Jia, Gomez et al. 2012). Through these repeated motifs it is believed that Fam21 binds to Vps35, with the more distal repeats being more important for this interaction than the proximal repeats. In vivo, Fam21 will only interact with Vps35 if it is in complex with Vps29, therefore only interacting with an intact and functional retromer complex (Helfer, Harbour et al. 2013). Further to being responsible for the localisation of the WASH complex, the unstructured tail also contains a short motif that binds to actin uncapping proteins (Hernandez-Valladares, Kim et al. 2010).

The link between the retromer and the WASH complex has been further strengthened by studies looking into which proteins rely on the respective complexes for correct trafficking. A study with transgenic mice, which generated Wash1 knockout cells used cre-mediated excision of the gene to conditionally knock down the protein in certain cells, termed WASHout (Piotrowski, Gomez et al. 2013). This study showed defects in the recycling of certain proteins back to the PM, e.g. the EGFR, Glut-1 and CD28. Parallel studies have also highlighted the importance of the retromer in Glut-1 transport (Steinberg, Gallon et al. 2013). Another example would be that of CIMPR. Linking WASH to endosome-to-Golgi retrieval, the WASH complex has been shown to be involved with CIMPR trafficking to the Golgi, a process that also relies on the Snx component of the retromer (Arighi, Hartnell et al. 2004, Gomez and Billadeau 2009). Much like other members of the WASP complex superfamily, WASH is inherently inactive by itself. The activity of this complex is regulated by the E3 ubiquitin ligase TRIM27. Moreover, the activity of this enzyme is increased by another protein called MAGE-L2 (Hao, Doyle et al. 2013). This protein is recruited to endosomes via interactions with Vps35.

The WASH complex has also been linked with the trafficking and recycling of other membrane bound proteins and receptors back to the PM. Notable examples include: the transferrin receptor, α5β1 integrin and, along with Snx-27, the β-adrenergic

receptor (Derivery, Sousa et al. 2009, Temkin, Lauffer et al. 2011, Zech, Calaminus et al. 2011).

It has been proposed that the WASH complex aids the sorting of endosomal proteins through the generation of discrete actin micro-domains (Puthenveedu, Lauffer et al. 2010). Furthermore, Wash1 domains have been shown to coalesce with the inhibition of actin polymerisation (Derivery, Helfer et al. 2012). As with the retromer CSC, it is not clear how specificity for certain proteins to be sorted for either retrieval to the Golgi or recycled back to the PM is regulated. Current opinion believes that this is achieved via associated proteins to the complex, such as Snx27 (Temkin, Lauffer et al. 2011). Further to this, the WASH complex has also been associated with BLOC-1 (biogenesis of lysosomal-related organelles complex 1) and may be involved with lysosome related organelles such as melanosomes (Monfregola, Napolitano et al. 2010, Ryder, Vistein et al. 2013).

RNAi knockdown of components of the WASH complex leads to marked increase in tubulation of endosomes, which is believed to be due to a defect in membrane scission (Derivery, Sousa et al. 2009, Gomez and Billadeau 2009). It is noteworthy that this increased tubulation phenotype of endosomes was not observed with the WASHout system and only with RNA interference (Seaman, Gautreau et al. 2013). Mutations in components of the WASH complex have been shown to lead to particular neurological disorders. Mutations in strumpellin, for example, can lead to Hereditary spastic paraplegia (Valdmanis, Meijer et al. 2007, de Bot, Vermeer et al. 2013), while mutations to KIAA1033 can lead to destabilisation of the whole complex and can lead to late onset AD (Ropers, Derivery et al. 2011, Vardarajan, Bruesegem et al. 2012).

1.4. Receptor signalling

Cells express receptors on their cell surface as a method for sensing the extracellular environment. These receptors can then trigger a cascade of signalling events that allow the cell to respond to changes in their environment.

1.4.1. Growth factors

The discovery of growth factors was first reported in the 1950's by Levi-Montalcini and Cohen, the two would later receive a Nobel prize for much of the work they did around this period. Levi-Montalcini showed that a mouse sarcoma had an impact on the growth of a chick embryo's nervous system (Levi-Montalcini and Hamburger 1951, Levi-Montalcini 1952, Levi-Montalcini, Meyer et al. 1954). A few years later, the factor responsible for this observation was isolated from mouse sarcomas and then isolated again from snake venom (Cohen, Levi-Montalcini et al. 1954, Cohen and Levi-Montalcini 1956, Levi-Montalcini and Cohen 1956). This molecule was the first growth factor identified and is now known as Nerve growth factor (NGF) and over the next few years was followed by the subsequent identification of epidermal growth factor (EGF) by Cohen in the 1960's. Extracts from mice submaxillary glands could induce precocious eyelid opening and incisor eruption (Cohen 1962). These observations were reported to be due to increased keratinisation and epidermis growth, eventually leading to the isolation of the factor responsible for epidermal growth, EGF (Cohen and Elliott 1963, Cohen 1965). It was almost a decade later before human EGF was finally identified and isolated from human urine by Cohen (Cohen and Carpenter 1975, Starkey, Cohen et al. 1975). In the mid 1970's, EGF was shown to bind to cells and membranes. This observation was taken further, when ^{125}I-labelled EGF was shown to bind to fibroblasts before being degraded by the cells (Carpenter, Lembach et al. 1975). By the end of the decade, EGF had been shown to induce phosphorylation of endogenous proteins in A-432 tumour cells, providing insights into the molecular mechanisms by which cells would translate the growth factor signal into a biological response (Carpenter, King et al. 1978). The receptor for EGF (EGFR, also known as ErbB1) wasn't fully sequenced until 1984 (Ullrich, Coussens et al. 1984). Other members of the EGF receptor family (ErbB2-4) would be identified over the next few years (Stern, Heffernan et al. 1986, Plowman, Whitney et al. 1990, Plowman, Culouscou et al. 1993).

1.4.2. Receptor tyrosine kinases (RTKs)

The principal mechanism of action and main components of RTK signalling are highly conserved from *C. elegans* to humans (Lemmon and Schlessinger 2010). With the exception of the insulin receptor and insulin-like growth factor-1 (IGF-1) receptor, which exist as a disulphide bound inactive dimer (Ward, Lawrence et al. 2007), growth factors lead to the activation of RTKs by inducing dimerization of the receptor with another ligand bound receptor (Ullrich and Schlessinger 1990). The RTKs then trans-phosphorylate each other with the resulting phosphorylated tyrosine residue acting as an assembly site for downstream signalling molecules. By the end of the 1990's and early 2000's, crystal structures of RTK fragments began to emerge for many receptors such as: the VEGFR, TrkA, Eph receptor, Axl, Tie2 and the stem cell factor receptor KIT (Wiesmann, Fuh et al. 1997, Wiesmann, Ultsch et al. 1999, Himanen and Nikolov 2003, Barton, Tzvetkova-Robev et al. 2006, Sasaki, Knyazev et al. 2006, Liu, Chen et al. 2007).

There are 4 main types of dimerization that essentially all RTKS will fall into. These are dimerization mediated either: entirely by the ligand, entirely by the receptor, a mixture of both the receptor and the ligand or with the aid of an accessory molecule, e.g. heparin. With the example of the NGFR, dimerization is mediated entirely by the ligand, with no direct interaction between the receptors (Wehrman, He et al. 2007). Whereas with the EGFR, ligand binding results in a conformational change in the extracellular portion of the receptor. This leads to the region that is responsible for the dimerization being available to interact with a neighbouring receptor (Garrett, McKern et al. 2002, Ogiso, Ishitani et al. 2002). Stem cell factor ligand is able to form a dimer with itself. This allows it to essentially crosslink 2 KIT receptors that contains 2 Ig-like domains (D4 and D5), which also interact and strengthen the bond between the dimerising receptors (Yuzawa, Opatowsky et al. 2007). Finally, with the fibroblast growth factor receptor (FGFR) ligand, heparin and dimerised receptor all bind at the same region (the D2 domain) and cooperate to stabilise the dimer (Plotnikov, Schlessinger et al. 1999, Stauber, DiGabriele et al. 2000, Ibrahimi, Yeh et al. 2005). Once the RTKs have dimerised, trans-phosphorylation and activation of the receptors

tyrosine kinase domain (TKD) can occur, leading to downstream signalling events (Honegger, Kris et al. 1989).

Auto-phosphorylation of RTKs occurs in distinct phases. The first of these phases is responsible for relieving the auto-inhibition placed on the receptor and increasing the kinase activity of the intrinsic TKD (Lemmon and Schlessinger 2010). Despite the inactive form of TKDs varying substantially between different RTKs , the active form of these domains is actually very similar (Huse and Kuriyan 2002). This is because key regulatory components of TKDs need to adopt a specific configuration in order to allow for efficient transfer of phosphate groups, and therefore, increased kinase activity (Nolen, Taylor et al. 2004). Due to the differences in the inactive form, however, different regulatory mechanisms are exhibited between RTKs. The TKD can be auto-inhibited by its own activation loop, as seen with the insulin receptor and the FGFR (Hubbard 2004). A tyrosine in the activation loop of these RTKS sterically blocks the active site of the TKD. This tyrosine is trans-phosphorylated when the receptors bind their ligands, preventing it from sitting in the active site, providing access for ATP and substrates (Chen, Ma et al. 2007, Bae, Lew et al. 2009).

TKDs can also be auto-inhibited by regions outside of the TKD itself. As seen with the Musk receptor, Flt3 receptor, KIT receptor and the Eph family of receptors, the juxtamembrane region of the receptor can make extensive contacts with the TKD, e.g. in the activation loop, and therefore helps to stabilise the inactive form of the TKD (Till, Becerra et al. 2002, Griffith, Black et al. 2004, Mol, Dougan et al. 2004). Further phosphorylation of the TKD can lead to greater increases in its kinase activity. For example, Phosphorylation of Y553 in the juxtamembrane region precedes phosphorylation of Y754 in the activation loop of the Musk receptor (Till, Becerra et al. 2002). Mutations to RTKs that prevent the juxtamembrane regions interacting with the TKD are found in many cancers, as these lead to constitutively active receptors (Dibb, Dilworth et al. 2004). Another region of the receptors, that can provide auto-inhibition of the TKDs, is the C-terminal tail. This region contains a tyrosine that inhibits the TKD by also providing a steric block on the active site of the TKD that prevents substrate access (Shewchuk, Hassell et al. 2000, Niu, Peters et al. 2002).

The EGFR/ErbB family of receptors are unusual in their mode of activation, due to the fact that the activation loop doesn't require trans-phosphorylation for activation of the TKD (Zhang, Gureasko et al. 2006). Activation occurs when the C-lobe of one TKD interacts with the N-lobe of another TKD. This causes a conformational change in the second TKD that disrupts the auto-inhibition placed on it and allows it to adopt the active conformation (Boyer, Turchi et al. 2006, Qiu, Tarrant et al. 2008). The juxtamembrane region of these receptors is also important for TKD activation, but instead of helping to stabilise the inactive TKD form, it provides a pocket for the C-lobe of the activating TKD to sit in, aiding it to interact with the N-lobe of the receiving TKD (Jura, Endres et al. 2009, Red Brewer, Choi et al. 2009).

The second phase of auto-phosphorylation is responsible for creating phospho-tyrosine binding sites. Phosphorylation events within this phase occur in specific orders, e.g. Y583 in the kinase insert of the FGFR is phosphorylated first, followed by Y463 in the Juxtamembrane region and Y585 also in the kinase insert (Furdui, Lew et al. 2006). Phospho-tyrosines generated in this phase of auto-phosphorylation, provide binding sites on the receptor for the recruitment of SH2 domain and phospho-tyrosine binding (PTB) domain containing signalling adaptors (Mohammadi, Honegger et al. 1991, Pawson 2004). These proteins are recruited either directly to the RTK or to already docked accessory proteins, e.g. insulin receptor substrate 1 (IRS1) with the insulin receptor that becomes hyper-phosphorylated in response to RTK activation (Sun, Crimmins et al. 1993). From here, the RTK can activate a number of signalling pathways, such as the MAPK or Akt signalling pathways. Although these pathways were thought to be linear and operate in isolation of each other, it has become increasingly evident that they in fact form intertwined networks.

1.4.3. ErbB receptor family

The EGFR was the first RTK to be identified and, therefore, is the most heavily studied out of the RTK family of receptors (Wang 2017). The EGFR is a part of the ErbB subfamily of receptors, which includes, EGFR/ErbB1/Her1, ErbB2/Her2, ErbB3/Her3 and ErbB4/Her4 (Yarden and Sliwkowski 2001). These receptors can form both hetero-

and homodimers (Citri and Yarden 2006). Heterodimerisation is important for activation of all the ErbB receptors, due to the fact that ErbB2 has no direct ligand and ErbB3 has impaired kinase function (Carraway and Cantley 1994). Aberrant activation of ErbB receptors leads to tumourgenesis in many cancers, such as non-small cell lung cancer (NSCLC), breast, pancreatic, ovarian, head and neck, etc. (Arteaga and Engelman 2014). The ErbB2 receptor is highly implicated in breast and ovarian cancers. In these cancers, the receptor is associated with gene amplification leading to overexpression of the receptor. This occurs in approximately 20-25% of breast and ovarian cancers and is linked with poor prognosis (Slamon, Clark et al. 1987, Reese and Slamon 1997). The ErbB3 receptor exhibits a $1/1000^{th}$ the autophosphorylation activity of the EGFR. It has been linked to cancer, mainly due to its ability to promote oncogenic EGFR and ErbB2 receptor signalling (Gullick 1996). ErbB4 differs from the other members of the ErbB family as the receptor becomes cleaved after binding to its ligand. The full length receptor is 180kDa. After activation the 80kDa intracellular domain is cleaved and translocates to the nucleus in order to regulate gene transcription. This receptor is required for the development of the CNS, heart and mammary glands (Sardi, Murtie et al. 2006).

1.4.4. Endosomal RTK signalling

In 1979, Haigler, et al. showed that, when treated with epidermal growth factor (EGF), the number of EGF receptors (EGFR) present on the cell surface was reduced by 99%, and subsequently redistributed to internal compartments within the cells (Haigler, McKanna et al. 1979). Endocytosis in turn, became viewed as a down regulatory mechanism, by which the cell could attenuate growth factor signals in order to prevent aberrant cell growth (Beguinot, Lyall et al. 1984, Sorkin and von Zastrow 2002). However, insights indicating that this wasn't the full picture, in terms of the roles of the endosome, came in 1985 when Wiley, et al. observed that the rate of degradation of internalised EGFRs was slower than the rate of internalisation (Wiley, VanNostrand et al. 1985). Further studies by Sorkin et al., in 1988, showed that EGF did not dissociate from the EGFR in early endosomes, suggesting that the EGFR was still active after endocytosis (Sorkin, Teslenko et al. 1988).

In 1994, fractionation studies looked into EGFR and insulin receptor signalling. Both the EGFR and insulin receptor had been linked to the recruitment of Grb2, Sos and Shc, but the two receptors give different physiological responses, despite containing converging signalling pathways. Separation of plasma membrane and endosomal compartments after stimulation with either EGF or insulin, showed greater internalisation of the EGFR compared to the insulin receptor, and greater levels of tyrosine phosphorylation in endosomal compartments when stimulated with EGF, compared to stimulation with insulin (Di Guglielmo, Baass et al. 1994). These experiments indicated that internalisation of the EGFR to the endosome could be responsible for different physiological outcomes observed between the EGFR and the insulin receptor (Murphy, Padilla et al. 2009, Omerovic and Prior 2009).

In 1996, Vieira, et al. showed that inhibition of endocytosis increased EGF-dependent cell growth, and this was due to changes within the phosphorylation profile of the EGFR and its associated proteins. Interestingly, both hyper- and hypo-phosphorylation of EGFR associated proteins in the K44A dynamin mutant cells, compared to wild type (WT) cells was observed (Vieira, Lamaze et al. 1996). In 2001, Burke, et al. used an anti-EGFR antibody tagged with biotin via a disulphide bond. The biotin tag could then be removed from the cell surface with the addition of glutathione, while the internalised antibody would retain its tag (Burke, Schooler et al. 2001). This allowed them to analyse the differences in signalling within the normal physiological context of the cell. The results from the experiment show differential activation of EGFR associated proteins, at internal and cell surface locations.

At the same time, Wu, et al. was working on both EGF and NGF. While both growth factors induced transient Ras activation, only NGF caused prolonged Rap1 activation (Wu, Lai et al. 2001). Furthermore, activated Rap1, along with associated signalling complexes, was shown to be present at endosomes. Additionally, disruption of internal membranes within the cell resulted in Rap1 signalling being abolished, while having little to no effect on Ras activity (Wu, Lai et al. 2001). Later, in 2002 and 2004, studies by Wang et al. examined endosomal signalling of both EGFR and PDGFR. These studies used specific RTK inhibitors, along with blocking of recycling to deliver inactive

growth factor-receptor complexes to the endosome. From here, the inhibitors were washed out and endosomal signalling could be observed (Wang, Pennock et al. 2002, Wang, Pennock et al. 2004). These studies show that signal transduction can be initiated from endosomes and that this signal is sufficient to provide a biological response. They also expand the concept of endosomal signalling to RTKs other than the EGFR.

In 2012, the pioneering study by Vieira, et al. (Vieira, Lamaze et al. 1996) was revisited using more modern techniques. Endocytosis was inhibited using a dynamin inhibitor, Dynasore, instead of expression of the K44A mutant dynamin. Protein phosphorylation was then examined by phosphoproteomics to provide an unbiased global view of EGF and endocytosis dependent phosphorylation (Omerovic, Hammond et al. 2012). The results validate the general principle established by Vieira et al. but indicate some finding may be due to compensatory mechanisms caused by long term dynamin inhibition. This study also showed that phosphorylation of the ESCRT-0 complex by EGF is highly dependent on endocytosis. The studies described above introduce the concept of spatial regulation of RTKs, whereby, signals generated at the plasma membrane and the endosome will result in different signalling outcomes (Figure 1.7).

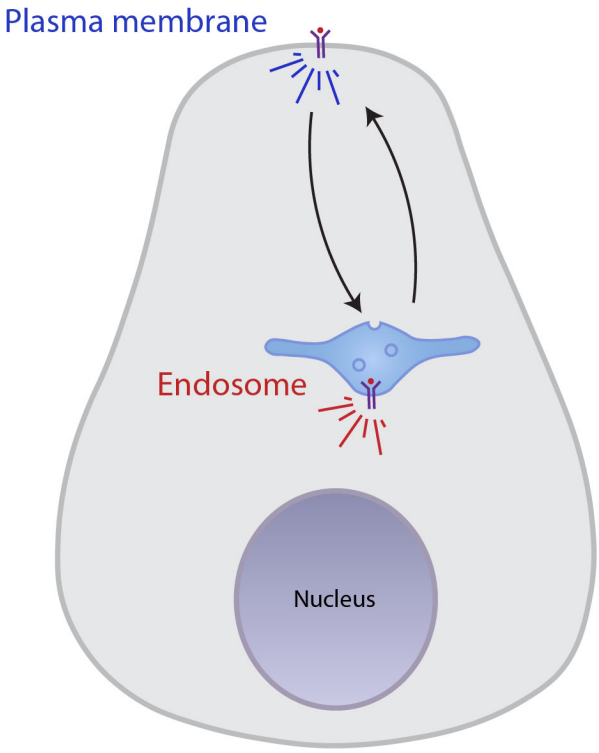

Figure 1.7 Spatial regulation of Receptor tyrosine kinases (RTKs). The receptor is activated at the plasma membrane, where it exposed to an array of signalling adaptors and effectors to elicit a biological response. Later, trafficking of the receptor to the endosome will result in the receptor being exposed to a different environment of adaptors and effectors, resulting in a distinct biologically response.

1.4.5. G-protein coupled receptors (GPCRs)

The GPCR family of the receptors makes up the largest group of receptors with almost a 1000 members (Fredriksson and Schioth 2005). Clinically, these receptors are very important with 34% of all FDA approved drugs targeting a GPCR. These receptors all share a 7 transmembrane (7TM) structure and are linked to second messenger generating enzymes via the action of heterotrimeric G-proteins (Gilman 1987). Much of what we know about these receptors was pioneered by research into the β-adrenergic receptor. This work done in the 1970's and 1980's by Lefkowitz would ultimately lead him to win the Nobel Prize in chemistry in 2012 for his efforts (Lefkowitz 2007).

Studies into the β-adrenergic receptor began before the GPCR class of receptors had even been described, and also before it was even known if the β-adrenergic receptor was even an individual molecule (Lefkowitz 2007). The biochemist Earl Sutherland even said at the time that it was possible the β-adrenergic receptor could be a binding site on Adenylate cyclase (AC) (Robison, Butcher et al. 1967). In the early-to-mid 1970's radio-ligands were generated for the β- and α-adrenergic receptor (Mukherjee, Caron et al. 1975), as well as for a number of other receptors such as glucagon, opioid and muscarinic cholinergic receptors (Rodbell, Birnbaumer et al. 1971, Pert and Snyder 1973, Yamamura and Snyder 1974). These tools helped to build on our understanding of the physiological outputs governed by the receptors they were targeted against. This work would be built upon further with these tools by the purification of many targeted receptors. Affinity chromatography, along with the radio ligands, would allow for the purification of the relatively sparse β-adrenergic receptor in 1972 (Lefkowitz, Haber et al. 1972). By the end of the decade, the 'ternary complex model' had been developed (De Lean, Stadel et al. 1980).

It was not until mid 1980's that the β-adrenergic receptor as a single molecule was finally accepted as a receptor. Reconstitution of the β-adrenergic receptor into xenopus erythrocytes allowed the previously unresponsive cells to respond to catecholamines (Cerione, Strulovici et al. 1983). A year later this experiment was taken a step further by also reconstituting G-proteins with the β-adrenergic receptor, creating a hormone responsive AC signalling system (Cerione, Sibley et al. 1984).

In 1986, the β-adrenergic receptor was cloned, a task only possible at the time due to the fact that the receptor is 'intron-less' (Dixon, Kobilka et al. 1986). The sequence revealed the receptor to have 7 membrane spanning regions with sequence homology to the 7TM structure of Rhodopsin. Until this point, Rhodopsin had not been thought of as a receptor and this finding changed the view that the 7TM structure was specific to light sensitive proteins (Ovchinnikov Yu 1982). Further sequencing of the other adrenergic receptors strengthened this argument (Kobilka, Matsui et al. 1987, Dohlman, Thorner et al. 1991). Over the next few years the 7TM class of receptors began to grow rapidly as more receptors were cloned, including the muscarinic

cholinergic receptor and substance K receptors (Kubo, Fukuda et al. 1986, Masu, Nakayama et al. 1987). By the beginning of the 1990's, a large number of olfactory receptors had been cloned (almost 500) with all of them turning out to be GPCRs (Buck and Axel 1991). By the end of the decade, many taste receptors had been given the same treatment (Hoon, Adler et al. 1999).

The α_2- and β_2- adrenergic receptors are an interesting pair of receptors and their study has given great insight into the structural function of GPCRs. These two receptors share a reasonably high degree of sequence homology, and interestingly both bind the same adrenergic ligands, but with opposite downstream effects. While the β_2 receptor will increase the activity of AC, the α_2 receptor will, in contrast, inhibit AC activity due to the binding of G_s and G_i respectively. A series of chimeras were generated in order to determine which regions of the receptor would translate to which function and where specificity for G-proteins could be determined (Kobilka, Kobilka et al. 1988). From these experiments performed in the late 1980's and early 1990's, it was determined that the third intracellular loop was responsible for G_s and G_i specificity, while ligand binding was determined by the membrane spanning domains (Ostrowski, Kjelsberg et al. 1992). It was also shown that residues in the distal region of the third intra cellular loop would provide important intra-receptor interactions that hold the receptor in an inactive state at rest. Binding of a ligand would lead to a conformational change allowing the receptor to 'relax' into its active state (Cotecchia, Exum et al. 1990). Mutations to these residues can be found in thyroid adenomas.

In the mid 1970's, it was first observed that repeated exposures to β-adrenergic receptor agonists would lead to reduced cellular responses. This desensitization is a key homeostasis process regulating GPCR function, but it was unclear at the time what was responsible for the phenomenon. A few years later it was shown that cells which had been desensitized to isoproterenol, exhibited receptors that migrated slower on polyacrylamide gels (Stadel, Nambi et al. 1982). Suggesting the presence of a post-translational modification (PTM) such as phosphorylation. This was later confirmed with the use of ^{32}Pi labelled phosphate (Stadel, Nambi et al. 1983). The enzyme

responsible for phosphorylating the β-adrenergic receptor wouldn't be identified until the end of the 1986 and was named β-adrenergic receptor kinase (βARK) but has since been renamed GRK2 (Benovic, Strasser et al. 1986). This enzyme appeared to be similar to an enzyme identified in rod cells, which was responsible for the phosphorylation of Rhodopsin (Wilden and Kuhn 1982). This family of kinases now contains 7 members (GRK1-7) (Pitcher, Freedman et al. 1998).

β-ARK was purified from bovine brain tissue and, interestingly, would lose its ability to desensitize the β-adrenergic receptor the further it was purified. An explanation for this would come from studies into Rhodopsin. A 48kDa protein (now called arrestin1) was shown to work with Rhodopsin kinase in order to deactivate Rhodopsin (Kuhn and Wilden 1987). This protein was able to restore the desensitizing effects of purified β-ARK (Benovic, Kuhn et al. 1987). β-arrestin1 and β-arrestin2 (also known as arrestin2 and 3 respectively) would soon be identified (Lohse, Benovic et al. 1990, Attramadal, Arriza et al. 1992).

GPCR phosphorylation by GRKs does not convey receptor desensitization per se, but rather generates high affinity binding sites for the arrestins (Lohse, Benovic et al. 1990, Gurevich, Dion et al. 1995). This series of events was first visualized in 1999 by Barak et al. (Barak, Warabi et al. 1999). Arrestins downregulate GPCR signal by reducing $G_{\alpha s}$ activation, thus hampering the production of further cAMP, and the recruitment of phosphodiesterase's to increase the rate of cAMP degradation (Perry, Baillie et al. 2002). Arrestins can also act as adaptors for proteins involved in clathrin mediated endocytosis in order to aid in the internalization of activated GPCRs (Ferguson, Menard et al. 1995, Laporte, Oakley et al. 1999). Once internalized to endosomal membranes, the GPCR is uncoupled from its ligand and re-sensitized before being recycled back to the plasma membrane (Yu, Lefkowitz et al. 1993, Krueger, Daaka et al. 1997). Arrestins are also responsible for the G-protein independent activation of MAP kinase pathways (Luttrell, Ferguson et al. 1999).

1.4.6. Endosomal GPCR signalling

Much like with RTKs, internalization of GPCRs was viewed as a mechanism to attenuate receptor signaling, with activation of heterotrimeric G proteins occurring at the plasma membrane (Figure 1.8). However, during the 1990's, multiple studies observed G proteins present at endo-membranes (Stow, de Almeida et al. 1991, de Almeida, Holtzman et al. 1994, Brand, Holtzman et al. 1996, Weiss, White et al. 1997), indicating that GPCR signaling may not be restricted to the plasma membrane (Irannejad and von Zastrow 2014). The first example of an endosomally derived GPCR signal came from study of Ste2 in 2006. When activated, Ste2 catalyzes guanine nucleotide exchange of the G_{α} subunit, allowing the βγ subunits to dissociate and transduce the receptors signal by activation of the MAP kinase pathway (Slessareva, Routt et al. 2006). This study showed that the G_{α} subunit conveyed part of the receptors signalling activity and that this took place at endosomes.

A few years later, in 2009, an immunotherapy study showed that the S1P1R receptor displayed sustained receptor activity at endosomes when the cells were treated with the drug; FTY720 (Mullershausen, Zecri et al. 2009). Another group investigating the thyroid-stimulating hormone (TSH) receptor show that receptor activity is poorly reversed after the hormone is washed out (Calebiro, Nikolaev et al. 2009). However, upon inhibition of endocytosis with the dynamin inhibitor, Dynasore, they were able to attenuate the persistent signal with removal of the TSH. Interestingly, this persistent signal produced by the TSHR continues after TSH has dissociated from the receptor (Werthmann, Volpe et al. 2012). Sustained cAMP signalling was observed with Parathyroid hormone (PTH) receptor in HEK293 cells adding further support for the notion of sustained GPCR activation occurring at endosomes (Ferrandon, Feinstein et al. 2009). Overexpression of Arrestins was also shown to prolong the PTHR signal, leading to the proposed mechanism by which Arrestins were responsible for sustained endosomal signalling of GPCRs (Feinstein, Wehbi et al. 2011).

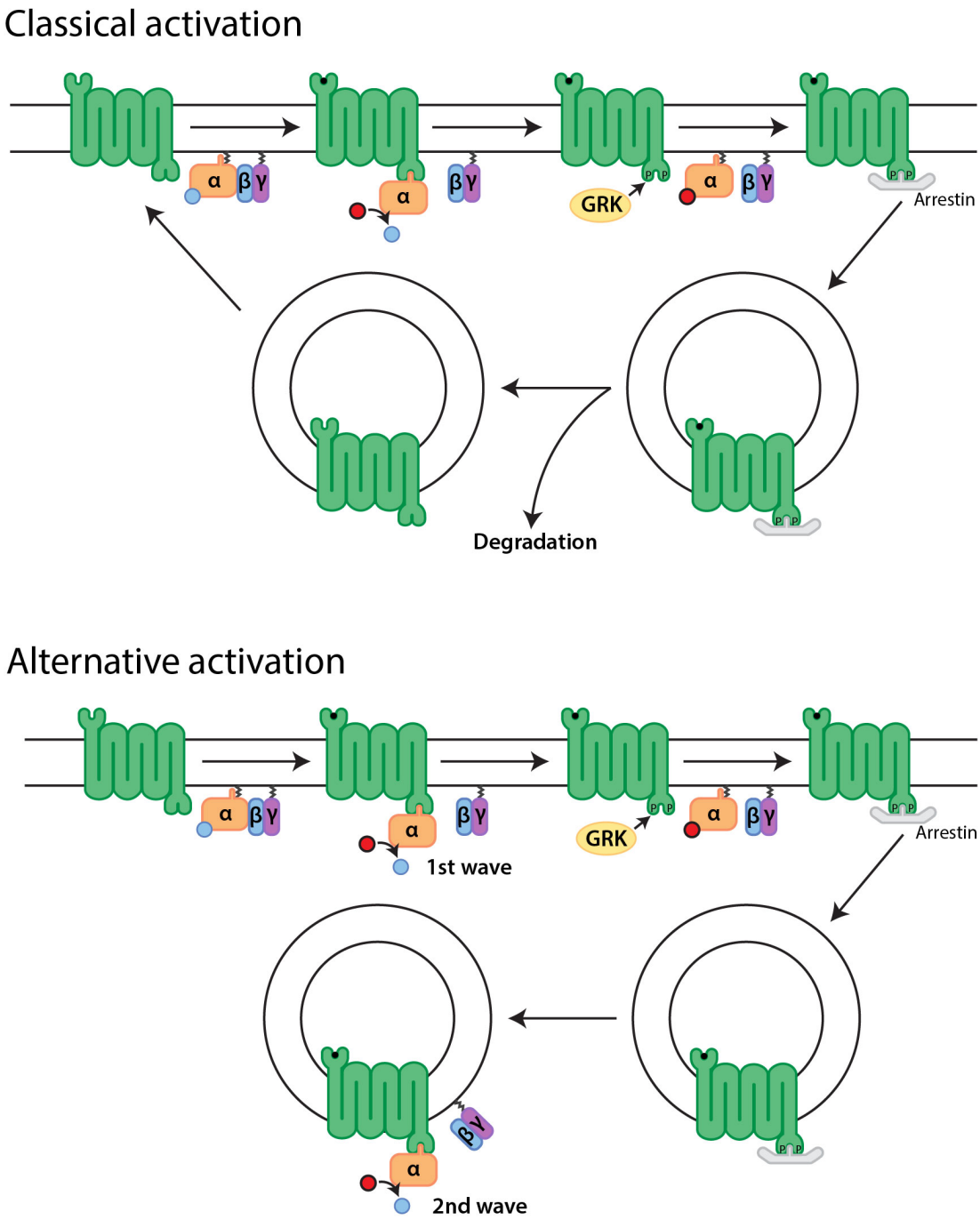

Figure 1.8 Classical and endosomal GPCR signalling. In both circumstances, binding of the ligand to the GPCR results in a conformational change in the receptor. This now allows the receptor to bind to the α subunit of the heterotrimeric G-proteins, causing it to displace GDP for GTP and become active. The α subunit dissociates from the βγ subunits and activates various effectors. The GPCR is then phosphorylated by GRK, allowing it to bind Arrestins. This results in the internalisation of the receptor. In the classical model, trafficking of the receptor to the endosome results in the attenuation of the signal and resetting of the receptor to be recycled back to the PM. However, in the alternative model, the GPCR can further activate heterotrimeric G-proteins at the endosome, resulting in a 2nd and more sustained wave of activation.

Further studies would report persistent GPCR signalling with the Vasopressin receptor, V2R, as well as an acute endosomal signal from the dopamine receptor, DRD1 (Kotowski, Hopf et al. 2011, Feinstein, Yui et al. 2013). Resulting in a revision of the proposed model that suggested the sustained endosomal signal resulted from a GPCR-Arrestin-$G_{\beta\gamma}$ complex (Wehbi, Stevenson et al. 2013).

Sustained cAMP signalling had previously been ruled out for the β-adrenergic receptor, however, in 2013, an elegant study using conformational biosensors of active G-proteins found that isoproterenol was able to induce endosomally active G-proteins (Irannejad, Tomshine et al. 2013). The same group also showed that the endosomal derived portion of the β-adrenergic receptor signal is responsible for the cells transcriptional response (Tsvetanova and von Zastrow 2014).

1.4.7. Crosstalk between GPCRs and RTKs

Traditionally, studies on GPCRs and RTKs have been performed in isolation. While this has been important for understanding the basic signalling of each family of receptors, rarely in nature will cells experience a growth factor or other ligand in isolation. In the mid 1990's it began to emerge that RTKs could be activated independent of their ligands, e.g. by various stress factors such as UV radiation (Knebel, Rahmsdorf et al. 1996, Goldkorn, Balaban et al. 1997). The term transactivation was coined in 1996 by Ullrich's lab when they showed that stimulation with endothelin-I, lysophosphatic acid (LPA) and thrombin, all lead to the phosphorylation of the EGFR (Daub, Weiss et al. 1996). This added to the observation that the PDGFR can be activated by angiotensin II (Linseman, Benjamin et al. 1995). By the end of the decade a number of GPCR ligands had been shown to activate RTKs but the mechanism for how this occurs had not been elucidated (Daub, Wallasch et al. 1997, Lee and Chao 2001, Peng, Myers et al. 2002).

In 1999, it was suggested that GPCR stimulation led to the activation of metalloproteinases and cleavage of, for example, heparin-binding EGF (HB-EGF) (Prenzel, Zwick et al. 1999). Further examples of metalloproteinase involvement in GPCR-RTK crosstalk were observed over the next few years in cardiac cells with the

angiotensin receptors, and in response to other factors such as *Helicobactor pylori* infection (Uchiyama-Tanaka, Matsubara et al. 2001, Asakura, Kitakaze et al. 2002, Wallasch, Crabtree et al. 2002). This gave rise to the 'triple membrane passing signalling' (TMPS) model, whereby the signal crosses the plasma membrane three times. Other mechanisms for the transactivation of RTKs have also been suggested. Src and Pyk were shown to interact with the EGFR in response to LPA receptor activation (Luttrell, Hawes et al. 1996, Keely, Calandrella et al. 2000). Src is capable of directly phsophorylating the EGFR (Biscardi, Maa et al. 1999). Another possible mechanism for the transactivation of RTKs is via the inhibition of protein tyrosine phosphatases (PTPs). H_2O_2 has been shown to inhibit PTPs (Sundaresan, Yu et al. 1995) and stimulation of some GPCRs can lead to H_2O_2 generation (Rhee, Bae et al. 2000).

Transactivation of RTKs by GPCRs has been more commonly observed throughout recent years as opposed to RTK activation of GPCRs. However there a few examples of evidence to suggest that RTKs are capable of GPCR transactivation (Delcourt, Bockaert et al. 2007). Pertussis toxin has been shown to mediate some of the actions of insulin via G proteins (Luttrell, Kilgour et al. 1990), suggesting the insulin receptors mitogenic effects are mediated by $G_{\beta\gamma}$ subunits (Luttrell, van Biesen et al. 1995, Dalle, Ricketts et al. 2001). A similar observation was also seen with FGF (Fedorov, Jones et al. 1998). In 1996, EGF was observed to activate adenylate cyclase via phosphorylation of $G_{\alpha s}$ subunit (Poppleton, Sun et al. 1996). Phosphorylation of $G_{\alpha i}$ prevents its reassociation with the βγ subunits and prolongs G protein activation (Alderton, Rakhit et al. 2001). The S1P receptor has also been shown to be activated in response to various RTKs, e.g. IGF-1, NGF and PDGF, via synthesis and secretion of the receptor ligands (Hobson, Rosenfeldt et al. 2001, Toman, Payne et al. 2004, El-Shewy, Johnson et al. 2006). The PDGFR has also been observed to transactivate S1P recetors in a ligand independent way (Waters, Sambi et al. 2003). Further to this, stimulation of $G_{\alpha i}$ has been shown to be important for both EGFR and PDGFR dependent migration (Shan, Chen et al. 2006) and inhibition of a S1P receptor blocks PDGF induced cell migration (Waters, Long et al. 2006).

1.5. Objectives

A major aim of the work described in this thesis is to expand upon our current knowledge surrounding the role of HRS in endosomal signalling and trafficking. In particular, I hoped to advance our understanding of the function of HRS phosphorylation. HRS is a prominent target of RTK activity, but despite this, the role of HRS phosphorylation is still up for contention. Furthermore, the profile of HRS phsophorylation changes when stimulating with different growth factors (Row, Clague et al. 2005). Here I attempt to bring clarity to the issue by assessing the phosphorylation dependent interactors of HRS and investigate the dynamics of HRS recruitment.

Work preceeding this project from our laboratory indicates that HRS may have a role as a signalling adaptor (Han liu, unpublished data; described in chapter three). I aimed to evaluate this hypothesis by examining the EGF dependent binding partners of HRS by mass spectrometry and to also establish proximity labelling techniques in the laboratory. Secondly, I aimed to build upon the existing tools and methodologies in order to investigate specific endosomally derived cAMP and protein kinase A (PKA) signalling. The purpose of this is to progress the field by developing a method for the direct visualisation of cAMP generation and PKA signalling at endosomes. I hope to introduce new tools for examining crosstalk between RTKs and GPCRs that in principle could be governed by HRS.

There is evidence that suggests phosphorylation of HRS may alter its binding properties with membranes (Urbé, Mills et al. 2000). I therefore aimed to visualise the dynamics of HRS recruitment to endosomes in response to growth factor stimulation. Tyrosine residues 329 and 334 of HRS have been identified as principal phosphorylation sites in response to EGFR activation (Urbé, Sachse et al. 2003). I utilised a HRS mutant lacking in these tyrosine residues to investigate the function of phosphorylation at these sites.

Chapter two: Materials and methods

2.1. Cell biology

2.1.1. Materials and Reagents

Dulbecco's Modified Eagle's Medium (DMEM) + GlutaMAX-I (#31966-021), Fetal bovine serum (FBS) (#10270), Penicillin and Streptomycin antibiotic mixture (#15140-122) and Minimum Essential Medium/Non-Essential Amino Acids (MEM/NEAA) (#11140-035) were purchased from Thermo Fisher Scientific. Trypsin-EDTA (#15400) and Opti-MEM (#409864), and Hygromycin B (#10687010) were from Invitrogen (Paisley, UK). GeneJuice® Transfection reagent (#70967-3) came from EMD Millipore (Darmstadt, Germany). Geneticin (G418) (#04727878001) was purchased from Roche Diagnostics. Wortmannin (#W1628), Forskolin (#F6886) and Isoproterenol (#I6504) were all supplied from Sigma-Aldrich (Dorset, UK). EGF (#AF100-15), TGFα (#100-16A) were purchased from Peprotech (London, UK) and EGF-AlexaFluor555 (#E35350) was from Fisher Scientific. SAR405 (#AOB6007) came from Aobious (MA, USA), Dyngo (#ab120689) was from Abcam (Cambridge, UK) and IBMX (#410957) was bought from EMD Millipore (Darmstadt, Germany). All cell culture plastics were purchased from Corning (NY, USA).

2.1.2. Cell culture

HeLa S3 Flp-In cells and HEK293 Flp-In cells were cultured in Dulbecco's Modified Eagle Medium supplemented with 10% Fetal bovine serum (FBS), 0.1mM MEM/Non-Essential Amino Acids (MEM/NEAA) and 100units/ml of Penicillin and Streptomycin. All cells were cultured at 37°C and in a humidified 5% CO_2 atmosphere. Confluent cells were split for maintenance at 1:4-1:6 dilutions every 2-3 days.

2.1.3. DNA transfection

Transient DNA transfections were performed using GeneJuice® in all cell lines. For a 35mm dish, cells were seeded into each dish and incubated overnight at 37°C. The following day, the culture medium was exchanged for 1ml of fresh full DMEM. 3µl of GeneJuice was then added to 100µl of Opti-MEM and mixed gently. After a 5-minute incubation at room temperature, 1µg of DNA was added to the Opti-MEM and mixed gently. The mixture was then incubated for 20 minutes at room temperature before being added to cells in a drop wise manner. Cells were fixed, harvested or used for live-cell imaging 24 hours after transfection.

2.1.4. Drug treatments

Generation of PtdIns(3)*P* was inhibited with either a 15-minute treatment of 1µM Wortmannin or a 2 hour treatment with 1µM SAR405. Dynamin inhibition was achieved from a 15-minute pre-treatment with 30µM Dyngo. The same concentration of Dyngo was maintained for the duration of the experiment. β-adrenergic receptors were stimulated with 10nM Isoproterenol for the indicated time periods. EGF receptors were stimulated with 20ng/ml of EGF or TGFα, unless otherwise stated. For experiments using fluorescent EGF, 1µg/ml of EGF-AlexaFluor555 was used. Where indicated, cells were serum starved 6 hours prior to growth factor stimulation.

2.2. Molecular biology

2.2.1. Reagents

Pfu Ultra II DNA polymerase (#600670) and Deoxynucleotide mix (#200415-51) were purchased from Agilent Technologies (Cheshire, UK). Agarose powder (#15510-019), DH5α competent cells (#18265017) and S.O.C medium (#S1797) were from Invitrogen (Paisley, UK). Rosetta™ (DE3) competent cells (#70954) were bought from Merck Millipore. Miniprep (#27106), HiSpeed Midiprep (#12643) and HiSpeed Maxiprep

(#12663), Gel extraction (#28704) kits and RNAase-free DNAase (#79254) were all purchased from Qiagen (Crawley, UK). All restriction endonucleases (RE), Quick Ligation kit (#M22000S), Purple Gel loading dye (#B7025S), 100bp (#N3231) and 1kb (#N3232) ladders were bought from New England Biolabs (Herts, UK). TAE buffer (#EC-872) was obtained from National Diagnostics (Hull, UK). All primers were purchased from Eurofins MWG Operon (Ebersberg, Germany). Zero Blunt™ TOPO™ PCR Cloning Kit (#450031), pEF5/FRT/V5 Directional TOPO™ Cloning Kit (#K603501), TOP10 competent cells (#C404003), One Shot® ccdB Survival™ 2 T1R Competent Cells (#A10460) and Snakeskin® pleated dialysis tubing (3,500MWCO) (#68035) were bought from Fisher Scientific (Loughborough, UK). Gateway™ BP Clonase™ II Enzyme mix (#11789020) and Gateway™ LR Clonase™ II Enzyme mix (#11791020) were purchased from Life Technologies (Paisley, UK). Isopropyl β-D-1-thiogalactopyranoside (IPTG) (#MB1008) was from Melford biolaboratories (Suffolk, UK). Ethidium Bromide (EtBr) (#E1510), Lysozyme (#L6876) and Imidazole (#I202-100G) were all from Sigma-Aldrich (Dorset, UK). 5ml HisTrap HP column (#17524801) and AKTA chromatography system are both from GE Healthcare Life Sciences (Buckinghamshire, UK). pcDNA-APEX2-NES (#49386) (Lam, Martell et al. 2015) and pCSDEST-APEX2-GBP (#67651) (Ariotti, Hall et al. 2015) were purchased from Addgene. pcDNA3.1-AKAR4-NES and pcDNA3.1-ICUE3 plasmids were a gift from Oliver Rocks (Max Delbrück Centre), and the pGFP-C1-Epac1-RA2 plasmid was a gift from Philip Stork (Oregon Health and Science University). A summary of all primers used can be found in table 2.1.

Name	Sequence (5'->3')	Length	Tm	GC content
DG-FFYVE-HinDIII-F	AGAAGCTTGGCACCATGGATGTTAGCAGAGAAGAGGCTCC	40	74.6	52.5%
DG-FFYVE-BamHI-R	AAGGATCCCCAGACCCAGATCCAGAAGTCCGATCTTCATC	40	74.6	53%
DG-ICUE3-3231F	GGGAGGTACCTGAGGATCTATGG	23	64.2	56%
DG-ICUE3-3253R	CCATAGATCCTCAGGTACCTCCC	23	64.2	56%
DG-ICUE3-2217F	TGTTGTCAACCCACAGGAAG	20	57.3	50%
DG-AKAR4-1107F	ACTAGGAGAAGACGGTAACC	20	57.3	50%
DG-APEX2-397F	GACCTAAGGTTCCATTCCAC	20	57.3	50%
DG-CFP-NES-R	CCTCAGGTTACAGGGTCAGGCGCTCCAGGGGGGGCAGGGTACCTCCCTTGTACAGCTC	58	>75	65.5%
DG-HRS-N-attB1F	GGGGACAAGTTTGTACAAAAAAGCAGGCTGGGGATCCACCATGGGGCGAGGCAGCGGCAC	60	>75	60%
DG-HRS-N-attB2R	GGGGACCACTTTGTACAAGAAAGCTGGGTGGTCGACTCAGTCAAAGGAGATGAGC	55	>75	52.7%
DG-RfB-Fwd	GCCTGACCCTGGACTCAACAAGTTTGTACAAAAAAGC	37	75	35.2%
DG-RfB-Rev	CTCGAGTTATATCAACCACTTTGTACAAG	29	65	38%
DG-APEX2-RfB-R	GTACAAACTTGTTGAGTCCAGGGTCAGGCGCTCCAG	36	>75	56%

Table 2.1 Summary of the primers used for cloning

2.2.2. Polymerase chain reaction (PCR)

PCR was used for DNA amplification in order to clone the FYVE domain from pcDNA3.1-GFP-FENSFYVE vector and add a Kozak sequence, a linker and BamHI and HindIII restriction sites. This PCR fragment was later used to add a FYVE domain to both cAMP and PKA FRET biosensors. PCR was also used for site-directed mutagenesis (SDM). The nuclear export sequence (NES) was re-introduced to pcDNA3.1-FF-AKAR4 CFP-only vector, after the SDM removed the sequence from the open reading frame (ORF). The RA2 domain from the Epac1-RA2 vector was also cloned by PCR in order to be introduced into the pcDNA3.1-FF-ICUE3 vector.

A two-step PCR was also used to create an APEX2 destination vector for Gateway cloning. Primers were designed to amplify the enzyme from the pcDNA3-APEX2 vector, without the constructs STOP codon. More primers were designed to amplify the RfB cassette such that the forward primer had an over lapping sequence to the reverse primer used to amplify the APEX2 enzyme. The second PCR step took the two PCR fragments along with the end primers to create the final DNA sequence, which was used to generate the destination vector. AttB sites were added to amplified HRS and mutant HRS (YYFF) to create gateway compatible PCR fragments. These fragments were amplified from pcDNA3-GFP-HRS and pcDNA3-GFP-HRS (YYFF) vectors.

Finally, PCR was used to add FRT sites to the APEX2 tagged HRS constructs from pcEXP221-APEX2-HRS and pcEXP221-APEX2-YYFF vectors, along with a cytosolic version of the enzyme from pcDNA3-APEX2-NES, to generate Flp-In compatible vectors. Examples of the PCR reactions and temperature cycles used are shown in tables 2.2 and 2.3 respectively.

	FFYVE	***Control***	
Water	Up to 38.5µl	38.5µl	
Plasmid	-µl	0µl	(50ng)
pfu buffer	5µl	5µl	
Primer 1	2.5µl	2.5µl	(0.5µM)
Primer 2	2.5µl	2.5µl	
dNTPs	0.5µl	0.5µl	
HS pfu ultra	1µl	1µl	
Total	50µl	50µl	

Table 2.2 Example PCR reaction setup

Stage	***No. Cycles***	***Temp***	***Duration***
1	1	95	2 mins
2	30	95	30 sec
		55	30 sec
		68	1 min/kb
3	1	68	10 mins

Table 2.3 Example PCR temperature cycles

2.2.3. TOPO cloning

TOPO Blunt-end cloning was used to generate sub-cloning vector intermediates for many of the DNA fragments that had been amplified by PCR. The blunt-end ligation is catalysed by the topoisomerase I enzyme, which is covalently ligated to a phosphate group at each end of a linearized PCR4®Blunt-TOPO vector. After PCR amplification, the PCR fragments were resolved on an agarose gel and visualised under UV light. The DNA band was then cut out from the gel and eluted using a Qiagen Gel Extraction kit. The eluted PCR product was ligated with the PCR4®Blunt-TOPO vector for 5 minutes at room temperature. Resulting cloning vectors were transformed into TOP10 cells as described in section 2.2.8.

2.2.4. Quick ligation

Quick ligation was used for the ligation of DNA fragments generated from RE digestion. These DNA fragments were then resolved in an agarose gel and visualised by UV. Bands corresponding to the correct fragment size would be cut out and eluted in the same manner described in the above section. The eluted DNA fragments were ligated at room temperature for 5 minutes. The ligated vectors were used to transform DH5α competent cells as described in section 2.2.8.

2.2.5. Gateway cloning

Gateway cloning was performed according to the manufacturer's instructions. Briefly, wild type and mutant HRS were flanked by attB sites using PCR as described in section 2.2.2. This PCR product was combined with 150ng of pDONR vector in a 1:1 ratio. The solution was made up to 8µl with TE buffer before 2µl of Gateway® BP Clonase® II enzyme mix was added to the mixture. The reaction was incubated at 25°C for 1 hour. 2µg of Proteinase K was added and the mixture was incubated for a further 10 minutes at 37°C. The reaction was then used to transform DH5α as described in section 2.2.8. This recombination reaction resulted in the generation of pENTR vectors containing

the wild type and mutant HRS sequences. These vectors were then used with the APEX2 destination vector to generate the final expression vectors. pENTR vectors were mixed with 150ng of the destination vector in a 1:1 ratio and made up to 8µl with TE buffer. 2µl of Gateway® LR Clonase® II enzyme mix was added to the mixture. The reaction was incubated for 1 hour at 25°C. 2µg of proteinase K was added and the mixture was incubated for a further 10 minutes at 37°C. DH5α bacterial cells were transformed with the LR reaction mixture as described in section 2.2.8.

2.2.6. Restriction endonuclease (RE) digestion

Generally, 500ng of DNA was used for test digests and 4-5µg was used when generating DNA fragments for cloning. Reaction mixtures were incubated for 1-4 hours at the optimal temperature dictated by the RE used, typically this was 37°C.

2.2.7. Agarose gel electrophoresis

Electrophoresis grade agarose powder was added to TAE buffer (40mM Tris-acetate, 1mM Na_2-EDTA) and heated in a microwave until the agarose was completely dissolved. Prepared agarose gels were typically 0.8-1.0% agarose (w/v). Ethidium Bromide (EtBr) was then added to a final concentration of 0.5µg/ml to allow for visualisation by UV light. The agarose was then poured and allowed to cool at room temperature. Samples were mixed with 6x sample buffer and loaded alongside 100bp or 1kb ladders. DNA gels were resolved in a horizontal midi electrophoresis tank (Fisher Scientific, Loughborough, UK) using TAE buffer. Gels were typically run for 40-60 minutes at 120V.

2.2.8. Bacteria transformation

Bacterial transformations were performed using either DH5α or TOP10 cells, unless otherwise stated. For each transformation, 50µl of bacteria was thawed on ice before having 2-3µl of DNA from a ligation reaction mixture added to the cells. The bacteria

were then heat shocked by incubation on ice for 20 minutes, 1-minute incubation in a water bath at 42°C, followed by a further 2 minutes on ice. 200µl of S.O.C. medium was then added and the bacteria were incubated at 225 rpm and 37°C for 1 hour. The bacterial culture was then spread onto LB agar plates with the appropriate antibiotic (Ampicillin: 100mg/ml or Kanamycin: 10mg/ml) and incubated at 37°C for overnight.

Between 4-6 colonies were selected per transformation. Each colony would be used to inoculate 5ml of LB broth with the appropriate antibiotic (Ampicillin: 100mg/ml or Kanamycin: 10mg/ml) and incubated for 16-18 hours at 37°C and 225rpm. DNA was then purified from the overnight bacterial culture using a Qiagen Miniprep kit, and tested using RE digestion. Positive colonies were further expanded in 150ml of LB broth with the appropriate antibiotic and incubated at 37°C and 225rpm for 16-18 hours. DNA was then purified using either a Qiagen Midiprep or Maxiprep kit. The purified DNA was then sent for sequencing at the DNA Sequencing Service (University of Dundee, UK). A glycerol stock was also made at this point, as described in the following section.

2.2.9. Glycerol stock

5ml of overnight bacterial culture was centrifuged at 3000g for 5 minutes. After discarding the supernatant, the pellet was re-suspended in 2ml of 40% glycerol in LB broth and stored at -80°C.

2.2.10. Nanotrap purification

Rosetta cells were transformed with the vector containing the GFP-nanotrap sequence as described in section 2.2.8. 5ml bacterial cultures were added to 500ml LB broth with the appropriate antibiotic and were incubated at 37°C and 225rpm for 2 hours. Samples were removed from the broth, and the OD_{600} was measured. If the measurement was below 0.6, the bacterial broth was returned to the incubator and re-measured every 30 minutes until the OD_{600} reached between 0.6 and 0.8. 1mM

IPTG was added to the broth and incubated for a further 4 hours at 225rpm and 37°C to induce protein expression. The broth was then centrifuged for 15 minutes at 3000g. The Supernatant was removed and the remaining pellet was flash frozen in liquid nitrogen and stored at -20°C until ready to be lysed.

Frozen pellets were thawed on ice. The bacteria were then lysed on ice in a lysis solution [5mM imidazole in IMAC buffer (20mM Tris pH 8, 300mM NaCl) supplemented with 0.5mg/ml lysozyme and DNAase] and sonicated on full speed for 5 x 20 seconds. The lysates were then ultra-centrifuged at 100,000g for 20 minutes. The supernatant was collected for further purification. The GFP-nanotrap was purified by affinity chromatography using a HisTrap column and increasing concentrations of imidazole to elute His-tagged proteins from the column. The eluate was collected in 1 ml fractions and analysed by SDS-PAGE. The purified GFP-nanotrap was then dialysed overnight in 3,500 MWCO dialysis tubing and dialysis buffer (25mM HEPES pH7.2, 150mM NaCl, 0.5mM DTT). The purified protein was flash frozen in liquid nitrogen and stored at -80°C. The nanobody was conjugated to sepharose beads according to manufactures instructions.

2.2.11. Generation of Flp-In stable cell lines

FRT-containing PCR product of APEX2-HRS, APEX2-YYFF and APEX2-NES were cloned into a pEF5/FRT/V5 TOPO vector to generate pEF5/FRT/V5-TOPO-APEX2-NES, pEF5/FRT/V5-TOPO-APEX2-HRS and pEF5/FRT/V5-TOPO-APEX2-YYFF Flp-In compatible vectors. These vectors were transfected into HeLa S3 Flp-In host cells along with pOG44 plasmid, to express the Flp recombinase in a 9:1 ratio. Expressing cells were selected and maintained using 150µg/ml Hygromycin B.

2.2.12. Generation of FRET biosensor expressing cell lines

HEK293 cells were transfected with pcDNA3.1-AKAR4-NES, pcDNA3.1-AKAR4-FF-NES, pcDNA3.1-ICUE4 and pcDNA3.1-ICUE4-FF constructs as described in section 2.1.3. 24

hours after transfection, the cells were treated with G418 (0.4mg/ml) antibiotic. They were maintained in the antibiotic for approximately two weeks, with the media exchanged every 3-4 days. Once single colonies were visible, they were individually picked into separate wells of a 24-well plate. The cells were maintained in antibiotic media.

2.3. Imaging

2.3.1. Materials and Reagents

For Live-cell imaging, µ-Dish 35mm (#81156) was purchased from Thistle scientific (Glasgow, UK). Hank's balanced salt solution (HBSS) (#14065-049) and HEPES (#15630-056) were purchased form Life technologies. 4',6-diamidino-2-phenylindole (DAPI) stain (#D1306) was bought from Invitrogen (Paisley, UK). Mowiol (#475904) was purchased from Merck Millipore. Glutaraldehyde (#AGR1020), Osmium (OsO_4) (#75632), 200 mesh copper grids (#AGG2450C) and pioloform (#AGR1275) were all purchased from Agar Scientific (Essex, UK). Uranyl acetate (UA) (#U007), Lead citrate (#L018) and resin (#T031) were from TAAB Laboratory equipment (Berkshire, UK). The dEYEmond Ultra 3mm 45° diamond knife (#A2013213) was bought from Scimed GmbH (Germany). 3,3'-Diaminobenzidine (DAB) (#D5905), Ethanol (#270741), Chloroform (#288306) and hydrogen peroxide (H_2O_2) (#H1009) were all purchased from Sigma-Aldrich (Dorset, UK). All solutions were made up in PBS unless otherwise stated.

2.3.2. Immunofluorescence staining (IF)

For immunofluorescence, cells were cultured on glass coverslips. The coverslips were washed twice with room temperature PBS, before being fixed in 4% paraformaldehyde (PFA) for 10 minutes. The coverslips were washed twice in PBS again and quenched by a 20-minute incubation in 50mM ammonium chloride (NH_4Cl). The cells were then

permeabilised with 0.2% Triton-X 100 in PBS for 4 minutes before being blocked in 10% goat serum for 30 minutes. The coverslips were then incubated in primary antibody in 5% goat serum for 20 minutes, and then washed in PBS three times for 5 minutes. The secondary antibody in 5% goat serum was then incubated with the coverslips for 20 minutes, followed by another three washes in PBS for 5 minutes. The coverslips were then rinsed in water and mounted onto Mowiol with or without the addition of 4',6-diamidino-2-phenylindole (DAPI) stain. All IF images were taken on either a Ziess scanning line or a 3i Marianas spinning disk confocal microscope, using a x63 objectives (Ziess). A summary of the antibodies used for immunofluorescence are shown in tables 2.4 and 2.5.

Target	Species	Source/Catalog No.	Incubation conditions
EEA-1	mouse	BD Transduction (#610456)	PFA, 1:500, 5% GS, 20 mins
HRS	rabbit	Home made (Sachse, Urbé et al. 2002)	PFA, 1:1000, 3% BSA, 2 hrs
Flag	mouse	Sigma (#F1804)	PFA, 1:1000, 3% BSA, 2 hrs

Table 2.4 Summary of the primary antibodies used for immunofluorescence

Sceondary antibody	Source/Catalog No.	Incubation conditions
Donkey anti-mouse AF350	Invitrogen (#A10035)	1:1000, 5% GS, 20 mins, RT
Donkey anti-rabbit AF350	Invitrogen (#A10039)	1:1000, 5% GS, 20 mins, RT
Donkey anti-rabbit AF488	Invitrogen (#A21206)	1:1000, 5% GS, 20 mins, RT
Donkey anti-rabbit AF594	Invitrogen (#A21207)	1:1000, 5% GS, 20 mins, RT
Donkey anti-mouse AF488	Invitrogen (#A21202)	1:1000, 5% GS, 20 mins, RT
Donkey anti-mouse AF594	Invitrogen (#A21203)	1:1000, 5% GS, 20 mins, RT

Table 2.5 Summary of the secondary antibodies used for immunofluorescence

2.3.3. Live-cell imaging

Live cell experiments were performed with a 3i Marianas spinning disk confocal microscope (3i intelligent imaging innovations, Germany) or a Ziess scanning line

confocal microscope where indicated. Cells were imaged in a humidified chamber at 37°C and 5% CO_2, unless otherwise stated. All cells were seeded in 35mm Ibidi dishes for imaging on both the spinning disk and scanning line confocal microscopes. Images were taken with a x63 objective (Ziess). Endosome numbers were counted using the Trackmate plug-in on ImageJ. Fluorescent intensities of endosomes were analysed using the slidebook6 software (3i).

2.3.4. FRET imaging

Cells were maintained in Hank's balanced salt solution and buffered using 25mM HEPES. Cells were imaged in a CO_2-independent, humidified chamber at 37°C. Cells were treated with Forskolin, IBMX, isoproterenol, Dyngo, and EGF as indicated by the respective figure legends and section 2.1.4. Images were all taken on a 3i Marianas spinning disk confocal microscope. For each image, three channels were captured denoted 'Donor' (447-517nm detection range, 445nm excitation), 'Acceptor' (515-569 detection range, 514nnm excitation) and 'Transfer' (515-569nm detection range, 445nm excitation) channels. For the FRET experiments, three fields of view were taken to generate an average for each biological repeat. The images were then analysed using the Slidebook 6 software (3i). For endosomal FRET sensor cell lines, a laplacian filter was applied to the acceptor channel, in order to generate an endosomal mask for analysis. The intensities were measured and background and bleed through corrected. FRET was calculated from the intensities using the following equation:

$$FRET = \frac{I_{Transfer} - \left(I_{Transfer(CFP-only)} \Big/ I_{Donor(CFP-only)} \; X \; I_{Donor}\right)}{I_{Donor}}$$

'I' represents intensity for the indicated channel (Miyawaki, Llopis et al. 1997). Bleed through correction factor calculated from cells expressing CFP-only versions of each biosensor.

2.3.5. Electron Microscopy (EM)

HeLa S3 Flp-In APEX2-HRS cells were fixed in 2.5% glutaraldehyde in 0.1M PB buffer pH7.4 for a total 2 minutes in a PELCO BioWave Pro (Ted Pella, USA) at 100W and 20Hg chamber pressure. The cells were then incubated in 1mg/ml DAB and 10mM H_2O_2 for 30 minutes at room temperature. The cells were then washed in 1M Cacodylate buffer and stained using 1% OsO_4 for a total of one minute in a PELCO BioWave Pro at 100W and 20Hg chamber pressure. The cells were further stained in 1% UA at 4°C overnight. The samples were dehydrated in increasing concentrations of ethanol before being embedded in TAAB medium resin and cured at 60°C for 48 hours. Thin sections (60-70nm) were cut with a Leica UC6 ultramicrotome using a dEYEmond Ultra 3mm 45° diamond knife, relaxed using chloroform and mounted on 200 mesh copper grids that had been coated with 0.3% pioloform in chloroform. Samples were post stained with lead citrate and 2% UA. Images were taken using a FEI 120kV tecnai G2 Spirit BioTwin transmission electron microscope (TEM) and AnaySIS software (Olympus, Germany).

2.4. Protein biochemistry

2.4.1. Reagents

Ponceau-S stain (#P7170), Hydrogen peroxide (H_2O_2) (#H1009), (±)-6-Hydroxy-2,5,7,8-tetramethylchromane-2-carboxylic acid (Trolox) (#238813), Ascorbic acid (#A-7631) and mammalian protease inhibitor (MPI) (#P8340) were all purchased from Sigma-Aldrich (Dorset, UK). PhosSTOP Phosphatase inhibitor cocktail tablets (#4906845001) were purchased from Roche (Sussex, UK). Marvel skimmed milk powder was obtained from Premier Brands, UK. Pierce 660-nm protein assay reagent (#22662) and Streptavidin magnetic beads (#88817) were bought from Life technologies (Paisley, UK). NHS-activated Sepharose 4 Fast Flow beads (#17-0906-01), Amersham ECL full range rainbow marker (#RPN800E) and Amersham Protran 0.45µm nitrocellulose membrane (#10600002) were purchased from GE healthcare (Buckinghamshire, UK).

Biotin-phenol (#LS-3500-0250) was from Iris Biotech GMBH and Sodium Azide (#AA14314-22) was from VWR (Leicestershire, UK). NuPAGE Bis-Tris 4-12% gels (1.5mm 10-well: #NP0303BOX, 1mm 20-well: #W61402A), NuPAGE MOPS (#NP0001-02) and NuPAGE MES (#NP0002-02) buffers were all obtained from Invitrogen (Paisley, UK). A summary of the antibodies used are shown in tables 2.4 and 2.5.

2.4.2. Cell lysis

Near confluent cells were washed three times on ice with PBS that had been chilled to 4°C. The cells were then lysed for 10 minutes on ice, using either nonidet P-40 (NP-40) lysis buffer (0.5% NP-40, 25mM Tris pH 7.5, 100mM NaCl, 50mM NaF) or RIPA lysis buffer (10mM Tris pH 7.5, 150mM NaCl, 1% Triton-X 100, 0.1% SDS, 1% sodium deoxycholate). Both NP-40 and RIPA buffer were supplemented with mammalian protease inhibitor cocktail (MPI). For experiments looking at phosphorylation, a phosphatase inhibitor was also added to the lysis buffer. Lysates were then centrifuged at 14,000g for 10 minutes, with the supernatant being collected. Samples were then stored at -20°C.

2.4.3. Protein assay

The protein concentration of cell lysates was measured using the Pierce 660-nm protein assay reagent. Protein assays were carried out as per the manufactures instructions. 125µg-2,000µg protein standards were used to establish a standard curve. For very concentrated samples, the lysate used for the protein assay was diluted 1:2. After a 5-minute incubation at room temperature, samples were read at OD_{660}.

2.4.4. Proximity labelling

For proximity labelling, the APEX2 peroxidase enzyme was used in order to tag nearby proteins with Biotin-phenol in the presence of H_2O_2 (Hung, Udeshi et al. 2016). When cells were ready to harvest, the cell medium was exchanged for fresh full medium

containing 500µM Biotin-phenol and incubated for 30 minutes at 37°C. Unless otherwise stated, labelling would be initiated by a 1-minute incubation of 1mM H_2O_2 at room temperature. Immediately afterwards, cells were placed on ice and washed three times with ice cold quenching solution (PBS supplemented with 10mM sodium ascorbate, 5mM Trolox and 10mM sodium azide). The cells were then lysed using NP-40 lysis buffer supplemented with MPI, 1mM PMSF and quenchers (10mM sodium ascorbate, 5mM Trolox and 10mM sodium azide).

2.4.5. Immunoprecipitation (IP)

Immunoprecipitation with GFP-nanotrap cross-linked to sepharose beads was performed immediately after cell lysis to avoid losing potential interactions from freeze-thaw cycles. Prior to immunoprecipitation, GFP-nanotrap sepharose beads were pre-washed in whichever lysis buffer was used to generate the cell lysates. With the exception of titration experiments, the sepharose beads were added to lysate samples in a ratio of 400µg protein sample per 10µl of beads. For Mass spectrometry experiments, 3-4mg of lysate was typically used per condition. Lysate samples were incubated on a rotating wheel at 4°C for 30 minutes. The beads were centrifuged at 1000g for 1 minute at 4°C and washed three times with YP-IP buffer (0.1% NP-40, 25mM Tris pH 7.5, 150mM NaCl) and once with 10mM Tris/HCl, pH7.5. The final pellet was then re-suspended in 1.5x SDS-PAGE sample buffer to elute the proteins bound to the beads.

For biotin IPs, streptavidin magnetic beads were pre-washed in the same lysis buffer used to generate lysates. Unless otherwise stated, the beads were added to lysate samples in a ratio of 360µg of protein lysate for 30µl of magnetic beads. For Mass spectrometry experiments, 2-3mg of lysate was typically used per condition, which are combined prior to the streptavidin pulldown. Lysates were incubated on a rotating wheel at room temperature for 1 hour. The beads were then pelleted on a magnetic rack for 1 minute. For each wash step, the wash buffer was added to the beads, the tubes were vortexed and incubated for 1 minute before being pelleted again on the

magnetic rack. The beads were washed twice with RIPA buffer, once with 1M KCl, once with 0.1M Na_2CO_3, once with 8M Urea in 10mM Tris-HCl pH 8.0 and finally twice again with RIPA buffer. The proteins were eluted from the beads with 3x sample buffer, 2mM biotin and 20mM DTT for 10 minutes at 98°C.

2.4.6. Sodium dodecyl sulphate polyacrylamide gel electrophoresis (SDS-PAGE)

Proteins were resolved by SDS-PAGE using precast NUPAGE 4-12% Bis-Tris gels. Prior to loading, protein samples were standardised to the same concentration and mixed with 5x sample buffer and heated to 98°C for 10 minutes. In general, 20µg of boiled protein samples were loaded in each well, depending on the abundance of the protein of interest. For IP's all of the eluted protein sample would be loaded for each condition. Rainbow protein ladder would be loaded alongside protein samples. Protein separation was typically performed at 200V for 55-60 minutes in MOPS running buffer, for small molecular weight proteins, MES running buffer would be used instead.

2.4.7. Western blotting

For Western blotting, proteins were transferred from polyacrylamide gels onto 0.45µm Protran nitrocellulose membranes. This was performed in transfer buffer (200ml ethanol, 800ml water, 14.4g Glycine and 3.03g Tris) ran at a constant current of 0.9A and 24V for 1 hour in a genie blotter. After being transferred, the nitrocellulose membrane was stained with Ponceau-S stain to check the transfer efficiency, equal loading of wells and DNA contamination. The Ponceau-S stain was washed off with either PBS or TBS before being blocked in 5% Marvel milk powder in either PBS or TBS containing 0.1% tween-20 (w/v) (PBS-T or TBS-T), unless otherwise stated, at room temperature for 1 hour. The membrane was then incubated in primary antibody according to the conditions described in table 2.6. Unused primary antibody was removed by three 5-minute washes in PBS-T or TBS-T, followed by incubation with IRDye conjugate-secondary antibodies (LI-COR Biosciences) for 1 hour. The

membranes were washed as above and visualised on a LI-COR Odessey imaging system. A summary of the antibodies used are shown in tables 2.6 and 2.7.

Target	Species	Source/Catalog No.	Incubation conditions
EEA-1	Mouse	BD Transduction (#610456)	1:1000, 5% milk in PBS-T, o/n, 4°C
EEA-1	Rabbit	Home made (MILLS, JONES et al. 1998)	1:1000, 5% milk in PBS-T, o/n, 4°C
HRS	Goat	Everest Biotech (#EB07211)	1:2000, 5% milk in PBS-T, o/n, 4°C
STAM2	Rabbit	Home made (Row, Clague et al. 2005)	1:1000, 5% milk in PBS-T, o/n, 4°C
PY334-HRS	Rabbit	Home made (Urbé, Sachse et al. 2003)	1:1000, 5% milk in TBS-T, o/n, 4°C, (blocked 5% BSA in TBS-T)
Actin	Rabbit	Sigma (#A2266)	1:10,000, 5% milk in PBS-T, 1 hr, RT
Actin	Mouse	Abcam (#Ab6276)	1:10,000, 5% milk in PBS-T, 1 hr, RT
GFP	Sheep	Home made (Prior, Harding et al. 2001)	1:5000, 5% milk in PBS-T, 1 hr, RT
Flag	Rabbit	Sigma (#F4725)	1:1000, 5% milk in PBS-T, o/n, 4°C

Table 2.6 Summary of the primary antibodies used for western blotting

Sceondary antibody	Source/Catalog No.	Incubation conditions
Donkey anti-mouse IRDye 800CW	LICOR (#926-32212)	1:10,000, 5% milk in PBS-T, 1h, RT
Donkey anti-mouse IRDye 680CW	LICOR (#926-32222)	1:10,000, 5% milk in PBS-T, 1h, RT
Donkey anti-rabbit IRDye 800CW	LICOR (#926-32213)	1:10,000, 5% milk in PBS-T, 1h, RT
Donkey anti-rabbit IRDye 680CW	LICOR (#926-32223)	1:10,000, 5% milk in PBS-T, 1h, RT
Donkey anti-sheep IRDye 800CW	LICOR (#926-32214)	1:10,000, 5% milk in PBS-T, 1h, RT
Donkey anti-sheep IRDye 680CW	LICOR (#926-32224)	1:10,000, 5% milk in PBS-T, 1h, RT

Table 2.7 Summary of the secondary antibodies used for western blotting

2.5. Mass spectrometry (MS)

2.5.1. Reagents

L-Lysine and L-Arginine free DMEM (#D633) were purchased from DC biosciences and the FBS (#FB-1001D/500) was from Biosera (France). All amino acids used for SILAC labelled media (Lys, #L8662; Arg, #A-8094; Pro, #P5607; Lys4, #616192; Arg6, #643440; Lys8, #608041; Arg10, #609033) and Iodoacetamide (IAA) (#T-6125) were purchased from Sigma-Aldrich, (Dorset, UK). Dithiothreitol (DTT) (#MB1015) was purchased from Melford biolaboratories (Suffolk, UK). Coomassie stain (#46-5034) was obtained from Invitrogen. LoBind Eppendorf tubes (#022431081) are from Eppendorf (Hamburg, Germany). HPLC grade water (#23595328), HPLC grade formic acid (#20318.297) and HPLC grade acetonitrile (ACN) (#20060320) were all bought from VWR (Leicestershire, UK). Mass spectrometry grade Trypsin Gold (#V5280) was purchased from Promega (WI, USA).

2.5.2. Stable isotope labelling by amino acids in cell culture (SILAC)

HeLa S3 Flp-In cell lines were cultured in either 'Light', 'Medium' or 'Heavy' SILAC medium for at least two weeks (6 passages) prior to experimentation to ensure optimal isotope labelling. SILAC medium was made up of DMEM supplemented with 10% dialysed FBS and amino acids to generate the 'Light', 'Medium' or 'Heavy' labelling. These amino acids are: 'Light' (L-Lysine, Lys-0; L-Arginine, Arg-0; L-Proline, Pro-0), 'Medium' (L-Lysine-$^{2}H_4$, Lys-4; L-Arginine-$^{13}C_6$, Arg-6; L-Proline, Pro-0) and 'Heavy' (L-Lysine-$^{2}H_6$-$^{15}N_2$, Lys-8; L-Arginine-$^{13}C_6$-$^{15}N_2$, Arg-10; L-Proline, Pro-0).

2.5.3. In-gel digest

Lysates were prepared as indicated in the relevant chapter, according to the methods outlined in sections 2.4.2, 2.4.3, 2.4.4 and 2.4.5. Protein samples were run on a NUPAGE 4-12% gel, as described in section 2.4.6. The gel was then fixed and stained

by using a coomassie stain as per the manufactures instructions. The gel was washed in water overnight to remove the excess stain. The loaded lane was then cut into bands and diced into small pieces using a stainless steel blade. The gel pieces were then transferred to LoBind Eppendorf tubes and de-stained using a solution of 50mM ammonium bicarbonate and 50% acetonitrile (ACN) for 10 minutes at 37°C. The de-staining step was repeated until all the stain was removed from the gel pieces. The gel pieces were then dehydrated in 100% ACN for 5 minutes. The supernatant was discarded and the gel pieces were placed in a speed vacuum for a further 5 minutes. 10mM DTT in 100mM ammonium bicarbonate was added to the gel pieces in order to reduce the protein samples. The gel pieces were incubated at 56°C for 1 hour, followed by a 30-minute incubation in 50mM iodoacetamide in 100mM ammonium bicarbonate at room temperature. Band pieces were then washed with 100mM ammonium bicarbonate for 15 minutes, before being dehydrated again with 100% ACN for 5 minutes and 5 minutes in a speed vacuum. The proteins within the gel pieces were digested by incubation with trypsin diluted in 40mM ammonium bicarbonate and 9% ACN at 37°C for 16 hours, at a trypsin: protein ratio of 1:25.

2.5.4. Peptide extraction

Once the trypsin digestion has been completed, an equal volume of ACN was added to each tube and incubated at 30°C for 30 minutes. The supernatant of each tube was then transferred to a fresh LoBind Eppendorf tube. The gel pieces were then incubated for 20 minutes in 1% formic acid. The supernatant was transferred to the collection tube. The formic acid incubation was repeated once more before 100% ACN was added to the gel pieces for 10 minutes. The supernatant was once again transferred to the collection tube. The collection tubes containing the peptide samples were placed in the speed vacuum until all the liquid had evaporated. Peptide samples were re-suspended in 25µl of 1% formic acid prior to mass spectrometry analysis.

2.5.5. Detection and identification

Peptides were separated using a nanoACQUITY UPLC system (Waters) coupled to a Proxeon nanoelectrospray source and LTQ-Orbitrap XL mass spectrometer (Thermo Fisher). 4µl of each sample was loaded onto a 180µm x 20mm, 5µm C18 symmetry trapping column (Waters) in 0.1% formic acid at 10-15µl/min. Peptides were then resolved on a 25cm x 75µm BEH-C18 column (Waters) on an ACN gradient and a 300nl/min flow rate. Mass spectrometry spectra (m/z 300-2000) were obtained at a resolution of 30,000 and collision energy at 35%, 30ms. The top five ions were subjected to MS/MS in the linear quadrapole ion trap. All spectra were acquired using the Xcalibur software (Thermo Fisher). MS spectra were analysed using MaxQuant (version 1.5.3.8) using default settings, with additional SILAC labelling and biotin variable modification.

Chapter three: Analysis of the HRS interactome in response to growth factor stimulation

The purpose of HRS phosphorylation in response to growth factor stimulation has remained elusive, despite being a topic that has been studied on numerous occasions (Urbé, Mills et al. 2000, Row, Clague et al. 2005, Stern, Visser Smit et al. 2007, Meijer, van Rotterdam et al. 2012). HRS is highly phosphorylated in response to EGF stimulation (Bache, Raiborg et al. 2002, Omerovic, Hammond et al. 2012), but previous work from my laboratory has shown this to have little, to no, effect on EGFR degradation kinetics. One alternative function could be that HRS acts as a signalling adaptor and that phosphorylation of the protein could change the suite of proteins present at the endosome.

Preliminary results from our laboratory investigated this idea by examining the differences in binding partners between GFP-tagged, HRS (WT) and a phosphorylation mutant (YYFF), which has had tyrosine residues 329 and 334 mutated to phenylalanine residues. The approached used stable cell lines generated with the Flp-In system to express the GFP-tagged proteins at near endogenous levels. Previous studies looking into the role of these phosphorylation sites have often used over-expression in their studies, which can lead to misinterpretation. The binding partners were then assessed by performing immunoprecipitation (IP) using a polyclonal anti-GFP antibody with SILAC labelled cells and analysed by mass spectrometry.

This data indicated a collection of hetero-trimeric G-proteins, along with the small GTPase Rac1, binding to HRS, with the G-proteins being enriched in the WT condition compared to the YYFF mutant (Liu, unpublished data). A follow-up experiment using a HRS antibody against the endogenous protein found Rac1 and the same collection of G-proteins enriched in the EGF stimulated condition compared to the starved

condition (Liu, unpublished data), suggesting that these interactions are EGF dependent.

However, inconsistencies exist between the individual repeats of the experiments that needed resolving. It may be possible to improve reproducibility by using a less variable antibody. One alternative, is to use the GFP-nanotrap. This is a 'nanobody' derived from the hypervariable region of a Llama antibody (Rothbauer, Zolghadr et al. 2008, Beghein and Gettemans 2017). Antibodies from *Camelidae* species are comprised of a single amino acid chain, in comparison to the two heavy and two light chains of conventional antibodies. The nanobody is then expressed from a bacterial plasmid enabling it to be purified in large quantities, whilst experiencing less batch-to-batch variation. Furthermore, the GFP-nanotrap has been shown to identify binding partners by proteomic analysis with higher efficiency compared to conventional GFP-antibodies (Galan, Paris et al. 2011).

One of the larger challenges faced with this experiment, is the fact that it is pushing the boundary of the signal-to-noise ratio. This is likely due to the transient nature of the interactions we are trying to identify. Previous studies into the binding partners of HRS have only identified a few strong interactors, namely STAM1/2 and Eps15 (Roxrud, Raiborg et al. 2008, Huttlin, Ting et al. 2015). However, it is known that HRS interacts with many more proteins, for example, through Yeast two hybrid (Y2H) experiments, HRS has been shown to bind to TSG101 (Pornillos, Higginson et al. 2003). HRS also contains a ubiquitin interacting motif and is important for the trafficking of ubiquitylated receptors, yet no receptors have been shown to bind to HRS by traditional IP techniques. It is possible that these potential interacting partners are binding only very weakly, and therefore transiently, to HRS.

APEX2 is the second generation of a modified peroxidase enzyme from the soy bean plant (Martell, Deerinck et al. 2012, Lam, Martell et al. 2015). The APEX2 enzyme is able to create phenoxyl free radicals from Biotin phenol in the presence of H_2O_2 and is used in proximity-labelling of proteins (Hwang and Espenshade 2016). The advantage of using this enzyme over other enzymes used for proximity-labelling, such

as BirA, is that it has a much higher activity level and can label proteins with Biotin within minutes, as opposed to hours with BirA (Mehta and Trinkle-Mulcahy 2016). This allows for greater time resolution and to study changes to interacting partners as a result of an acute treatment. Proximity-labelling should allow for better identification of transiently interacting proteins as these proteins can now be enriched through a direct interaction between the biotin modification and streptavidin conjugated beads (Hung, Udeshi et al. 2016).

3.1. Objectives:

The primary objective of this chapter was to investigate the potential difference in interacting partners between wild type HRS and the tyrosine point mutant under conditions of EGF stimulation, in order to assess the role of phosphorylation at Y329/334. The secondary objective of this chapter was to assess the suitability of proximity-ligation techniques for use with mass spectrometry.

3.2. Results

3.2.1. Purification of GFP-nanotrap antibody

I began by purifying the GFP-nanotrap in order to conjugate the nanobody to sepharose beads. The GFP-nanotrap plasmid was introduced into *E. coli* and induced with IPTG. After the cells were lysed by sonication, the GFP-nanotrap was purified using an imidazole gradient on a His-Trap column. The purification of the nanobody is shown in Figure 3.1. A single large peak is seen on the UV trace (blue line) as the concentration of imidazole increases. The flow-through was collected into 1ml fractions, indicated by the red strokes on Figure 3.1(A). The two larger strokes indicate the fractions taken from the purification. Samples of these fractions were taken for analysis by SDS-PAGE (Figure 3.1(B)).

Samples from every stage of the purification process have been taken to quality control the purification process (Figure 3.1(C)). The +/- IPTG conditions represent the protein abundance in the bacteria before and after induction of the GFP-nanotrap by IPTG. The nanobody is 13KDa in size, which is clearly shown to be induced by IPTG, along with several other large bands. After lysis, the bacterial solution was ultracentrifuged. Samples from both the supernatant and pellet from this step were retained for analysis. This step removes one of the large unspecific bands. A portion of the GFP-nanotrap also appears to be removed at this step. The bound and unbound fractions represent the proteins which were passed through the His-Trap column. The fractions analysed in Figure 3.1(B) are pooled to generate the bound fraction in Figure 3.1(C). The vast majority of the unspecific bands are removed by the His-Trap column, leaving a relatively pure batch of the GFP-nanotrap.

After conjugating the nanobody to sepharose beads, a quality control experiment was performed to optimise the ratio of lysate-to-beads needed to obtain the best results for immunoprecipitation (IP). GFP-HRS expressing HeLa cells were harvested for the IP, with varying amounts of the protein lysate added to 10µl of sepharose beads (Figure 3.1(D)). Similar amounts of GFP-tagged HRS are pulled down across all conditions. In the unbound fraction, increasing amounts of GFP-HRS are seen as the protein amounts increase. Only small amounts can be seen in the unbound fraction of the 100µg and 200µg conditions. The intensity of the 800µg and 1000µg bands are much larger, indicating that the beads are saturated with material. A moderate band can be seen with the 400µg condition and as such, it was decided that this ratio of lysate-to-beads was to be used in future experiments. This condition will ensure that the beads have bound to as much material as possible.

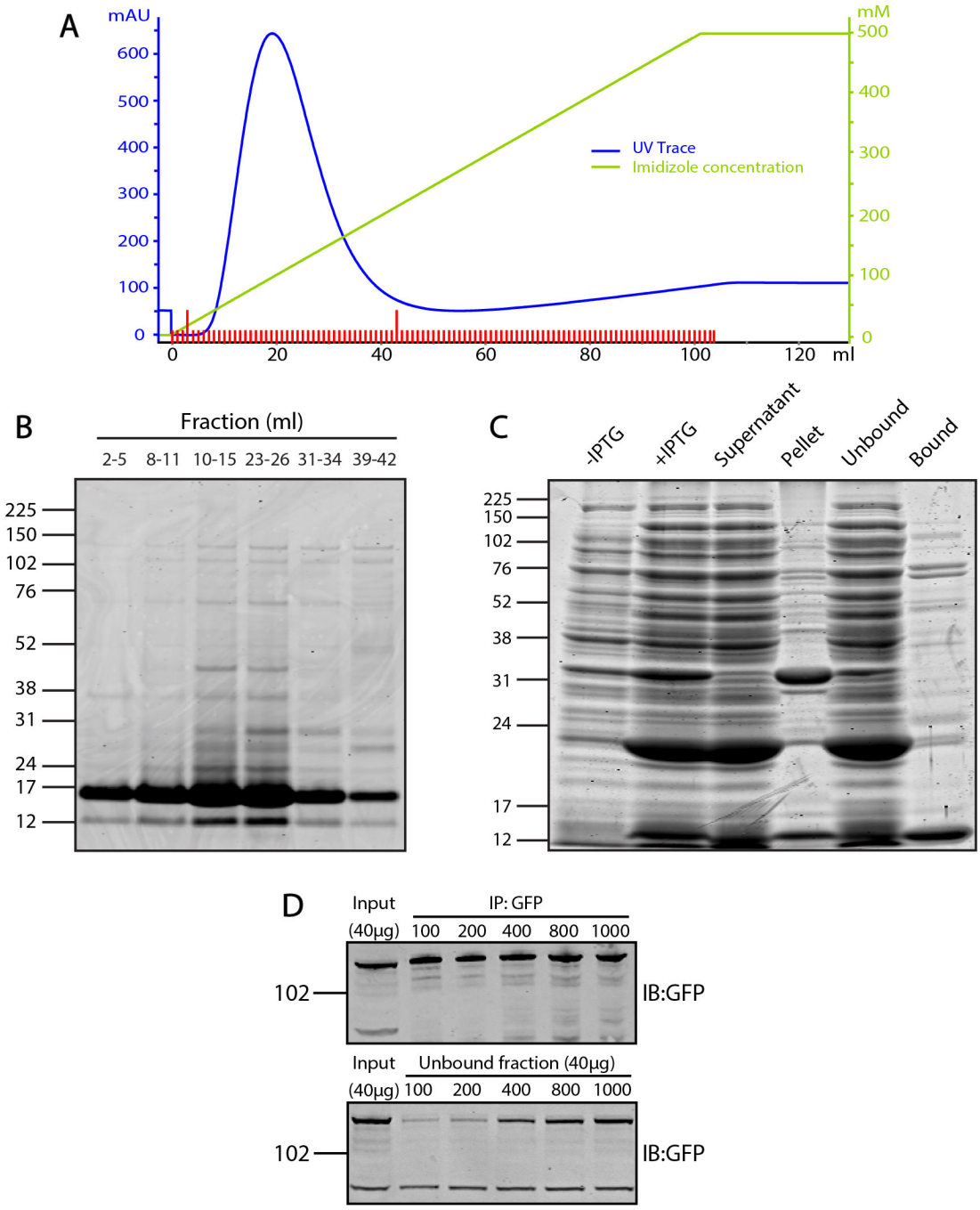

Figure 3.1 Purification of GFP-nanotrap. (A) Affinity chromatography UV trace (blue line) taken during the elution of the GFP-nanotrap off a His-Trap column with increasing concentrations of imidazole (green line). Red ticks represent the collected fractions. **(B)** SDS-PAGE of the fractions indicated by the two larger red ticks in (A). **(C)** SDS-PAGE analysis of samples taken at various points during the purification process. The bound fraction represents the pooling of the fractions in (B). **(D)** GFP-HRS cell line lysate titration for the GFP-nanotrap after conjugation to sepharose beads.

3.2.2. Characterisation of GFP-cell lines

For these experiments, the GFP-tagged cell lines described above were used. These cell lines include a GFP only control and GFP tagged to both the wild type HRS and the phosphorylation mutant YYFF. These cell lines were counter stained with an anti-EEA1 antibody. As shown in Figure 3.2(A), both the wild type and the mutant HRS localise to endosomes that overlap with EEA1 positive endosomes. By immunofluorescence, no defects or differences can be seen in the localisation in the mutant HRS compared to the wild type.

The purpose of using the Flp-In system to generate the GFP cell-lines, was to create isogenic cell lines that express the tagged proteins at equal levels, which are at near endogenous levels. As previously mentioned, over-expression of HRS can lead to a dominant negative phenotype in the normal trafficking and degradation of receptors. The levels of HRS were assessed in all the cell lines by western blotting. The GFP tag on the proteins we have introduced increases their molecular weight and so the endogenous and GFP-tagged proteins can be differentiated by gel electrophoresis. As shown by the blot in Figure 3.2(B), the total levels of HRS in the wild type cell line and the mutant cell line are similar to the levels of HRS in the GFP only control. Expression of the GFP-tagged HRS leads to a reduction in the endogenous HRS levels, with the majority of the total HRS pool in these cell lines made up of the tagged proteins that are being expressed.

Next, the ability of the GFP-tagged HRS proteins to be phosphorylated was assessed. This was achieved by stimulating the cell lines with 20ng/ml of EGF for the indicated time points. Phosphorylation of the residual endogenous HRS can be seen in all the cell lines, with peak phosphorylation occurring at 8 minutes. The signal then diminishes after 30 minutes of stimulation. In addition to the endogenous HRS, phosphorylation to the GFP-tagged HRS can be seen in the wild type cell line but not in the YYFF mutant. As the phospho-antibody is targeted to the tyrosine sites that have been mutated in the mutant cell line, the absence of the phosphorylation bands in the up-shifted position for the mutant cell line was expected (Figure 3.2(C)).

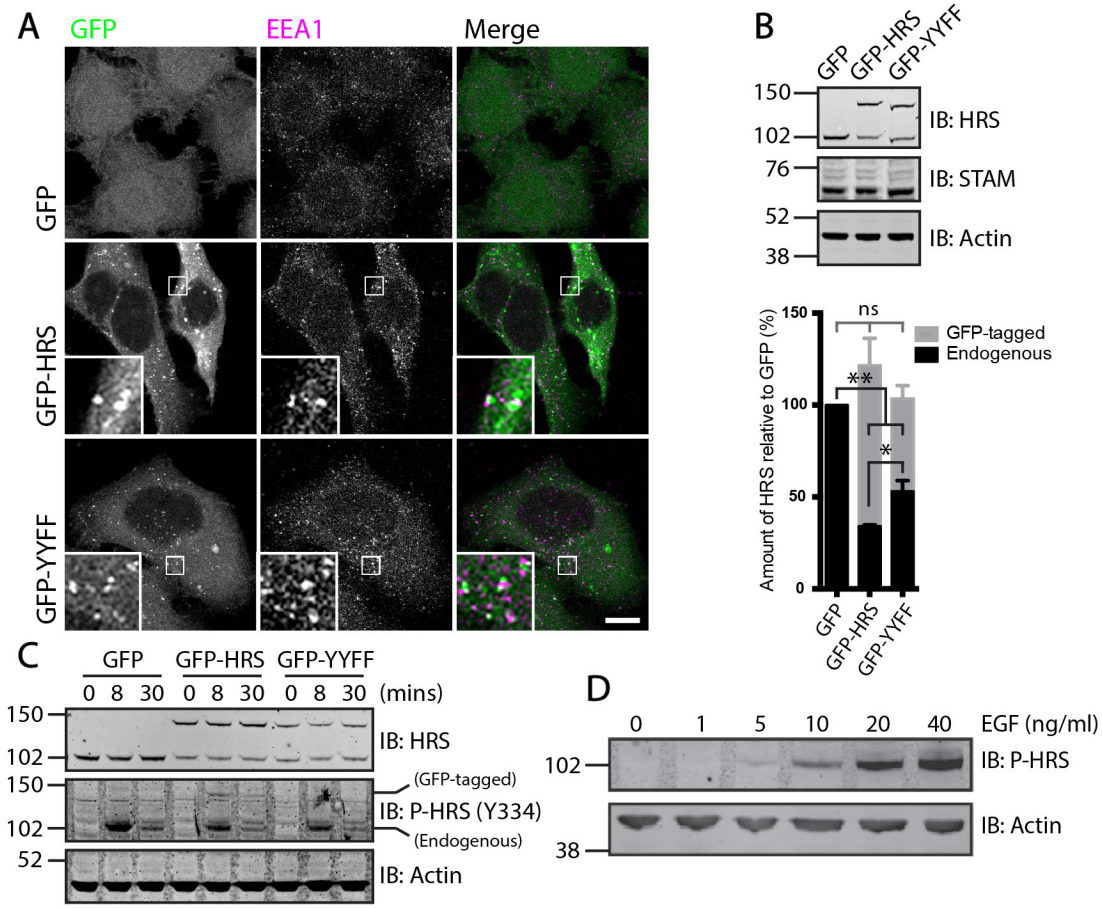

Figure 3.2 GFP-Cell line characterisation and optimisation. (A) HeLa S3 Flp-In cells stably expressing GFP-tagged constructs co-stained with an anti-EEA1 antibody. Scale bar = 10µm **(B)** Western blot assessing the relative levels of GFP-tagged HRS constructs compared to endogenous levels. Values normalised to HRS levels of GFP control. N = 3. Error bars represent standard deviation. One-way ANOVA with Tukey's multiple comparisons test, * $P < 0.01$, ** $P < 0.0001$. **(C&D)** HeLa S3 GFP Flp-In cells were serum starved for 6 hours and then **(C)** stimulated with 20ng/ml EGF for the indicated time periods, or **(D)** stimulated for 8 minutes with the indicated concentration of EGF.

Further optimisation was undertaken for the following experiments. The concentration of EGF was titrated to ensure a high enough concentration was being used to obtain full phosphorylation without over saturating the signalling pathway. The cell lines were stimulated with the indicated concentrations of EGF for 8 minutes and then blotted for with an anti-phospho-HRS antibody. As seen in Figure 3.2(D), peak phosphorylation was seen with 20ng/ml and 40ng/ml concentrations. Although the 40ng/ml condition appeared to exhibit slightly higher levels of phosphorylation than the 20ng/ml condition, the increase was only small and suggests that 40ng/ml would

be an over-saturating concentration of EGF. Hence, for the remaining experiments, 20ng/ml of EGF will be used whenever the cells are stimulated with the growth factor.

3.2.3. GFP cell line mass spectrometry results

To analyse the differences in interacting partners between wild type HRS and mutant HRS, the GFP-tagged cell lines were assessed by mass spectrometry. Each cell line was grown in a separate SILAC media for two weeks, with the GFP only control labelled with 'light' media (Lys 0, Arg 0), the wild type cell line labelled with 'medium' media (Lys 4, Arg 6), and the mutant cell line labelled with 'heavy' media (Lys 8, Arg 10). See section 2.5.2 for more details on the SILAC labelling. After stimulation with 20ng/ml of EGF for 8 minutes, the cell lines were immunoprecipitated (IP) separately using the GFP-nanobody conjugated to sepharose beads. The elutions were then mixed 1:1:1 and process for mass spectrometry (see schematic in Figure 3.3(A)). Cells were serum starved for 6 hours prior to stimulation.

Comparing the wild type cell lines to the GFP control (Figure 3.3(B)), we can see the largest enrichments in the wild type cell line from the GFP IP are: HRS, STAM, STAM2 and the ribosomal protein, RPL14. Apart from these well-established interacting proteins, no other proteins (except RPL14) showed any significant enrichment outside the background signal seen around the baseline. The same can be seen with the mutant cell line, when compared to the GFP only control cells. A handful of proteins are indicated as significantly de-enriched in the mutant cell line, though only to a small degree. These are: an actin-like protein ACTL8, an uncharacterised protein and the proteasome complex subunit PSME1. Both of these de-enrichments can possibly be explained by untagged GFP being more like to interact with these proteins due to its cytosolic localisation.

Assessing this experiment from a technical standpoint, we have to conclude that it was successful. HRS and STAM give the experiment an internal control. These proteins interact together strongly and are well established. Since these proteins are enriched in both the wild type and mutant cell lines, the results cannot be discounted as a

mistake in performing the experiment. The proteins identified in this experiment to be significantly altered between conditions appear to be of little biological relevance in the context HRS function.

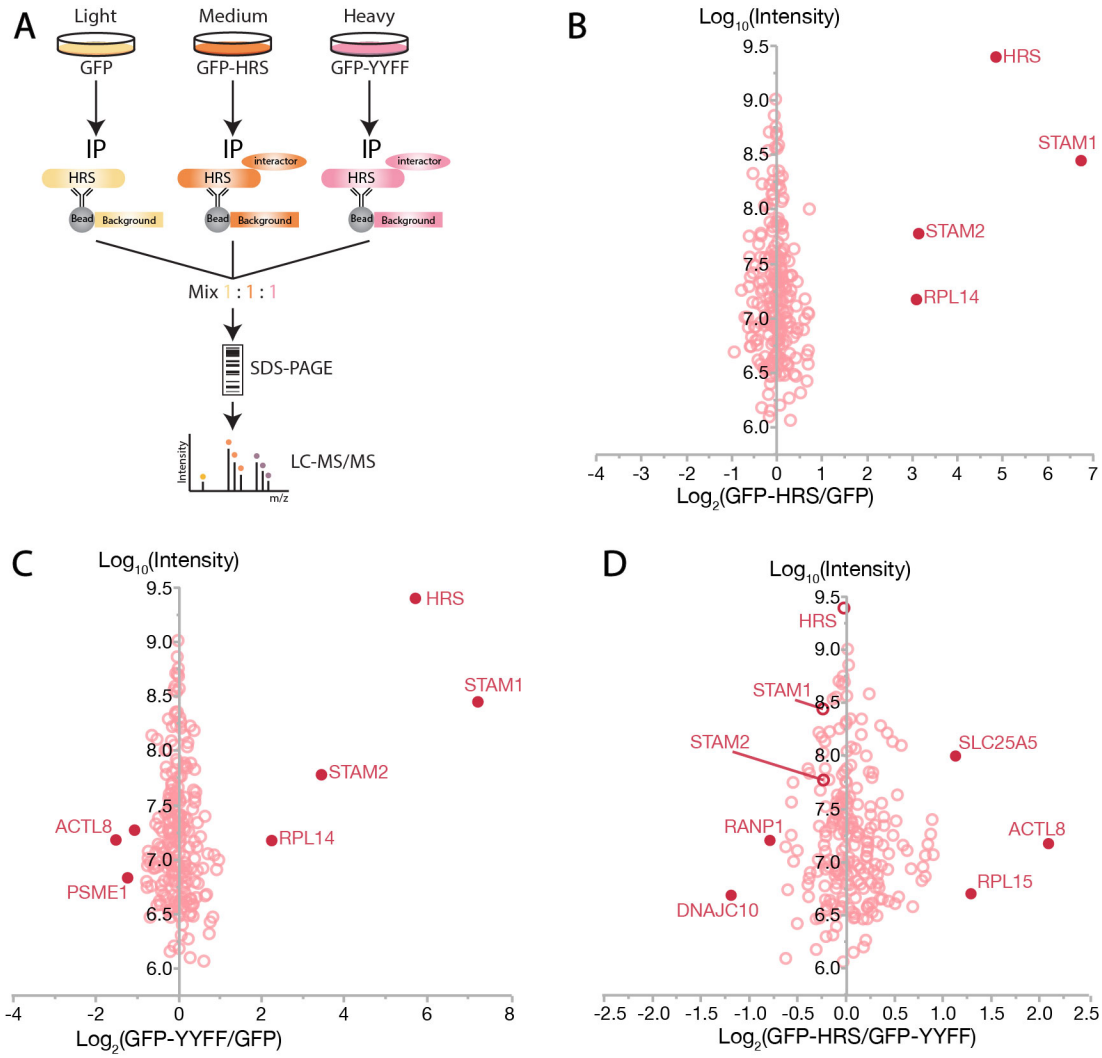

Figure 3.3 GFP-HRS interactome in EGF stimulated HeLa S3 Flp-In cells. (A) Workflow of the SILAC experiment using the stable GFP cell lines. In gel digest was carried out on the samples prior to analysis with LC-MS/MS. Log_2 transformed ratios plotted against Log_{10} transformed intensities for **(B)** GFP-HRS versus GFP, **(C)** GFP-YYFF versus GFP and **(D)** GFP-HRS versus GFP-YYFF. Filled circles represent proteins which show significant ratio changes. Significance B, false discovery rate (FDR) < 0.05.

The results described above suggest that any potential interaction with the G-proteins would be very weak and transient. It may be that these interactions are too transient to be reliably detected by traditional IP techniques. As a result, proximity-ligation

techniques were employed to attempt to detect these transient interactions. Out of the various methods for proximity-ligation, the APEX2 enzyme was chosen over the promiscuous BirA enzyme used in the BioID system. The reason for this is because the APEX2 enzyme allows for greater time resolution than BioID, since APEX2 has been shown to tag proteins with biotin within minutes, as opposed to hours with the BirA enzyme (Trinkle-Mulcahy 2019).

Further to this, a tool has been developed that combines the APEX enzyme with the GFP-nanotrap for faster screening of any GFP-tagged protein by electron microscopy (Ariotti, Hall et al. 2015). We aimed to assess whether this technique can be used for the detection of protein-protein interactions via mass spectrometry. Using the same GFP-tagged cell lines as used above, the APEX2-nanotrap was transfected into each cell line (Figure 3.4). The nanobody portion of the construct should direct the APEX2 enzyme to the GFP-tagged proteins.

Using this system for these experiments also offers another benefit over the traditional IP methodology. As labelling with biotin occurs prior to cell lysis, the samples can be combined prior to biotin-streptavidin IP (Figure 3.4(C)). This will reduce the variation that may be introduced between samples when they are immunoprecipitated separately. The Biotin-streptavidin bond is a very strong and therefore allows for much harsher washes to be used as well.

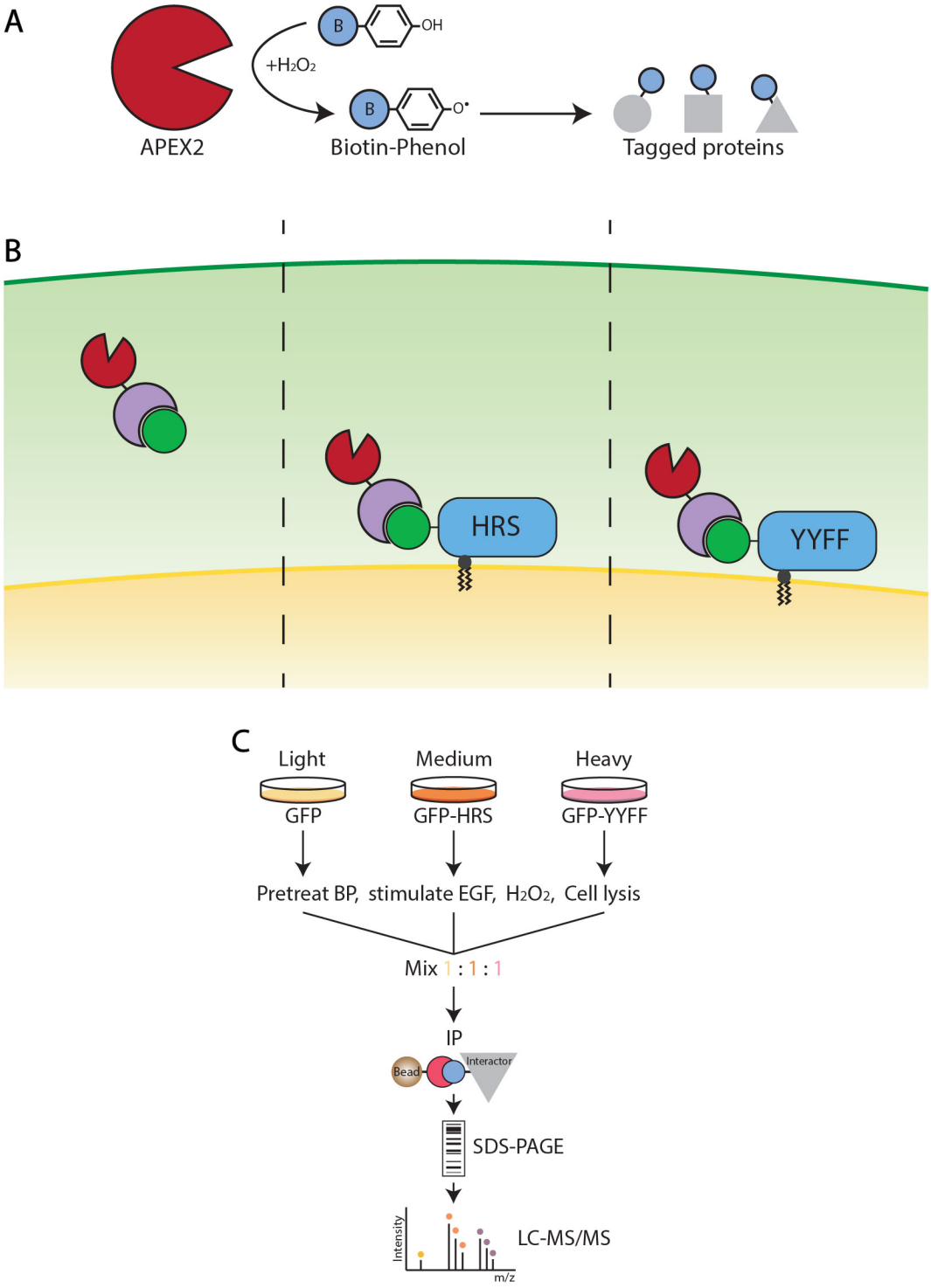

Figure 3.4 Schematic diagram of the experimental setup for using APEX2-nanotrap. **(A)** Simplified mechanism of how the APEX2 enzyme tags nearby proteins with biotin phenol in the presence of H_2O_2. **(B)** APEX2 enzyme is attached to the GFP-nanotrap and used in the HeLa S3 Flp-In GFP-tagged cell lines. **(C)** Workflow of SILAC experiment using the stable cell lines and APEX2-nanotrap. Cells were stimulated with 20ng/ml EGF following a 6-hour serum starvation and 30-minute pre-treatment with Biotin-phenol. Labelling of interacting proteins is induced by the addition of H_2O_2. Cell lysates are then mixed in a 1:1:1 ratio before enrichment by Streptavidin pulldown.

3.2.4. Enrichment of biotin-labelled proteins using APEX2

A control experiment was performed to assess the ability of APEX2 to label proteins with biotin and determine if an enriched pool of these proteins could be obtained (Figure 3.5). The GFP-tagged cell lines were transfected with the APEX2-nanotrap construct 24 hours prior to labelling. Labelling was activated by the addition of H_2O_2 for 1 minute. The cells were quickly quenched and then lysed. A control condition was set up for each cell line, which was not transfected with the APEX2 enzyme and did not have H_2O_2 added to induce labelling.

The top panel of Figure 3.5 shows the total amount of protein on the blot. Samples are taken from all parts of the streptavidin IP. The Input and flow-through (first supernatant taken from the IP prior to washing) show no difference in the total amounts of protein between cell lines and positive and negative controls. This shows that equal concentrations were used for all the conditions in the IP. An increase in the total protein is seen in the positive controls of the bound fraction compared to the non-labelled negative control. After looking at the total protein, the blot was then probed for biotin using a streptavidin antibody. Stronger staining can be seen in the positive controls compared to the negative controls, suggesting that the enzyme is effectively labelling proteins with biotin. The bound fraction shows a massively increased enrichment of biotinylated proteins compared to the input and flow-through fractions, showing that the biotinylated proteins have been enriched by the streptavidin IP.

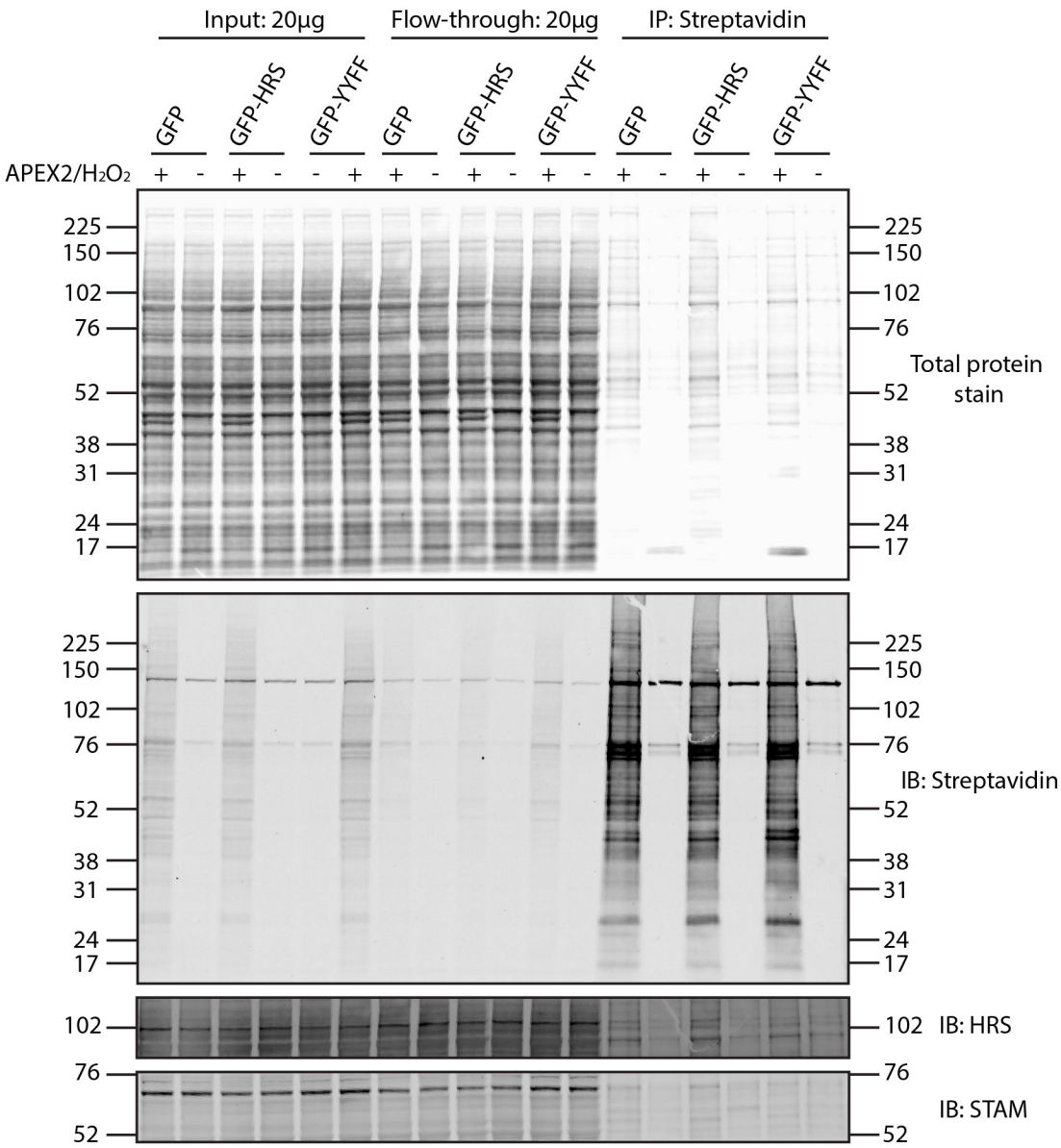

Figure 3.5 Enrichment of biotin-labelled proteins by APEX2-nanotrap. HeLa S3 Flp-In GFP cell lines transfected with APEX2-nanotrap were incubated with biotin-phenol. Biotinylation was stimulated in the cells where indicated before the cells were lysed and a streptavidin IP was performed. The top panel shows the total proteins present in each lane. The second panel was probed with a streptavidin antibody to show the levels of biotinylation. The bottom two panels were probed for HRS and STAM.

3.2.5. APEX2-nanotrap approach for mass spectrometry identifies a larger pool of proteins

The SILAC labelled cell lines were transfected with the APEX2-nanotrap construct 24 hours prior to labelling, as mentioned above. The cells were then stimulated with 20ng/ml of EGF at 37°C for 8 minutes before H_2O_2 was added for 1 minute at room temperature to activate the biotin labelling by the APEX2 enzyme. Cells were lysed and the lysates mixed prior to immunoprecipitation. The samples were then processed for mass spectrometry. The first observation from the data obtained using the APEX2-nanotrap approach was that much more material had been detected compared to the previous mass spectrometry experiment.

From the graphs generated (Figure 3.6), the majority of proteins fall around the base line, creating a large background signal. I was encouraged to see that a collection of G-proteins, and Rac1, had been identified in the dataset. These proteins, however, fall within the large background 'cloud' of proteins, and thus, we have to conclude that they are not enriched in this dataset.

Further problems arise in the dataset when looking for HRS and STAM to act as the internal controls for the experiment. HRS was not identified at all in the dataset, while STAM1 also failed to make it out of the background 'cloud'. This casts doubt over the validity of these results if a strong enrichment of the bait protein, or its most common binding partner, hasn't been obtained.

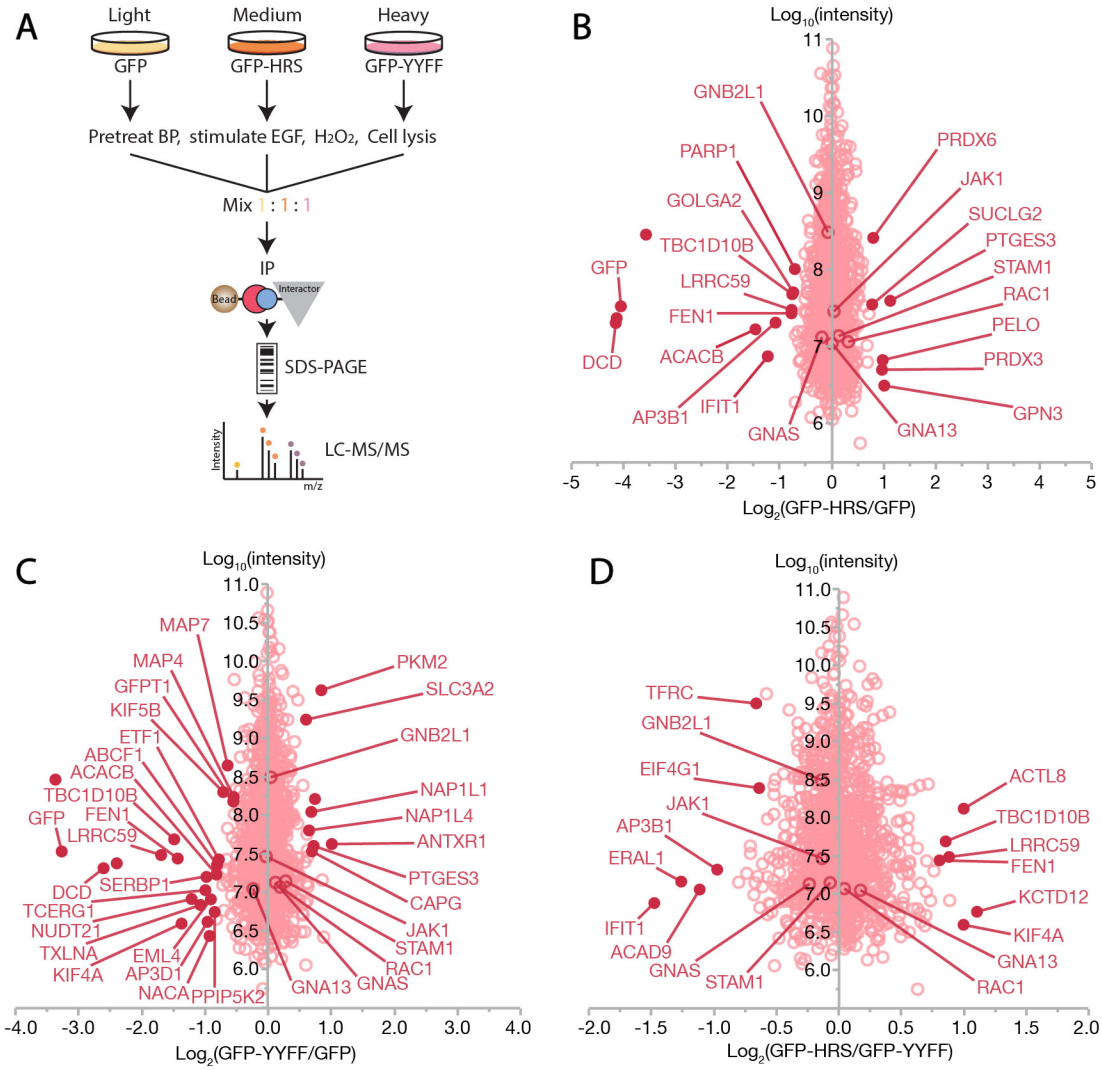

Figure 3.6 GFP-HRS interactome in EGF stimulated HeLa S3 Flp-In cells transfected with APEX2-nanotrap. (A) Workflow of SILAC experiment using the stable cell lines and APEX2-nanotrap. In gel digest was carried out on the samples prior to analysis with LC-MS/MS. Log2 transformed ratios plotted against Log10 transformed intensities for **(B)** GFP-HRS versus GFP, **(C)** GFP-YYFF versus GFP and **(D)** GFP-HRS versus GFP-YYFF. Filled circles represent proteins which show significant ratio changes. Significance B, false discovery rate (FDR) < 0.05.

3.2.6. Abundant cytosolic proteins make up the largest intensities in the dataset

Upon further examination of the results, I noticed that the proteins which displayed the largest intensities, tended to be very abundant cytosolic proteins. For example, tubulin subunits as well as actin subunits had some of the highest intensities in the dataset (Figure 3.7(A)). Moreover, these proteins tended to have similar levels between conditions, meaning that there was no enrichment in any condition. This may

have been due to the nature of this approach. The APEX2-nanotrap was overexpressed via transient transfection and as such would be in excess of the GFP-tagged constructs. This would mean that there was more than likely, an excess of the enzyme, which is unable to bind to a GFP molecule. The excess enzyme would then be generating biotin-phenoxyl radicals in the cytosol, potentially explaining why the proteins with the highest intensities are abundant cytosolic proteins.

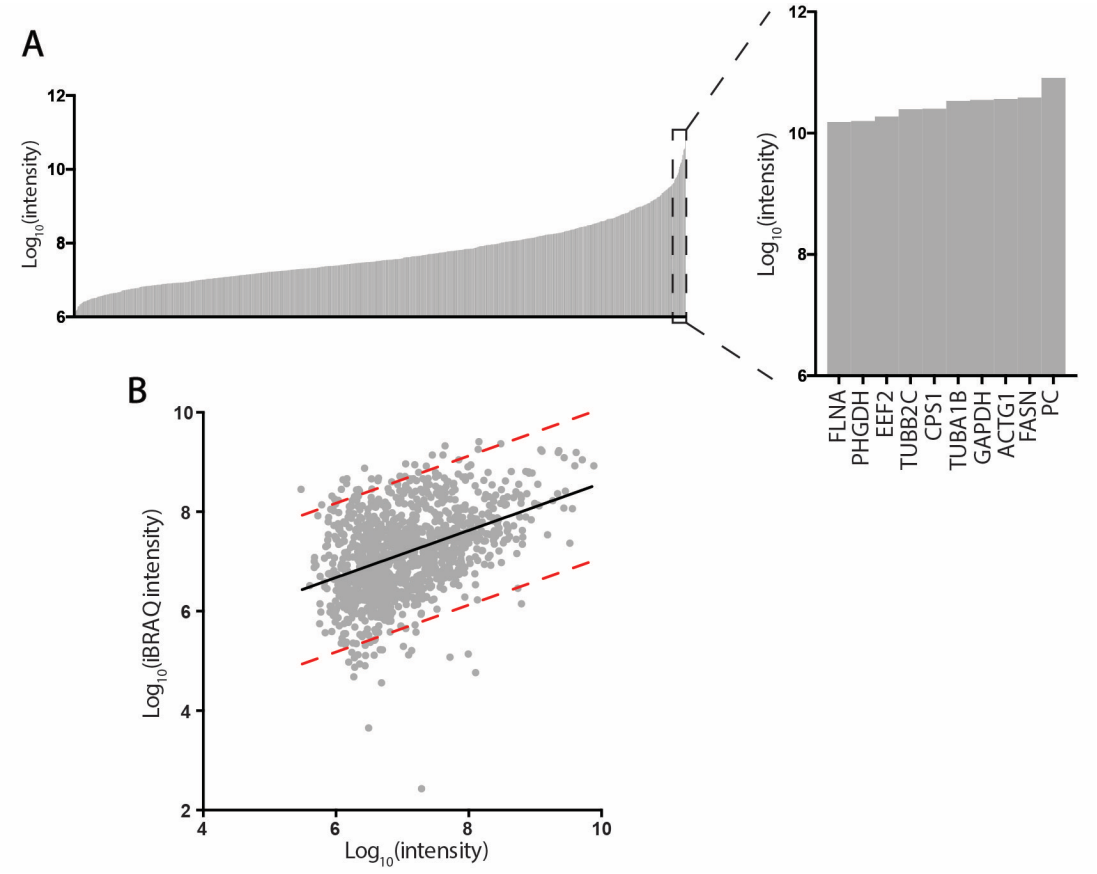

Figure 3.7 intensity analysis of HRS interactome generated with APEX2-tagged nanotrap. (A) intensity histogram of proteins identified using APEX2-nanotrap. Highlighted are the ten highest intensity proteins. **(B)** Intensities from the APEX2-nanotrap mass spectrometry experiment were compared to the HeLa copy number dataset generated from (Nagaraj, Wisniewski et al. 2011). Pearson r = 0.4243, P < 0.0001.

To examine this further, I took the intensities of all the proteins within my dataset and compared them to the copy number for HeLa cells from a dataset published by Matthias Mann and colleagues (Nagaraj, Wisniewski et al. 2011) (Figure 3.7(B)). There was a correlation between the intensities of the biotinylated proteins in the APEX2-nanotrap dataset and the copy number dataset from Matthias Mann. This suggests that there is not a specific enrichment of proteins interacting with HRS with the APEX2-nanotrap.

3.2.7. Generation of APEX2-tagged HRS cell lines

Due to the issues brought about from the overexpression of the APEX2 enzyme in the last approach. I decided to make cell lines using the same Flp-In system used to generate the GFP-tagged cell lines. The idea is that all of the APEX2 enzyme will now be associated with HRS as they would be directly linked to each other. This would hopefully, reduce the background signal significantly and maybe eliminate the abundant cytosolic proteins from the subsequent datasets. Using the Flp-In system also ensures that the HRS constructs are being expressed at a similar level to what is seen under normal physiological conditions. A schematic of the experimental setup is shown in Figure 3.8. This set up mirrors that which was used for the GFP-tagged cell lines, with lysate collection and IP methodology being identical to the APEX2-nanotrap approach. Generation of the cell lines is described in section 2.2.11.

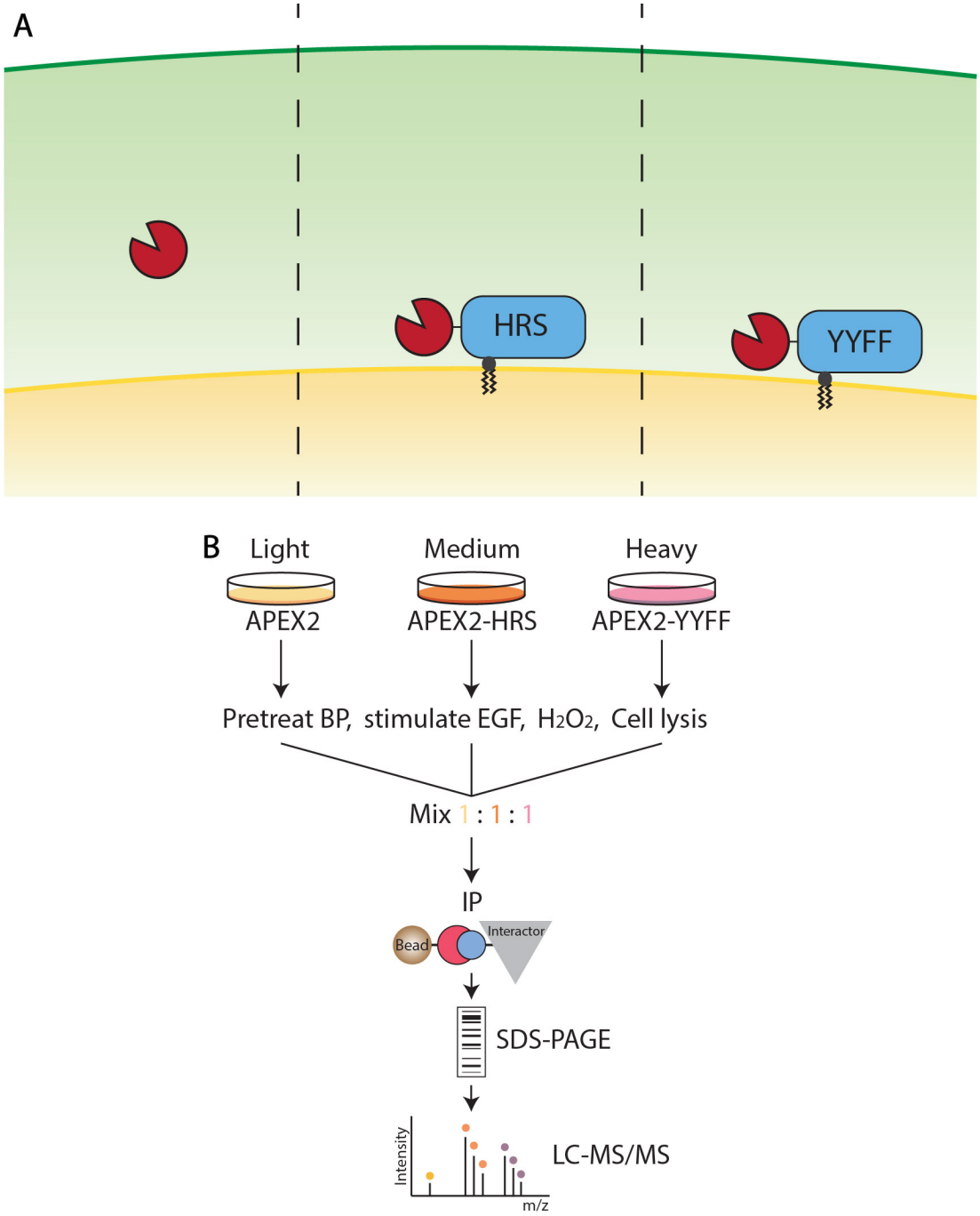

Figure 3.8 Schematic diagram of the experimental setup for using APEX2-tagged HRS. (A) APEX2 enzyme is attached directly to HRS and stably expressed in HeLa S3 Flp-In cell lines. **(B)** Workflow of SILAC experiment using the APEX2 cell lines. Cells were stimulated with 20ng/ml EGF following a 6-hour serum starvation and 30-minute pre-treatment with Biotin-phenol. Labelling of interacting proteins is induced by the addition of H_2O_2. Cell lysates were then mixed in a 1:1:1 ratio before enrichment by Streptavidin pulldown.

3.2.8. APEX2-tagged cell line characterisation and IP optimisation

The APEX2 enzyme contains a Flag tag. In order to visualise the localisation of APEX2 in the three cell lines, APEX2 expressing cell lines were co-stained with an anti-HRS and an anti-Flag antibody (Figure 3.9(A)). Both the APEX2-HRS and APEX2-YYFF expressing cells show co-localisation between the anti-HRS and anti-Flag antibodies. No co-localisation is seen between the two antibodies in the APEX2 only cells.

By Western blot, APEX2-HRS and APEX2-YYFF constructs are expressed at similar levels to the endogenous HRS in the APEX only cell lines. The endogenous HRS levels within the WT and mutant HRS cell lines decreases with the presence of the APEX2-HRS constructs. This is a similar phenomenon that was seen with the GFP-HRS cell lines used above.

The APEX2 cell lines also respond to 20ng/ml of EGF as per the GFP cell lines. APEX2-HRS shows a P-HRS band appearing after 8 minutes of EGF stimulation, which has decreased after 30 minutes of stimulation. These bands are not seen in the APEX2 only or the mutant HRS cell lines.

Since the previous IP was optimised for cell lines expressing higher levels of the APEX2 enzyme, the amount of protein lysate would need to be titrated for a given amount of streptavidin beads. Increasing amounts of protein lysate were used with 30µl of magnetic beads to assess how much of the beads will be used in the MS experiment. As shown in the bottom panel of Figure 3.9(D), as the protein amount used increases, so does the strength of the biotinylated bands. Looking at the unbound fraction, there does not seem to be an increase of biotinylated bands until a slight increase seen in the 1000µg condition. This suggests that at 1000µg of protein, the beads are reaching saturation.

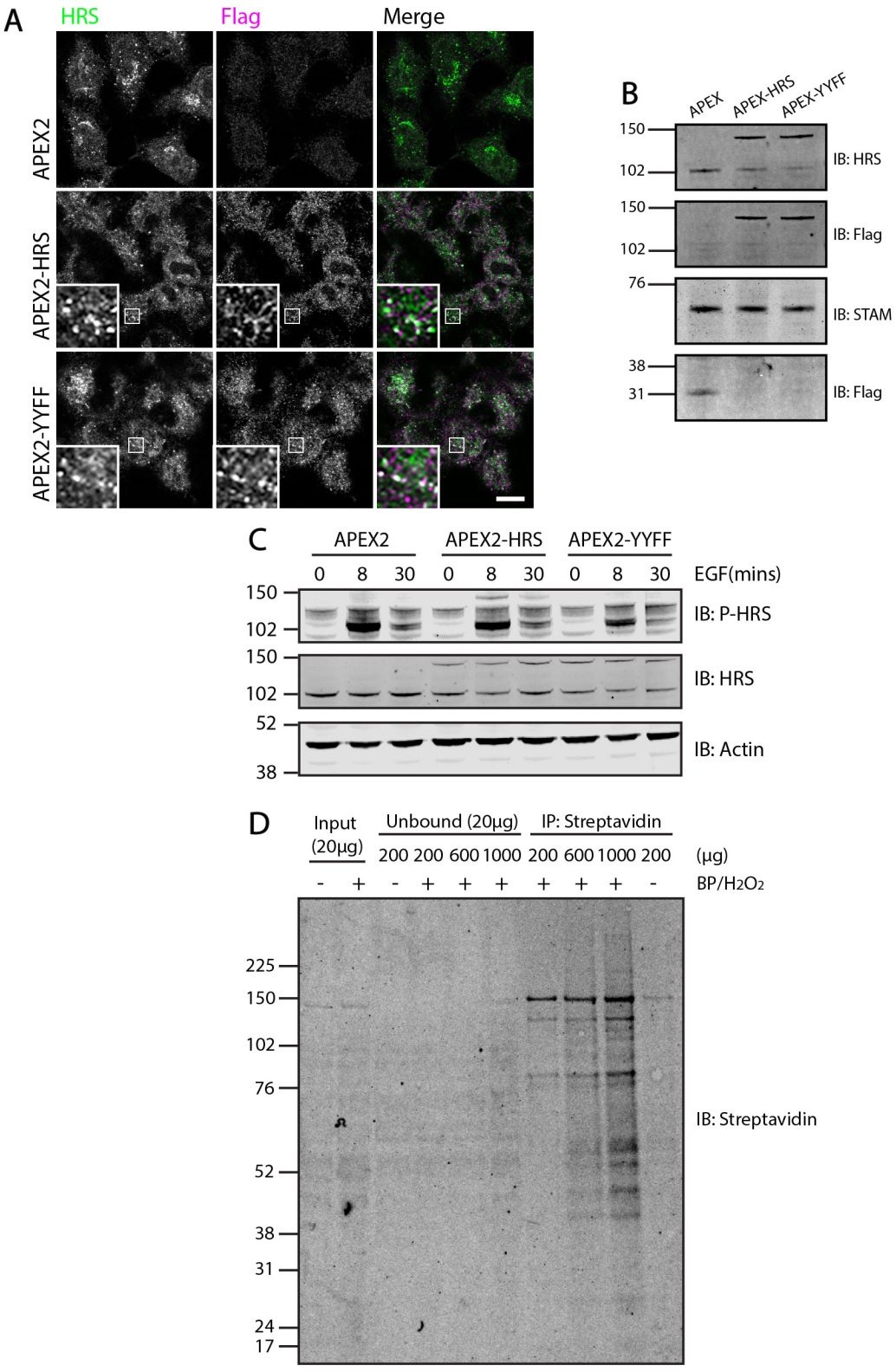

Figure 3.9 APEX2 Cell line characterisation and optimisation. (A) HeLa S3 Flp-In cells stably expressing APEX2-tagged constructs co-stained with anti-Flag and anti-HRS antibodies. Scale bar = 10µm **(B)** Western blot assessing the relative levels of APEX2-tagged HRS constructs compared to endogenous levels. **(C)** APEX2 Flp-In cells were serum starved for 6 hours and then stimulated with 20ng/ml EGF for the indicated time periods. **(D)** APEX2 cell line lysate titration against streptavidin beads. Indicated amounts of protein lysate were loaded onto 30µl of beads.

3.2.9. APEX2 cell line mass spectrometry results

The first observation that can be made from the APEX2 cell line mass spectrometry, is that far fewer biotin-labelled proteins have been identified compared to using the APEX2-nanotrap approach. This is due to a much lower expression of the APEX2 enzyme.

Looking at both the wild type and mutant HRS compared to GFP, several proteins are identified as up regulated in both conditions (Figure 3.10(B)). These are: the tRNA synthase LARS, the serine/threonine kinase STK10, the non-muscle myosin heavy chain MYH14 and the E1 ubiquitin enzyme UBA1. Enriched in the mutant cell line was several proteins involved in RNA regulation: RIOK2, RPL3 and RPL7; as well as a couple of metabolic enzymes, PMK2 and GPI (Figure 3.10(C)). Perhaps the most interesting enrichment was of the E3 ligase deltex-3-like (DTX3L), which was enriched in the wild type HRS condition compared to both the APEX2 only control and the mutant HRS cell lines (Figure 3.10(B&D)). This indicates that the interaction between this E3 ligase and HRS is dependent on the phosphorylation of tyrosine residues 329 and 334.

As with the APEX2-nanotrap approach, I looked for HRS and STAM in the dataset to use as an internal control. Despite the APEX2 enzyme being directly linked to HRS, neither HRS or STAM were identified in the dataset. Furthermore, the collection of heterotrimeric G-proteins, along with Rac1, were also absent from this dataset. This lack of a positive internal control raises concern over the validity of the mass spectrometry results.

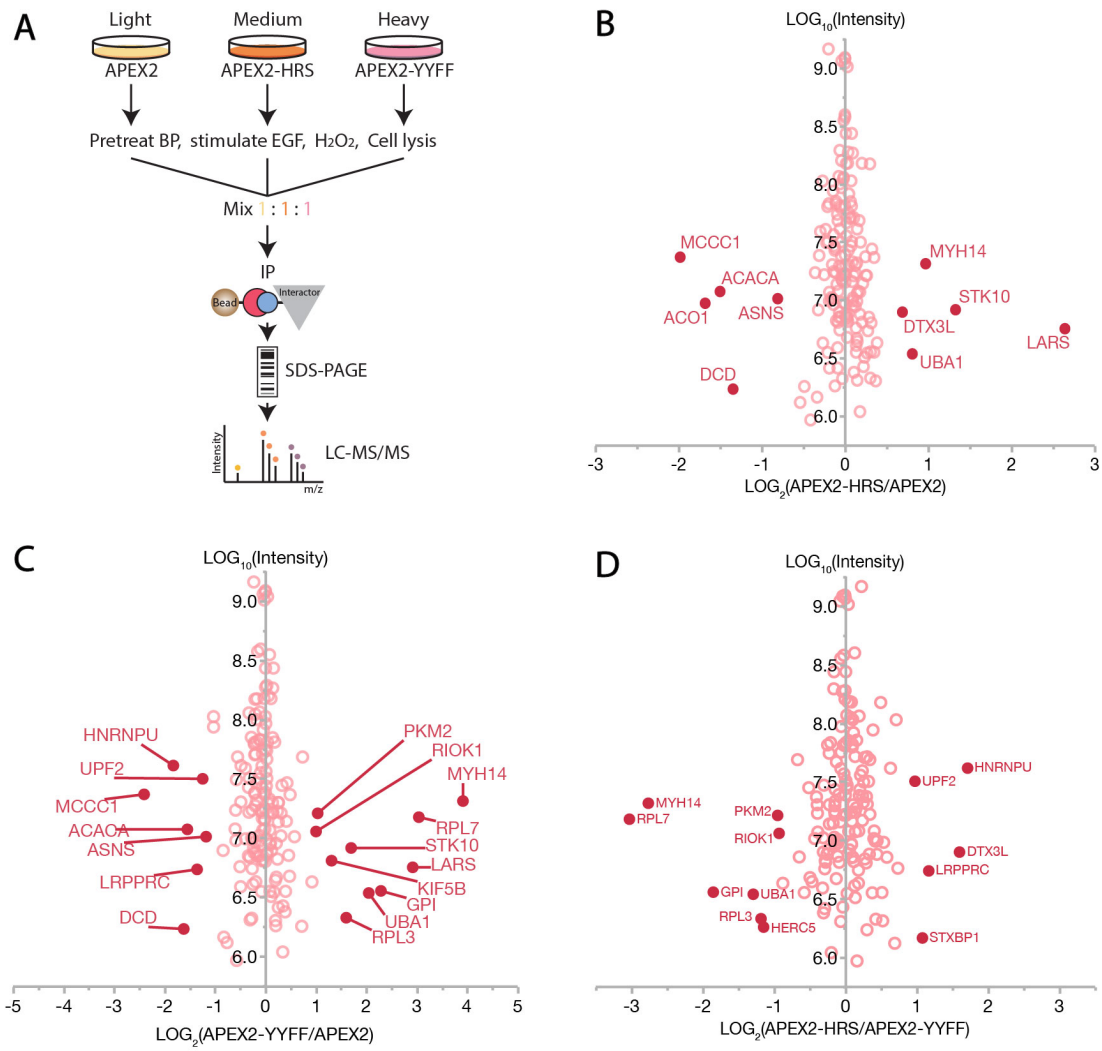

Figure 3.10 APEX2-HRS interactome in EGF stimulated HeLa S3 Flp-In cells. (A) Workflow of the SILAC experiment using the stable APEX2 cell lines. In gel digest was carried out on the samples prior to analysis with LC-MS/MS. Log_2 transformed ratios plotted against Log_{10} transformed intensites for **(B)** APEX2-HRS versus APEX2, **(C)** APEX2-YYFF versus APEX2 and **(D)** APEX2-HRS versus APEX2-YYFF. Filled circles represent proteins which show significant ratio changes. Significance B, false discovery rate (FDR) < 0.05.

3.3. Summary of results

- Only strong, well established interaction partners were identified by mass spectrometry from the traditional GFP IP
- Over-expression of APEX2-nanotrap in the GFP cell lines lead to a high background signal, with predominantly abundant cytosolic proteins being identified.
- Mass spectrometry analysis of biotin labelled proteins from the APEX2 cell lines identified proteins associated with range of biological processes. These include: RNA regulation, components of the ubiquitin cascade pathway and a couple of metabolic enzymes.
- The E3 ligase DTX3L was enriched in the wild type APEX2-HRS cell lines compared to both the mutant HRS (APEX2-YYFF) and APEX2 only cell lines.
- Neither method of proximity labelling managed to identify the possible HRS-dependent enrichment of heterotrimeric G-proteins.

3.4. Discussion

As mentioned in the introduction to this chapter, the transient nature of these potential interactions makes them very difficult to measure. Evident by the initial mass spectrometry experiment, where only STAM1 and STAM2 were identified as interacting partners of HRS, despite the literature showing many other proteins are capable of interacting with HRS (Huttlin, Ting et al. 2015).

APEX2-nanotrap is a tool used in electron microscopy to create a modular system for the visualisation of GFP-labelled proteins (Ariotti, Hall et al. 2015). The enzyme is linked to the anti-GFP nanobody and introduced into cells via a transient transfection. The GFP-nanotrap localises APEX2 to GFP-tagged proteins. This method has been successfully employed in electron microscopy studies. In this chapter, I attempted to determine if this methodology could be used for the detection of protein-protein

interactions via mass spectrometry. Successfully utilising this method would allow for the rapid proximity-labelling analysis of GFP-tagged proteins. Over-expression of the APEX2-nanotrap led to a huge excess of the probe compared to GFP-tagged HRS. The result of this was a high background noise level. The largest intensity proteins within the dataset were predominantly abundant cytosolic proteins and lacked specificity for HRS.

To overcome these caveats, the APEX2 enzyme was tagged directly to HRS and expressed the construct in cells using the Flp-In system. This should avoid the issue of the enzyme being expressed in excess and vastly improve the specificity of the method. The resulting mass spectrometry dataset using the APEX2 cell lines certainly contained much less material than the preceding dataset and identified a completely different set of proteins (Figures 3.6 and 3.10). However, HRS and STAM failed to be labelled by APEX2, despite the enzyme being directly tagged to HRS. It is possible that the expression of APEX2 is too low in these cell lines to obtain reliable mass spectrometry data. The amount of material identified in the APEX cell line mass spectrometry experiments was comparable to the traditional GFP IP experiments, however.

It is worth considering the possibility that HRS may be poorly labelled by the biotin phenol free radicals generated by the APEX2 enzyme. An interesting preprint article studying the 'biotinome' suggests that biotin modifications preferentially favour intrinsically disordered regions (IDRs) (Minde, Ramakrisna et al. 2018). This provides a possible explanation for the absence of HRS in both proximity-labelling experiments. It may then be difficult to use HRS and STAM as internal controls when using proximity-labelling techniques.

With this in mind, the results of the APEX2 cell line experiment can be considered, albeit with caution, without the presence of HRS and STAM. Two metabolic enzymes, pyruvate kinase isozyme M2 (PKM2) and glucose-6-phosphate isomerase (GPI), were identified in the APEX2 cell line dataset. PKM2 and GPI were enriched in the mutant cell lines compared to both the APEX2 only control and wild type HRS conditions. This

suggests that HRS phosphorylation inhibits the interaction between HRS and these enzymes. A study on CXCR4 has shown that various components of the ESCRT machinery mediate the CXCR4-induced activation of Akt (Verma and Marchese 2015). This study suggests that the ESCRT machinery regulates Akt activity by mediating the degradation of DEPTOR, an mTORC2 complex antagonist. The mTORC2 complex regulates certain aspects of cellular metabolism, providing a potential link between the two identified metabolic enzymes and ESCRT-0.

The ubiquitin-activating enzyme UBA1 was also identified in both the wild type and mutant HRS cell lines. Along with it was the E3 ligase, deltex-3-like (DTX3L), which was enriched in the wild type condition compared to both the APEX2 only control and the mutant HRS cell lines. Interestingly, DTX3L has been shown to regulate another E3 ligase atrophin-1 interacting protein 4 (AIP4), independently from its own E3 ligase activity (Holleman and Marchese 2014). This prevents AIP4 from ubiquitylating components of ESCRT-0, thus promoting the degradation of the cytokine receptor CXCR4. DTX3L is recruited to endosomes upon CXCR4 activation and knockdown of the E3 ligase by siRNA, leads to both HRS and STAM exhibiting a more cytosolic distribution in the context of CXCL12 stimulation. Furthermore, the authors also show that DTX3L interacts with both HRS and STAM. This is built upon by the data described here, which suggests that this interaction is dependent on phosphorylation of tyrosine residues 329 and 334 in the context of EGF stimulation.

The role of DTX3L in CXCR4 signalling, according to the study by Holleman and Marchese, is to aid in the degradation of the cytokine receptor by attenuating AIP4 dependent ubiquitylation of HRS and STAM. The mass spectrometry data obtained from the APEX2 cell lines suggests that this concept may also extend to RTK signalling.

Chapter four: Development of endosomal biosensors for cAMP and PKA

The classical model of GPCR signalling envisions that activation of the receptor, and subsequent effectors, occurs at the plasma membrane. Binding of the ligand by the receptor leads to a conformational change at the cytosolic tail. This allows it to activate the α subunit of hetero-trimeric G-proteins by exchanging GDP for GTP. Later, after binding of β-arrestin, the GPCR is internalised to the endosome. Here the signal is then down-regulated and the receptor reset before being recycled back to the plasma membrane.

More recently, this view has shifted. Increasing evidence has shown that a second wave of activation can occur at endosomes and that this produces a more prolonged cAMP signal compared to the plasma membrane signal (Irannejad and von Zastrow 2014). This phenotype was initially identified with the parathyroid hormone receptor and thyroid stimulating hormone (TSH) receptor (Calebiro, Nikolaev et al. 2009, Ferrandon, Feinstein et al. 2009), but has subsequently been shown to be exhibited in various other GPCRs including the β_2-adrenergic receptor (Irannejad, Tomshine et al. 2013). Furthermore, work with the β_2-adrenergic receptor also showed that the prolonged endosomal signal was responsible for the transcriptional response (Tsvetanova and von Zastrow 2014).

Despite the increasing evidence to support this model, no direct measurements of endosomally produced cAMP have been recorded. Current methods have looked at differences in the global cAMP population after various manipulations to receptor trafficking. In order to measure endosomal cAMP production and signalling, I proposed to use the FRET based cAMP and PKA biosensors, ICUE3 and AKAR4, and modify their location to endosomes.

The indicator of cAMP using Epac (ICUE) FRET based biosensor was first developed in 2004 by sandwiching cyan and yellow fluorophores around a full length Epac1 (DiPilato, Cheng et al. 2004). Upon binding cAMP, Epac1 undergoes a large conformational change. This moves the fluorophores further apart and reduces the FRET between them. The ICUE3 sensor is the third generation for the biosensor with an improved dynamic range over previous iterations (DiPilato and Zhang 2009)(Figure 4.1).

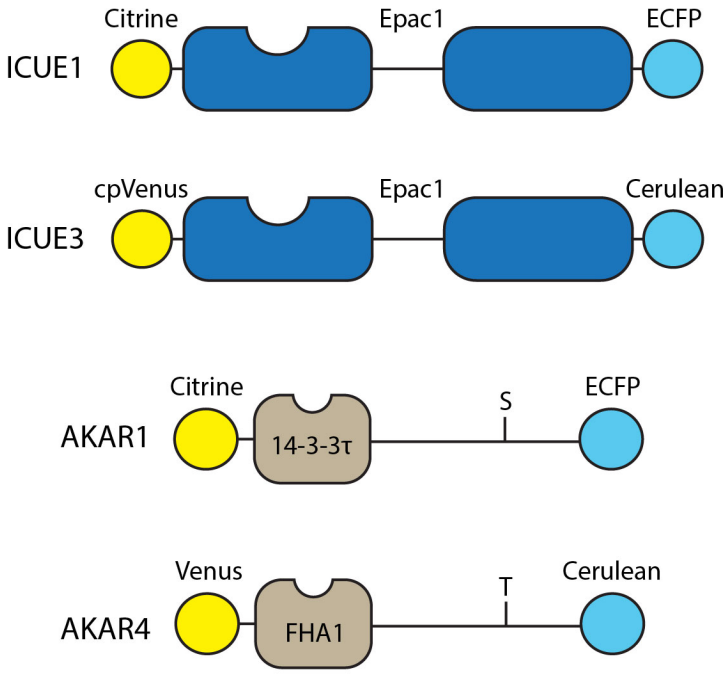

Figure 4.1 Evolution of PKA and cAMP biosensors. Multiple versions of the cAMP, indicator of cAMP using Epac (ICUE), and PKA, A-kinase activity reporter (AKAR), biosensors have been generated. Different fluorescent protein variants have been used in order to improve the intensity and dynamic range of FRET measurements. The phosphoamino acid domain has also been changed in AKAR4 over the earlier iteration. 14-3-3τ has been replaced by Forkhead associated domain (FHA1).

A-kinase activity reporter (AKAR) developed in 2001, is a FRET based biosensor containing a substrate sequence for PKA and a phosphorylation recognition domain to induce a conformational change in response to PKA activity (Zhang, Ma et al. 2001). In contrast to the ICUE biosensor, AKAR is open under non-stimulated conditions. When PKA becomes active, it phosphorylates the pseudo-substrate. The phosphorylation recognition domain now binds to the phosphorylated amino acid, resulting in the

sensor folding up and an increase in FRET. The AKAR4 sensor is the latest iteration of the biosensor (Depry, Allen et al. 2011).

Organelles are identified by the GTPases and specific lipids present on the cytosolic surface (Behnia and Munro 2005). Early endosomes are in part identified by the phosphoinositide PtdIns(3)*P* (Di Paolo and De Camilli 2006). This phosphoinositide species is generated by the class III phosphoinositide 3-kinase, Vps34 (Schu, Takegawa et al. 1993), which is recruited to endosomes by the GTPase, Rab5. Proteins bind to PtdIns(3)*P* through an interaction with their FYVE domain (Gaullier, Simonsen et al. 1998). The FYVE domain is named after the first 4 proteins it was found in (Fab1, YOTB, Vac1 and EEA1) when it was shown to be required for the endosomal localisation of EEA1 (Stenmark, Aasland et al. 1996). The FYVE domain has since been identified on numerous endosomal proteins, many of which are critical for endosomal function. Overexpression of FYVE domain containing proteins can therefore saturate the PtdIns(3)*P* available for binding and disrupt normal endosome function, as is seen with HRS overexpression (Chin, Raynor et al. 2001).

4.1. Objectives

My aim for the work described in this chapter was to develop FRET based biosensors for the study of endosomal cAMP generation and PKA signalling. The resulting FRET sensors will then be used to determine if manipulation of HRS will lead to altered cAMP and PKA signalling.

4.2. Results

4.2.1. GFP-FENSFYVE construct localises to endosomes

In order to localise the AKAR4 and ICUE3 constructs to endosomes, a FYVE domain was added to the N-terminus of each construct. The FYVE domain can localise GFP to PtdIns(3)*P* containing membranes. This has been achieved previously through the use of a double FYVE domain from HRS (Gillooly, Morrow et al. 2000). However, a single FYVE domain from FENS has been found to be sufficient to localise GFP to endosomes. GFP-FENSFYVE (referred to as GFP-FF from here onwards) co-localises with the early endosomal marker EEA1 in HeLa cells (Figure 4.2(A)). Since the FYVE domain binds to PtdIns(3)*P*, then disruption to the generation of this phospholipid should cause endosomal proteins to fall off the endosome. This is shown when endosomal localisation of GFP-FF is lost after treatment with the VPS34 inhibitor SAR405 (Figure 4.2(B)).

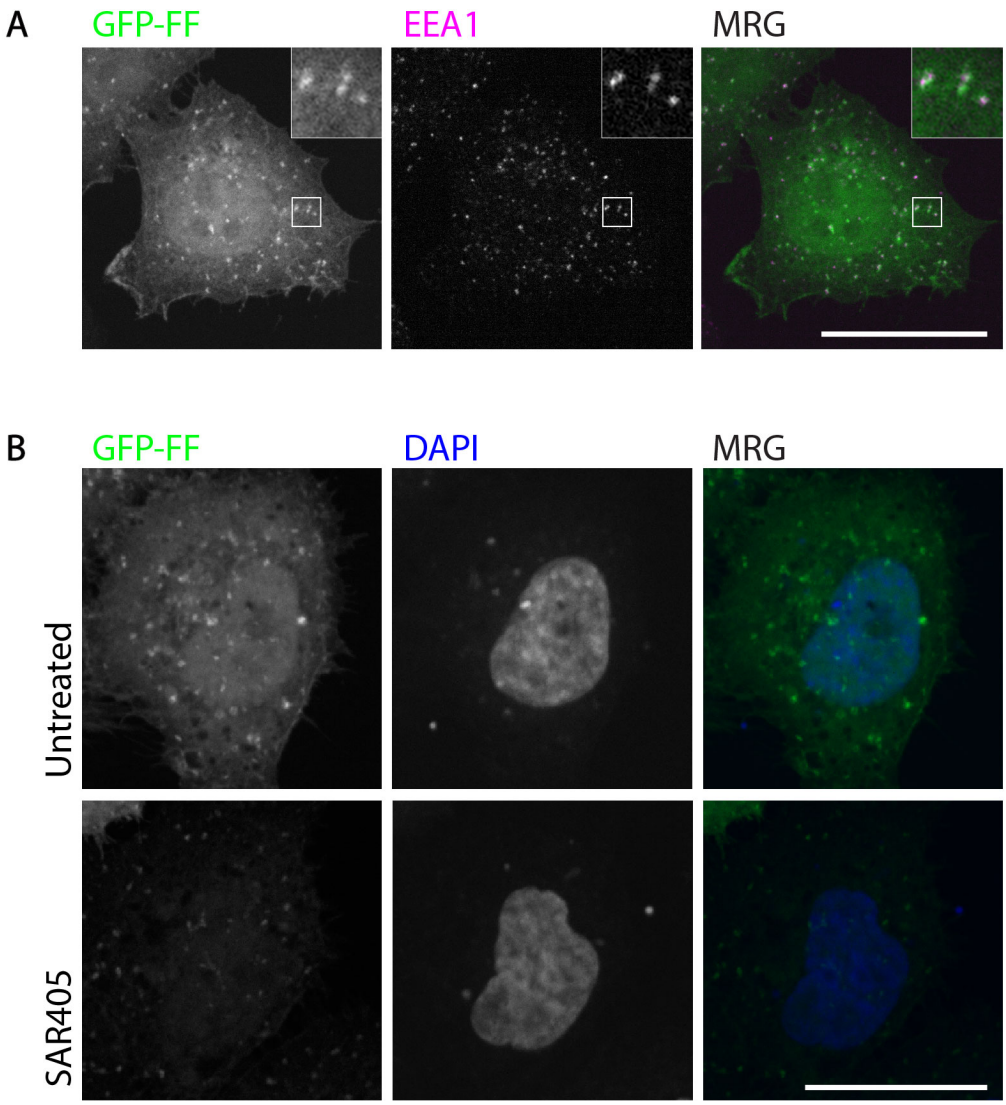

Figure 4.2 GFP-FENSFYVE localises to early endosomes. HeLa cells transfected with GFP-FENSFYVE (FF) and **(A)** co-stained with an anti-EEA1 antibody. **(B)** HeLa cells transfected with GFP-FF and treated for 2 hours with either DMSO (untreated) or 1µM of the VPS34 inhibitor, SAR405. Scale bar = 10µm.

4.2.2. FYVE domain localises AKAR4 to endosomes

The FYVE domain was cloned from the GFP-FF construct via PCR and inserted in front of the AKAR4 construct, as demonstrated in the schematic in Figure 4.3(A). AKAR4 with the cloned FYVE domain (AKAR4-FF) showed co-localisation with EEA1 (Figure 4.3(B)). This localisation was lost following treatment with the VPS34 inhibitor SAR405 as well as the less specific PI-3-K inhibitor Wortmannin (Figure 4.3(C)).

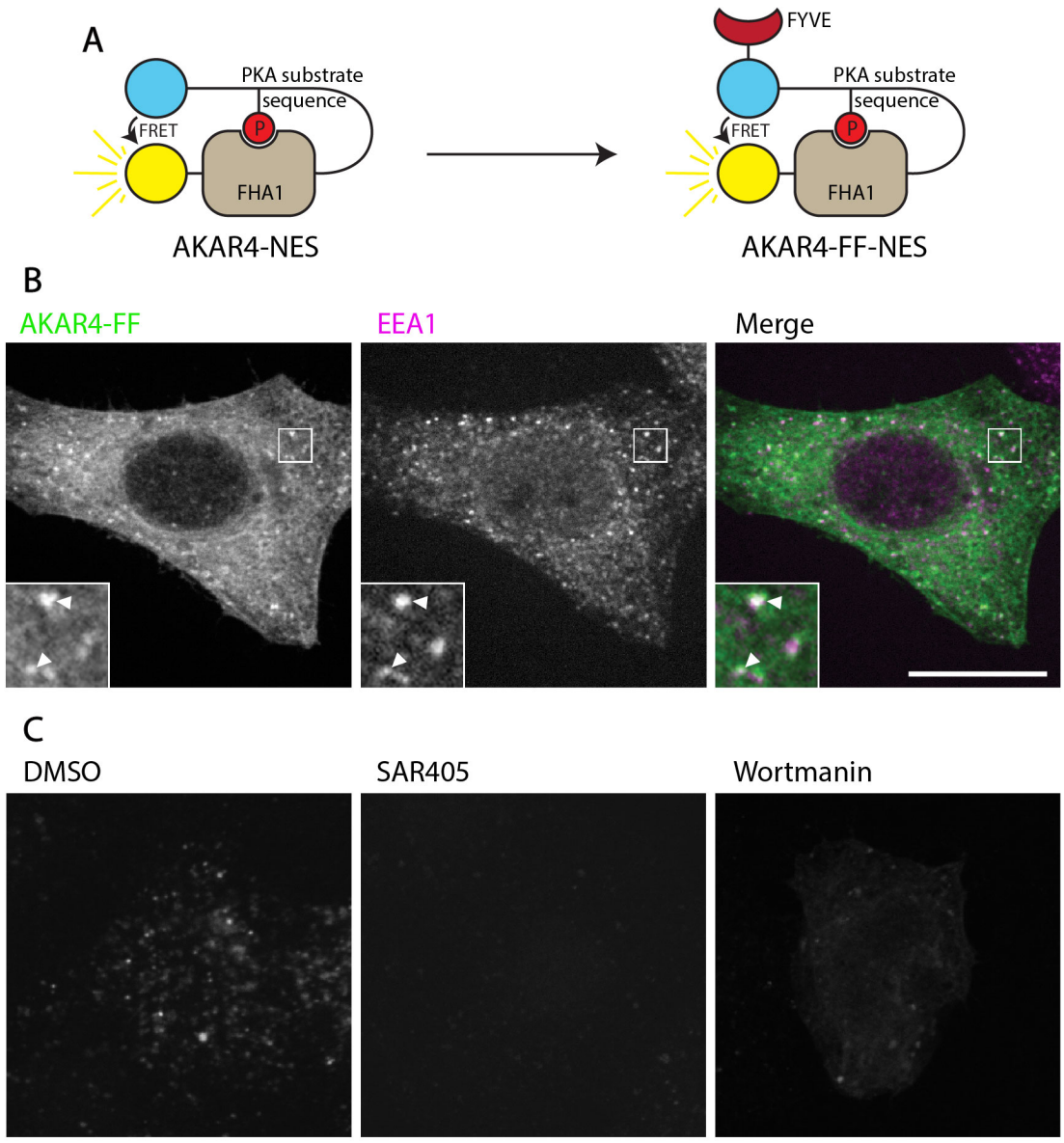

Figure 4.3 Localisation of endosomal AKAR4 to early endosomes. (A) Schematic diagram of cytosolic and endosomal AKAR4, PKA FRET sensors. Endosomal AKAR4 (AKAR4-FF) was made by attaching the FYVE domain from GFP-FF. **(B)** HeLa cells transfected with AKAR4-FF and co-stained with an anti-EEA1 antibody. **(C)** HeLa cells transfected with AKAR4-FF were treated with either 1 µM Wortmannin for 15mins, or 1 µM of SAR405 for 2 hours. Cells underwent a Saponin extraction prior to PFA fixation. Scale bar = 10µm.

4.2.3. Generation of CFP-only control for the AKAR4 and AKAR4-FF constructs

The AKAR4 construct was generated using Venus and Cerulean fluorophores (Depry, Allen et al. 2011), and thus the excitation spectra overlap with one another, as is often the case with FRET pairs. This means that control measures need to be taken in order to determine what proportion of the FRET Emission channel is due to the appropriate fluorophore and allow us to eliminate the contaminating light from our measurements, known as bleed through. In order to determine the bleed through of the donor channel, a CFP-only control was developed for the AKAR4 constructs. This was achieved by introducing a premature stop codon immediately prior to the Venus fluorophore. The stop codon was introduced via site directed mutagenesis. As shown by Figure 4.4, emission from the YFP is completely abolished in the CFP-only controls for both AKAR4 and AKAR4-FF.

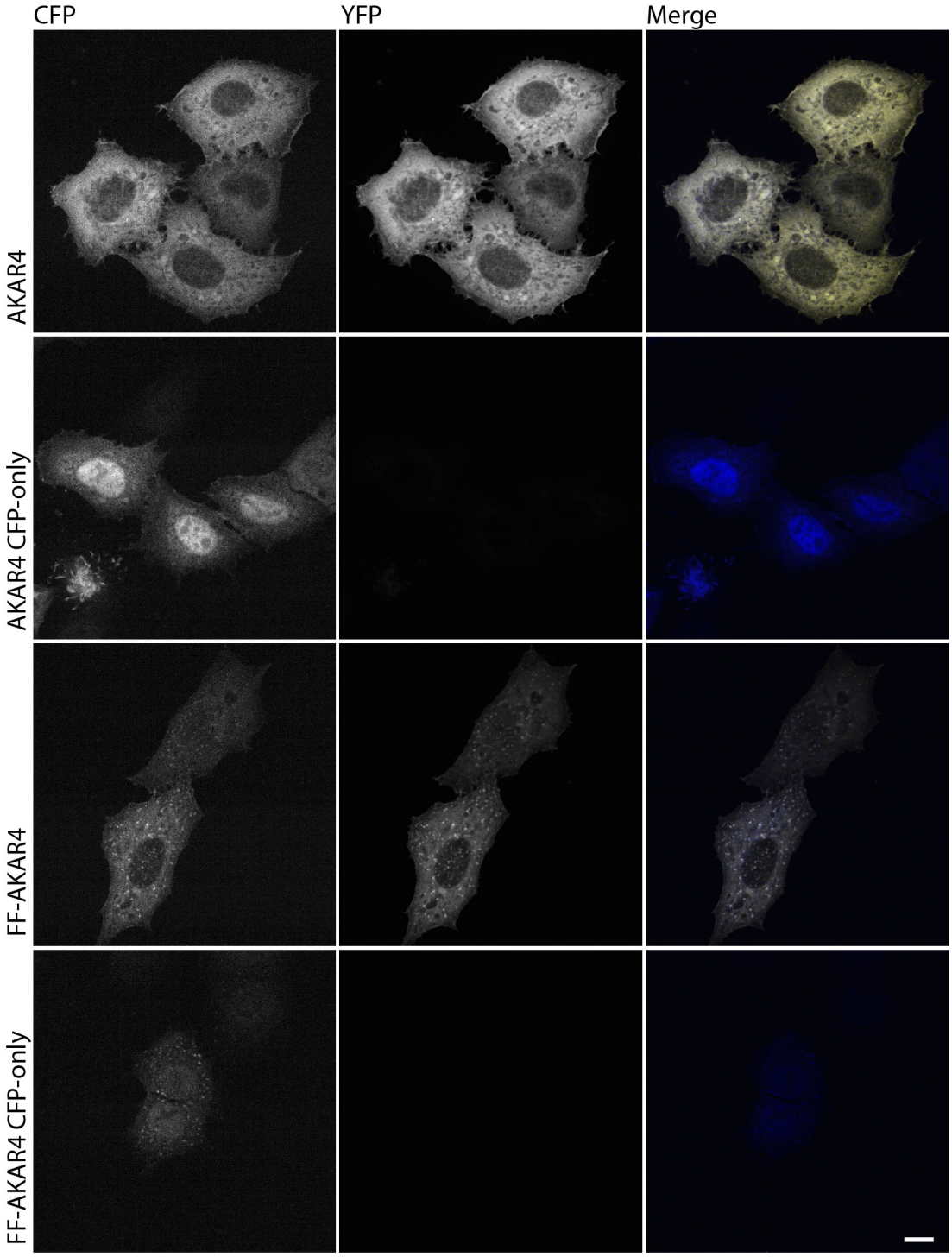

Figure 4.4 Expression of CFP and YFP fluorophores of AKAR4 CFP-only controls. HeLa cells transfected with full length and CFP-only versions of the cytosolic and endosomal AKAR4 constructs. Scale bar = 10µm.

4.2.4. CFP-only constructs for AKAR4 and AKAR4-FF exhibit increased nuclear localisation

From Figure 4.4, both of the CFP-only constructs are observed exhibiting an increased nuclear localisation. This is due to the AKAR4 construct expressing a nuclear export sequence (NES) at its C-terminus. This sequences acts as a signal to exclude proteins from the nucleus. Introducing a premature stop codon prior to the Venus fluorophore not only removed the fluorophore, but also the NES from the FRET sensor. This issue was easily resolved with further cloning, by reintroducing the NES to the CFP-only constructs, demonstrated by the schematic in Figure 4.5(A). Exclusion of the FRET sensors from the nucleus is rescued by the re-addition of the NES (Figure 4.5(B)).

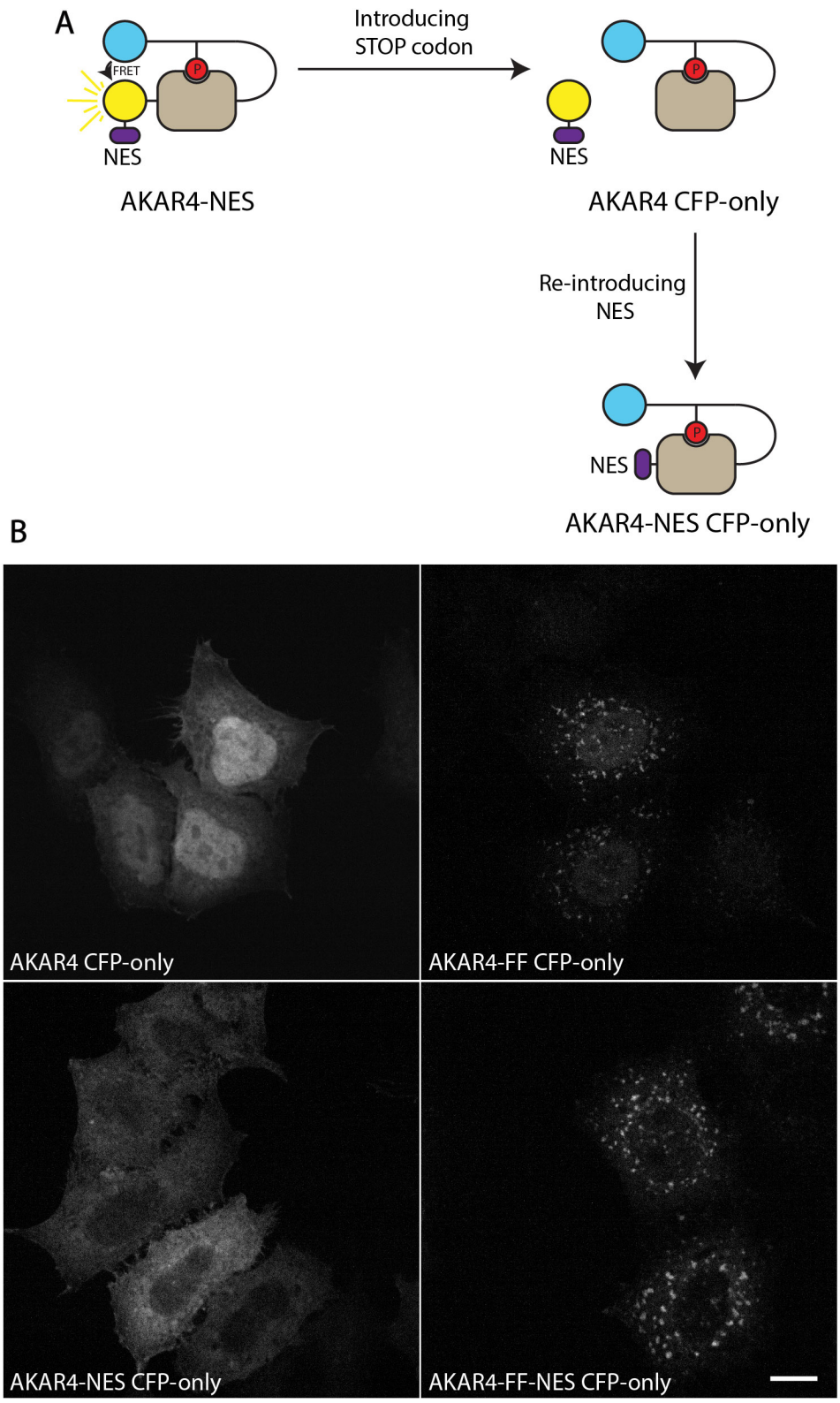

Figure 4.5 Re-introducing the NES on the CFP-only versions of the AKAR4 constructs. (A) Schematic diagram depicted the loss and re-introductions of the NES to the AKAR4 CFP-only constructs. **(B)** HeLa cells transfected with cytosolic and endosomal AKAR4 constructs, with or without the NES. YFP channel shown. Scale Bar = 10µm.

4.2.5. FYVE domain poorly localises ICUE3 to endosomes

After successfully localising the AKAR4 construct to endosomes with the FYVE domain from FENS, the same method was employed for the ICUE3 cAMP FRET sensor. Despite cloning the FYVE domain into ICUE3 exactly the same way as with AKAR4-FF, the construct displayed unusual localisation (Figure 4.6). ICUE3 with the attached FYVE domain (ICUE3-FF) co-localised poorly with EEA1 and appeared to be distributed to puncta in the nucleus. It is unclear if this construct has localised specifically to a subset of endosomes or if a portion of endosomes have been redistributed to the perinuclear region due to the presence of the ICUE3-FF construct.

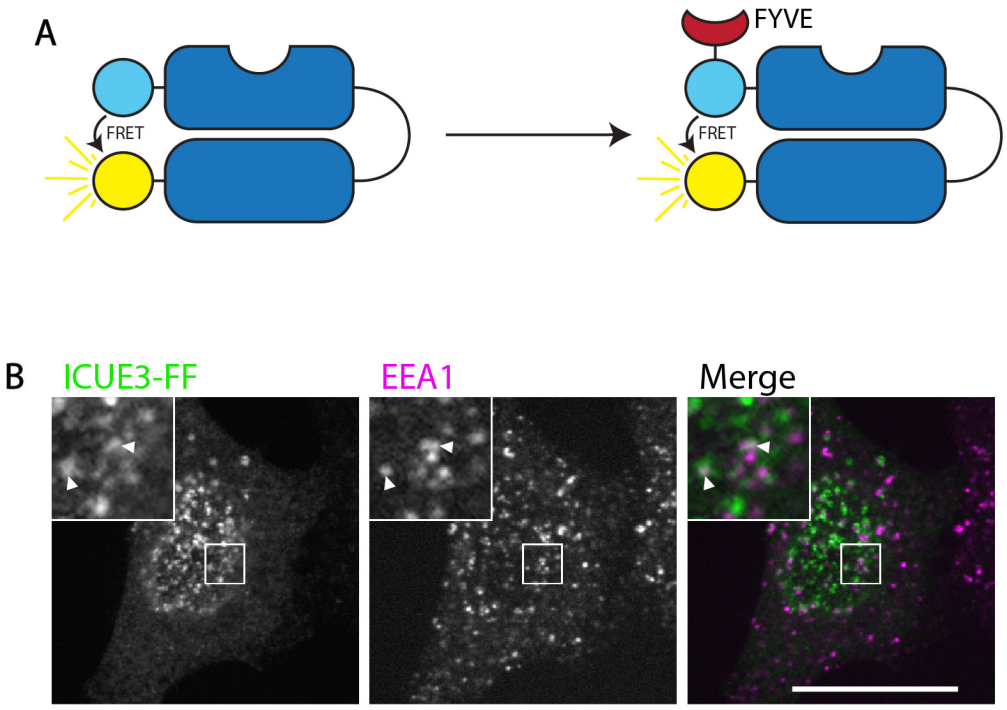

Figure 4.6 ICUE3-FF localises poorly to early endosomes. (A) Schematic diagram of cytosolic and endosomal ICUE3, cAMP FRET sensors. ICUE3-FF was made by attaching the FYVE domain from GFP-FF. **(B)** HeLa cells transfected with ICUE3-FF and co-stained with an anti-EEA1 antibody. Scale Bar = 10µm.

4.2.6. RA domain from Epac2 improves localisation of endosomal cAMP FRET sensor.

To determine the cause of the mis-localisation of ICUE3-FF, I decided to look into the literature surrounding Epac localisation. Epac is activated in the presence of cAMP and, in turn, leads to the activation of Rap1, a Ras super family member. For efficient activation of Rap1, Epac1 requires the interaction of Ran and Ran binding protein (RanBP). This interaction occurs through the Ras associated (RA) domain and also anchors Epac1 to the nuclear pore. Interestingly, when comparing the localisation of both Epac isoforms, Epac1 displays localisation to the nuclear envelope, while Epac2 does not (Liu, Takahashi et al. 2010). Since the RA domain is the region responsible for interaction with the nuclear pore protein Ran, the authors speculated that differences in this region were responsible for the altered distribution of the two isoforms. By replacing the RA domain of Epac1 with the RA domain of Epac2 (RA2), they effectively abolished the nuclear localisation of Epac1. Here, this strategy was employed with the endosomal ICUE3 construct by swapping the RA domain with that from Epac2 (RA2) to create a new construct which will now be termed ICUE4, demonstrated by the schematic in Figure 4.7(A). Though this did not completely abolish the nuclear staining seen with ICUE3-FF, it did effectively redistribute the construct. The ICUE4-FF construct displayed puncta in the cell periphery, which co-localised with EEA1. Furthermore, these peripheral puncta, but not the nuclear localisation, disappeared following treatment with Wortmannin and SAR405 (Figure 4.7(B)). From this I can confidently conclude that the ICUE4-FF construct localises to PtdIns(3)*P* positive endosomes.

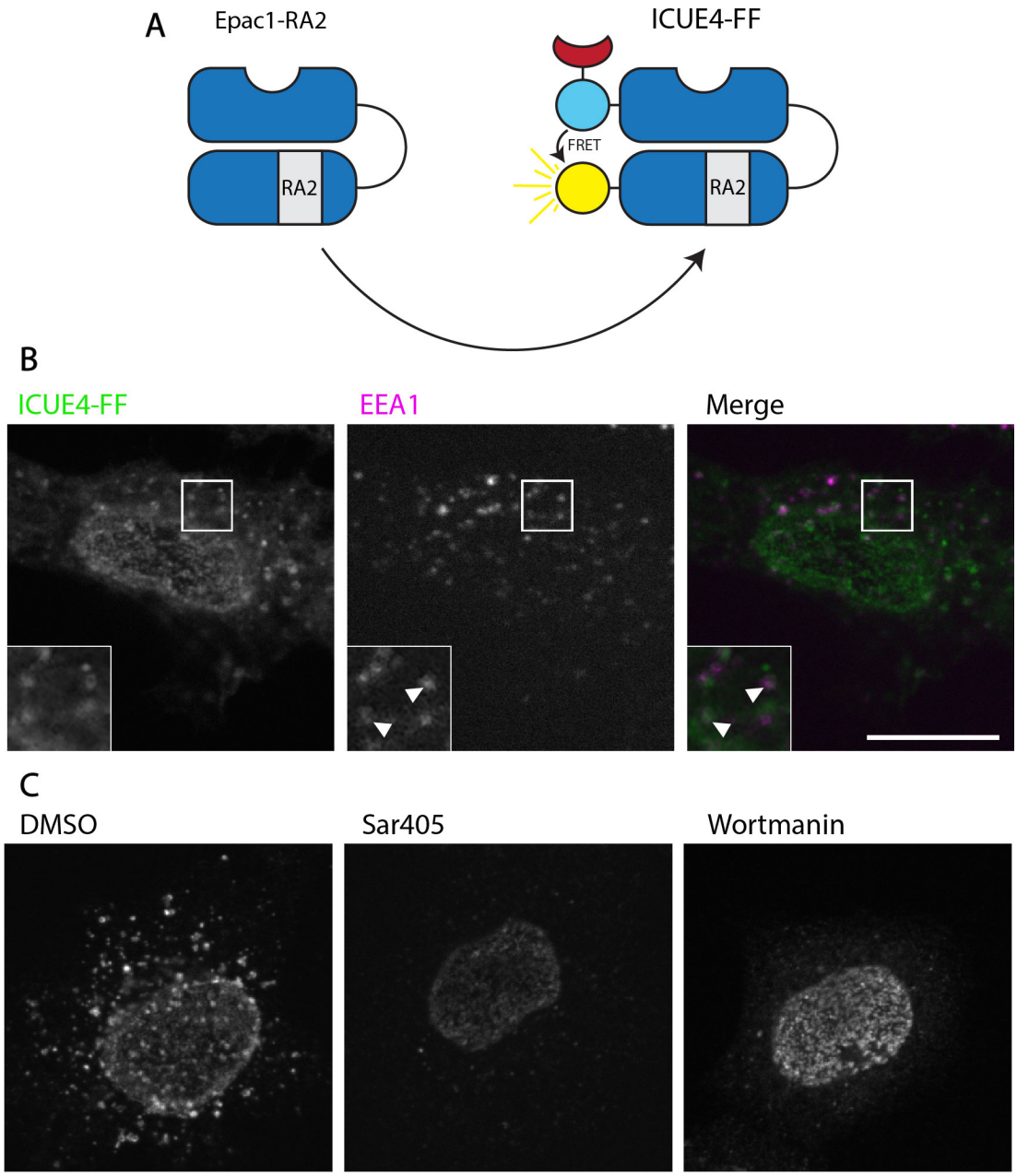

Figure 4.7 Localisation of endosomal ICUE4 to early endosomes. (A) Schematic diagram of how ICUE4-FF was made by exchanging the RA2 domain from Epac1-RA2 with the RA domain of ICUE3. **(B)** HeLa cells transfected with ICUE4-FF and co-stained with an anti-EEA1 antibody. **(C)** HeLa cells transfected with ICUE4-FF were treated with either 1 µM Wortmannin for 15mins, or 1 µM of Sar405 for 2 hours. Cells underwent a Saponin extraction prior to PFA fixation. Scale bar = 10µm.

4.2.7. ICUE4 construct is still functional as a cAMP biosensor.

A mutated version of the ICUE3 cAMP sensor was created by Zhangs group, which is unable to open up and remains in an always closed conformation. Further examination of the ICUE4 construct generated showed that the point mutation responsible for preventing the sensor from opening up, and thus function, would fall within the RA region exchanged in order to improve the localisation of the biosensor. This raised the question as to whether or not the new ICUE4 biosensor could function at all as a sensor for cAMP. To test this, the emission ratio of both the ICUE4 and the ICUE3 biosensors was measured after treatment of the β_2-adrenergic receptor agonist, isoproterenol. Treatment with isoproterenol causes an increase in cAMP levels. The cAMP then interacts with the biosensor and allow it to open up, as long as it is still able to undergo a conformational change. This should lead to a measurable decrease in FRET. The ICUE4 still exhibited changes to the emission ratios of the fluorophores, due to changes in FRET (Figure 4.8). This suggests that the ICUE4 biosensor can still undergo a conformational change in the presence of cAMP.

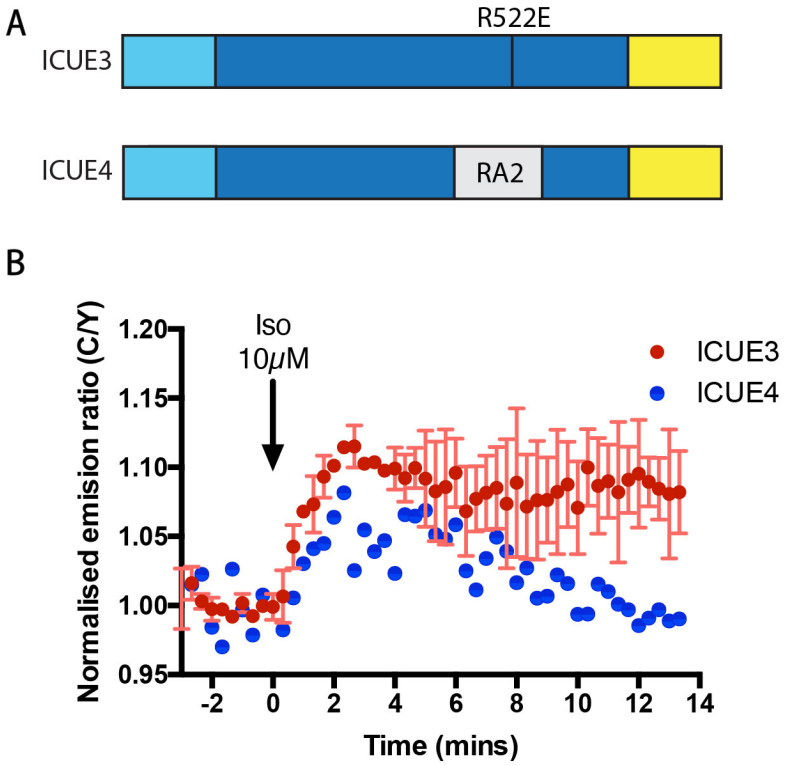

Figure 4.8 ICUE4 construct still able to undergo a conformational change in response to cAMP. (A) Schematic diagram showing the point mutation, that prevents ICUE3 from opening, in the region that is exchanged to create ICUE4. **(B)** Emission ratio time course of ICUE3 and ICUE4 in response to 10μM isoproterenol (Iso). Error bars represent range. N = 1-2.

4.2.8. Generation of CFP-only control for cAMP sensors.

As with the AKAR4 constructs, a CFP-only control is necessary to determine the bleed through of the CFP emission into the FRET transfer channel. As seen in Figure 4.9, the YFP emission is abolished in the CFP-only controls. Unlike with the AKAR4 constructs, the ICUE constructs exist in a closed conformation initially, before opening up in the presence of cAMP. This means the FRET is high in low cAMP conditions and explains why the CFP emission is low in the full length construct and becomes stronger once the acceptor fluorophore is removed, and thus removes the FRET transfer with it.

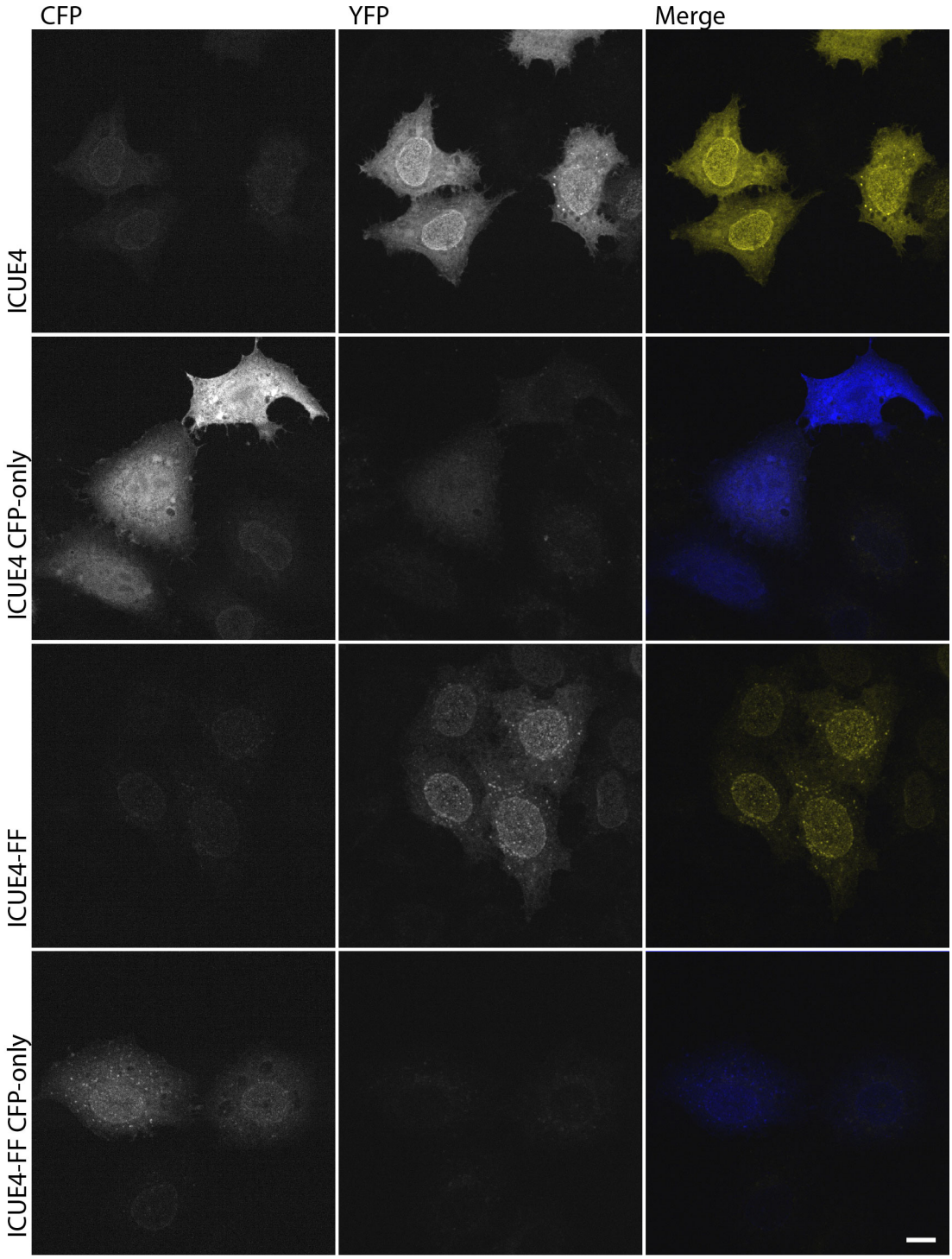

Figure 4.9 Expression of CFP and YFP fluorophores of ICUE4 CFP-only controls. HeLa cells transfected with full length and CFP-only versions of the cytosolic and endosomal ICUE4 constructs. All images levelled to the same for comparison. Scale bar = 10µm.

4.2.9. Generation of FRET biosensor cell lines

Many endosomal proteins rely on FYVE domains binding to PtdIns(3)*P* for their localisation. Due to this, it is important to be careful when expressing proteins with these domains, as seen with the dominant negative effects of HRS over-expression. Therefore, stably expressing cell lines for the cAMP and PKA biosensors were made. Furthermore, the cell lines would provide more consistent intensities of the fluorophores from cell to cell. This is important as relative intensities of the fluorophores can have an impact on FRET measurements and uniform expression will improve the reliability of the measurements.

The FRET biosensors were introduced into HEK293 cells via random integration and single colonies picked to generate clones. This would produce clones which were expressing the sensors at different levels, allowing me to choose one that would be appropriate for further experiments. Figure 4.10 shows the YFP acceptor expression levels for each cell line generated. For cytosolic versions of the FRET sensors, the exact expression doesn't need to be as stringently controlled. For these cell lines the clones which showed the brightest expression were chosen. For the AKAR4 cell lines, this was clone AK-3, and for the ICUE4 cell lines, this was either clone IC-2 or IC-7. IC-7 was chosen due to the fact that IC-2 grew at a very slow rate. The cell lines expressing the endosomal version of the FRET sensors need to be chosen more carefully. For the AKAR4-FF cell lines, clones AKF-3, AKF-5, AKF-9 and AKF-10 gave a very low expression level. These cell lines would be difficult to get FRET measurements from and so were discounted. Clone AKF-4 exhibited enlarged endosomes, indicating that normal endosomal function was disrupted. Due to this, clone AKF-2 was used for the following experiments. For the ICUE4-FF cell lines, only ICF-3 and ICF-9 were bright enough to obtain FRET measurements. Despite the clone ICF-3 being brighter, clone ICF-9 was chosen because the ICF-3 clone appeared to be a mixed population of cells, with some cell being brighter than others.

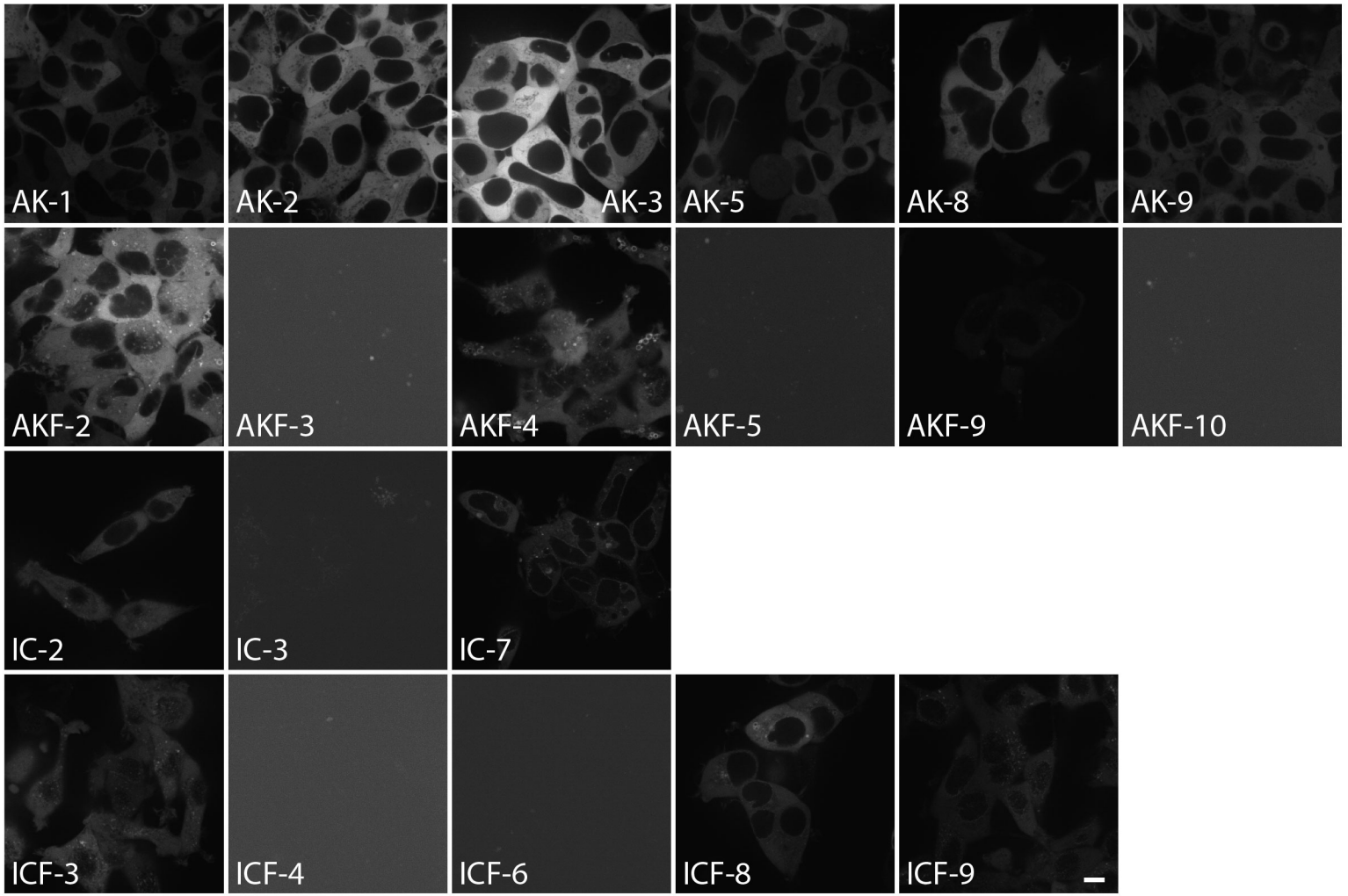

Figure 4.10 Expression of FRET biosensors in Hek293 cell line clones. AK = AKAR4 expressing clones, AKF = AKAR4-FF expressing clones, IC = ICUE4 expressing clones and ICF = ICUE4-FF expressing clones. Scale bar = 10µm.

4.2.10 Endosomal cAMP and PKA biosensor struggle to distinguish endosomal signals from the total signal

In order to test whether the endosomal FRET biosensors were giving solely an endosomal measurement for cAMP and PKA activity, a dynamin inhibitor was utilised to block endocytosis and see how this may affect endosomal and cytosolic FRET measurements after stimulation with the β_2-adrenergic receptor agonist, isoproterenol. A Laplacian filter was applied to images of cells expressing the endosomal FRET sensor in order to solely measure endosomal cAMP and PKA signalling. As is seen in Figure 4.11, after stimulation with 10µM isoproterenol, the CFP/YFP ratio of both the ICUE4 and ICUE4-FF cAMP sensors increases, indicating a decrease in FRET and an increase in the levels of cAMP. In the presence of the dynamin inhibitor, Dyngo, the cytosolic cAMP sensor showed a slightly slower increase in the CFP/YFP ratio compared to the DMSO control. Though I hypothesized that there would not be any change in this measurement, a small change like the one observed can easily be explained by the dynamin inhibitor preventing the endosomal produced cAMP from being generated.

Issues begin to arise when examining the endosomal cAMP sensor. The ICUE4-FF shows similar kinetics to the cytosolic biosensor, which shouldn't be the case as the β_2-adrenergic receptors first need to be endocytosed in order to begin signalling from the endosome. This would only occur after a few minutes. Secondly, upon treatment with 30µM Dyngo, the endosomal sensor only shows a very small decrease in the CFP/YFP ratio.

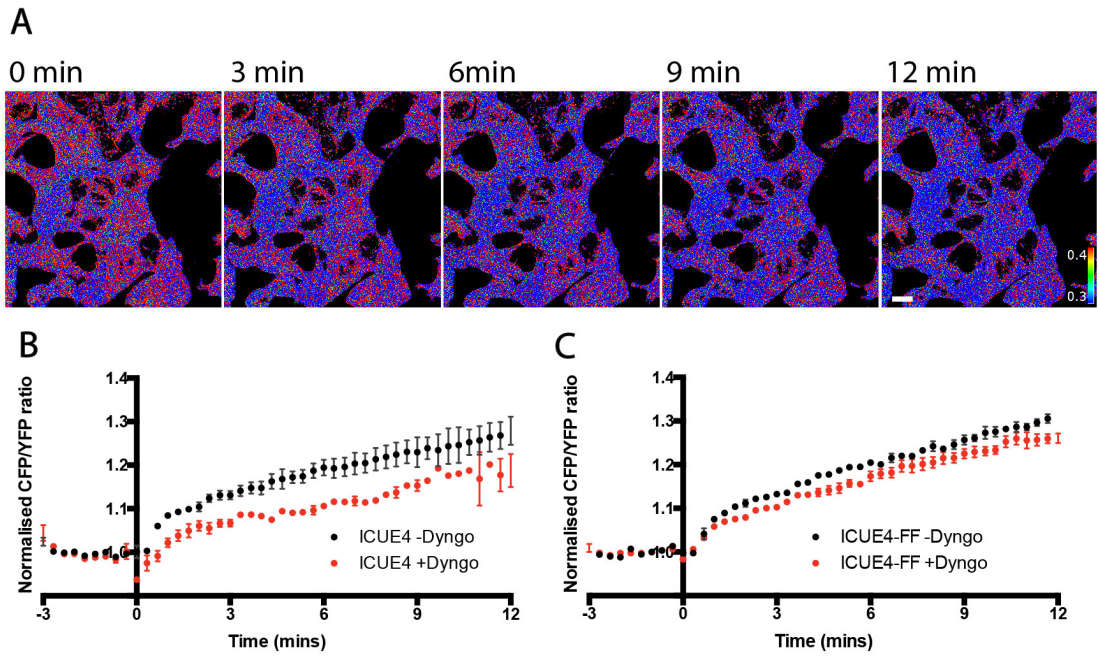

Figure 4.11 Proof of principle experiment for endosomal cAMP biosensor. (A) Pseudo-coloured images of endosomal ICUE4-FF expressing cells. Red represents a high amount of FRET and therefore low levels of cAMP. **(B & C)** Normalised CFP/YFP ratios of the **(B)** cytosolic ICUE4 and **(C)** endosomal ICUE4-FF biosensors after the addition of 10µM isoproterenol at 0 minutes. Scale bar = 10µm. Error bars represent SEM. N = 3. Data analysed using multiple T-tests, $P < 0.05$.

With the PKA sensor, no significant difference is seen when the cytosolic AKAR4 expressing cell line is treated with the dynamin inhibitor, Dyngo, compared to the DMSO control (Figure 4.12). This result was what was expected and could point towards a difference in preferences for the PKA pathway at the plasma membrane as no reduction in the YFP/CFP ratio is seen with the presence of Dyngo, despite a small decrease in total cAMP production. As with the endosomal cAMP sensor, AKAR4-FF also shows no significant decrease in the measured YFP/CFP ratios when the cells are pre-treated with Dyngo. The kinetics of the endosomal AKAR4-FF biosensor are different to the cytosolic version of AKAR4. The AKAR4-FF biosensor appears to show higher levels of FRET for longer. This contrasts from the ICUE4 biosensor where the cytosolic and endosomal biosensors exhibit the same kinetics as each other.

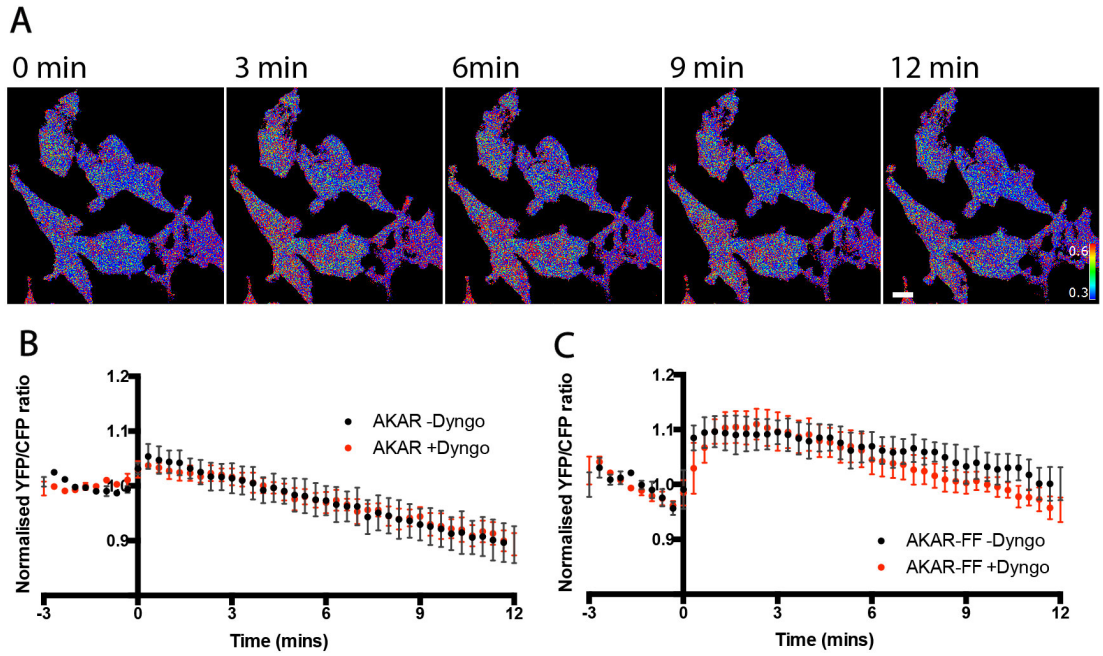

Figure 4.12 Proof of principle experiment for endosomal PKA biosensor. (A) Pseudo-coloured images of endosomal AKAR4-FF expressing cells. Red represents a high amount of FRET and therefore high levels of PKA activity. **(B & C)** Normalised YFP/CFP ratios of the **(B)** cytosolic AKAR4 and **(C)** endosomal AKAR4-FF biosensors after the addition of 10µM isoproterenol at 0 minutes. Scale bar = 10µm. Error bars represent SEM. N = 3. Data analysed using multiple T-tests, P > 0.05.

To examine the difference in FRET kinetics, the Laplacian filter, which was used for the FRET analysis, was applied to generate the pixel intensity for the FRET pseudo colour images. This creates an image that highlights the endosomes and reduces the intensity of the cytosol pixels (Figure 4.13). Comparing the two pseudo colour images, certain regions of the binary mask image appeared to stand out (highlighted by white arrowheads). Some of these regions matched up with the endosomes indicated by the Laplacian filter. Suggesting that PKA signalling at some of the endosomes may be distinguishable from the cytosol based on their FRET. These endosomes identified in the binary image are still difficult to distinguish by eye.

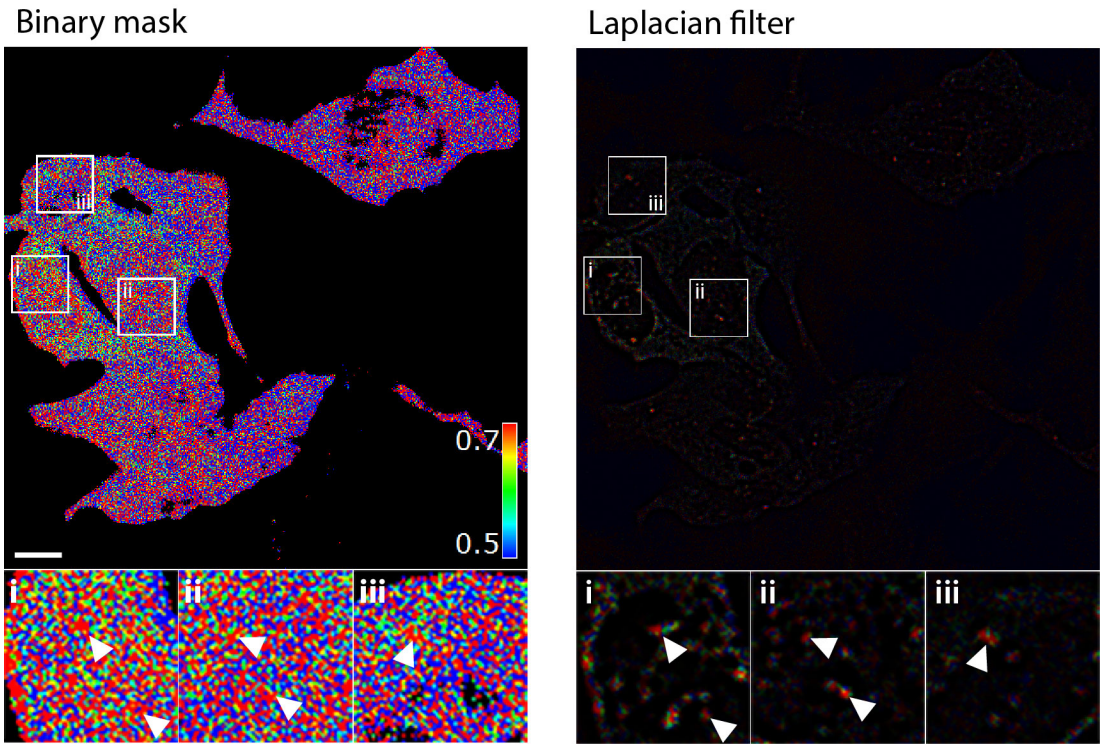

Figure 4.13 FRET from AKAR4-FF expressing cells visualised using different methods. HEK293 cells stably expressing the endosomal AKAR4-FF biosensor after 9 minutes of stimulation with isoproterenol. Both images depict the same cells with the pseudo colour image generated by different methods. The hue for each image is generated from the FRET analysis carried out by slidebook. On the left, the intensity of each pixel is generated from a binary mask and so is either 0 or 1. On the right, the intensity of each pixel comes from a Laplacian filter of the acceptor channel. Scale bar = 10µm. See supplementary movies 1 and 2 for FRET pseudo colour videos using both of these methods.

4.3. Summary of results

- The FYVE domain was sufficient by itself to localise the AKAR4 construct to endosomes.
- Additional modifications were required to localise the ICUE3 construct to endosomes, resulting in the generation of the ICUE4 construct.
- The FRET biosensors localised to endosomes were unable to effectively distinguish endosomally derived cAMP generation or PKA signalling.

4.4. Discussion

The aim of this chapter was to develop tools that would allow me to study the endosomal generation of cAMP and its downstream signalling pathways. This area of research is one that has gained interest over the last few years and there is a need to improve upon the existing tools.

Ultimately, I was unable to generate the endosome localised FRET based biosensors that could reliably differentiate PKA activity or cAMP produced specifically at the endosome (Figures 4.11 and 4.12). The development of such tools, however, may be a challenging endeavour due to the nature of the molecules being measured, particularly with regards to cAMP. cAMP is a small, diffusible second messenger molecule, and as a result could be too diffusible to spatially differentiate the various sub-populations. Discrete microdomains have been well established for Ca^{2+} signalling. However, the diffusion rate of Ca^{2+} is approximately 10x lower than the diffusion rate of cAMP ($50\mu m^2s^{-1}$ opposed to $500\mu m^2s^{-1}$) (Zaccolo, Magalhaes et al. 2002). This would explain why ICUE4-FF would have similar kinetics in response to isoproterenol to its cytosolic counterpart. Diffusion is a much quicker process than endocytosis, providing a reason as to why the endosomal signals were not abolished when endocytosis was supposedly blocked by the dynamin inhibitor. cAMP would still be generated at the plasma membrane, and this pool is detectable by the FRET sensor localised at the endosomes. I had hoped that phosphodiesterases would contain the second messenger into distinct microdomains, but this appears not to be the case in the above experiments. Blocking of endocytosis by Dyngo was not properly validated, however, raising doubt over the validity of the results.

The duration of PKA activation determined by the endosomal PKA biosensor differed from the cytosolic version. Furthermore, it is possible to distinguish endosomes from the FRET measurements. It may, therefore, be possible to further improve upon the current endosomal AKAR4 biosensor. The cell lines expressing the biosensor still displayed a relatively large cytosolic background. Further work may be able to reduce

this background and ultimately improve the signal-to-noise ratio. Expressing the biosensor in cells using a Flp-In system that allows for inducible expression may provide more stringent control over the expression of the sensor in order to provide a better signal for FRET measurements. An additional approach could be to improve the affinity of the FRET sensor for endosomes. The FYVE domain of HRS alone is insufficient to localise GFP to endosomes, but by doubling this FYVE domain, endosomal localisation is achieved (Gillooly, Morrow et al. 2000). The FYVE domain of FENS, used here, has a higher affinity for PtdIns(3)*P* than the FYVE domain of HRS. a single copy of FENS FYVE domain is sufficient to localise GFP to endosomes (Figure 4.2). Doubling the FENS FYVE domain on the biosensors should improve their affinity to PtdIns(3)*P* further and reduce the cytosolic background.

As I was also experiencing difficulty confirming the interactions between HRS and various G-proteins, at this point I decided to move on from this approach and examine other areas of HRS function not related to the crosstalk of RTKs and GPCRs.

Chapter five: HRS dynamics in response to growth factor stimulation

Conventionally, it is believed that the function of HRS is to corral ubiquitylated receptors via interactions through its UIM and VHS domains (Raiborg, Bache et al. 2002, Urbé, Sachse et al. 2003). HRS can also bind to TSG101 of the ESCRT-I complex, via a PSAP motif (Pornillos, Alam et al. 2002, Bache, Brech et al. 2003). This allows HRS to pass the ubiquitylated receptors to the rest of the ESCRT machinery and ultimately leads to degradation of the receptors. Depletion or overexpression of HRS leads to disruption of normal degradation processes (Chin, Raynor et al. 2001, Urbé, Sachse et al. 2003). This prevents receptor down regulation leading to an accumulation of the receptor at endosomes.

More recently, we have been able to show that HRS also plays a role in the recruitment of WASH to endosomes (MacDonald, Brown et al. 2018). The WASH complex is responsible for generating actin rich-domains on endosomes (Derivery, Sousa et al. 2009). Depletion of HRS led to a decreased localisation of WASH to endosomes and disruption of constitutive recycling of both the EGFR and the metalloproteinase MT1-MMP. This suggests that HRS could have a much more central role in the sorting of transmembrane proteins at endosomes, by being responsible for the recruitment of recycling machinery, such as the WASH complex, as well as the other components of the ESCRT machinery.

The HRS/WASH axis controls the sorting of the EGFR, but since HRS is phosphorylated downstream of EGFR activation, the dynamics of this relationship between the receptor and the HRS/WASH axis is currently unknown (MacDonald, Brown et al. 2018). If HRS is involved in the recruitment of both degradation and recycling machinery, how is this balance controlled? How does HRS react to the incoming cargo? Furthermore, trafficking of the EGFR is altered, depending on the ligand to which it binds (Roepstorff, Grandal et al. 2009).

The function of HRS phosphorylation is a topic that is still controversial. Studies have shown that the distribution of HRS is altered dependent on its phosphorylation state. A larger portion of phosphorylated HRS is found in the cytosol compared to membrane bound fractions, despite the fact that phosphorylation occurs at the endosomes (Urbé, Mills et al. 2000). Could the phosphorylation of HRS be important to how it reacts to the incoming cargo? Is the recruitment of the degradation and recycling machineries altered by HRS phosphorylation?

In order to ascertain answers to some of these questions, I use the GFP-tagged HRS Flp-In cell lines described in chapter three. These cells express the GFP-tagged HRS constructs at near endogenous levels. This is important in order to look at normally functioning endosomes, as over-expression of HRS leads to a dominant-negative effect that disrupts the endosomes normal function and dynamics. This is due to the fact that many proteins localise to endosomes through interactions with PtdIns(3)*P*. Over-expression of a FYVE domain containing protein leads to sequestration of PtdIns(3)*P*, changing the stoichiometry of endosomal proteins. As these cells express GFP-tagged HRS, they allow for real-time observations of HRS recruitment and dynamics at endosomes.

5.1. Objectives

The objective of this chapter is to investigate the dynamic response of HRS to growth factor stimulation and determine the subsequent effect on the recruitment of downstream effectors. By using the same GFP cell lines described in chapter three, I aim to determine if the tyrosine mutant (YYFF) behaves differently to wild type HRS.

5.2. Results

5.2.1. EGF stimulation leads to an increase in HRS positive endosomes

The GFP-HRS Flp-In cell lines are powerful tools for the study of HRS. They allow for the visualisation of HRS without the disruption associated with overexpression. These cells were used to assess the effect of EGF on HRS in real time. 20ng/ml of EGF was added to GFP-HRS cell line and the cells were visualised continually on a spinning disk confocal for the next 10 minutes (Figure 5.1). An increase in the number of fluorescent puncta was observed after the addition of the EGF. This does not necessarily suggest that EGF leads to an increase in the number endosomes, but shows an increase in the number of HRS positive endosomes. See supplementary video 3 for the movie of Figure 5.1.

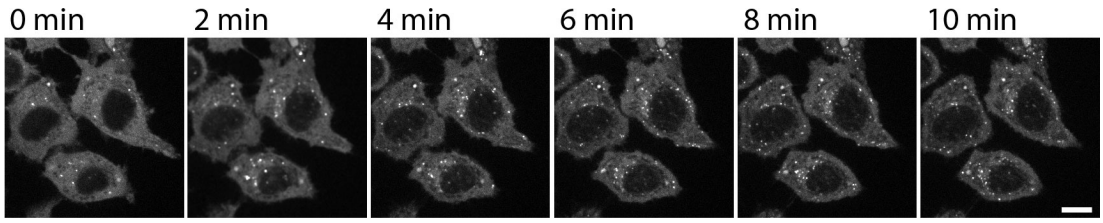

Figure 5.1 Time-lapse of GPF-HRS positive endosomes in response to EGF stimulation. GFP-HRS expressing HeLa cells were stimulated with 20ng/ml of EGF and immediately placed on the microscope for live-cell imaging. Scale bar = 10µm. See supplementary movie 3 for a video of the time-lapse images.

5.2.2. HRS positive endosome increase is not dependent on phosphorylation

After seeing the number of HRS positive endosomes increase in response to EGF stimulation, I decided to see if there might be any difference with the phosphorylation mutant HRS cell line. This cell line has two tyrosine residues, Y329 and Y334, mutated to phenylalanine residues. Both cell lines were stimulated with EGF and imaged continuously over the next 30 minutes. The number of endosomes was counted using the Trackmate plug-in on ImageJ. As can be seen in Figure 5.2, there was no significant difference to the increase in HRS positive endosomes in response to EGF between the

wild type and the phosphorylation mutant HRS. The analysis also shows that there was an increase of about 40% in the number of HRS positive endosomes.

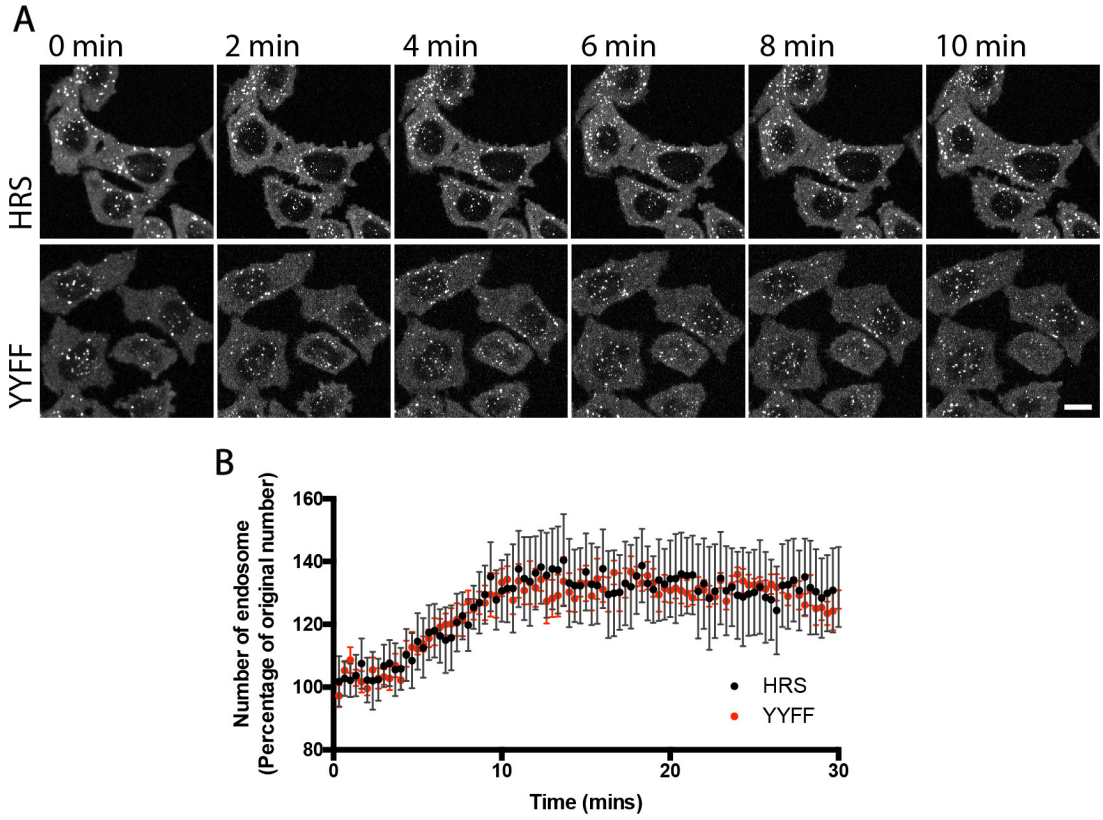

Figure 5.2 Response of wild type and mutant HRS to EGF stimulation. (A) GFP-HRS and GFP-YYFF expressing HeLa cells were stimulated with 20ng/ml of EGF and immediately placed on the microscope for live-cell imaging. Scale bar = 10µm. **(B)** The number of HRS positive endosomes was counted and displayed as a percentage of the original number. Error bars represent SEM. N = 5. Data points after every 5 minutes were analysed. T-test, $P > 0.05$ at all time points.

5.2.3. Transferrin does not lead to an increase in HRS positive endosomes

To confirm that the increase in HRS positive endosomes is in response to EGF, the effect stimulating the GFP-HRS cell lines with EGF was compared to the addition of Transferrin. GFP-HRS Flp-In cells were imaged immediately after the addition of either EGF or Transferrin and the number of HRS positive endosomes was counted (Figure 5.3(A)). As seen before, the number of HRS positive endosomes increased with stimulation of EGF. With the addition of Transferrin, however, there was no increase in the number of HRS positive endosomes. Interestingly, there was actually a gradual decrease in the number HRS positive endosomes over the time, resulting in

approximately half the number of puncta after 10 minutes. This is likely due to bleaching of the GFP. However, due to the lack of biological repeats there was no significant difference between the two.

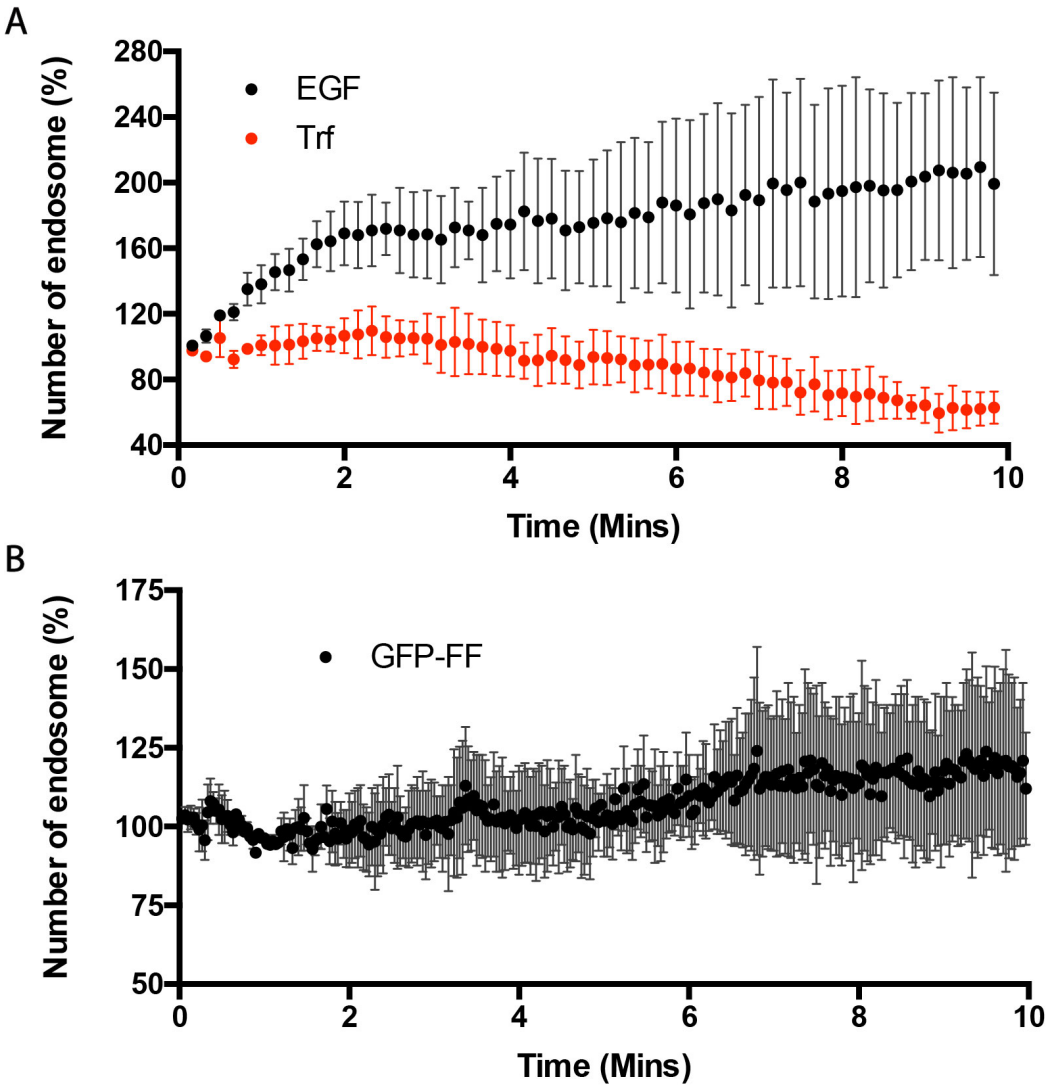

Figure 5.3 Endosome count control experiments. (A) GFP-HRS expressing HeLa cells were treated with 20ng/ml of EGF or transferrin (Trf) and immediately placed on the microscope for live-cell imaging. The number of HRS positive endosomes was counted. **(B)** HeLa cells transiently transfected with GFP-FENSFYVE (GFP-FF) were stimulated with 20ng/ml of EGF. The number of GFP-FF positive endosomes was counted. Error bars represent range. N = 2.

5.2.4. EGF does not increase PtdIns(3)*P* positive endosomes

HRS is localised to endosomes via its FYVE domain. The FYVE domain binds to PtdIns(3)*P* on early endosomes. If the number of HRS positive endosomes is increasing

in response to EGF, a logical explanation for this is that EGF is increasing the activity of the PI-3-kinase, VPS34, in order to increase the amount of PtdIns(3)*P* positive endosomes. To assess this, HeLa cells were transfected with the endosomal marker, GFP-FENSFYVE (Figure 5.3(B)). The FYVE domain from FENS is sufficient enough to localise to PtdIns(3)*P* by itself, enabling it to act as a marker for early endosomes (Ridley, Ktistakis et al. 2001). The GFP-FF positive endosomes showed no distinct increase in the number of endosomes in response to EGF. There does appear to be a slight gradual increase over time, however this is insignificant in comparison to the increase in HRS positive endosomes. This suggests HRS is being specifically recruited to endosomes in response to EGF stimulation, without a general increase in the number of endosomes, or their PtdIns(3)*P* status.

5.2.5. HRS is recruited to EGF positive vesicles

If HRS is being specifically recruited to endosomes without this increase being simply down to an increase in the number of endosomes, the question arises, how is HRS being recruited to the endosomes? One function of HRS is to bind to ubiquitylated receptors in order to corral them together into specific microdomains for degradation. Could the incoming cargo, i.e. activated EGFR, therefore be responsible for recruiting HRS? To examine this, the GFP-HRS cell line was stimulated with EGF that had been conjugated to the fluorescent dye Alexafluor-555 (AF555). By using this fluorescent dye, the endocytosed receptors could be visualised as they were being transported to endosomes (Figure 5.4). As shown by the time-lapse image, The EGF-AF555 can be seen at the plasma membrane at the start of the experiment. As the experiment progresses, the fluorescent protein starts to be internalised into the cell in vesicles. Following an individual vesicle (arrowheads) it can clearly be seen that the magenta puncta (EGF-AF555) slowly starts to become white, indicating the accumulation of the green fluorescence from GFP-HRS. There does not appear to be a fusion event with nearby GFP-HRS positive endosomes but rather the gradual recruitment of HRS to the cargo containing vesicles.

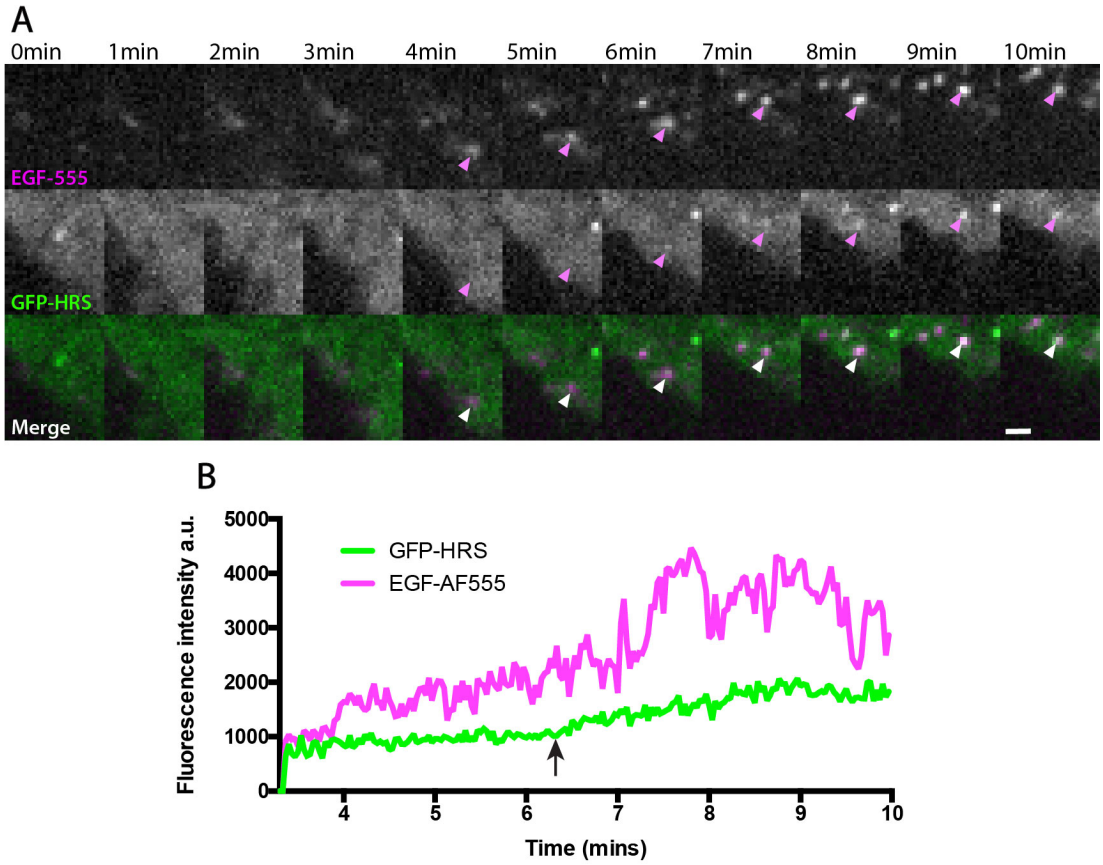

Figure 5.4 Recruitment of GFP-HRS after stimulation with fluorescent EGF. (A) Time-lapse of GFP-HRS expressing HeLa cells after stimulation with EGF-AF555. Scale bar = 1µm. **(B)** The fluorescent intensities of both channels was measured for the vesicle indicated by the arrowheads. Black arrow indicates an upward inflection in GFP intensity. See supplementary movie 4 for a video of the time-lapse images in (A).

5.2.6. WASH is recruited to endosomes in response to EGF

As mentioned above, our group was able to show that HRS is responsible for recruiting WASH to endosomes (MacDonald, 2018). Because of this, I wondered if WASH would react in a similar manner to HRS in response to EGF. I hypothesised that the number of WASH positive endosomes would increase in response to EGF to a similar extent as HRS positive endosomes.

To begin with, the number of WASH positive endosomes starts to increase after stimulation with EGF (Figure 5.5). However, this increase is short lived and very quickly begins to go down. It is possible that this immediate increase may be an artefact from

the imaging. As can be seen in Figure 5.5(A), the background intensity increases after the first image. The downward trend of the number of WASH positive endosomes begins while HRS is still being recruited to endosomes. Furthermore, the number of WASH positive endosomes continues to decrease below pre-stimulated levels, ending at approximately 66% of the original number by the end of the experiment, while the number of HRS positive endosomes remains above its original levels. From the images, it can clearly be seen that GFP-WASH is displaying a more cytosolic localisation compared to the beginning.

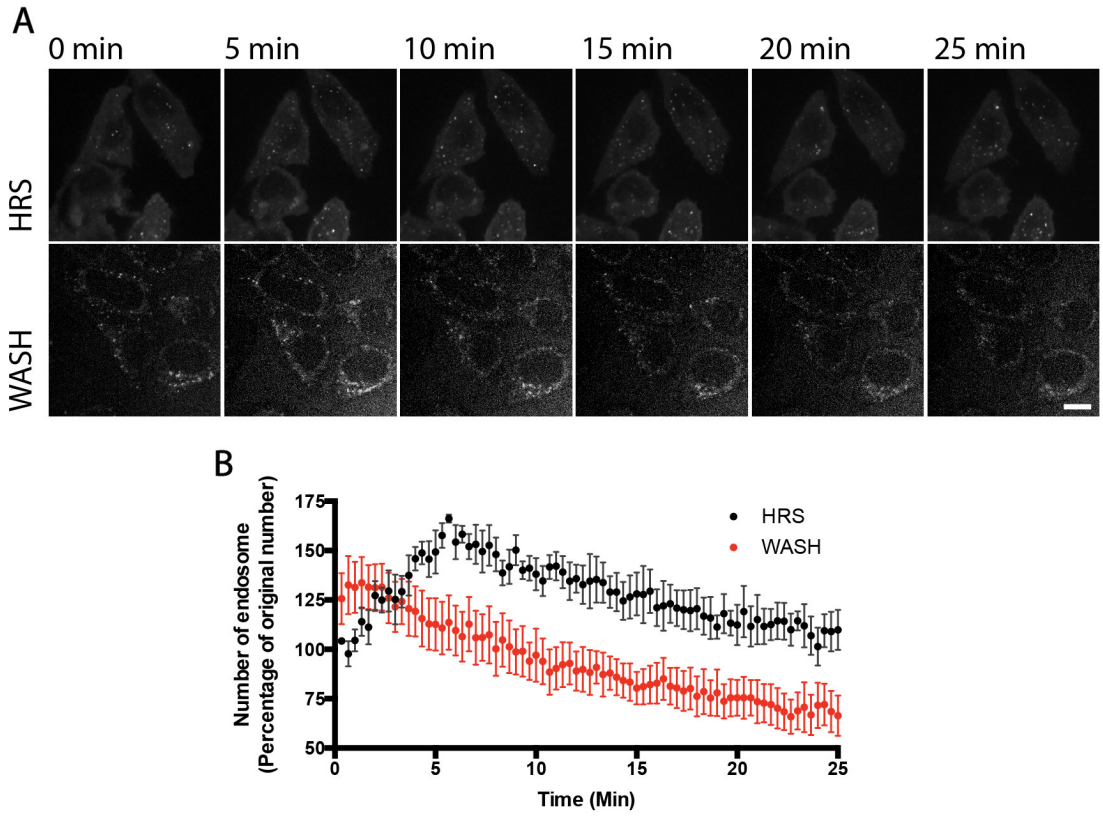

Figure 5.5 Response of WASH to EGF stimulation. (A) Time-lapse of GFP-WASH and GFP-HRS expressing HeLa cells after stimulation with 20ng/ml EGF. Live-cell imaging took place immediately after stimulation. Scale bar = 10µm. **(B)** The number of HRS and WASH positive endosomes with in the cells, displayed as a percentage of the original number. Error bars represent SEM. N = 3. See supplementary movie 5 for a video of the GFP-WASH cells from (A). Data points after every 5 minutes were analysed. T-test, $P < 0.05$ at 10, 15,20 and 25mins.

5.2.7. TGFα increases the number of HRS positive endosomes similarly to EGF

Different EGFR ligands have different effects on the trafficking of the receptor in response to stimulation (Roepstorff, Grandal et al. 2009). EGF, for example, leads to a proportion of the internalised receptors being degraded, with the remaining receptors recycled back to the plasma membrane. Stimulation with TGFα, however, leads to recycling of almost all of the internalised EGFR, with very little being directed towards degradation.

Due to the fact that WASH was recruited to endosomes differently than HRS, I decided to examine whether the recruitment of HRS differed in response to TGFα instead of EGF. GFP-HRS cells were stimulated with equal concentrations of EGF and TGFα and measured the number of HRS positive endosomes over time. Over the first 10 minutes, the number of HRS positive endosomes increased at the exact same rate with both EGF and TGFα (Figure 5.6). At the later time points, TGFα appeared to show a small decrease in the number of HRS positive endosomes compared to EGF, but this did not reach significance.

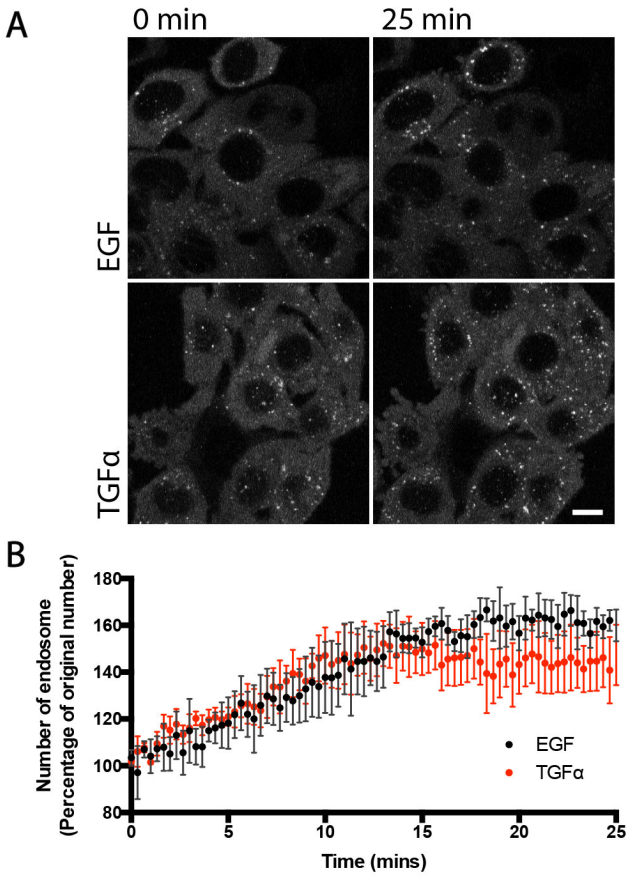

Figure 5.6 The effect of EGF and TGFα on HRS. (A) Representative images of GFP-HRS expressing HeLa cells after stimulation of 20ng/ml stimulation of EGF or TGFα. Scale bar = 10µm. **(B)** The number of HRS positive endosomes in the cells, displayed as a percentage of the original number. Error bars represent SEM. N = 3. Data points after every 5 minutes were analysed. T-test, $P > 0.05$ at all time points.

5.2.8. The HRS phosphorylation mutant shows a smaller increase in endosomes with TGFα

The HRS phosphorylation mutant (YYFF) shows no difference in its recruitment to endosomes compared to wild type HRS when stimulated with EGF. As activation of different RTKs lead to differential phosphorylation patterns of the receptor and HRS (Row, 2005), I wanted to determine whether the phosphorylation mutant would react to TGFα in a similar manner to EGF, as seen with the wild type HRS cells. When stimulated with EGF the number of HRS positive endosomes increase by 40-60% with both the wild type and the phosphorylation mutant. However, when stimulated with TGFα the HRS (YYFF) cells appeared to exhibit a smaller increase in the number of HRS

positive endosomes, increasing by approximately 25% (Figure 5.7), however this difference did not reach statistical significance. The peak number of positive endosomes occurred earlier with TGFα than with EGF and subsequently began to decrease gradually over time. After 25 minutes of TGFα simulation, the number of HRS positive endosomes had almost returned to the original levels. Further biological repeats could increase the power of the experiment.

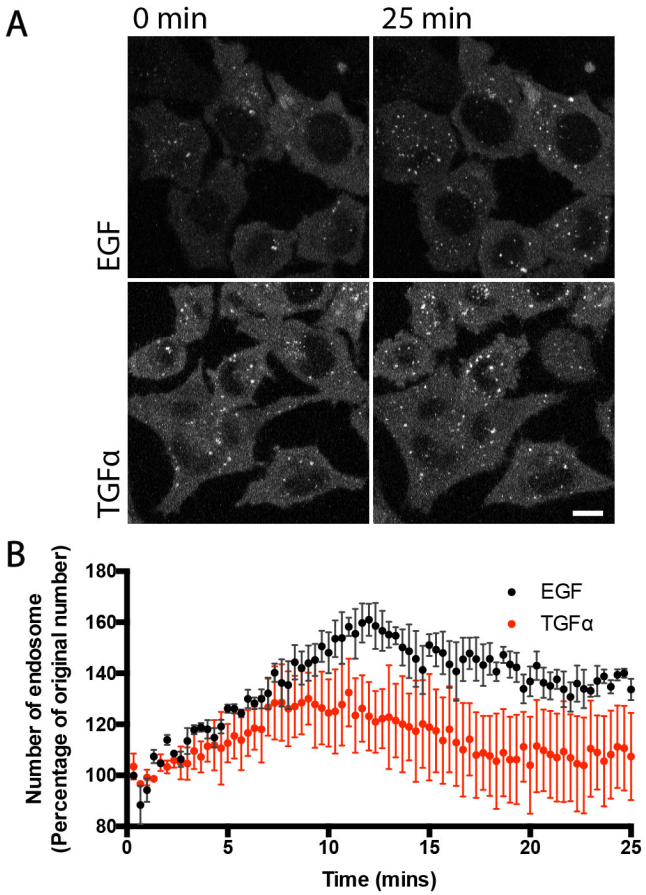

Figure 5.7 The effect of EGF and TGFα on mutant HRS (YYFF). (A) Representative images of GFP-YYFF expressing HeLa cells after stimulation of 20ng/ml stimulation of EGF or TGFα. Scale bar = 10μm. **(B)** The number of HRS positive endosomes in the cells, displayed as a percentage of the original number. Error bars represent SEM. N = 3. Data points after every 5 minutes were analysed. T-test, $P > 0.05$ at all time points.

5.2.9. APEX2-HRS cells allow for easy visualisation of the flat endosomal clathrin coat

Despite experiencing trouble with the APEX2-HRS cell line for mass spectrometry, I decided to see if I they could be used for electron microscopy (EM). The APEX2 enzyme is able to generate diaminobenzidine (DAB) radicals, which aggregate together and form an electron dense stain. These cells should allow me to visualise the sub-cellular localisation of HRS by electron microscopy.

APEX2-HRS cells were incubated with DAB prior to fixation. The cells were then incubated with H_2O_2 and prepared for EM. Figure 5.8 shows multiple examples of APEX2-HRS staining on endosomes. The DAB staining appears to localise to a distinct microdomain on the endosomes (arrowheads). The membrane within this region appears flatter than the rest of the endosome. These regions show the morphological characteristics of the flat clathrin coat present on endosomes (Futter, Gibson et al. 1998). These regions have otherwise been challenging to visualise, however, the APEX2-HRS cell line has provided a simple method for imagining these regions.

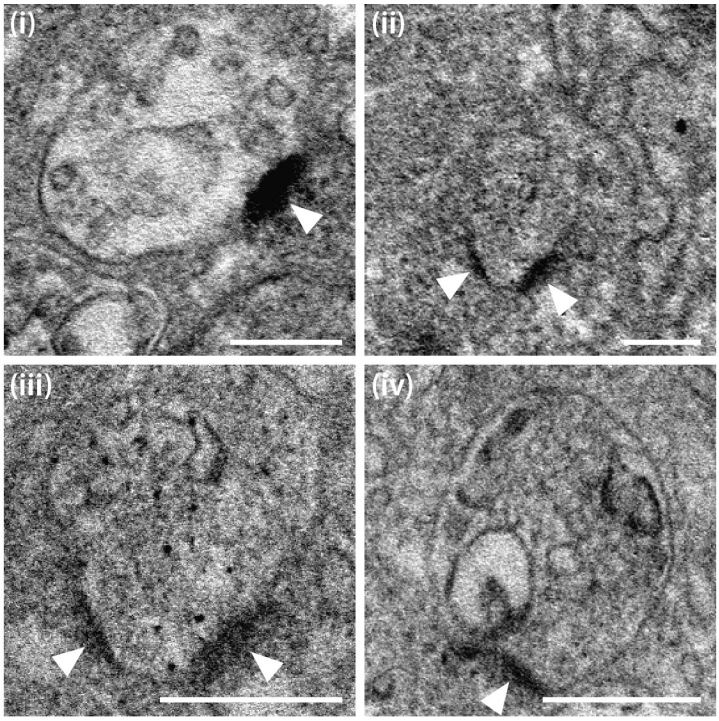

Figure 5.8 Electron microscopy of APEX2-HRS expressing HeLa cells. (i-iv) Representative images of endosomes with APEX2-HRS expressed. Staining induced by incubation with 1mg/ml DAB and 10mM H_2O_2 for 30 minutes. Scale bar = 200nm.

5.2.10. HRS phosphorylation does not affect concerted HRS recruitment waves

A recent paper published at the end of experimentation, described waves of recruitment of various components of the ESCRT machinery (Wenzel, Schultz et al. 2018). By analysing individual endosomes, they identified concerted waves in the fluorescence intensity of HRS, TSG101 and various CHMPs in response to EGF stimulation. Analysis of the experiments described in this chapter have focused on the population of HRS positive endosomes as a whole and not at an individual level. Retrospective analysis of the data identified similar recruitment waves for HRS and also for the HRS mutant (YYFF), suggesting that phosphorylation at Y329 and Y334 has no effect on this concerted recruitment pattern (Figure 5.9).

Interestingly, recruitment of HRS to a newly formed EGF positive vesicle did not appear to demonstrate these waves of recruitment (Figure 5.4(B)), with only established endosomes displaying this characteristic.

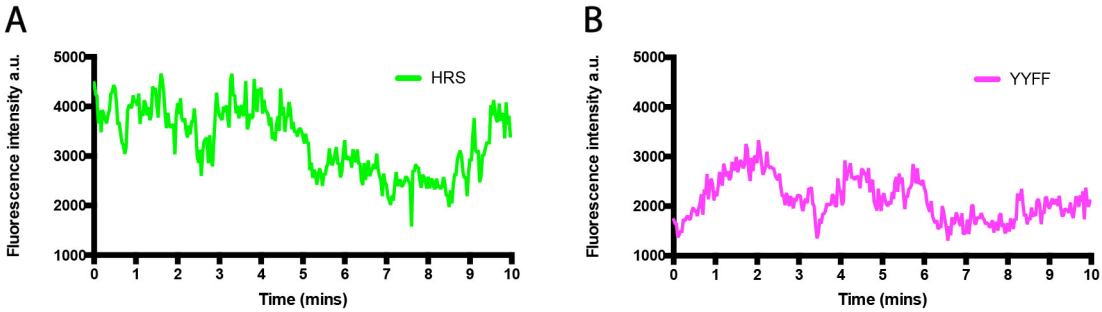

Figure 5.9. Concerted recruitment waves of wild type and mutant HRS. (A & B) Fluorescent intensities of individual vesicles from **(A)** wild type and **(B)** mutant HRS expressing HeLa cells after stimulation with 20ng/ml of EGF.

5.3. Summary of results

- EGF stimulation leads to an increase in the number of HRS positive endosomes in wild type and mutant cells
- Recruitment of HRS occurs on nascent vesicles.
- Phosphorylation plays a role in the response of HRS to TGFα but not to EGF.
- Despite HRS being responsible for recruiting WASH to endosomes, WASH is not recruited in response to EGF.
- Clathrin microdomains can be clearly visualised in APEX2-HRS expressing cells.

5.4. Discussion

The aim of this chapter was to study HRS dynamically in response to growth factor stimulation. This has previously been difficult to study due to the fact that overexpression of HRS leads to a dominant negative effect on endosomal function. Here, I used HeLa cells which are stably expressing either wild type GFP-HRS or a phosphorylation mutant GFP-HRS (YYFF). These proteins were introduced using the Flp-In system, generating isogenic cell lines which express the tagged proteins at near endogenous levels. These cells have allowed me to study the dynamics of HRS recruitment without disruption to endosome morphology or function.

A study from Haugen et al. at the end of 2017 examined the binding kinetics of HRS and Eps15 and how this regulated RTK degradation (Haugen, Skjeldal et al. 2017). They show a transient drop in fluorescence intensity of endosomal HRS around 8 minutes after EGF stimulation. They also report a decrease in the immobile fraction of HRS after performing FRAP experiments. These findings fit in with previous finding from my laboratory that show a greater proportion of phosphorylated HRS in the cytosol than on endosomes (Urbé, Mills et al. 2000). However, this transient drop in endosomal HRS fluorescence is a finding which I have been unable to observe in the experiments described above. Furthermore, FRAP experiments performed by a colleague found the opposite effect on the immobile fraction of HRS, observing an increase in the immobile fraction after stimulation with EGF (Macdonald, unpublished results). The results did show that the HRS phosphorylation mutant had no change to its immobile fraction in response to EGF stimulation, which is in accordance to the data from Haugen et al. (Haugen, Skjeldal et al. 2017).

The findings of this chapter disagree with some of the results reported by Haugen et al., despite the fact that both studies use stably expressing cell lines to study HRS dynamics. This drop in fluorescence may be a phenotype of human fibroblast (M1) cells used in their study and therefore not present in the HeLa cells used here (Haugen, Skjeldal et al. 2017). Another explanation for the discrepancies could be due to their co-expression of a MHC-class-II-associated chaperone invariant chain (Ii-Mep4), which leads to enlarged endosomes. This is an alternative to enlarging endosomes with the Rab5 mutant, Rab5(Q79L), and therefore doesn't affect Rab5 to Rab7 conversion or EEA1 binding dynamics (Skjeldal, Strunze et al. 2012). It may also be possible that the observations found within this study are an artefact of enlarging endosomes.

Binding dynamics of HRS was studied in another paper from 2018. Wenzel et al. used lentivirus-generated cell lines expressing various ESCRT components tagged to fluorescent markers (Wenzel, Schultz et al. 2018). This resulted in the expression of mCherry-HRS at near endogenous levels. Importantly, this study doesn't manipulate endosomes in any other way. Wenzel et al. showed that HRS, TSG101 and various

CHMPs are recruited to endosomal membranes in concerted waves. Each wave results in the formation of an intraluminal vesicle (ILV). It's worth noting that this study used HeLa cells and also didn't observe a drop in fluorescence intensity after 8 minutes of stimulation with EGF. Retrospective analysis of the data in this chapter reveals similar waves of HRS recruitment, though the waves are less clear than those reported by Wenzel et al. This is most likely due to the slight differences in the experimental set up. The study from Wenzel et al. stimulated with a high concentration of EGF (200ng/ml opposed to 20ng/ml) for 2 minutes before washing the growth factor out and imaging the cells. In my experiments EGF wasn't washed out and was present in the media throughout imaging.

The increase in HRS positive endosomes appears to be due to the recruitment of HRS to newly formed vesicles containing the endocytosed receptor. These vesicles appear not to be positive for PtdIns(3)*P*, as the number of GFP-FF positive endosomes did not increase with stimulation of EGF. This somewhat contradicts a study from early 2018 which examined the activation of an AGC kinase family member, SGK3 (Malik, Macartney et al. 2018). The study found that stimulation with 50ng/ml of IGF1 would increase the levels of PtdIns(3)*P*. This was performed on fixed samples in HEK293 cells and with a purified PtdIns(3)*P* probe, so did not dynamically examined the effect of IGF1 on the levels of PtdIns(3)*P*. It is feasible to believe the effect on PtdIns(3)*P* is cell type and growth factor dependent.

Recruitment of HRS appears to be mediated by the incoming cargo. HRS interacts with ubiquitylated receptors via double-sided UIM and VHS domains (Raiborg, Bache et al. 2002). This interaction could be responsible for recruitment of HRS to endosomes in response to EGF stimulation. Ubiquitin has previously been shown to be sufficient for the recruitment of the HRS binding partner, Eps15 (Gucwa and Brown 2014). It is possible that these two proteins are recruited to endosomes in a similar fashion to one another. Equally, recruitment of either protein could be mediated by the interaction with the other.

Different growth factors provide different phosphorylation profiles on both HRS and STAM (Row, Clague et al. 2005, Francavilla, Papetti et al. 2016). This may provide an

explanation for why the HRS phosphorylation mutant reacted differently to stimulation with EGF and TGFα. With recruitment and phosphorylation of HRS being mediated by the incoming cargo, it suggests that the endocytosed RTK is priming HRS to recruit the appropriate downstream effectors. EGF pushes the EGFR more towards degradation while TGFα encourages the receptor to be recycled back to the plasma membrane (Roepstorff, Grandal et al. 2009). Therefore, it is possible that stimulation with EGF will encourage the recruitment of the rest of the ESCRT machinery and stimulation with TGFα will lead HRS to recruit the WASH complex.

The APEX2-HRS cell lines allowed HRS to be visualised by electron microscopy. They reveal distinct microdomains that resemble, flat clathrin coated domains (Futter, Gibson et al. 1998, Sachse, Urbé et al. 2002). These domains can be difficult to visualise. HRS appears to be confined to microdomains on flat regions of endosomes. Further studies from our collaborators have visualised the phosphorylation mutant (YYFF) by EM (data not shown). The heavy staining from the DAB in the APEX2-YYFF expressing cells appeared to be less confined and was present on tubular regions of endosomes. Phosphorylation of HRS at Y329 and Y334 may be responsible for defining the distinct clathrin microdomains on endosomes. These domains are present in non-stimulated cells, however, so it is unclear how phosphorylation of HRS will impact this process.

Chapter six: Final discussion

6.1. APEX2 cell lines as tools

The APEX2 enzyme is a reagent for proximity ligation that offers advantages over the previously established BioID method due to its short labelling time (Mehta and Trinkle-Mulcahy 2016). Tagging with biotin occurs within minutes as opposed to hours, and therefore provides a 'snapshot' of interacting proteins. This enzyme was developed for the study of mitochondria and has been very effective at labelling the whole proteome of the organelle matrix. The mitochondria are, however enclosed organelles, limiting the diffusion of biotin-phenol free radicals. Extra precautions are required in order to examine the cytosolic face of organelles, including mitochondria, and thus, there are limited studies to my knowledge that utilise this enzyme on the cytosolic facing membrane of organelles (Hung, Zou et al. 2014, Hung, Lam et al. 2017). The first example of this kind of study was for the investigation of signalling events in primary cilia (Mick, Rodrigues et al. 2015). Access to the primary cilia is, however, tightly controlled. Though this study is the first to demonstrate that proximity labelling can be applied to proteomics of non-membrane bound organelles, this isn't a truly open example of proximity labelling proteomics.

In 2017, Lobingier et al., demonstrated that APEX2 can be used on endosomes and show that the enzyme can also be used to examine a specific protein network (Lobingier, Huttenhain et al. 2017). The authors tagged the β-adrenergic receptor with APEX2 to examine the proteins which engage with the receptor as it traffics from the plasma membrane to the endosome. They targeted the APEX2 enzyme to various compartments to use as 'compartment references' in order to spatially resolve the specific protein network from what they term as 'bystanders', i.e. proteins which are present in close proximity to the protein network but are not directly involved (Lobingier, Huttenhain et al. 2017). This approach works well for the β-adrenergic receptor, since it is a transmembrane receptor, and therefore only exists on lipid membranes. The additional challenge faced when applying these approaches to

proximity ligation of HRS interactors, is that the membrane interaction of HRS is very dynamic, with a large pool of HRS existing in the cytosol. This makes the task of deciding which compartment reference to use difficult.

More recently, a study investigating interactors of Rab21, utilised the APEX2 enzyme for proximity labelling proteomics (Del Olmo, Lauzier et al. 2019). As with HRS, Rabs also have a dynamic association with membranes. The study expressed APEX2 tagged Rab proteins using Flp-In T-REx cells. This allows the expression of the APEX2 enzyme to be modulated by stimulation with doxycycline. The study doesn't provide a comparison between the endogenous or APEX2-tagged Rabs, so it isn't clear how the expression of the APEX2 enzyme compares to the experiments described in chapter three of this thesis. The number of proteins identified in this study was much higher than in the APEX-HRS cell line dataset, which leads me to believe that APEX2 may have been expressed at higher levels than in my own experiments. This is further supported by the fact that 'bystanders' typically seen at endosomes, such as EEA1, were absent from my APEX2 cell line dataset (Figure 3.10). The Flp-In T-REx system may provide a better system for expressing APEX2-HRS constructs as it provides more control over the expression levels of the enzyme.

As mentioned in section 3.4, it may be possible that HRS is poorly labelled when using the APEX2 enzyme for proximity labelling. HRS and STAM tyrosine residues are highly phosphorylated in response to EGF stimulation (Omerovic, Hammond et al. 2012). Biotin-phenol radicals generated by APEX2 preferentially bind to tyrosine (Hung, Zou et al. 2014). This raises the question of whether tyrosine phosphorylation prevents APEX2 from labelling HRS with biotin-phenol. In addition, tyrosine is a hydrophobic amino acid and as a result only about ~15% of tyrosine residues are surface accessible in folded proteins (Lins, Thomas et al. 2003). In contrast, biotin radicals generated by BioID label lysine residues (Li, Li et al. 2017). Lysine residues are approximately 50% surface accessible, suggesting that proximity labelling by BioID, may be able to label proteins to a much larger extent. With the advent of TurboID, a version of the BioID system that is capable of labelling proteins with biotin within 10 minutes, it may provide a better option moving forward than the APEX2 enzyme (Branon, Bosch et al.

2018). It is worth noting that HRS also experiences ubiquitin modifications, and so a combination of the two approaches may be required.

For electron microscopy, these APEX2 cell lines did work well. The images shown in Figure 5.8 show HRS localised in regions which resemble flat clathrin microdomains. This raises the question of why the enzyme did not work as well for analysing protein-protein interactions as it did for EM. The reason is most likely due to how the heavy stain is generated. The APEX2 enzyme generates DAB free radical, similar to creating biotin-phenol free radical. However, the DAB free radical species is not then tagging neighbouring proteins. It forms a precipitate at the site where it was formed (Martell, Deerinck et al. 2012). This mitigates the potential labelling issues found when labelling HRS with biotin-phenol.

6.2. HRS recruitment to endosomes

6.2.1. DTX3L and HRS recruitment

Recruitment of the ubiquitin E3 ligase, DTX3L, to endosomes has previously been reported after stimulation with CXCL12 (Holleman and Marchese 2014). Furthermore, when DTX3L is knocked down by siRNA, cells which have been stimulated with CXCL12 show reduced recruitment of ESCRT-0 proteins onto endosomes. I have now shown that DTX3L interacts with HRS in an EGF dependent manner (Figure 3.10). It's possible that this interaction acts to modulate the levels of HRS ubiquitylation and prevent HRS exhibiting auto-inhibition of itself through the UIM binding to its own ubiquitin modifications (Hoeller, Crosetto et al. 2006), allowing the UIM to be open for interactions with other ubiquitylated proteins. This interpretation is consistent with both my observations and the observation from Holleman and Marchese that ESCRT-0 exhibits a reduced endosomal localisation due to DTX3L siRNA KD (Holleman and Marchese 2014).

In the work presented in chapter five, I show that HRS is recruited directly to endocytosed vesicles containing EGF. My leading hypothesis for this observation is that HRS is recruited to these vesicles by the interaction between the ubiquitylated EGFR and the UBDs of HRS. Traditionally, recruitment of HRS to endosomes is thought to be mediated by its FYVE domain (Raiborg, Bremnes et al. 2001), however, the effect of EGF stimulation on the levels of PtdIns(3)*P* don't correlate with the recruitment of HRS. Since DTX3L has been shown to modulate the level of ubiquitylation of HRS and STAM by AIP4, it would therefore be interesting to incorporate this finding into the work described in chapter five regarding HRS recruitment.

6.2.2. HRS recruitment in response to TGFα

Stimulation with EGF leads to an increase in the number of HRS positive puncta. This recruitment was unaffected in the HRS phosphorylation mutant (YYFF) (see figure 5.2). EGF leads to a proportion of the internalised EGFR to be degraded, with the remainder recycled back to the plasma membrane. Stimulation of the EGFR with TGFα however leads to the majority of the receptor to be recycled (Roepstorff, Grandal et al. 2009). When assessing the recruitment of HRS in response to TGFα stimulation, I found that the HRS mutant (YYFF) to be recruited less than wild type HRS (Figure 5.7). This leads me to suggest that tyrosine residues 329 and 334 may be involved in recruiting recycling machinery to endosomes. Endosomal recruitment of the recycling complex WASH is mediated in part by HRS, though the mechanism by which this occurs is unclear (MacDonald, Brown et al. 2018).

Recycling of the EGFR when stimulated with TGFα is believed to be due to the dissociation rate between the ligand and the receptor. TGFα dissociates from the EGFR at a less acidic pH than EGF and so is uncoupled from the EGFR at the early endosome (Ebner and Derynck 1991). This was thought to encourage the recycling of the receptor rather than its degradation. The data described in the present study suggests that this may be a more active process and dependent on the particular phosphorylation status of HRS.

6.3. HRS 'priming'

This leads me to a working model to guide future work, whereby HRS plays a more central role in endosomal sorting and is 'primed' to respond depending on the incoming cargo (Figure 6.1). HRS is primed based on the phosphorylation and ubiquitin code, determined by upstream signalling molecules. Receptors that are primarily degraded, phosphorylate HRS in a way that primes it for degradation processes, encouraging HRS to recruit the degradation machinery. Conversely, receptors that need recycling will lead to a different pattern of phosphorylation and ubiquitin modification that encourage the recruitment of recycling machinery components, such as WASH. The particular pattern of post-translational modifications leads to a differential response with regards to endosomal sorting, trafficking and signalling.

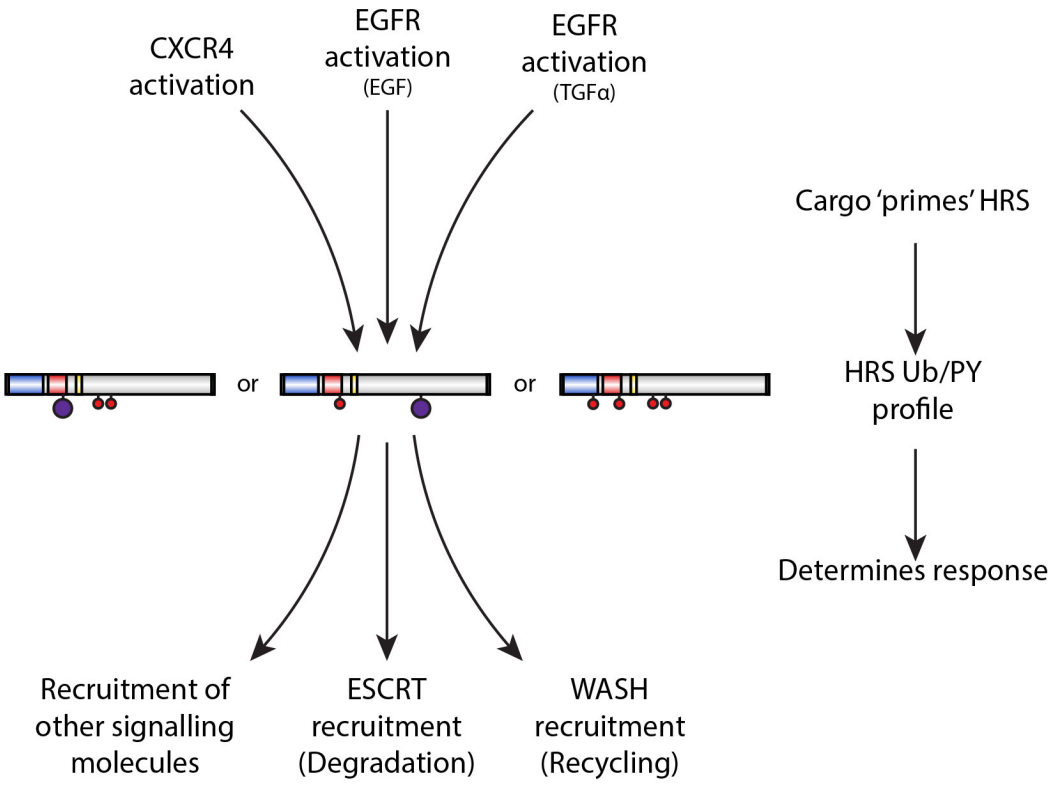

Figure 6.1 A working model for HRS 'priming'. The activated receptors being trafficked to the endosomes 'primes' HRS by inducing a particular pattern of phosphorylation (red circles) and ubiquitin (purple circles) modifications. This profile of modifications then determines the response of HRS to the incoming cargo by recruitment of either degradation machinery, recycling machinery or other signalling molecules.

6.4. Future work

6.4.1. Further advancements of the APEX2 and FRET cell lines generated

The development of molecular tools and cell lines was a major objective of the work undertaken. Further work is, however, required in order to improve upon those generated here. Measurements of cAMP at endosomes may be a more challenging endeavour due to the diffusion rate of the second messenger. Regulation of PKA is more tightly controlled and so improvements to the cell lines generated may be possible. I had generated cell lines by random integration so that I could choose an appropriately expressing cell line. With hindsight, it may have been more beneficial to use inducible Flp-In cell lines such as the Flp-In T-REx system. This would have allowed for more stringent control over the expression of the cytosolic and endosomal PKA biosensors.

Generation of the APEX2-HRS cell lines using the method described was the most applicable in terms of HRS biology. It led to the expression of the APEX2-HRS constructs at near endogenous levels. This was appropriate for the use of the cells lines in electron microscopy but may have led to the APEX2 enzyme being expressed at too low of a level to achieve reliable labelling with biotin phenol. Utilising the Flp-In T-REx system may also allow for better control over the expression of these constructs. This would allow for the expression to be fine-tuned to better manage the balance between APEX2 expression and negatively impacting HRS function.

As HRS is heavily tyrosine phosphorylated in response to many growth factors, labelling with biotin phenol by APEX2 may lead to the poor labelling of HRS. In this vein, it may be more appropriate to use the turboID enzyme for proximity labelling of HRS interactors, as this enzyme leads to the labelling of lysine residues instead of tyrosine. The reduced labelling time of this enzyme over its predecessors, may allow for appropriate time resolution that is required for studying the EGF dependent

binding partners of HRS. However, since HRS also experiences ubiquitin modification, the combination of both enzymes used in conjunction may be required.

6.4.2. Further work on the recruitment of HRS

My leading hypothesis for the recruitment of HRS to EGF positive vesicles is through interaction of its UBDs with ubiquitylated receptors. An obvious next step to assess this notion would be to repeat the endosomal recruitment experiments with perturbations to the UIM and VHS domain of HRS, as well as to the FYVE domain. If the EGF dependent increase in HRS positive puncta is abolished with the UBD mutants, this would provide strong evidence that incoming cargo is responsible for the initial recruitment of HRS.

It would also be interesting to see how DTX3L affects HRS recruitment. Assessing how treatment with DTX3L siRNA would affect the dynamics of HRS recruitment would take the work by Holleman and Marchese a step further. The experiment described by their study was in the context of CXCL12 stimulation, it would also be interesting to see if acute stimulation with this ligand also had an impact on HRS recruitment. Furthermore, DTX3L was identified in the mass spectrometry dataset, which was in the context of EGF stimulation. DTX3L is recruited to endosomes in response to CXCL12 stimulation, it may also be recruited to endosomes in response to EGF stimulation. Visualisation of DTX3L recruitment may provide further insights into the regulation of HRS recruitment.

6.4.3. Further work on assessing HRS 'priming'

HRS has previously been shown to be partly responsible for the recruitment of WASH (MacDonald, Brown et al. 2018). EGF stimulation didn't lead to an increase in WASH positive puncta despite increasing the number of HRS positive puncta. As mentioned above, TGFα is an EGFR ligand that encourages the receptor to be recycled rather than degraded. It would be intriguing to determine if TGFα would have a different effect on

the recruitment of WASH than EGF. I hypothesise that the different responses of HRS are due to differential phosphorylation and ubiquitin modifications to HRS. Differential phosphorylation profile of HRS has been observed with different growth factor receptors (Row, Clague et al. 2005, Francavilla, Papetti et al. 2016). Tyrosine residues 329 and 334 were used in this study due to their identification by Urbé et al. (Urbé, Sachse et al. 2003). Phosphorylation at these residues appeared to affect the recruitment of HRS in response to TGFα but not EGF (Figures 5.6 and 5.7). Further tyrosine mutants could be generated to determine if any of them are involved in the EGF induced recruitment of HRS.

The identification of the E3 ligase DTX3L highlights the potential role of HRS ubiquitylation in ligand-induced HRS recruitment. Manipulation to the ubiquitylation of HRS is likely to alter the dynamics of its recruitment. This can be achieved through perturbations to DTX3L, AIP4 or by direct manipulations to lysine residues on HRS itself. The resulting experiments would hopefully provide further evidence to support the concept of HRS 'priming' as well as provide further mechanistic insights into this process.

6.5. Concluding remarks

The aim of the work described in this thesis, was to establish HRS as a signalling adaptor involved in the crosstalk between RTKs and GPCRS, as well as ascertain the function of HRS phosphorylation. I was unable to confirm the EGF dependent interactions of HRS with the collection of G-proteins found in the preliminary work described in the beginning of chapter three. I did, however, identify a connection between HRS and the E3 ligase DTX3L. DTX3L has been implicated with the signalling of CXCR4. This interaction between HRS and DTX3L provides supporting evidence to the notion that HRS may be acting as a signalling adaptor in order to mediate certain aspects of RTK and GPCR crosstalk.

My work on FRET based biosensors for the measurements of endosomal cAMP production and endosomal PKA signalling will need further development. The purpose of generating these tools was to use them to provide further evidence of HRS mediating the crosstalk between RTKs and GPCRs. Due to the diffusion rate of cAMP, it may not be possible to create a tool specifically for the study of endosomal cAMP production. It may still be possible to improve the cell lines created for endosomal PKA signalling and generate reliable FRET measurements.

Finally, by visualising the dynamics of HRS recruitment in response to acute stimulation of EGF, I show that HRS is recruited directly to EGF positive vesicles, in a manner that appears to be independent of PtdIns(3)*P* levels. Furthermore, I show a difference in the recruitment of the tyrosine mutant HRS (YYFF) compared to wild type HRS in response to TGFα stimulation, but not with EGF stimulation. This provides evidence that the phosphorylation profile of HRS may dictate the way in which it responds to incoming cargo.

Appendix

Supplementary movie 1 Pseudo colour movie of FRET from AKAR4-FF expressing cells stimulated with Isoproterenol. Pixel intensities derived from a binary mask of the acceptor channel.

Supplementary movie 2 Pseudo colour movie of FRET from the same AKAR4-FF expressing cells stimulated with Isoproterenol. Pixel intensities derived from a Laplacian filter of the acceptor channel.

Supplementary movie 3 GFP-HRS expressing HeLa cells stimulated with 20ng/ml of EGF. Movie of time-lapse images in Figure 5.1.

Supplementary movie 4 GFP-HRS expressing HeLa cells stimulated with EGF-AF555. Movie of time-lapse images in Figure 5.4.

Supplementary movie 5 GFP-WASH expressing HeLa cells stimulated with 20ng/ml of EGF. Movie of time-lapse images in Figure 5.5.

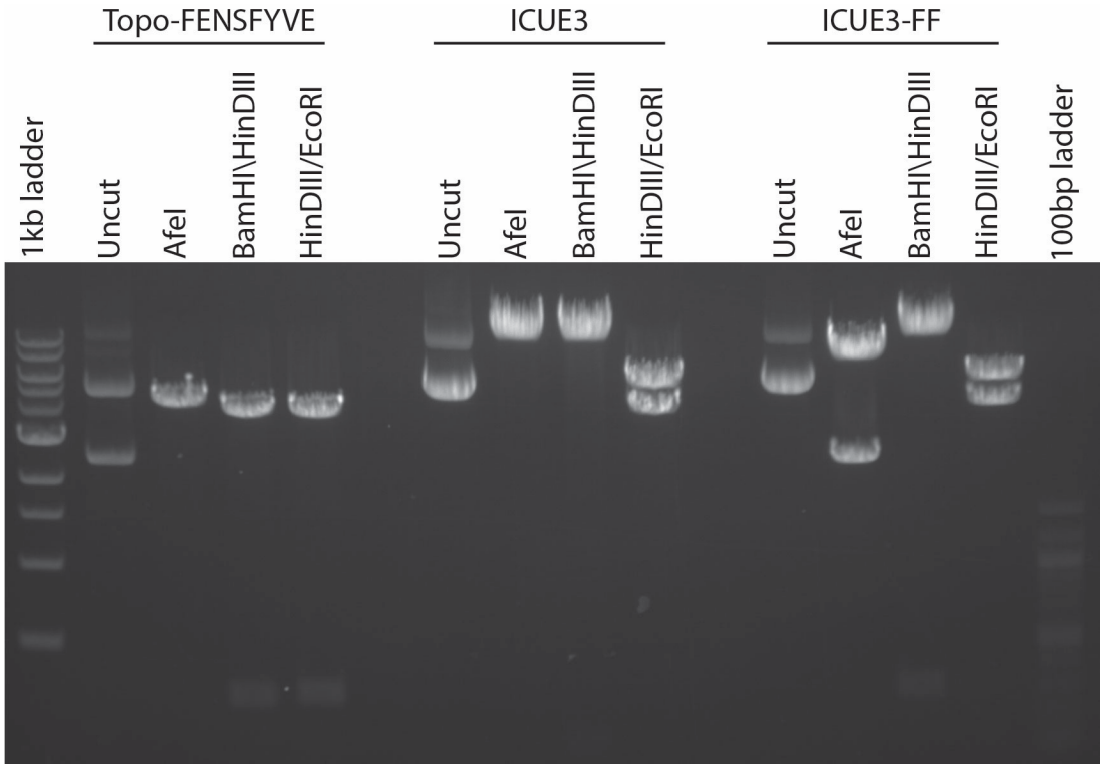

Supplementary Figure 1 Test digests of the intermediate vectors generated with creating endosomal ICUE3. Plasmid maps of the vectors used with restriction sites can be found in Supplementary Figures 2-4. The final generated vectors were sent for sequencing.

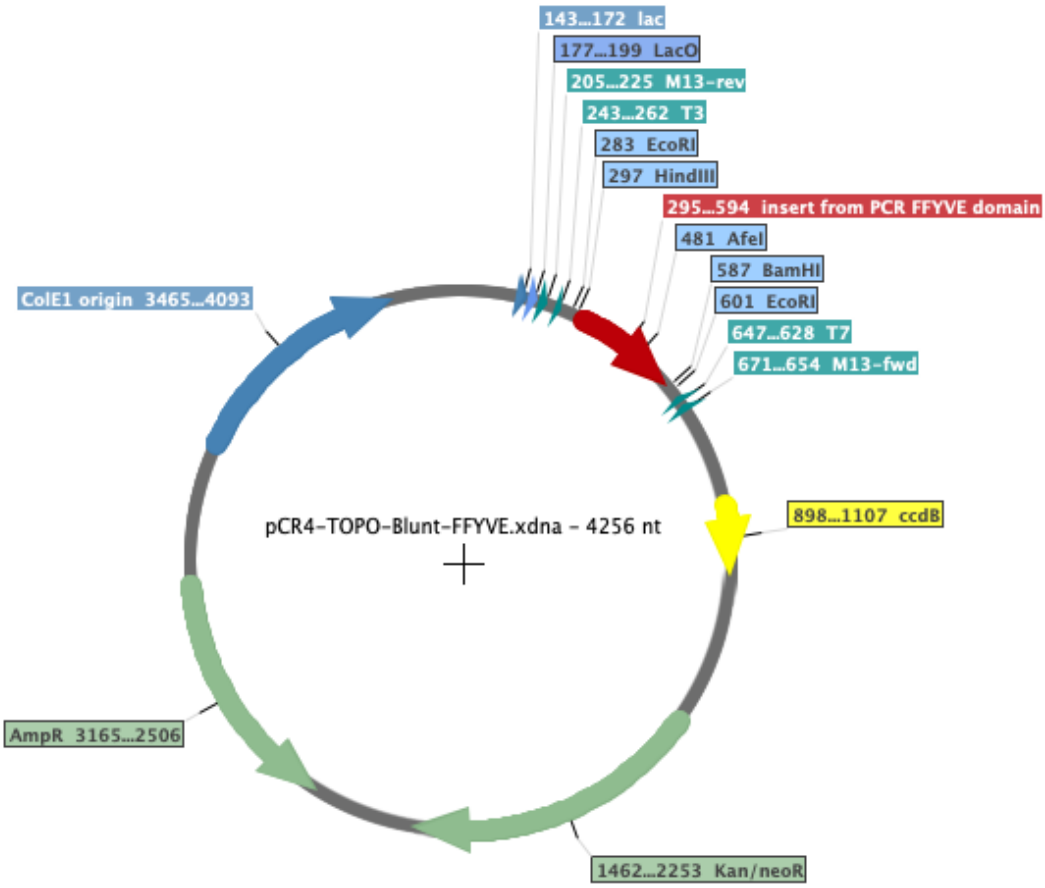

Supplementary Figure 2 Plasmid map of pCR4-TOPO-Blunt-FFYVE vector. Plasmid map show the locations of the restriction sites used in Supplementary Figure 1.

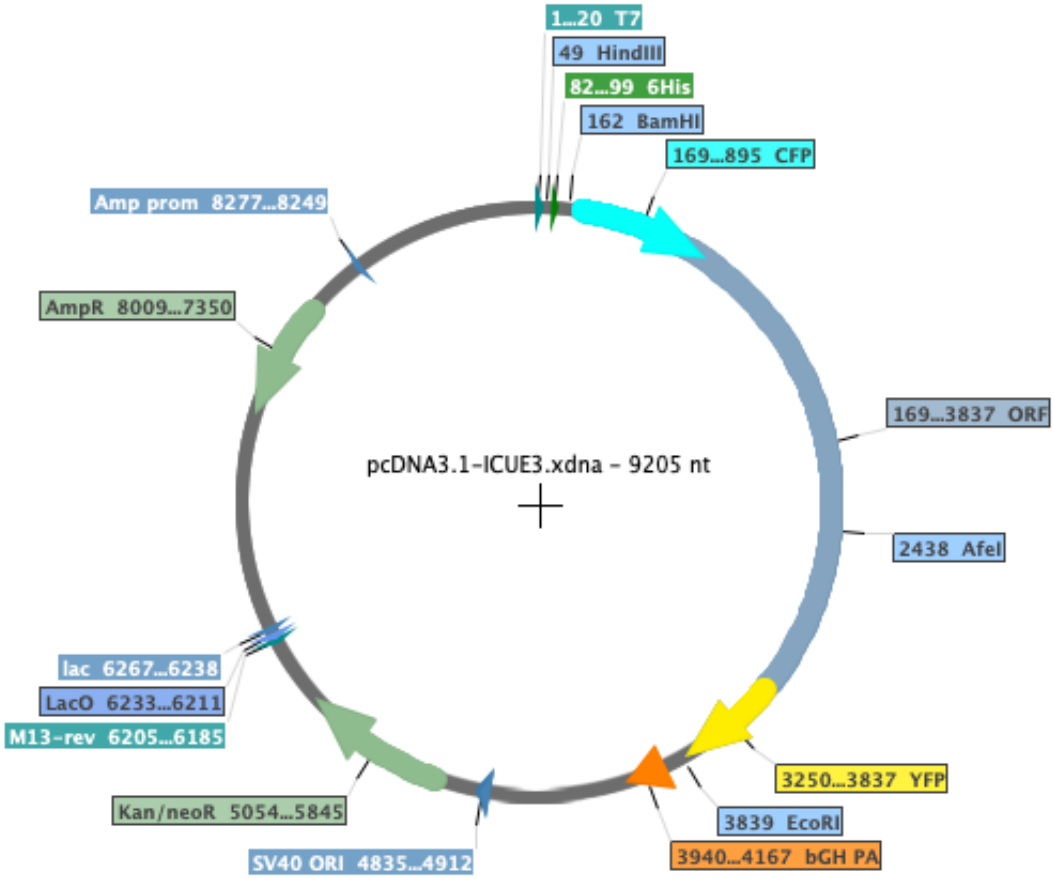

Supplementary Figure 3 Plasmid map of pcDNA3.1-ICUE3 vector. Plasmid map show the locations of the restriction sites used in Supplementary Figure 1.

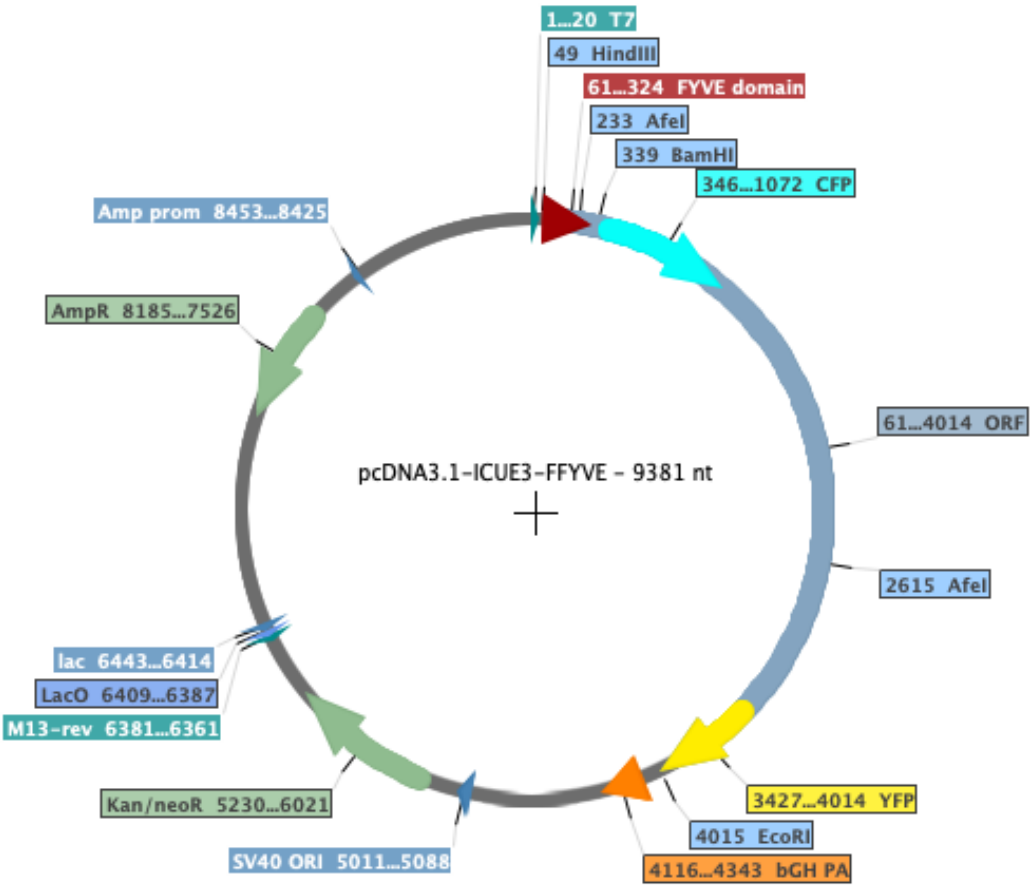

Supplementary Figure 4 Plasmid map of pcDNA3.1-ICUE3-FFYVE vector. Plasmid map show the locations of the restriction sites used in Supplementary Figure 1.

Bibliography

Akutsu, M., M. Kawasaki, Y. Katoh, T. Shiba, Y. Yamaguchi, R. Kato, K. Kato, K. Nakayama and S. Wakatsuki (2005). "Structural basis for recognition of ubiquitinated cargo by Tom1-GAT domain." FEBS Lett **579**(24): 5385-5391.

Alam, S. L., J. Sun, M. Payne, B. D. Welch, B. K. Blake, D. R. Davis, H. H. Meyer, S. D. Emr and W. I. Sundquist (2004). "Ubiquitin interactions of NZF zinc fingers." Embo J **23**(7): 1411-1421.

Alderton, F., S. Rakhit, K. C. Kong, T. Palmer, B. Sambi, S. Pyne and N. J. Pyne (2001). "Tethering of the platelet-derived growth factor beta receptor to G-protein-coupled receptors. A novel platform for integrative signaling by these receptor classes in mammalian cells." J Biol Chem **276**(30): 28578-28585.

Anderson, R. G., M. S. Brown and J. L. Goldstein (1977). "Role of the coated endocytic vesicle in the uptake of receptor-bound low density lipoprotein in human fibroblasts." Cell **10**(3): 351-364.

Anderson, R. G., J. L. Goldstein and M. S. Brown (1977). "A mutation that impairs the ability of lipoprotein receptors to localise in coated pits on the cell surface of human fibroblasts." Nature **270**(5639): 695-699.

Appelmans, F., R. Wattiaux and C. De Duve (1955). "Tissue fractionation studies. 5. The association of acid phosphatase with a special class of cytoplasmic granules in rat liver." Biochem J **59**(3): 438-445.

Arighi, C. N., L. M. Hartnell, R. C. Aguilar, C. R. Haft and J. S. Bonifacino (2004). "Role of the mammalian retromer in sorting of the cation-independent mannose 6-phosphate receptor." J Cell Biol **165**(1): 123-133.

Ariotti, N., T. E. Hall, J. Rae, C. Ferguson, K. A. McMahon, N. Martel, R. E. Webb, R. I. Webb, R. D. Teasdale and R. G. Parton (2015). "Modular Detection of GFP-Labeled Proteins for Rapid Screening by Electron Microscopy in Cells and Organisms." Dev Cell **35**(4): 513-525.

Arrigo, A. P., K. Tanaka, A. L. Goldberg and W. J. Welch (1988). "Identity of the 19S 'prosome' particle with the large multifunctional protease complex of mammalian cells (the proteasome)." Nature **331**(6152): 192-194.

Arstila, A. U. and B. F. Trump (1968). "Studies on cellular autophagocytosis. The formation of autophagic vacuoles in the liver after glucagon administration." Am J Pathol **53**(5): 687-733.

Arteaga, C. L. and J. A. Engelman (2014). "ERBB receptors: from oncogene discovery to basic science to mechanism-based cancer therapeutics." Cancer Cell **25**(3): 282-303.

Asakura, M., M. Kitakaze, S. Takashima, Y. Liao, F. Ishikura, T. Yoshinaka, H. Ohmoto, K. Node, K. Yoshino, H. Ishiguro, H. Asanuma, S. Sanada, Y. Matsumura, H. Takeda, S. Beppu, M. Tada, M. Hori and S. Higashiyama (2002). "Cardiac hypertrophy is inhibited by antagonism of ADAM12 processing of HB-EGF: metalloproteinase inhibitors as a new therapy." Nat Med **8**(1): 35-40.

Asao, H., Y. Sasaki, T. Arita, N. Tanaka, K. Endo, H. Kasai, T. Takeshita, Y. Endo, T. Fujita and K. Sugamura (1997). "Hrs is associated with STAM, a signal-transducing adaptor molecule." J. Biol. Chem. **272**: 32785-32791.

Ashford, T. P. and K. R. Porter (1962). "Cytoplasmic components in hepatic cell lysosomes." J Cell Biol **12**: 198-202.

Attramadal, H., J. L. Arriza, C. Aoki, T. M. Dawson, J. Codina, M. M. Kwatra, S. H. Snyder, M. G. Caron and R. J. Lefkowitz (1992). "Beta-arrestin2, a novel member of the arrestin/beta-arrestin gene family." J Biol Chem **267**(25): 17882-17890.

Babst, M., D. J. Katzmann, E. J. Estepa-Sabal, T. Meerloo and S. D. Emr (2002). "Escrt-III: an endosome-associated heterooligomeric protein complex required for mvb sorting." Dev Cell **3**(2): 271-282.

Babst, M., D. J. Katzmann, W. B. Snyder, B. Wendland and S. D. Emr (2002). "Endosome-associated complex, ESCRT-II, recruits transport machinery for protein sorting at the multivesicular body." Dev Cell **3**(2): 283-289.

Bache, K. G., A. Brech, A. Mehlum and H. Stenmark (2003). "Hrs regulates multivesicular body formation via ESCRT recruitment to endosomes." J Cell Biol **162**(3): 435-442.

Bache, K. G., C. Raiborg, A. Mehlum, I. H. Madshus and H. Stenmark (2002). "Phosphorylation of Hrs downstream of the epidermal growth factor receptor." Eur J Biochem **269**(16): 3881-3887.

Bache, K. G., C. Raiborg, A. Mehlum and H. Stenmark (2003). "STAM and Hrs are subunits of a multivalent ubiquitin-binding complex on early endosomes." J Biol Chem **278**(14): 12513-12521.

Bache, K. G., T. Slagsvold, A. Cabezas, K. R. Rosendal, C. Raiborg and H. Stenmark (2004). "The growth-regulatory protein HCRP1/hVps37A is a subunit of mammalian ESCRT-I and mediates receptor down-regulation." Mol Biol Cell **15**(9): 4337-4346.

Bae, J. H., E. D. Lew, S. Yuzawa, F. Tome, I. Lax and J. Schlessinger (2009). "The selectivity of receptor tyrosine kinase signaling is controlled by a secondary SH2 domain binding site." Cell **138**(3): 514-524.

Banta, L. M., J. S. Robinson, D. J. Klionsky and S. D. Emr (1988). "Organelle assembly in yeast: characterization of yeast mutants defective in vacuolar biogenesis and protein sorting." J Cell Biol **107**(4): 1369-1383.

Barak, L. S., K. Warabi, X. Feng, M. G. Caron and M. M. Kwatra (1999). "Real-time visualization of the cellular redistribution of G protein-coupled receptor kinase 2 and beta-arrestin 2 during homologous desensitization of the substance P receptor." J Biol Chem **274**(11): 7565-7569.

Barton, W. A., D. Tzvetkova-Robev, E. P. Miranda, M. V. Kolev, K. R. Rajashankar, J. P. Himanen and D. B. Nikolov (2006). "Crystal structures of the Tie2 receptor ectodomain and the angiopoietin-2-Tie2 complex." Nat Struct Mol Biol **13**(6): 524-532.

Beghein, E. and J. Gettemans (2017). "Nanobody Technology: A Versatile Toolkit for Microscopic Imaging, Protein-Protein Interaction Analysis, and Protein Function Exploration." Front Immunol **8**: 771.

Beguinot, L., R. M. Lyall, M. C. Willingham and I. Pastan (1984). "Down-regulation of the epidermal growth factor receptor in KB cells is due to receptor internalization and subsequent degradation in lysosomes." Proc Natl Acad Sci U S A **81**(8): 2384-2388.

Behnia, R. and S. Munro (2005). "Organelle identity and the signposts for membrane traffic." Nature **438**(7068): 597-604.

Bellare, P., E. C. Small, X. Huang, J. A. Wohlschlegel, J. P. Staley and E. J. Sontheimer (2008). "A role for ubiquitin in the spliceosome assembly pathway." Nat Struct Mol Biol **15**(5): 444-451.

Benovic, J. L., H. Kuhn, I. Weyand, J. Codina, M. G. Caron and R. J. Lefkowitz (1987). "Functional desensitization of the isolated beta-adrenergic receptor by the beta-adrenergic receptor kinase: potential role of an analog of the retinal protein arrestin (48-kDa protein)." Proc Natl Acad Sci U S A **84**(24): 8879-8882.

Benovic, J. L., R. H. Strasser, M. G. Caron and R. J. Lefkowitz (1986). "Beta-adrenergic receptor kinase: identification of a novel protein kinase that phosphorylates the agonist-occupied form of the receptor." Proc Natl Acad Sci U S A **83**(9): 2797-2801.

Bhagatji, P., R. Leventis, J. Comeau, M. Refaei and J. R. Silvius (2009). "Steric and not structure-specific factors dictate the endocytic mechanism of glycosylphosphatidylinositol-anchored proteins." J Cell Biol **186**(4): 615-628.

Bienko, M., C. M. Green, N. Crosetto, F. Rudolf, G. Zapart, B. Coull, P. Kannouche, G. Wider, M. Peter, A. R. Lehmann, K. Hofmann and I. Dikic (2005). "Ubiquitin-binding domains in Y-family polymerases regulate translesion synthesis." Science **310**(5755): 1821-1824.

Bilodeau, P. S., J. L. Urbanowski, S. C. Winistorfer and R. C. Piper (2002). "The Vps27p Hse1p complex binds ubiquitin and mediates endosomal protein sorting." Nat Cell Biol **4**(7): 534-539.

Biscardi, J. S., M. C. Maa, D. A. Tice, M. E. Cox, T. H. Leu and S. J. Parsons (1999). "c-Src-mediated phosphorylation of the epidermal growth factor receptor on Tyr845 and Tyr1101 is associated with modulation of receptor function." J Biol Chem **274**(12): 8335-8343.

Bishop, N. and P. Woodman (2001). "TSG101/mammalian VPS23 and mammalian VPS28 interact directly and are recruited to VPS4-induced endosomes." J Biol Chem **276**(15): 11735-11742.

Blake, T. J., M. Shapiro, H. C. Morse, 3rd and W. Y. Langdon (1991). "The sequences of the human and mouse c-cbl proto-oncogenes show v-cbl was generated by a large truncation encompassing a proline-rich domain and a leucine zipper-like motif." Oncogene **6**(4): 653-657.

Boyer, L., L. Turchi, B. Desnues, A. Doye, G. Ponzio, J. L. Mege, M. Yamashita, Y. E. Zhang, J. Bertoglio, G. Flatau, P. Boquet and E. Lemichez (2006). "CNF1-induced ubiquitylation and proteasome destruction of activated RhoA is impaired in Smurf1-/- cells." Mol Biol Cell **17**(6): 2489-2497.

Brand, S. H., E. J. Holtzman, D. A. Scher, D. A. Ausiello and J. L. Stow (1996). "Role of myristoylation in membrane attachment and function of G alpha i-3 on Golgi membranes." Am J Physiol **270**(5 Pt 1): C1362-1369.

Branon, T. C., J. A. Bosch, A. D. Sanchez, N. D. Udeshi, T. Svinkina, S. A. Carr, J. L. Feldman, N. Perrimon and A. Y. Ting (2018). "Efficient proximity labeling in living cells and organisms with TurboID." Nat Biotechnol **36**(9): 880-887.

Brzovic, P. S., A. Lissounov, D. E. Christensen, D. W. Hoyt and R. E. Klevit (2006). "A UbcH5/ubiquitin noncovalent complex is required for processive BRCA1-directed ubiquitination." Mol Cell **21**(6): 873-880.

Bucci, C., R. G. Parton, I. Mather, H. Stunnnenberg, K. Simons, B. Hoflack and M. Zerial (1992). "The small GTPase rab5 functions as a regulatory factor in the early endocytic pathway." Cell **70**: 715-728.

Buck, L. and R. Axel (1991). "A novel multigene family may encode odorant receptors: a molecular basis for odor recognition." Cell **65**(1): 175-187.

Bugarcic, A., Y. Zhe, M. C. Kerr, J. Griffin, B. M. Collins and R. D. Teasdale (2011). "Vps26A and Vps26B subunits define distinct retromer complexes." Traffic **12**(12): 1759-1773.

Burke, P., K. Schooler and H. S. Wiley (2001). "Regulation of epidermal growth factor signaling by endocytosis and intracellular trafficking." Mol. Biol. Cell **12**: 1897-1910.

Calebiro, D., V. O. Nikolaev, M. C. Gagliani, T. de Filippis, C. Dees, C. Tacchetti, L. Persani and M. J. Lohse (2009). "Persistent cAMP-signals triggered by internalized G-protein-coupled receptors." PLoS Biol **7**(8): e1000172.

Campsteijn, C., M. Vietri and H. Stenmark (2016). "Novel ESCRT functions in cell biology: spiraling out of control?" Curr Opin Cell Biol **41**: 1-8.

Canal, F., E. Anthony, A. Lescure, E. Del Nery, J. Camonis, F. Perez, B. Ragazzon and C. Perret (2015). "A kinome siRNA screen identifies HGS as a potential target for liver cancers with oncogenic mutations in CTNNB1." BMC Cancer **15**: 1020.

Carlsson, S. R., J. Roth, F. Piller and M. Fukuda (1988). "Isolation and characterization of human lysosomal membrane glycoproteins, h-lamp-1 and h-lamp-2. Major sialoglycoproteins carrying polylactosaminoglycan." J Biol Chem **263**(35): 18911-18919.

Carlton, J. G. and J. Martin-Serrano (2007). "Parallels between cytokinesis and retroviral budding: a role for the ESCRT machinery." Science **316**(5833): 1908-1912.

Carpenter, G., L. King, Jr. and S. Cohen (1978). "Epidermal growth factor stimulates phosphorylation in membrane preparations in vitro." Nature **276**(5686): 409-410.

Carpenter, G., K. J. Lembach, M. M. Morrison and S. Cohen (1975). "Characterization of the binding of 125-I-labeled epidermal growth factor to human fibroblasts." J Biol Chem **250**(11): 4297-4304.

Carraway, K. L., 3rd and L. C. Cantley (1994). "A neu acquaintance for erbB3 and erbB4: a role for receptor heterodimerization in growth signaling." Cell **78**(1): 5-8.

Ceresa, B. P. and S. L. Schmid (2000). "Regulation of signal transduction by endocytosis." Curr. Op. Cell Biol. **12**: 204-210.

Cerione, R. A., D. R. Sibley, J. Codina, J. L. Benovic, J. Winslow, E. J. Neer, L. Birnbaumer, M. G. Caron and R. J. Lefkowitz (1984). "Reconstitution of a hormone-sensitive adenylate cyclase system. The pure beta-adrenergic receptor and guanine nucleotide regulatory protein confer hormone responsiveness on the resolved catalytic unit." J Biol Chem **259**(16): 9979-9982.

Cerione, R. A., B. Strulovici, J. L. Benovic, C. D. Strader, M. G. Caron and R. J. Lefkowitz (1983). "Reconstitution of beta-adrenergic receptors in lipid vesicles: affinity chromatography-purified receptors confer catecholamine responsiveness on a heterologous adenylate cyclase system." Proc Natl Acad Sci U S A **80**(16): 4899-4903.

Chen, H., J. Ma, W. Li, A. V. Eliseenkova, C. Xu, T. A. Neubert, W. T. Miller and M. Mohammadi (2007). "A molecular brake in the kinase hinge region regulates the activity of receptor tyrosine kinases." Mol Cell **27**(5): 717-730.

Chen, J., N. Hou, C. Zhang, Y. Teng, X. Cheng, Z. Li, J. Ren, J. Zeng, R. Li, W. Wang, X. Yang and Y. Lan (2015). "Smooth Muscle Hgs Deficiency Leads to Impaired Esophageal Motility." Int J Biol Sci **11**(7): 794-802.

Chin, L.-S., M. C. Raynor, X. Wei, H.-Q. Chen and L. Li (2001). "Hrs interacts with sorting Nexin 1 and regulates degradation of Epidermal Growth Factor Receptor." J. Biol. Chem. **276**: 7069-7078.

Christoforidis, S., M. Miaczynska, K. Ashman, M. Wilm, L. Zhao, S.-C. Yip, M. D. Waterfield, J. M. Backer and M. Zerial (1999). "Phosphatidylinositol-3-OH kinases are rab5 effectors." Nature Cell Biol. **1**: 249-252.

Chu, T., J. Sun, S. Saksena and S. D. Emr (2006). "New component of ESCRT-I regulates endosomal sorting complex assembly." J Cell Biol **175**(5): 815-823.

Ciechanover, A. (2005). "Intracellular protein degradation: from a vague idea thru the lysosome and the ubiquitin-proteasome system and onto human diseases and drug targeting." Cell Death Differ **12**(9): 1178-1190.

Ciechanover, A., Y. Hod and A. Hershko (1978). "A heat-stable polypeptide component of an ATP-dependent proteolytic system from reticulocytes. ." Biochem Biophys Res Commun **425**(3): 565-570.

Citri, A. and Y. Yarden (2006). "EGF-ERBB signalling: towards the systems level." Nat Rev Mol Cell Biol **7**(7): 505-516.

Clague, M. and S. Urbe (2010). "Ubiquitin: Same Molecule, Different Degradation Pathways." Cell **143**(5): 682-685.

Clague, M. J. and S. Urbe (2003). "Hrs function: viruses provide the clue." Trends Cell Biol **13**(12): 603-606.

Clark, S. L., Jr. (1957). "Cellular differentiation in the kidneys of newborn mice studies with the electron microscope." J Biophys Biochem Cytol **3**(3): 349-362.

Claude, A. (1946). "Fractionation of mammalian liver cells by differential centrifugation; experimental procedures and results." J Exp Med **84**: 61-89.

Cohen, S. (1962). "Isolation of a mouse submaxillary gland protein accelerating incisor eruption and eyelid opening in the new-born animal." J Biol Chem **237**: 1555-1562.

Cohen, S. (1965). "The stimulation of epidermal proliferation by a specific protein (EGF)." Dev Biol **12**(3): 394-407.

Cohen, S. and G. Carpenter (1975). "Human epidermal growth factor: isolation and chemical and biological properties." Proc Natl Acad Sci U S A **72**(4): 1317-1321.

Cohen, S. and G. A. Elliott (1963). "The stimulation of epidermal keratinization by a protein isolated from the submaxillary gland of the mouse." J Invest Dermatol **40**: 1-5.

Cohen, S. and R. Levi-Montalcini (1956). "A NERVE GROWTH-STIMULATING FACTOR ISOLATED FROM SNAKE VENOM." Proc Natl Acad Sci U S A **42**(9): 571-574.

Cohen, S., R. Levi-Montalcini and V. Hamburger (1954). "A NERVE GROWTH-STIMULATING FACTOR ISOLATED FROM SARCOM AS 37 AND 180." Proc Natl Acad Sci U S A **40**(10): 1014-1018.

Cotecchia, S., S. Exum, M. G. Caron and R. J. Lefkowitz (1990). "Regions of the alpha 1-adrenergic receptor involved in coupling to phosphatidylinositol hydrolysis and enhanced sensitivity of biological function." Proc Natl Acad Sci U S A **87**(8): 2896-2900.

Cozier, G. E., J. Carlton, A. H. McGregor, P. A. Gleeson, R. D. Teasdale, H. Mellor and P. J. Cullen (2002). "The phox homology (PX) domain-dependent, 3-phosphoinositide-mediated association of sorting nexin-1 with an early sorting endosomal compartment is required for its ability to regulate epidermal growth factor receptor degradation." J Biol Chem **277**(50): 48730-48736.

Dalle, S., W. Ricketts, T. Imamura, P. Vollenweider and J. M. Olefsky (2001). "Insulin and insulin-like growth factor I receptors utilize different G protein signaling components." J Biol Chem **276**(19): 15688-15695.

Daub, H., C. Wallasch, A. Lankenau, A. Herrlich and A. Ullrich (1997). "Signal characteristics of G protein-transactivated EGF receptor." Embo j **16**(23): 7032-7044.

Daub, H., F. U. Weiss, C. Wallasch and A. Ullrich (1996). "Role of transactivation of the EGF receptor in signalling by G-protein-coupled receptors." Nature **379**(6565): 557-560.

de Almeida, J. B., E. J. Holtzman, P. Peters, L. Ercolani, D. A. Ausiello and J. L. Stow (1994). "Targeting of chimeric G alpha i proteins to specific membrane domains." J Cell Sci **107 (Pt 3)**: 507-515.

de Bot, S. T., S. Vermeer, W. Buijsman, A. Heister, M. Voorendt, A. Verrips, H. Scheffer, H. P. Kremer, B. P. van de Warrenburg and E. J. Kamsteeg (2013). "Pure adult-onset spastic paraplegia caused by a novel mutation in the KIAA0196 (SPG8) gene." J Neurol **260**(7): 1765-1769.

de Duve, C. (2004). "My love affair with insulin." J Biol Chem **279**(21): 21679-21688.

de Duve, C. (2005). "The lysosome turns fifty." Nat Cell Biol **7**(9): 847-849.

De Duve, C., B. C. Pressman, R. Gianetto, R. Wattiaux and F. Appelmans (1955). "Tissue fractionation studies. 6. Intracellular distribution patterns of enzymes in rat-liver tissue." Biochem J **60**(4): 604-617.

De Lean, A., J. M. Stadel and R. J. Lefkowitz (1980). "A ternary complex model explains the agonist-specific binding properties of the adenylate cyclase-coupled beta-adrenergic receptor." J Biol Chem **255**(15): 7108-7117.

Del Olmo, T., A. Lauzier, C. Normandin, R. Larcher, M. Lecours, D. Jean, L. Lessard, F. Steinberg, F. M. Boisvert and S. Jean (2019). "APEX2-mediated RAB proximity labeling identifies a role for RAB21 in clathrin-independent cargo sorting." EMBO Rep **20**(2).

Delcourt, N., J. Bockaert and P. Marin (2007). "GPCR-jacking: from a new route in RTK signalling to a new concept in GPCR activation." Trends Pharmacol Sci **28**(12): 602-607.

Depry, C., M. D. Allen and J. Zhang (2011). "Visualization of PKA activity in plasma membrane microdomains." Mol Biosyst **7**(1): 52-58.

Derivery, E. and A. Gautreau (2010). "Evolutionary conservation of the WASH complex, an actin polymerization machine involved in endosomal fission." Commun Integr Biol **3**(3): 227-230.

Derivery, E., E. Helfer, V. Henriot and A. Gautreau (2012). "Actin polymerization controls the organization of WASH domains at the surface of endosomes." PLoS One **7**(6): e39774.

Derivery, E., C. Sousa, J. J. Gautier, B. Lombard, D. Loew and A. Gautreau (2009). "The Arp2/3 activator WASH controls the fission of endosomes through a large multiprotein complex." Dev Cell **17**(5): 712-723.

Di Fiore, P. P. and G. N. Gill (1999). "Endocytosis and mitogenic signalling." Curr. Op. Cell Biol. **11**: 483-488.

Di Guglielmo, G. M., P. C. Baass, W.-J. Ou, B. I. Posner and J. J. M. Bergeron (1994). "Compartmentalization of SHC, GRB2 and mSOS, and hyperphosphorylation of Raf-1 by EGF but not insulin in liver parenchyma." EMBO J. **13**: 4269-4277.

Di Paolo, G. and P. De Camilli (2006). "Phosphoinositides in cell regulation and membrane dynamics." Nature **443**(7112): 651-657.

Dibb, N. J., S. M. Dilworth and C. D. Mol (2004). "Switching on kinases: oncogenic activation of BRAF and the PDGFR family." Nat Rev Cancer **4**(9): 718-727.

Dikic, I., S. Wakatsuki and K. J. Walters (2009). "Ubiquitin-binding domains - from structures to functions." Nat Rev Mol Cell Biol **10**(10): 659-671.

Ding, J., L. Su and G. Gao (2011). "Hrs inhibits citron kinase-mediated HIV-1 budding via its FYVE domain." Protein Cell **2**(6): 470-476.

DiPilato, L. M., X. Cheng and J. Zhang (2004). "Fluorescent indicators of cAMP and Epac activation reveal differential dynamics of cAMP signaling within discrete subcellular compartments." Proc Natl Acad Sci U S A **101**(47): 16513-16518.

DiPilato, L. M. and J. Zhang (2009). "The role of membrane microdomains in shaping beta2-adrenergic receptor-mediated cAMP dynamics." Mol Biosyst **5**(8): 832-837.

Dixon, R. A., B. K. Kobilka, D. J. Strader, J. L. Benovic, H. G. Dohlman, T. Frielle, M. A. Bolanowski, C. D. Bennett, E. Rands, R. E. Diehl, R. A. Mumford, E. E. Slater, I. S. Sigal, M. G.

Caron, R. J. Lefkowitz and C. D. Strader (1986). "Cloning of the gene and cDNA for mammalian beta-adrenergic receptor and homology with rhodopsin." Nature **321**(6065): 75-79.

Dohlman, H. G., J. Thorner, M. G. Caron and R. J. Lefkowitz (1991). "Model systems for the study of seven-transmembrane-segment receptors." Annu Rev Biochem **60**: 653-688.

Du, X., A. S. Kazim, A. J. Brown and H. Yang (2012). "An essential role of Hrs/Vps27 in endosomal cholesterol trafficking." Cell Rep **1**(1): 29-35.

Dunn, K. W. and F. R. Maxfield (1992). "Delivery of ligands from sorting endosomes to late endosomes occurs by maturation of sorting endosomes." J. Cell Biol. **117**: 301-310.

Dunn, K. W., T. E. McGraw and F. R. Maxfield (1989). "Iterative fractionation of recycling receptors from lysosomally destined ligands in an early sorting endosome." J. Cell Biol. **109**: 3303-3314.

Dupre, S. and R. Haguenauer-Tsapis (2001). "Deubiquitination step in the endocytic pathway of yeast plasma membrane proteins: crucial role of Doa4p ubiquitin isopeptidase." Mol Cell Biol **21**(14): 4482-4494.

Eaton, S. (2008). "Retromer retrieves wntless." Dev Cell **14**(1): 4-6.

Ebner, R. and R. Derynck (1991). "Epidermal growth factor and transforming growth factor-alpha: differential intracellular routing and processing of ligand-receptor complexes." Cell Regul **2**(8): 599-612.

El-Sayed, A. and H. Harashima (2013). "Endocytosis of gene delivery vectors: from clathrin-dependent to lipid raft-mediated endocytosis." Mol Ther **21**(6): 1118-1130.

El-Shewy, H. M., K. R. Johnson, M. H. Lee, A. A. Jaffa, L. M. Obeid and L. M. Luttrell (2006). "Insulin-like growth factors mediate heterotrimeric G protein-dependent ERK1/2 activation by transactivating sphingosine 1-phosphate receptors." J Biol Chem **281**(42): 31399-31407.

Etlinger, J. D. and A. L. Goldberg (1977). "A soluble ATP-dependent proteolytic system responsible for the degradation of abnormal proteins in reticulocytes." Proc Natl Acad Sci U S A **74**(1): 54-58.

Fan, J., K. Jiang, Y. Liu and J. Jia (2013). "Hrs promotes ubiquitination and mediates endosomal trafficking of smoothened in Drosophila hedgehog signaling." PLoS One **8**(11): e79021.

Fedorov, Y. V., N. C. Jones and B. B. Olwin (1998). "Regulation of myogenesis by fibroblast growth factors requires beta-gamma subunits of pertussis toxin-sensitive G proteins." Mol Cell Biol **18**(10): 5780-5787.

Feinstein, T. N., V. L. Wehbi, J. A. Ardura, D. S. Wheeler, S. Ferrandon, T. J. Gardella and J. P. Vilardaga (2011). "Retromer terminates the generation of cAMP by internalized PTH receptors." Nat Chem Biol **7**(5): 278-284.

Feinstein, T. N., N. Yui, M. J. Webber, V. L. Wehbi, H. P. Stevenson, J. D. King, Jr., K. R. Hallows, D. Brown, R. Bouley and J. P. Vilardaga (2013). "Noncanonical control of vasopressin receptor type 2 signaling by retromer and arrestin." J Biol Chem **288**(39): 27849-27860.

Ferguson, S. S., L. Menard, L. S. Barak, W. J. Koch, A. M. Colapietro and M. G. Caron (1995). "Role of phosphorylation in agonist-promoted beta 2-adrenergic receptor sequestration. Rescue of a sequestration-defective mutant receptor by beta ARK1." J Biol Chem **270**(42): 24782-24789.

Ferrandon, S., T. N. Feinstein, M. Castro, B. Wang, R. Bouley, J. T. Potts, T. J. Gardella and J. P. Vilardaga (2009). "Sustained cyclic AMP production by parathyroid hormone receptor endocytosis." Nat Chem Biol **5**(10): 734-742.

Fjorback, A. W., M. Seaman, C. Gustafsen, A. Mehmedbasic, S. Gokool, C. Wu, D. Militz, V. Schmidt, P. Madsen, J. R. Nyengaard, T. E. Willnow, E. I. Christensen, W. B. Mobley, A. Nykjaer and O. M. Andersen (2012). "Retromer binds the FANSHY sorting motif in SorLA to regulate amyloid precursor protein sorting and processing." J Neurosci **32**(4): 1467-1480.

Francavilla, C., M. Papetti, K. T. Rigbolt, A. K. Pedersen, J. O. Sigurdsson, G. Cazzamali, G. Karemore, B. Blagoev and J. V. Olsen (2016). "Multilayered proteomics reveals molecular switches dictating ligand-dependent EGFR trafficking." Nat Struct Mol Biol **23**(6): 608-618.

Fredriksson, R. and H. B. Schioth (2005). "The repertoire of G-protein-coupled receptors in fully sequenced genomes." Mol Pharmacol **67**(5): 1414-1425.

Fu, Q. S., C. J. Zhou, H. C. Gao, Y. J. Jiang, Z. R. Zhou, J. Hong, W. M. Yao, A. X. Song, D. H. Lin and H. Y. Hu (2009). "Structural basis for ubiquitin recognition by a novel domain from human phospholipase A2-activating protein." J Biol Chem **284**(28): 19043-19052.

Furdui, C. M., E. D. Lew, J. Schlessinger and K. S. Anderson (2006). "Autophosphorylation of FGFR1 kinase is mediated by a sequential and precisely ordered reaction." Mol Cell **21**(5): 711-717.

Futter, C. E., A. Gibson, E. H. Allchin, S. Maxwell, L. J. Ruddock, G. Odorizzi, D. Domingo, I. S. Trowbridge and C. R. Hopkins (1998). "In polarized MDCK cells basolateral vesicles arise from clathrin-g-adaptin coated domains on endosomal tubules." J. Cell Biol. **141**: 611-623.

Futter, C. E., A. Pearse, L. J. Hewlett and C. R. Hopkins (1996). "Multivesicular endosomes containing internalized EGF-EGF receptor complexes mature and then fuse directly with lysosomes." J Cell Biol **132**(6): 1011-1023.

Galan, J. A., L. L. Paris, H. J. Zhang, J. Adler, R. L. Geahlen and W. A. Tao (2011). "Proteomic studies of Syk-interacting proteins using a novel amine-specific isotope tag and GFP nanotrap." J Am Soc Mass Spectrom **22**(2): 319-328.

Garrett, T. P., N. M. McKern, M. Lou, T. C. Elleman, T. E. Adams, G. O. Lovrecz, H. J. Zhu, F. Walker, M. J. Frenkel, P. A. Hoyne, R. N. Jorissen, E. C. Nice, A. W. Burgess and C. W. Ward (2002). "Crystal structure of a truncated epidermal growth factor receptor extracellular domain bound to transforming growth factor alpha." Cell **110**(6): 763-773.

Garrus, J. E., U. K. von Schwedler, O. W. Pornillos, S. G. Morham, K. H. Zavitz, H. E. Wang, D. A. Wettstein, K. M. Stray, M. Cote, R. L. Rich, D. G. Myszka and W. I. Sundquist (2001). "Tsg101 and the vacuolar protein sorting pathway are essential for HIV-1 budding." Cell **107**(1): 55-65.

Gaullier, J.-M., A. Simonsen, A. D'Arrigo, B. Bremnes and H. Stenmark (1998). "FYVE fingers bind PtdIns(3)P." Nature **394**: 432-433.

Gershlick, D. C. and M. Lucas (2017). "Endosomal Trafficking: Retromer and Retriever Are Relatives in Recycling." Curr Biol **27**(22): R1233-r1236.

Geuze, H. J., J. W. Slot, G. J. Strous, A. Hasilik and K. von Figura (1985). "Possible pathways for lysosomal enzyme delivery." J Cell Biol **101**(6): 2253-2262.

Geuze, H. J., J. W. Slot, G. J. Strous, H. F. Lodish and A. L. Schwartz (1983). "Intracellular site of asialoglycoprotein receptor-ligand uncoupling: double-label immunoelectron microscopy during receptor-mediated endocytosis." Cell **32**(1): 277-287.

Gill, D. J., H. Teo, J. Sun, O. Perisic, D. B. Veprintsev, S. D. Emr and R. L. Williams (2007). "Structural insight into the ESCRT-I/-II link and its role in MVB trafficking." Embo j **26**(2): 600-612.

Gillooly, D. J., I. C. Morrow, M. Lindsay, R. Gould, N. J. Bryant, J. M. Gaullier, R. G. Parton and H. Stenmark (2000). " Localization of phosphatidylinositol 3-phosphate in yeast and mammalian cells." EMBO. J. **19**: 4577-4588.

Gillooly, D. J., A. Simonsen and H. Stenmark (2001). "Cellular functions of phosphatidylinositol 3-phosphate and FYVE domain proteins." Biochem J **355**(Pt 2): 249-258.

Gilman, A. G. (1987). "G proteins: transducers of receptor-generated signals." Annu Rev Biochem **56**: 615-649.

Goldknopf, I. L. and H. Busch (1977). "Isopeptide linkage between nonhistone and histone 2A polypeptides of chromosomal conjugate-protein A24." Proc Natl Acad Sci U S A **74**(3): 864-868.

Goldkorn, T., N. Balaban, M. Shannon and K. Matsukuma (1997). "EGF receptor phosphorylation is affected by ionizing radiation." Biochim Biophys Acta **1358**(3): 289-299.

Goldstein, J. L., R. G. Anderson and M. S. Brown (1979). "Coated pits, coated vesicles, and receptor-mediated endocytosis." Nature **279**(5715): 679-685.

Gomez, T. S. and D. D. Billadeau (2009). "A FAM21-containing WASH complex regulates retromer-dependent sorting." Dev Cell **17**(5): 699-711.

Gorden, P., J. L. Carpentier, S. Cohen and L. Orci (1978). "Epidermal growth factor: morphological demonstration of binding, internalization, and lysosomal association in human fibroblasts." Proc Natl Acad Sci U S A **75**(10): 5025-5029.

Gorvel, J. P., P. Chavrier, M. Zerial and J. Gruenberg (1991). "Rab 5 controls early endosome fusion in vitro." Cell **64**: 915-925.

Griffith, J., J. Black, C. Faerman, L. Swenson, M. Wynn, F. Lu, J. Lippke and K. Saxena (2004). "The structural basis for autoinhibition of FLT3 by the juxtamembrane domain." Mol Cell **13**(2): 169-178.

Gucwa, A. L. and D. A. Brown (2014). "UIM domain-dependent recruitment of the endocytic adaptor protein Eps15 to ubiquitin-enriched endosomes." BMC Cell Biol **15**: 34.

Gullick, W. J. (1996). "The c-erbB3/HER3 receptor in human cancer." Cancer Surv **27**: 339-349.

Gurevich, V. V., S. B. Dion, J. J. Onorato, J. Ptasienski, C. M. Kim, R. Sterne-Marr, M. M. Hosey and J. L. Benovic (1995). "Arrestin interactions with G protein-coupled receptors. Direct binding studies of wild type and mutant arrestins with rhodopsin, beta 2-adrenergic, and m2 muscarinic cholinergic receptors." J Biol Chem **270**(2): 720-731.

Haigler, H. T., J. A. McKanna and S. Cohen (1979). "Direct visualisation of the binding and internalisation of a ferritin conjugate of epidermal growth factor in human carcinoma cells A-431." J. Cell Biol. **81**: 382-395.

Hanson, P. I. and A. Cashikar (2012). "Multivesicular body morphogenesis." Annu Rev Cell Dev Biol **28**: 337-362.

Hao, Y. H., J. M. Doyle, S. Ramanathan, T. S. Gomez, D. Jia, M. Xu, Z. J. Chen, D. D. Billadeau, M. K. Rosen and P. R. Potts (2013). "Regulation of WASH-dependent actin polymerization and protein trafficking by ubiquitination." Cell **152**(5): 1051-1064.

Harbour, M. E., S. Y. Breusegem, R. Antrobus, C. Freeman, E. Reid and M. N. Seaman (2010). "The cargo-selective retromer complex is a recruiting hub for protein complexes that regulate endosomal tubule dynamics." J Cell Sci **123**(Pt 21): 3703-3717.

Harbour, M. E., S. Y. Breusegem and M. N. Seaman (2012). "Recruitment of the endosomal WASH complex is mediated by the extended 'tail' of Fam21 binding to the retromer protein Vps35." Biochem J **442**(1): 209-220.

Harterink, M., F. Port, M. J. Lorenowicz, I. J. McGough, M. Silhankova, M. C. Betist, J. R. T. van Weering, R. van Heesbeen, T. C. Middelkoop, K. Basler, P. J. Cullen and H. C. Korswagen (2011). "A SNX3-dependent retromer pathway mediates retrograde transport of the Wnt sorting receptor Wntless and is required for Wnt secretion." Nat Cell Biol **13**(8): 914-923.

Hasseine, L. K., J. Murdaca, F. Suavet, S. Longnus, S. Giorgetti-Peraldi and E. Van Obberghen (2007). "Hrs is a positive regulator of VEGF and insulin signaling." Exp Cell Res **313**(9): 1927-1942.

Haugen, L. H., F. M. Skjeldal, T. Bergeland and O. Bakke (2017). "Endosomal binding kinetics of Eps15 and Hrs specifically regulate the degradation of RTKs." Sci Rep **7**(1): 17962.

Helenius, A., J. Kartenbeck, K. Simons and E. Fries (1980). "On the entry of Semliki forest virus into BHK-21 cells." J Cell Biol **84**(2): 404-420.

Helfer, E., M. E. Harbour, V. Henriot, G. Lakisic, C. Sousa-Blin, L. Volceanov, M. N. J. Seaman and A. Gautreau (2013). "Endosomal recruitment of the WASH complex: active sequences and mutations impairing interaction with the retromer." Biol Cell **105**(5): 191-207.

Henne, W. M., N. J. Buchkovich and S. D. Emr (2011). "The ESCRT Pathway." Dev Cell **21**(1): 77-91.

Hernandez-Valladares, M., T. Kim, B. Kannan, A. Tung, A. H. Aguda, M. Larsson, J. A. Cooper and R. C. Robinson (2010). "Structural characterization of a capping protein interaction motif defines a family of actin filament regulators." Nat Struct Mol Biol **17**(4): 497-503.

Hershko, A., H. Heller, S. Elias and A. Ciechanover (1983). "Components of ubiquitin-protein ligase system. Resolution, affinity purification, and role in protein breakdown." J Biol Chem **258**(13): 8206-8214.

Hicke, L., H. L. Schubert and C. P. Hill (2005). "Ubiquitin-binding domains." Nat Rev Mol Cell Biol **6**(8): 610-621.

Hierro, A., J. Sun, A. S. Rusnak, J. Kim, G. Prag, S. D. Emr and J. H. Hurley (2004). "Structure of the ESCRT-II endosomal trafficking complex." Nature **431**(7005): 221-225.

Higgs, H. N. and T. D. Pollard (1999). "Regulation of actin polymerization by Arp2/3 complex and WASp/Scar proteins." J Biol Chem **274**(46): 32531-32534.

Himanen, J. P. and D. B. Nikolov (2003). "Eph signaling: a structural view." Trends Neurosci **26**(1): 46-51.

Hirano, S., M. Kawasaki, H. Ura, R. Kato, C. Raiborg, H. Stenmark and S. Wakatsuki (2006). "Double-sided ubiquitin binding of Hrs-UIM in endosomal protein sorting." Nat Struct Mol Biol **13**(3): 272-277.

Hobson, J. P., H. M. Rosenfeldt, L. S. Barak, A. Olivera, S. Poulton, M. G. Caron, S. Milstien and S. Spiegel (2001). "Role of the sphingosine-1-phosphate receptor EDG-1 in PDGF-induced cell motility." Science **291**(5509): 1800-1803.

Hoeller, D., N. Crosetto, B. Blagoev, C. Raiborg, R. Tikkanen, S. Wagner, K. Kowanetz, R. Breitling, M. Mann, H. Stenmark and I. Dikic (2006). "Regulation of ubiquitin-binding proteins by monoubiquitination." Nat Cell Biol **8**(2): 163-169.

Hofmann, K. and P. Bucher (1996). "The UBA domain: a sequence motif present in multiple enzyme classes of the ubiquitination pathway." Trends Biochem Sci **21**(5): 172-173.

Hofmann, K. and L. Falquet (2001). "A ubiquitin-interacting motif conserved in components of the proteasomal and lysosomal protein degradation systems." TIBS **26**: 347-350.

Holleman, J. and A. Marchese (2014). "The ubiquitin ligase deltex-3l regulates endosomal sorting of the G protein-coupled receptor CXCR4." Mol Biol Cell **25**(12): 1892-1904.

Honegger, A. M., R. M. Kris, A. Ullrich and J. Schlessinger (1989). "Evidence that autophosphorylation of solubilized receptors for epidermal growth factor is mediated by intermolecular cross-phosphorylation." Proc Natl Acad Sci U S A **86**(3): 925-929.

Hoon, M. A., E. Adler, J. Lindemeier, J. F. Battey, N. J. Ryba and C. S. Zuker (1999). "Putative mammalian taste receptors: a class of taste-specific GPCRs with distinct topographic selectivity." Cell **96**(4): 541-551.

Horazdovsky, B. F., B. A. Davies, M. N. Seaman, S. A. McLaughlin, S. Yoon and S. D. Emr (1997). "A sorting nexin-1 homologue, Vps5p, forms a complex with Vps17p and is required for recycling the vacuolar protein-sorting receptor." Mol Biol Cell **8**(8): 1529-1541.

Huang, S. H., L. Zhao, Z. P. Sun, X. Z. Li, Z. Geng, K. D. Zhang, M. V. Chao and Z. Y. Chen (2009). "Essential role of Hrs in endocytic recycling of full-length TrkB receptor but not its isoform TrkB.T1." J Biol Chem **284**(22): 15126-15136.

Hubbard, S. R. (2004). "Juxtamembrane autoinhibition in receptor tyrosine kinases." Nat Rev Mol Cell Biol **5**(6): 464-471.

Hung, V., S. S. Lam, N. D. Udeshi, T. Svinkina, G. Guzman, V. K. Mootha, S. A. Carr and A. Y. Ting (2017). "Proteomic mapping of cytosol-facing outer mitochondrial and ER membranes in living human cells by proximity biotinylation." Elife **6**.

Hung, V., N. D. Udeshi, S. S. Lam, K. H. Loh, K. J. Cox, K. Pedram, S. A. Carr and A. Y. Ting (2016). "Spatially resolved proteomic mapping in living cells with the engineered peroxidase APEX2." Nat Protoc **11**(3): 456-475.

Hung, V., P. Zou, H. W. Rhee, N. D. Udeshi, V. Cracan, T. Svinkina, S. A. Carr, V. K. Mootha and A. Y. Ting (2014). "Proteomic mapping of the human mitochondrial intermembrane space in live cells via ratiometric APEX tagging." Mol Cell **55**(2): 332-341.

Huse, M. and J. Kuriyan (2002). "The conformational plasticity of protein kinases." Cell **109**(3): 275-282.

Huttlin, E. L., L. Ting, R. J. Bruckner, F. Gebreab, M. P. Gygi, J. Szpyt, S. Tam, G. Zarraga, G. Colby, K. Baltier, R. Dong, V. Guarani, L. P. Vaites, A. Ordureau, R. Rad, B. K. Erickson, M. Wuhr, J. Chick, B. Zhai, D. Kolippakkam, J. Mintseris, R. A. Obar, T. Harris, S. Artavanis-Tsakonas, M. E. Sowa, P. De Camilli, J. A. Paulo, J. W. Harper and S. P. Gygi (2015). "The BioPlex Network: A Systematic Exploration of the Human Interactome." Cell **162**(2): 425-440.

Hwang, J. and P. J. Espenshade (2016). "Proximity-dependent biotin labelling in yeast using the engineered ascorbate peroxidase APEX2." Biochem J **473**(16): 2463-2469.

Ibrahimi, O. A., B. K. Yeh, A. V. Eliseenkova, F. Zhang, S. K. Olsen, M. Igarashi, S. A. Aaronson, R. J. Linhardt and M. Mohammadi (2005). "Analysis of mutations in fibroblast growth factor (FGF) and a pathogenic mutation in FGF receptor (FGFR) provides direct evidence for the symmetric two-end model for FGFR dimerization." Mol Cell Biol **25**(2): 671-684.

Irannejad, R., J. C. Tomshine, J. R. Tomshine, M. Chevalier, J. P. Mahoney, J. Steyaert, S. G. Rasmussen, R. K. Sunahara, H. El-Samad, B. Huang and M. von Zastrow (2013). "Conformational biosensors reveal GPCR signalling from endosomes." Nature **495**(7442): 534-538.

Irannejad, R. and M. von Zastrow (2014). "GPCR signaling along the endocytic pathway." Curr Opin Cell Biol **27**: 109-116.

Jia, D., T. S. Gomez, D. D. Billadeau and M. K. Rosen (2012). "Multiple repeat elements within the FAM21 tail link the WASH actin regulatory complex to the retromer." Mol Biol Cell **23**(12): 2352-2361.

Jia, D., T. S. Gomez, Z. Metlagel, J. Umetani, Z. Otwinowski, M. K. Rosen and D. D. Billadeau (2010). "WASH and WAVE actin regulators of the Wiskott-Aldrich syndrome protein (WASP) family are controlled by analogous structurally related complexes." Proc Natl Acad Sci U S A **107**(23): 10442-10447.

Joazeiro, C. A., S. S. Wing, H. Huang, J. D. Leverson, T. Hunter and Y. C. Liu (1999). "The tyrosine kinase negative regulator c-Cbl as a RING-type, E2-dependent ubiquitin-protein ligase." Science **286**(5438): 309-312.

Jura, N., N. F. Endres, K. Engel, S. Deindl, R. Das, M. H. Lamers, D. E. Wemmer, X. Zhang and J. Kuriyan (2009). "Mechanism for activation of the EGF receptor catalytic domain by the juxtamembrane segment." Cell **137**(7): 1293-1307.

Kanaseki, T. and K. Kadota (1969). "The "vesicle in a basket". A morphological study of the coated vesicle isolated from the nerve endings of the guinea pig brain, with special reference to the mechanism of membrane movements." J Cell Biol **42**(1): 202-220.

Kato, M., K. Miyazawa and N. Kitamura (2000). "A de-ubiquitinating enzyme UBPY interacts with the SH3 domain of Hrs binding protein via a novel binding motif Px(V/I)(D/N)RxxKP." J. Biol. Chem. 275: 37481-37487.

Katzmann, D. J., M. Babst and S. D. Emr (2001). "Ubiquitin-dependent sorting into the multivesicular body pathway requires the function of a conserved endosomal protein sorting complex, ESCRT-1." Cell 106: 145-155.

Katzmann, D. J., G. Odorizzi and S. D. Emr (2002). "Receptor downregulation and multivesicular-body sorting." Nat Rev Mol Cell Biol 3(12): 893-905.

Katzmann, D. J., S. Sarkar, T. Chu, A. Audhya and S. D. Emr (2004). "Multivesicular body sorting: ubiquitin ligase Rsp5 is required for the modification and sorting of carboxypeptidase S." Mol Biol Cell 15(2): 468-480.

Katzmann, D. J., C. J. Stefan, M. Babst and S. D. Emr (2003). "Vps27 recruits ESCRT machinery to endosomes during MVB sorting." J Cell Biol 162(3): 413-423.

Keely, S. J., S. O. Calandrella and K. E. Barrett (2000). "Carbachol-stimulated transactivation of epidermal growth factor receptor and mitogen-activated protein kinase in T(84) cells is mediated by intracellular Ca2+, PYK-2, and p60(src)." J Biol Chem 275(17): 12619-12625.

Kirkin, V., T. Lamark, Y. S. Sou, G. Bjorkoy, J. L. Nunn, J. A. Bruun, E. Shvets, D. G. McEwan, T. H. Clausen, P. Wild, I. Bilusic, J. P. Theurillat, A. Overvatn, T. Ishii, Z. Elazar, M. Komatsu, I. Dikic and T. Johansen (2009). "A role for NBR1 in autophagosomal degradation of ubiquitinated substrates." Mol Cell 33(4): 505-516.

Knebel, A., H. J. Rahmsdorf, A. Ullrich and P. Herrlich (1996). "Dephosphorylation of receptor tyrosine kinases as target of regulation by radiation, oxidants or alkylating agents." Embo j 15(19): 5314-5325.

Kobilka, B. K., T. S. Kobilka, K. Daniel, J. W. Regan, M. G. Caron and R. J. Lefkowitz (1988). "Chimeric alpha 2-,beta 2-adrenergic receptors: delineation of domains involved in effector coupling and ligand binding specificity." Science 240(4857): 1310-1316.

Kobilka, B. K., H. Matsui, T. S. Kobilka, T. L. Yang-Feng, U. Francke, M. G. Caron, R. J. Lefkowitz and J. W. Regan (1987). "Cloning, sequencing, and expression of the gene coding for the human platelet alpha 2-adrenergic receptor." Science 238(4827): 650-656.

Kojima, K., Y. Amano, K. Yoshino, N. Tanaka, K. Sugamura and T. Takeshita (2014). "ESCRT-0 protein hepatocyte growth factor-regulated tyrosine kinase substrate (Hrs) is targeted to endosomes independently of signal-transducing adaptor molecule (STAM) and the complex formation with STAM promotes its endosomal dissociation." J Biol Chem 289(48): 33296-33310.

Komada, M. and N. Kitamura (1995). "Growth-factor-induced tyrosine phosphorylation of hrs, a novel 115-kilodalton protein with a structurally conserved putative zinc finger domain." Mol. Cell Biol. **15**: 6213-6221.

Komada, M. and P. Soriano (1999). "Hrs, a FYVE finger protein localized to early endosomes is implicated in vesicular traffic and required for ventral folding morphogenisis." Genes Dev. **13**: 1475-1485.

Kostelansky, M. S., C. Schluter, Y. Y. Tam, S. Lee, R. Ghirlando, B. Beach, E. Conibear and J. H. Hurley (2007). "Molecular architecture and functional model of the complete yeast ESCRT-I heterotetramer." Cell **129**(3): 485-498.

Kostelansky, M. S., J. Sun, S. Lee, J. Kim, R. Ghirlando, A. Hierro, S. D. Emr and J. H. Hurley (2006). "Structural and functional organization of the ESCRT-I trafficking complex." Cell **125**(1): 113-126.

Kotowski, S. J., F. W. Hopf, T. Seif, A. Bonci and M. von Zastrow (2011). "Endocytosis promotes rapid dopaminergic signaling." Neuron **71**(2): 278-290.

Krueger, K. M., Y. Daaka, J. A. Pitcher and R. J. Lefkowitz (1997). "The role of sequestration in G protein-coupled receptor resensitization. Regulation of beta2-adrenergic receptor dephosphorylation by vesicular acidification." J Biol Chem **272**(1): 5-8.

Kubo, T., K. Fukuda, A. Mikami, A. Maeda, H. Takahashi, M. Mishina, T. Haga, K. Haga, A. Ichiyama, K. Kangawa and et al. (1986). "Cloning, sequencing and expression of complementary DNA encoding the muscarinic acetylcholine receptor." Nature **323**(6087): 411-416.

Kuhn, H. and U. Wilden (1987). "Deactivation of photoactivated rhodopsin by rhodopsin-kinase and arrestin." J Recept Res **7**(1-4): 283-298.

Kumari, S., S. Mg and S. Mayor (2010). "Endocytosis unplugged: multiple ways to enter the cell." Cell Res **20**(3): 256-275.

Kurzchalia, T. V., P. Dupree, R. G. Parton, R. Kellner, H. Virta, M. Lehnert and K. Simons (1992). "VIP21, a 21-kD membrane protein is an integral component of trans-Golgi-network-derived transport vesicles." J Cell Biol **118**(5): 1003-1014.

Lam, S. S., J. D. Martell, K. J. Kamer, T. J. Deerinck, M. H. Ellisman, V. K. Mootha and A. Y. Ting (2015). "Directed evolution of APEX2 for electron microscopy and proximity labeling." Nat Methods **12**(1): 51-54.

Langelier, C., U. K. von Schwedler, R. D. Fisher, I. De Domenico, P. L. White, C. P. Hill, J. Kaplan, D. Ward and W. I. Sundquist (2006). "Human ESCRT-II complex and its role in human immunodeficiency virus type 1 release." J Virol **80**(19): 9465-9480.

Laporte, S. A., R. H. Oakley, J. Zhang, J. A. Holt, S. S. G. Ferguson, M. G. Caron and L. S. Barak (1999). "The b2-adrenergic receptor/b-arrestin complex recruits the clathrin adaptor AP-2 during endocytosis." Proc. Natl. Acad. Sci. **96**: 3712-3717.

Lee, F. S. and M. V. Chao (2001). "Activation of Trk neurotrophin receptors in the absence of neurotrophins." Proc Natl Acad Sci U S A **98**(6): 3555-3560.

Lee, S., Y. C. Tsai, R. Mattera, W. J. Smith, M. S. Kostelansky, A. M. Weissman, J. S. Bonifacino and J. H. Hurley (2006). "Structural basis for ubiquitin recognition and autoubiquitination by Rabex-5." Nat Struct Mol Biol **13**(3): 264-271.

Lefkowitz, R. J. (2007). "Seven transmembrane receptors: something old, something new." Acta Physiol (Oxf) **190**(1): 9-19.

Lefkowitz, R. J., E. Haber and D. O'Hara (1972). "Identification of the cardiac beta-adrenergic receptor protein: solubilization and purification by affinity chromatography." Proc Natl Acad Sci U S A **69**(10): 2828-2832.

Lemmon, M. A. and J. Schlessinger (2010). "Cell signaling by receptor tyrosine kinases." Cell **141**(7): 1117-1134.

Levi-Montalcini, R. (1952). "Effects of mouse tumor transplantation on the nervous system." Ann N Y Acad Sci **55**(2): 330-344.

Levi-Montalcini, R. and S. Cohen (1956). "IN VITRO AND IN VIVO EFFECTS OF A NERVE GROWTH-STIMULATING AGENT ISOLATED FROM SNAKE VENOM." Proc Natl Acad Sci U S A **42**(9): 695-699.

Levi-Montalcini, R. and V. Hamburger (1951). "Selective growth stimulating effects of mouse sarcoma on the sensory and sympathetic nervous system of the chick embryo." J Exp Zool **116**(2): 321-361.

Levi-Montalcini, R., H. Meyer and V. Hamburger (1954). "In vitro experiments on the effects of mouse sarcomas 180 and 37 on the spinal and sympathetic ganglia of the chick embryo." Cancer Res **14**(1): 49-57.

Levkowitz, G., H. Waterman, S. A. Ettenberg, M. Katz, A. Y. Tsygankov, I. Alroy, S. Lavi, K. Iwai, Y. Reiss, A. Ciechanover, S. Lipkowitz and Y. Yarden (1999). "Ubiquitin ligase activity and tyrosine phosphorylation underlie suppression of growth factor signaling by c-Cbl/Sli-1." Mol. Cell **4**: 1029-1040.

Li, L. and S. N. Cohen (1996). "Tsg101: a novel tumor susceptibility gene isolated by controlled homozygous functional knockout of allelic loci in mammalian cells." Cell **85**(3): 319-329.

Li, P., J. Li, L. Wang and L. J. Di (2017). "Proximity Labeling of Interacting Proteins: Application of BioID as a Discovery Tool." Proteomics **17**(20).

Lins, L., A. Thomas and R. Brasseur (2003). "Analysis of accessible surface of residues in proteins." Protein Sci **12**(7): 1406-1417.

Linseman, D. A., C. W. Benjamin and D. A. Jones (1995). "Convergence of angiotensin II and platelet-derived growth factor receptor signaling cascades in vascular smooth muscle cells." J Biol Chem **270**(21): 12563-12568.

Liu, C., M. Takahashi, Y. Li, T. J. Dillon, S. Kaech and P. J. Stork (2010). "The interaction of Epac1 and Ran promotes Rap1 activation at the nuclear envelope." Mol Cell Biol **30**(16): 3956-3969.

Liu, H., X. Chen, P. J. Focia and X. He (2007). "Structural basis for stem cell factor-KIT signaling and activation of class III receptor tyrosine kinases." Embo j **26**(3): 891-901.

Lloyd, T. E., R. Atkinson, M. N. Wu, Y. Zhou, G. Pennetta and H. J. Bellen (2002). "Hrs regulates endosome membrane invagination and tyrosine kinase receptor signaling in Drosophila." Cell **108**: 261-269.

Lobingier, B. T., R. Huttenhain, K. Eichel, K. B. Miller, A. Y. Ting, M. von Zastrow and N. J. Krogan (2017). "An Approach to Spatiotemporally Resolve Protein Interaction Networks in Living Cells." Cell **169**(2): 350-360 e312.

Lohi, O. and V. P. Lehto (2001). "STAM/EAST/Hbp adapter proteins - integrators of signalling pathways." FEBS Lett. **508**: 287-290.

Lohse, M. J., J. L. Benovic, J. Codina, M. G. Caron and R. J. Lefkowitz (1990). "beta-Arrestin: a protein that regulates beta-adrenergic receptor function." Science **248**(4962): 1547-1550.

Losko, S., F. Kopp, A. Kranz and R. Kolling (2001). "Uptake of the ATP-binding cassette (ABC) transporter Ste6 into the yeast vacuole is blocked in the doa4 Mutant." Mol Biol Cell **12**(4): 1047-1059.

Lu, Q., L. W. Hope, M. Brasch, C. Reinhard and S. N. Cohen (2003). "TSG101 interaction with HRS mediates endosomal trafficking and receptor down-regulation." Proc Natl Acad Sci U S A **100**(13): 7626-7631.

Luhtala, N. and G. Odorizzi (2004). "Bro1 coordinates deubiquitination in the multivesicular body pathway by recruiting Doa4 to endosomes." J Cell Biol **166**(5): 717-729.

Luo, Z., M. Ge, J. Chen, Q. Geng, M. Tian, Z. Qiao, L. Bai, Q. Zhang, C. Zhu, Y. Xiong, K. Wu, F. Liu, Y. Liu and J. Wu (2017). "HRS plays an important role for TLR7 signaling to orchestrate inflammation and innate immunity upon EV71 infection." PLoS Pathog **13**(8): e1006585.

Luttrell, L., E. Kilgour, J. Larner and G. Romero (1990). "A pertussis toxin-sensitive G-protein mediates some aspects of insulin action in BC3H-1 murine myocytes." J Biol Chem **265**(28): 16873-16879.

Luttrell, L. M., S. S. Ferguson, Y. Daaka, W. E. Miller, S. Maudsley, G. J. Della Rocca, F. Lin, H. Kawakatsu, K. Owada, D. K. Luttrell, M. G. Caron and R. J. Lefkowitz (1999). "Beta-arrestin-dependent formation of beta2 adrenergic receptor-Src protein kinase complexes." Science **283**(5402): 655-661.

Luttrell, L. M., B. E. Hawes, T. van Biesen, D. K. Luttrell, T. J. Lansing and R. J. Lefkowitz (1996). "Role of c-Src tyrosine kinase in G protein-coupled receptor- and Gbetagamma subunit-mediated activation of mitogen-activated protein kinases." J Biol Chem **271**(32): 19443-19450.

Luttrell, L. M., T. van Biesen, B. E. Hawes, W. J. Koch, K. Touhara and R. J. Lefkowitz (1995). "G beta gamma subunits mediate mitogen-activated protein kinase activation by the tyrosine kinase insulin-like growth factor 1 receptor." J Biol Chem **270**(28): 16495-16498.

MacDonald, E., L. Brown, A. Selvais, H. Liu, T. Waring, D. Newman, J. Bithell, D. Grimes, S. Urbe, M. J. Clague and T. Zech (2018). "HRS-WASH axis governs actin-mediated endosomal recycling and cell invasion." J Cell Biol **217**(7): 2549-2564.

Machesky, L. M., S. J. Atkinson, C. Ampe, J. Vandekerckhove and T. D. Pollard (1994). "Purification of a cortical complex containing two unconventional actins from Acanthamoeba by affinity chromatography on profilin-agarose." J Cell Biol **127**(1): 107-115.

Malik, N., T. Macartney, A. Hornberger, K. E. Anderson, H. Tovell, A. R. Prescott and D. R. Alessi (2018). "Mechanism of activation of SGK3 by growth factors via the Class 1 and Class 3 PI3Ks." Biochem J **475**(1): 117-135.

Mamo, A., F. Jules, K. Dumaresq-Doiron, S. Costantino and S. Lefrancois (2012). "The role of ceroid lipofuscinosis neuronal protein 5 (CLN5) in endosomal sorting." Mol Cell Biol **32**(10): 1855-1866.

Marchese, A. and J. L. Benovic (2001). "Agonist-promoted ubiquitination of the G protein-coupled receptor CXCR4 mediates lysosomal sorting." J Biol Chem **276**(49): 45509-45512.

Martell, J. D., T. J. Deerinck, Y. Sancak, T. L. Poulos, V. K. Mootha, G. E. Sosinsky, M. H. Ellisman and A. Y. Ting (2012). "Engineered ascorbate peroxidase as a genetically encoded reporter for electron microscopy." Nat Biotechnol **30**(11): 1143-1148.

Masu, Y., K. Nakayama, H. Tamaki, Y. Harada, M. Kuno and S. Nakanishi (1987). "cDNA cloning of bovine substance-K receptor through oocyte expression system." Nature **329**(6142): 836-838.

Maxfield, F. R., J. Schlessinger, Y. Shechter, I. Pastan and M. C. Willingham (1978). "Collection of insulin, EGF and alpha2-macroglobulin in the same patches on the surface of cultured fibroblasts and common internalization." Cell **14**(4): 805-810.

McCullough, J., P. E. Row, O. Lorenzo, M. Doherty, R. Beynon, M. J. Clague and S. Urbe (2006). "Activation of the endosome-associated ubiquitin isopeptidase AMSH by STAM, a component of the multivesicular body-sorting machinery." Curr Biol **16**(2): 160-165.

McNally, K. E., R. Faulkner, F. Steinberg, M. Gallon, R. Ghai, D. Pim, P. Langton, N. Pearson, C. M. Danson, H. Nagele, L. L. Morris, A. Singla, B. L. Overlee, K. J. Heesom, R. Sessions, L. Banks, B. M. Collins, I. Berger, D. D. Billadeau, E. Burstein and P. J. Cullen (2017). "Retriever is a multiprotein complex for retromer-independent endosomal cargo recycling." Nat Cell Biol **19**(10): 1214-1225.

Mehta, V. and L. Trinkle-Mulcahy (2016). "Recent advances in large-scale protein interactome mapping." F1000Res **5**.

Meijer, I. M., W. van Rotterdam, E. J. van Zoelen and J. E. van Leeuwen (2012). "Recycling of EGFR and ErbB2 is associated with impaired Hrs tyrosine phosphorylation and decreased deubiquitination by AMSH." Cell Signal **24**(11): 1981-1988.

Mick, D. U., R. B. Rodrigues, R. D. Leib, C. M. Adams, A. S. Chien, S. P. Gygi and M. V. Nachury (2015). "Proteomics of Primary Cilia by Proximity Labeling." Dev Cell **35**(4): 497-512.

Miller, K., J. Beardmore, H. Kanety, J. Schlessinger and C. R. Hopkins (1986). "Localization of the epidermal growth factor (EGF) receptor within the endosome of EGF-stimulated epidermoid carcinoma (A431) cells." J Cell Biol **102**(2): 500-509.

MILLS, I., A. JONES and M. CLAGUE (1998). "Involvement of the endosomal autoantigen EEA1 in homotypic fusion of early endosomes." CURRENT BIOLOGY **8**(15): 881-884.

Miura, S. and Y. Mishina (2011). "Hepatocyte growth factor-regulated tyrosine kinase substrate (Hgs) is involved in BMP signaling through phosphorylation of SMADS and TAK1 in early mouse embryo." Dev Dyn **240**(11): 2474-2481.

Miyawaki, A., J. Llopis, R. Heim, J. M. McCaffery, J. A. Adams, M. Ikura and R. Y. Tsien (1997). "Fluorescent indicators for Ca2+ based on green fluorescent proteins and calmodulin." Nature **388**(6645): 882-887.

Mizuno, E., K. Kawahata, M. Kato, N. Kitamura and M. Komada (2003). "STAM proteins bind ubiquitinated proteins on the early endosome via the VHS domain and ubiquitin-interacting motif." Mol Biol Cell **14**(9): 3675-3689.

Mohammadi, M., A. M. Honegger, D. Rotin, R. Fischer, F. Bellot, W. Li, C. A. Dionne, M. Jaye, M. Rubinstein and J. Schlessinger (1991). "A tyrosine-phosphorylated carboxy-terminal peptide of the fibroblast growth factor receptor (Flg) is a binding site for the SH2 domain of phospholipase C-gamma 1." Mol Cell Biol **11**(10): 5068-5078.

Mol, C. D., D. R. Dougan, T. R. Schneider, R. J. Skene, M. L. Kraus, D. N. Scheibe, G. P. Snell, H. Zou, B. C. Sang and K. P. Wilson (2004). "Structural basis for the autoinhibition and STI-571 inhibition of c-Kit tyrosine kinase." J Biol Chem **279**(30): 31655-31663.

Monfregola, J., G. Napolitano, M. D'Urso, P. Lappalainen and M. V. Ursini (2010). "Functional characterization of Wiskott-Aldrich syndrome protein and scar homolog (WASH), a bi-modular nucleation-promoting factor able to interact with biogenesis of lysosome-related organelle subunit 2 (BLOS2) and gamma-tubulin." J Biol Chem **285**(22): 16951-16957.

Mu, F. T., J. M. Callaghan, O. Steele-Mortimer, H. Stenmark, R. G. Parton, P. L. Campbell, J. McCluskey, J. P. Yeo, E. P. Tock and B. H. Toh (1995). "EEA1, an early endosome-associated protein. EEA1 is a conserved alpha-helical peripheral membrane protein flanked by cysteine "fingers" and contains a calmodulin-binding IQ motif." J Biol Chem **270**(22): 13503-13511.

Mukherjee, C., M. G. Caron, M. Coverstone and R. J. Lefkowitz (1975). "Identification of adenylate cyclase-coupled beta-adrenergic receptors in frog erythrocytes with (minus)-[3-H] alprenolol." J Biol Chem **250**(13): 4869-4876.

Mukherjee, S., R. N. Ghosh and F. R. Maxfield (1997). "Endocytosis." Physiol. Rev. **77**: 759-803.

Mullershausen, F., F. Zecri, C. Cetin, A. Billich, D. Guerini and K. Seuwen (2009). "Persistent signaling induced by FTY720-phosphate is mediated by internalized S1P1 receptors." Nat Chem Biol **5**(6): 428-434.

Murphy, J. E., B. E. Padilla, B. Hasdemir, G. S. Cottrell and N. W. Bunnett (2009). "Endosomes: a legitimate platform for the signaling train." Proc Natl Acad Sci U S A **106**(42): 17615-17622.

Nabhan, J. F., R. Hu, R. S. Oh, S. N. Cohen and Q. Lu (2012). "Formation and release of arrestin domain-containing protein 1-mediated microvesicles (ARMMs) at plasma membrane by recruitment of TSG101 protein." Proc Natl Acad Sci U S A **109**(11): 4146-4151.

Nagaraj, N., J. R. Wisniewski, T. Geiger, J. Cox, M. Kircher, J. Kelso, S. Paabo and M. Mann (2011). "Deep proteome and transcriptome mapping of a human cancer cell line." Mol Syst Biol **7**: 548.

Nagata, T., K. Murata, R. Murata, S. L. Sun, Y. Saito, S. Yamaga, N. Tanaka, K. Tamai, K. Moriya, N. Kasai, K. Sugamura and N. Ishii (2014). "Hepatocyte growth factor regulated tyrosine kinase substrate in the peripheral development and function of B-cells." Biochem Biophys Res Commun **443**(2): 351-356.

Nakada-Tsukui, K., Y. Saito-Nakano, V. Ali and T. Nozaki (2005). "A retromerlike complex is a novel Rab7 effector that is involved in the transport of the virulence factor cysteine protease in the enteric protozoan parasite Entamoeba histolytica." Mol Biol Cell **16**(11): 5294-5303.

Nakatogawa, H., K. Suzuki, Y. Kamada and Y. Ohsumi (2009). "Dynamics and diversity in autophagy mechanisms: lessons from yeast." Nat Rev Mol Cell Biol **10**(7): 458-467.

Nielsen, M. S., C. Gustafsen, P. Madsen, J. R. Nyengaard, G. Hermey, O. Bakke, M. Mari, P. Schu, R. Pohlmann, A. Dennes and C. M. Petersen (2007). "Sorting by the cytoplasmic domain of the amyloid precursor protein binding receptor SorLA." Mol Cell Biol **27**(19): 6842-6851.

Nisar, S., E. Kelly, P. J. Cullen and S. J. Mundell (2010). "Regulation of P2Y1 receptor traffic by sorting Nexin 1 is retromer independent." Traffic **11**(4): 508-519.

Niu, X. L., K. G. Peters and C. D. Kontos (2002). "Deletion of the carboxyl terminus of Tie2 enhances kinase activity, signaling, and function. Evidence for an autoinhibitory mechanism." J Biol Chem **277**(35): 31768-31773.

Nolen, B., S. Taylor and G. Ghosh (2004). "Regulation of protein kinases; controlling activity through activation segment conformation." Mol Cell **15**(5): 661-675.

Nothwehr, S. F., S. A. Ha and P. Bruinsma (2000). "Sorting of yeast membrane proteins into an endosome-to-Golgi pathway involves direct interaction of their cytosolic domains with Vps35p." J Cell Biol **151**(2): 297-310.

Nothwehr, S. F. and A. E. Hindes (1997). "The yeast VPS5/GRD2 gene encodes a sorting nexin-1-like protein required for localizing membrane proteins to the late Golgi." J Cell Sci **110 (Pt 9)**: 1063-1072.

Novikoff, A. B., H. Beaufay and C. De Duve (1956). "Electron microscopy of lysosomerich fractions from rat liver." J Biophys Biochem Cytol **2**(4 Suppl): 179-184.

Odorizzi, G., M. Babst and S. D. Emr (1998). "Fab1p PtdIns(3)P 5-kinase function essential for protein sorting in the multivesicular body." Cell **95**: 847-858.

Odorizzi, G., D. J. Katzmann, M. Babst, A. Audhya and S. D. Emr (2003). "Bro1 is an endosome-associated protein that functions in the MVB pathway in Saccharomyces cerevisiae." J Cell Sci **116**(Pt 10): 1893-1903.

Ogiso, H., R. Ishitani, O. Nureki, S. Fukai, M. Yamanaka, J. H. Kim, K. Saito, A. Sakamoto, M. Inoue, M. Shirouzu and S. Yokoyama (2002). "Crystal structure of the complex of human epidermal growth factor and receptor extracellular domains." Cell **110**(6): 775-787.

Ohashi, E., K. Tanabe, Y. Henmi, K. Mesaki, Y. Kobayashi and K. Takei (2011). "Receptor sorting within endosomal trafficking pathway is facilitated by dynamic actin filaments." PLoS One **6**(5): e19942.

Ohsumi, Y. (2014). "Historical landmarks of autophagy research." Cell Res **24**(1): 9-23.

Olmos, Y., L. Hodgson, J. Mantell, P. Verkade and J. G. Carlton (2015). "ESCRT-III controls nuclear envelope reformation." Nature **522**(7555): 236-239.

Omerovic, J., D. E. Hammond, I. A. Prior and M. J. Clague (2012). "Global Snapshot of the Influence of Endocytosis upon EGF Receptor Signaling Output." Journal of Proteome Research **11**(11): 5157-5166.

Omerovic, J. and I. A. Prior (2009). "Compartmentalized signalling: Ras proteins and signalling nanoclusters." Febs j **276**(7): 1817-1825.

Oshima, R., T. Hasegawa, K. Tamai, N. Sugeno, S. Yoshida, J. Kobayashi, A. Kikuchi, T. Baba, A. Futatsugi, I. Sato, K. Satoh, A. Takeda, M. Aoki and N. Tanaka (2016). "ESCRT-0 dysfunction compromises autophagic degradation of protein aggregates and facilitates ER stress-mediated neurodegeneration via apoptotic and necroptotic pathways." Sci Rep **6**: 24997.

Ostrowski, J., M. A. Kjelsberg, M. G. Caron and R. J. Lefkowitz (1992). "Mutagenesis of the beta 2-adrenergic receptor: how structure elucidates function." Annu Rev Pharmacol Toxicol **32**: 167-183.

Ovchinnikov Yu, A. (1982). "Rhodopsin and bacteriorhodopsin: structure-function relationships." FEBS Lett **148**(2): 179-191.

Pawson, T. (2004). "Specificity in signal transduction: from phosphotyrosine-SH2 domain interactions to complex cellular systems." Cell **116**(2): 191-203.

Pearse, B. M. (1975). "Coated vesicles from pig brain: purification and biochemical characterization." J Mol Biol **97**(1): 93-98.

Pearse, B. M. (1976). "Clathrin: a unique protein associated with intracellular transfer of membrane by coated vesicles." Proc Natl Acad Sci U S A **73**(4): 1255-1259.

Pellinen, T., A. Arjonen, K. Vuoriluoto, K. Kallio, J. A. Fransen and J. Ivaska (2006). "Small GTPase Rab21 regulates cell adhesion and controls endosomal traffic of beta1-integrins." J Cell Biol **173**(5): 767-780.

Pellinen, T., S. Tuomi, A. Arjonen, M. Wolf, H. Edgren, H. Meyer, R. Grosse, T. Kitzing, J. K. Rantala, O. Kallioniemi, R. Fassler, M. Kallio and J. Ivaska (2008). "Integrin trafficking regulated by Rab21 is necessary for cytokinesis." Dev Cell **15**(3): 371-385.

Penengo, L., M. Mapelli, A. G. Murachelli, S. Confalonieri, L. Magri, A. Musacchio, P. P. Di Fiore, S. Polo and T. R. Schneider (2006). "Crystal structure of the ubiquitin binding domains of rabex-5 reveals two modes of interaction with ubiquitin." Cell **124**(6): 1183-1195.

Peng, H., J. Myers, X. Fang, E. K. Stachowiak, P. A. Maher, G. G. Martins, G. Popescu, R. Berezney and M. K. Stachowiak (2002). "Integrative nuclear FGFR1 signaling (INFS) pathway mediates activation of the tyrosine hydroxylase gene by angiotensin II, depolarization and protein kinase C." J Neurochem **81**(3): 506-524.

Perry, S. J., G. S. Baillie, T. A. Kohout, I. McPhee, M. M. Magiera, K. L. Ang, W. E. Miller, A. J. McLean, M. Conti, M. D. Houslay and R. J. Lefkowitz (2002). "Targeting of cyclic AMP degradation to beta 2-adrenergic receptors by beta-arrestins." Science **298**(5594): 834-836.

Pert, C. B. and S. H. Snyder (1973). "Opiate receptor: demonstration in nervous tissue." Science **179**(4077): 1011-1014.

Piotrowski, J. T., T. S. Gomez, R. A. Schoon, A. K. Mangalam and D. D. Billadeau (2013). "WASH knockout T cells demonstrate defective receptor trafficking, proliferation, and effector function." Mol Cell Biol **33**(5): 958-973.

Pitcher, J. A., N. J. Freedman and R. J. Lefkowitz (1998). "G protein-coupled receptor kinases." Annu Rev Biochem **67**: 653-692.

Plotnikov, A. N., J. Schlessinger, S. R. Hubbard and M. Mohammadi (1999). "Structural basis for FGF receptor dimerization and activation." Cell **98**(5): 641-650.

Plowman, G. D., J. M. Culouscou, G. S. Whitney, J. M. Green, G. W. Carlton, L. Foy, M. G. Neubauer and M. Shoyab (1993). "Ligand-specific activation of HER4/p180erbB4, a fourth member of the epidermal growth factor receptor family." Proc Natl Acad Sci U S A **90**(5): 1746-1750.

Plowman, G. D., G. S. Whitney, M. G. Neubauer, J. M. Green, V. L. McDonald, G. J. Todaro and M. Shoyab (1990). "Molecular cloning and expression of an additional epidermal growth factor receptor-related gene." Proc Natl Acad Sci U S A **87**(13): 4905-4909.

Poole, B., S. Ohkuma and M. J. Warburton (1977). "The accumulation of weakly basic substances in lysosomes and the inhibition of intracellular protein degradation." Acta Biol Med Ger **36**(11-12): 1777-1788.

Poppleton, H., H. Sun, D. Fulgham, P. Bertics and T. B. Patel (1996). "Activation of Gsalpha by the epidermal growth factor receptor involves phosphorylation." J Biol Chem **271**(12): 6947-6951.

Pornillos, O., S. L. Alam, D. R. Davis and W. I. Sundquist (2002). "Structure of the Tsg101 UEV domain in complex with the PTAP motif of the HIV-1 p6 protein." Nat Struct Biol **9**(11): 812-817.

Pornillos, O., S. L. Alam, R. L. Rich, D. G. Myszka, D. R. Davis and W. I. Sundquist (2002). "Structure and functional interactions of the Tsg101 UEV domain." Embo J **21**(10): 2397-2406.

Pornillos, O., J. E. Garrus and W. I. Sundquist (2002). "Mechanisms of enveloped RNA virus budding." Trends Cell Biol **12**(12): 569-579.

Pornillos, O., D. S. Higginson, K. M. Stray, R. D. Fisher, J. E. Garrus, M. Payne, G. P. He, H. E. Wang, S. G. Morham and W. I. Sundquist (2003). "HIV Gag mimics the Tsg101-recruiting activity of the human Hrs protein." J Cell Biol **162**(3): 425-434.

Prag, G., S. Misra, E. A. Jones, R. Ghirlando, B. A. Davies, B. F. Horazdovsky and J. H. Hurley (2003). "Mechanism of ubiquitin recognition by the CUE domain of Vps9p." Cell **113**(5): 609-620.

Prenzel, N., E. Zwick, H. Daub, M. Leserer, R. Abraham, C. Wallasch and A. Ullrich (1999). "EGF receptor transactivation by G-protein-coupled receptors requires metalloproteinase cleavage of proHB-EGF." Nature **402**(6764): 884-888.

Prior, I. A., A. Harding, J. Yan, J. Sluimer, R. G. Parton and J. F. Hancock (2001). "GTP-dependent segregation of H-ras from lipid rafts is required for biological activity." Nat Cell Biol **3**(4): 368-375.

Puthenveedu, M. A., B. Lauffer, P. Temkin, R. Vistein, P. Carlton, K. Thorn, J. Taunton, O. D. Weiner, R. G. Parton and M. von Zastrow (2010). "Sequence-dependent sorting of recycling proteins by actin-stabilized endosomal microdomains." Cell **143**(5): 761-773.

Qiu, C., M. K. Tarrant, S. H. Choi, A. Sathyamurthy, R. Bose, S. Banjade, A. Pal, W. G. Bornmann, M. A. Lemmon, P. A. Cole and D. J. Leahy (2008). "Mechanism of activation and inhibition of the HER4/ErbB4 kinase." Structure **16**(3): 460-467.

Rabinovitz, M. and J. M. Fisher (1964). "CHARACTERISTICS OF THE INHIBITION OF HEMOGLOBIN SYNTHESIS IN RABBIT RETICULOCYTES BY THREO-ALPHA-AMINO-BETA-CHLOROBUTYRIC ACID." Biochim Biophys Acta **91**: 313-322.

Rahighi, S., F. Ikeda, M. Kawasaki, M. Akutsu, N. Suzuki, R. Kato, T. Kensche, T. Uejima, S. Bloor, D. Komander, F. Randow, S. Wakatsuki and I. Dikic (2009). "NEMO binding to linear ubiquitin chains is essential for NF-κB activation." Cell **in press**.

Raiborg, C., K. G. Bache, D. J. Gillooly, I. H. Madshus, E. Stang and H. Stenmark (2002). "Hrs sorts ubiquitinated proteins into clathrin -coated microdomains of early endosomes." Nature Cell Biol. **4**: 394-398.

Raiborg, C., K. G. Bache, D. J. Gillooly, I. H. Madshus, E. Stang and H. Stenmark (2002). "Hrs sorts ubiquitinated proteins into clathrin-coated microdomains of early endosomes." Nat Cell Biol **4**(5): 394-398.

Raiborg, C., B. Bremnes, A. Mehlum, D. J. Gillooly, A. D'Arrigo, E. Stang and H. Stenmark (2001). "FYVE and coiled-coil domains determine the specific localisation of Hrs to early endosomes." J Cell Sci **114**(Pt 12): 2255-2263.

Raiborg, C., K. Gronvold Bache, A. Mehlum, E. Stang and H. Stenmark (2001). "Hrs recruits clathrin to early endosomes." EMBO J. **20**: 5008-5021.

Raiborg, C. and H. Stenmark (2002). "Hrs and endocytic sorting of ubiquitinated membrane proteins." Cell Struct Funct **27**(6): 403-408.

Raymond, C. K., I. Howald-Stevenson, C. A. Vater and T. H. Stevens (1992). "Morphological classification of the yeast vacuolar protein sorting mutants: evidence for a prevacuolar compartment in class E vps mutants." Mol. Biol. Cell **3**: 1389-1402.

Red Brewer, M., S. H. Choi, D. Alvarado, K. Moravcevic, A. Pozzi, M. A. Lemmon and G. Carpenter (2009). "The juxtamembrane region of the EGF receptor functions as an activation domain." Mol Cell **34**(6): 641-651.

Reese, D. M. and D. J. Slamon (1997). "HER-2/neu signal transduction in human breast and ovarian cancer." Stem Cells **15**(1): 1-8.

Reggiori, F. and H. R. Pelham (2001). "Sorting of proteins into multivesicular bodies: ubiquitin-dependent and -independent targeting." EMBO J. **20**: 5176-5186.

Reyes-Turcu, F. E., J. R. Horton, J. E. Mullally, A. Heroux, X. Cheng and K. D. Wilkinson (2006). "The ubiquitin binding domain ZnF UBP recognizes the C-terminal diglycine motif of unanchored ubiquitin." Cell **124**(6): 1197-1208.

Rhee, S. G., Y. S. Bae, S. R. Lee and J. Kwon (2000). "Hydrogen peroxide: a key messenger that modulates protein phosphorylation through cysteine oxidation." Sci STKE **2000**(53): pe1.

Ridley, S. H., N. Ktistakis, K. Davidson, K. E. Anderson, M. Manifava, C. D. Ellson, P. Lipp, M. Bootman, J. Coadwell, A. Nazarian, H. Erdjument-Bromage, P. Tempst, M. A. Cooper, J. W. Thuring, Z. Y. Lim, A. B. Holmes, L. R. Stephens and P. T. Hawkins (2001). "FENS-1 and DFCP1 are FYVE domain-containing proteins with distinct functions in the endosomal and Golgi compartments." J Cell Sci **114**(Pt 22): 3991-4000.

Rink, J., E. Ghigo, Y. Kalaidzidis and M. Zerial (2005). "Rab conversion as a mechanism of progression from early to late endosomes." Cell **122**(5): 735-749.

Robinson, J. S., D. J. Klionsky, L. M. Banta and S. D. Emr (1988). "Protein sorting in Saccharomyces cerevisiae:isolation of mutants defective in the delivery and processing of multiple vacuolar hydrolases." Mol. Cell Biol. **8**: 4936-4948.

Robison, G. A., R. W. Butcher and E. W. Sutherland (1967). "Adenyl cyclase as an adrenergic receptor." Ann N Y Acad Sci **139**(3): 703-723.

Rodbell, M., L. Birnbaumer, S. L. Pohl and H. M. Krans (1971). "The glucagon-sensitive adenyl cyclase system in plasma membranes of rat liver. V. An obligatory role of guanylnucleotides in glucagon action." J Biol Chem **246**(6): 1877-1882.

Roepstorff, K., M. V. Grandal, L. Henriksen, S. L. Knudsen, M. Lerdrup, L. Grovdal, B. M. Willumsen and B. van Deurs (2009). "Differential effects of EGFR ligands on endocytic sorting of the receptor." Traffic **10**(8): 1115-1127.

Rojas, R., T. van Vlijmen, G. A. Mardones, Y. Prabhu, A. L. Rojas, S. Mohammed, A. J. Heck, G. Raposo, P. van der Sluijs and J. S. Bonifacino (2008). "Regulation of retromer recruitment to endosomes by sequential action of Rab5 and Rab7." J Cell Biol **183**(3): 513-526.

Ropers, F., E. Derivery, H. Hu, M. Garshasbi, M. Karbasiyan, M. Herold, G. Nurnberg, R. Ullmann, A. Gautreau, K. Sperling, R. Varon and A. Rajab (2011). "Identification of a novel candidate gene for non-syndromic autosomal recessive intellectual disability: the WASH complex member SWIP." Hum Mol Genet **20**(13): 2585-2590.

Roth, M. G. (2006). "Clathrin-mediated endocytosis before fluorescent proteins." Nat Rev Mol Cell Biol **7**(1): 63-68.

Roth, T. F. and K. R. Porter (1964). "Yolk protein uptake in the oocyte of the mosquito Aedes Aegypti L." J. Cell Biol. **20**: 313-332.

Rothbauer, U., K. Zolghadr, S. Muyldermans, A. Schepers, M. C. Cardoso and H. Leonhardt (2008). "A versatile nanotrap for biochemical and functional studies with fluorescent fusion proteins." Mol Cell Proteomics **7**(2): 282-289.

Rothberg, K. G., J. E. Heuser, W. C. Donzell, Y.-S. Ying, J. R. Glenney and R. G. W. Anderson (1992). "Caveolin, a protein component of caveolae membrane coats." Cell **68**: 673-682.

Rothman, J. H. and T. H. Stevens (1986). "Protein sorting in yeast: mutants defective in vacuole biogenesis mislocalize vacuolar proteins into the late secretory pathway." Cell **47**(6): 1041-1051.

Rotty, J. D., C. Wu and J. E. Bear (2013). "New insights into the regulation and cellular functions of the ARP2/3 complex." Nat Rev Mol Cell Biol **14**(1): 7-12.

Row, P. E., M. J. Clague and S. Urbe (2005). "Growth factors induce differential phosphorylation profiles of the Hrs-Stam complex: a common node in signaling networks with signal specific properties." Biochem J **389**: 629-636.

Roxrud, I., C. Raiborg, N. M. Pedersen, E. Stang and H. Stenmark (2008). "An endosomally localized isoform of Eps15 interacts with Hrs to mediate degradation of epidermal growth factor receptor." J Cell Biol **180**(6): 1205-1218.

Ryder, P. V., R. Vistein, A. Gokhale, M. N. Seaman, M. A. Puthenveedu and V. Faundez (2013). "The WASH complex, an endosomal Arp2/3 activator, interacts with the Hermansky-Pudlak syndrome complex BLOC-1 and its cargo phosphatidylinositol-4-kinase type IIalpha." Mol Biol Cell **24**(14): 2269-2284.

Sachse, M., S. Urbé, V. Oorschot, G. J. Strous and J. Klumperman (2002). "Bilayered clathrin coats on endosomal vacuoles are involved in protein sorting toward lysosomes." Mol. Biol. Cell **13**: 1313-1328.

Saksena, S. and S. D. Emr (2009). "ESCRTs and human disease." Biochem Soc Trans **37**(Pt 1): 167-172.

Saksena, S., J. Wahlman, D. Teis, A. E. Johnson and S. D. Emr (2009). "Functional reconstitution of ESCRT-III assembly and disassembly." Cell **136**(1): 97-109.

Sardi, S. P., J. Murtie, S. Koirala, B. A. Patten and G. Corfas (2006). "Presenilin-dependent ErbB4 nuclear signaling regulates the timing of astrogenesis in the developing brain." Cell **127**(1): 185-197.

Sasaki, T., P. G. Knyazev, N. J. Clout, Y. Cheburkin, W. Gohring, A. Ullrich, R. Timpl and E. Hohenester (2006). "Structural basis for Gas6-Axl signalling." Embo j **25**(1): 80-87.

Sbrissa, D., O. C. Ikonomov and A. Shisheva (1999). "PIKfyve, a mammalain otholog of yeast Fab1p lipid kinase, synthesizes 5-phosphoinositides." J. Biol. Chem. **274**: 21589-21597.

Sbrissa, D., O. C. Ikonomov and A. Shisheva (2002). "Phosphatidylinositol 3-phosphate-interacting domains in PIKfyve. Binding specificity and role in PIKfyve. Endomenbrane localization." J Biol Chem **277**(8): 6073-6079.

Schmidt, O. and D. Teis (2012). "The ESCRT machinery." Curr Biol **22**(4): R116-120.

Schoenheimer, R., S. Ratner and D. Rittenberg (1939). "THE PROCESS OF CONTINUOUS DEAMINATION AND REAMINATION OF AMINO ACIDS IN THE PROTEINS OF NORMAL ANIMALS." Science **89**(2308): 272-273.

Schreiner, P., X. Chen, K. Husnjak, L. Randles, N. Zhang, S. Elsasser, D. Finley, I. Dikic, K. J. Walters and M. Groll (2008). "Ubiquitin docking at the proteasome through a novel pleckstrin-homology domain interaction." Nature **453**(7194): 548-552.

Schu, P. V., K. Takegawa, M. J. Fry, J. H. Stack, M. D. Waterfield and S. D. Emr (1993). "Phosphatidylinositol 3-kinase encoded by yeast VPS34 gene essential for protein sorting." Science **260**: 88-91.

Scoles, D. R., Y. Qin, V. Nguyen, D. H. Gutmann and S. M. Pulst (2005). "HRS inhibits EGF receptor signaling in the RT4 rat schwannoma cell line." Biochem Biophys Res Commun **335**(2): 385-392.

Seaman, M. N. (2004). "Cargo-selective endosomal sorting for retrieval to the Golgi requires retromer." J Cell Biol **165**(1): 111-122.

Seaman, M. N. (2012). "The retromer complex - endosomal protein recycling and beyond." J Cell Sci **125**(Pt 20): 4693-4702.

Seaman, M. N., A. Gautreau and D. D. Billadeau (2013). "Retromer-mediated endosomal protein sorting: all WASHed up!" Trends Cell Biol **23**(11): 522-528.

Seaman, M. N., M. E. Harbour, D. Tattersall, E. Read and N. Bright (2009). "Membrane recruitment of the cargo-selective retromer subcomplex is catalysed by the small GTPase Rab7 and inhibited by the Rab-GAP TBC1D5." J Cell Sci **122**(Pt 14): 2371-2382.

Seaman, M. N., E. G. Marcusson, J. L. Cereghino and S. D. Emr (1997). "Endosome to Golgi retrieval of the vacuolar protein sorting receptor, Vps10p, requires the function of the VPS29, VPS30, and VPS35 gene products." J Cell Biol **137**(1): 79-92.

Shan, D., L. Chen, D. Wang, Y. C. Tan, J. L. Gu and X. Y. Huang (2006). "The G protein G alpha(13) is required for growth factor-induced cell migration." Dev Cell **10**(6): 707-718.

Shewchuk, L. M., A. M. Hassell, B. Ellis, W. D. Holmes, R. Davis, E. L. Horne, S. H. Kadwell, D. D. McKee and J. T. Moore (2000). "Structure of the Tie2 RTK domain: self-inhibition by the nucleotide binding loop, activation loop, and C-terminal tail." Structure **8**(11): 1105-1113.

Shi, H., R. Rojas, J. S. Bonifacino and J. H. Hurley (2006). "The retromer subunit Vps26 has an arrestin fold and binds Vps35 through its C-terminal domain." Nat Struct Mol Biol **13**(6): 540-548.

Shih, S. C., G. Prag, S. A. Francis, M. A. Sutanto, J. H. Hurley and L. Hicke (2003). "A ubiquitin-binding motif required for intramolecular monoubiquitylation, the CUE domain." Embo j **22**(6): 1273-1281.

Shih, S. C., K. E. Sloper-Mould and L. Hicke (2000). "Monoubiquitin carries a novel internalization signal that is appended to activated receptors." Embo J **19**(2): 187-198.

Shim, S., L. A. Kimpler and P. I. Hanson (2007). "Structure/function analysis of four core ESCRT-III proteins reveals common regulatory role for extreme C-terminal domain." Traffic **8**(8): 1068-1079.

Simpson, J. C., G. Griffiths, M. Wessling-Resnick, J. A. Fransen, H. Bennett and A. T. Jones (2004). "A role for the small GTPase Rab21 in the early endocytic pathway." J Cell Sci **117**(Pt 26): 6297-6311.

Skjeldal, F. M., S. Strunze, T. Bergeland, E. Walseng, T. F. Gregers and O. Bakke (2012). "The fusion of early endosomes induces molecular-motor-driven tubule formation and fission." J Cell Sci **125**(Pt 8): 1910-1919.

Slagsvold, T., R. Aasland, S. Hirano, K. G. Bache, C. Raiborg, D. Trambaiano, S. Wakatsuki and H. Stenmark (2005). "Eap45 in mammalian ESCRT-II binds ubiquitin via a phosphoinositide-interacting GLUE domain." J Biol Chem.

Slamon, D. J., G. M. Clark, S. G. Wong, W. J. Levin, A. Ullrich and W. L. McGuire (1987). "Human breast cancer: correlation of relapse and survival with amplification of the HER-2/neu oncogene." Science **235**(4785): 177-182.

Slessareva, J. E., S. M. Routt, B. Temple, V. A. Bankaitis and H. G. Dohlman (2006). "Activation of the phosphatidylinositol 3-kinase Vps34 by a G protein alpha subunit at the endosome." Cell **126**(1): 191-203.

Small, S. A., K. Kent, A. Pierce, C. Leung, M. S. Kang, H. Okada, L. Honig, J. P. Vonsattel and T. W. Kim (2005). "Model-guided microarray implicates the retromer complex in Alzheimer's disease." Ann Neurol **58**(6): 909-919.

Sorkin, A. and M. von Zastrow (2002). "Signal transduction and endocytosis; close encounters of many kinds." Nature Rev. Mol. Cell Biol. **3**: 600-614.

Sorkin, A. D., L. V. Teslenko and N. N. Nikolsky (1988). "The endocytosis of epidermal growth factor in A431 cells: a pH of microenvironment and the dynamics of receptor complex dissociation." Exp Cell Res **175**(1): 192-205.

Sotelo, J. R. and K. R. Porter (1959). "An electron microscope study of the rat ovum." J Biophys Biochem Cytol **5**(2): 327-342.

Stadel, J. M., P. Nambi, T. N. Lavin, S. L. Heald, M. G. Caron and R. J. Lefkowitz (1982). "Catecholamine-induced desensitization of turkey erythrocyte adenylate cyclase. Structural alterations in the beta-adrenergic receptor revealed by photoaffinity labeling." J Biol Chem **257**(16): 9242-9245.

Stadel, J. M., P. Nambi, R. G. Shorr, D. F. Sawyer, M. G. Caron and R. J. Lefkowitz (1983). "Catecholamine-induced desensitization of turkey erythrocyte adenylate cyclase is associated with phosphorylation of the beta-adrenergic receptor." Proc Natl Acad Sci U S A **80**(11): 3173-3177.

Stamenova, S. D., M. E. French, Y. He, S. A. Francis, Z. B. Kramer and L. Hicke (2007). "Ubiquitin binds to and regulates a subset of SH3 domains." Mol Cell **25**(2): 273-284.

Starkey, R. H., S. Cohen and D. N. Orth (1975). "Epidermal growth factor: identification of a new hormone in human urine." Science **189**(4205): 800-802.

Stauber, D. J., A. D. DiGabriele and W. A. Hendrickson (2000). "Structural interactions of fibroblast growth factor receptor with its ligands." Proc Natl Acad Sci U S A **97**(1): 49-54.

Steinberg, F., M. Gallon, M. Winfield, E. C. Thomas, A. J. Bell, K. J. Heesom, J. M. Tavare and P. J. Cullen (2013). "A global analysis of SNX27-retromer assembly and cargo specificity reveals a function in glucose and metal ion transport." Nat Cell Biol **15**(5): 461-471.

Steinberg, F., K. J. Heesom, M. D. Bass and P. J. Cullen (2012). "SNX17 protects integrins from degradation by sorting between lysosomal and recycling pathways." J Cell Biol **197**(2): 219-230.

Stenmark, H., R. Aasland, B.-H. Toh and A. D'Arrigo (1996). "Endosomal localization of the autoantigen EEA1 is mediated by a zinc-binding FYVE finger." J. Biol. Chem. **271**: 24048-24054.

Stern, D. F., P. A. Heffernan and R. A. Weinberg (1986). "p185, a product of the neu proto-oncogene, is a receptorlike protein associated with tyrosine kinase activity." Mol Cell Biol **6**(5): 1729-1740.

Stern, K. A., G. D. Visser Smit, T. L. Place, S. Winistorfer, R. C. Piper and N. L. Lill (2007). "Epidermal growth factor receptor fate is controlled by Hrs tyrosine phosphorylation sites that regulate Hrs degradation." Mol Cell Biol **27**(3): 888-898.

Stow, J. L., J. B. de Almeida, N. Narula, E. J. Holtzman, L. Ercolani and D. A. Ausiello (1991). "A heterotrimeric G protein, G alpha i-3, on Golgi membranes regulates the secretion of a heparan sulfate proteoglycan in LLC-PK1 epithelial cells." J Cell Biol **114**(6): 1113-1124.

Sun, X. J., D. L. Crimmins, M. G. Myers, Jr., M. Miralpeix and M. F. White (1993). "Pleiotropic insulin signals are engaged by multisite phosphorylation of IRS-1." Mol Cell Biol **13**(12): 7418-7428.

Sundaresan, M., Z. X. Yu, V. J. Ferrans, K. Irani and T. Finkel (1995). "Requirement for generation of H2O2 for platelet-derived growth factor signal transduction." Science **270**(5234): 296-299.

Sundquist, W. I., H. L. Schubert, B. N. Kelly, G. C. Hill, J. M. Holton and C. P. Hill (2004). "Ubiquitin recognition by the human TSG101 protein." Mol Cell **13**(6): 783-789.

Swarbrick, J. D., D. J. Shaw, S. Chhabra, R. Ghai, E. Valkov, S. J. Norwood, M. N. Seaman and B. M. Collins (2011). "VPS29 is not an active metallo-phosphatase but is a rigid scaffold required for retromer interaction with accessory proteins." PLoS One **6**(5): e20420.

Tabuchi, M., I. Yanatori, Y. Kawai and F. Kishi (2010). "Retromer-mediated direct sorting is required for proper endosomal recycling of the mammalian iron transporter DMT1." J Cell Sci **123**(Pt 5): 756-766.

Takata, H., M. Kato, K. Denda and N. Kitamura (2000). "A hrs binding protein having a Src homology 3 domain is involved in intracellular degradation of growth factors and their receptors." Genes Cells **5**(1): 57-69.

Takeshita, T., T. Arita, H. Asao, N. Tanaka, M. Higuchi, H. Kuroda, K. Kaneko, H. Munakata, Y. Endo, T. Fujita and K. Sugamura (1996). "Cloning of a novel signal-transducing adaptor molecule containing an SH3 domain and ITAM." Biochem Biophys Res Commun **225**(3): 1035-1039.

Takeshita, T., T. Arita, M. Higuchi, H. Asao, K. Endo, H. Kuroda, N. Tanaka, K. Murata, N. Ishii and K. Sugamura (1997). "STAM, signal transducing adaptor molecule, is associated with

Janus kinases and involved in signaling for cell growth and c-myc induction." Immunity **6**(4): 449-457.

Tamai, K., M. Toyoshima, N. Tanaka, N. Yamamoto, Y. Owada, H. Kiyonari, K. Murata, Y. Ueno, M. Ono, T. Shimosegawa, N. Yaegashi, M. Watanabe and K. Sugamura (2008). "Loss of hrs in the central nervous system causes accumulation of ubiquitinated proteins and neurodegeneration." Am J Pathol **173**(6): 1806-1817.

Tanaka, N., K. Kaneko, H. Asao, H. Kasai, Y. Endo, T. Fujita, T. Takeshita and K. Sugamura (1999). "Possible involvement of a novel STAM-associated molecule "AMSH" in intracellular signal transduction mediated by cytokines." J Biol Chem **274**(27): 19129-19135.

Teis, D., S. Saksena and S. D. Emr (2008). "Ordered assembly of the ESCRT-III complex on endosomes is required to sequester cargo during MVB formation." Dev Cell **15**(4): 578-589.

Temkin, P., B. Lauffer, S. Jager, P. Cimermancic, N. J. Krogan and M. von Zastrow (2011). "SNX27 mediates retromer tubule entry and endosome-to-plasma membrane trafficking of signalling receptors." Nat Cell Biol **13**(6): 715-721.

Teo, H., D. J. Gill, J. Sun, O. Perisic, D. B. Veprintsev, Y. Vallis, S. D. Emr and R. L. Williams (2006). "ESCRT-I core and ESCRT-II GLUE domain structures reveal role for GLUE in linking to ESCRT-I and membranes." Cell **125**(1): 99-111.

Teo, H., O. Perisic, B. Gonzalez and R. L. Williams (2004). "ESCRT-II, an endosome-associated complex required for protein sorting: crystal structure and interactions with ESCRT-III and membranes." Dev Cell **7**(4): 559-569.

Terrell, J., S. Shih, R. Dunn and L. Hicke (1998). "A function for monoubiquitination in the internalization of a G protein-coupled receptor." Mol Cell **1**(2): 193-202.

Thien, C. B. F., F. Walker and W. Y. Langdon (2001). "Ring finger mutations that abolish c-Cbl directed polyubiquitination and down-regulation of the EGF receptor are insufficient for cell transformation." Mol. Cell **7**: 355-365.

Till, J. H., M. Becerra, A. Watty, Y. Lu, Y. Ma, T. A. Neubert, S. J. Burden and S. R. Hubbard (2002). "Crystal structure of the MuSK tyrosine kinase: insights into receptor autoregulation." Structure **10**(9): 1187-1196.

Toman, R. E., S. G. Payne, K. R. Watterson, M. Maceyka, N. H. Lee, S. Milstien, J. W. Bigbee and S. Spiegel (2004). "Differential transactivation of sphingosine-1-phosphate receptors modulates NGF-induced neurite extension." J Cell Biol **166**(3): 381-392.

Toyoshima, M., N. Tanaka, J. Aoki, Y. Tanaka, K. Murata, M. Kyuuma, H. Kobayashi, N. Ishii, N. Yaegashi and K. Sugamura (2007). "Inhibition of tumor growth and metastasis by depletion of vesicular sorting protein Hrs: its regulatory role on E-cadherin and beta-catenin." Cancer Res **67**(11): 5162-5171.

Trinkle-Mulcahy, L. (2019). "Recent advances in proximity-based labeling methods for interactome mapping." F1000Res **8**.

Tsukada, M. and Y. Ohsumi (1993). "Isolation and characterization of autophagy-defective mutants of Saccharomyces cerevisiae." FEBS Lett **333**(1-2): 169-174.

Tsvetanova, N. G. and M. von Zastrow (2014). "Spatial encoding of cyclic AMP signaling specificity by GPCR endocytosis." Nat Chem Biol.

Uchiyama-Tanaka, Y., H. Matsubara, Y. Nozawa, S. Murasawa, Y. Mori, A. Kosaki, K. Maruyama, H. Masaki, Y. Shibasaki, S. Fujiyama, A. Nose, O. Iba, T. Hasagawa, E. Tateishi, S. Higashiyama and T. Iwasaka (2001). "Angiotensin II signaling and HB-EGF shedding via metalloproteinase in glomerular mesangial cells." Kidney Int **60**(6): 2153-2163.

Uddin, M., A. Ratanatharathorn, D. Armstrong, P. Kuan, A. Aiello, E. Bromet, S. Galea, K. Koenen, B. Luft, K. Ressler, D. Wildman, C. Nievergelt and A. Smith (2018). "Epigenetic meta-analysis across three civilian cohorts identifies NRG1 and HGS as blood-based biomarkers for post-traumatic stress disorder." Epigenomics. **10**(12): 1585-1601.

Ullrich, A., L. Coussens, J. S. Hayflick, T. J. Dull, A. Gray, A. W. Tam, J. Lee, Y. Yarden, T. A. Libermann, J. Schlessinger and et al. (1984). "Human epidermal growth factor receptor cDNA sequence and aberrant expression of the amplified gene in A431 epidermoid carcinoma cells." Nature **309**(5967): 418-425.

Ullrich, A. and J. Schlessinger (1990). "Signal transduction by receptors with tyrosine kinase activity." Cell **61**(2): 203-212.

Ullrich, O., S. Reinsch, S. Urbe, M. Zerial and R. G. Parton (1996). "Rab11 regulates recycling through the pericentriolar recycling endosome." J. Cell Biol. **135**: 913-924.

Urbé, S., I. G. Mills, H. Stenmark, N. Kitamura and M. J. Clague (2000). "Endosomal localization and receptor dynamics determine tyrosine phosphorylation of hepatocyte growth factor-regulated tyrosine kinase substrate." Mol Cell Biol **20**(20): 7685-7692.

Urbé, S., M. Sachse, P. E. Row, C. Preisinger, F. A. Barr, G. Strous, J. Klumperman and M. J. Clague (2003). "The UIM domain of Hrs couples receptor sorting to vesicle formation." J. Cell Sci. **116**: 4169-4179.

Valdmanis, P. N., I. A. Meijer, A. Reynolds, A. Lei, P. MacLeod, D. Schlesinger, M. Zatz, E. Reid, P. A. Dion, P. Drapeau and G. A. Rouleau (2007). "Mutations in the KIAA0196 gene at the SPG8 locus cause hereditary spastic paraplegia." Am J Hum Genet **80**(1): 152-161.

van der Sluijs, P., M. Hull, P. Webster, P. Male, B. Goud and I. Mellman (1992). "The small GTP-binding protein rab4 controls an early sorting event on the endocytic pathway." Cell **70**: 729-740.

van der Sluijs, P., M. Hull, A. Zahraoui, A. Tavitian, B. Goud and I. Mellman (1991). "The small GTP-binding protein rab4 is associated with early endosomes." Proc. Natl. Acad. Sci. **88**: 6313-6317.

Vardarajan, B. N., S. Y. Bruesegem, M. E. Harbour, R. Inzelberg, R. Friedland, P. St George-Hyslop, M. N. Seaman and L. A. Farrer (2012). "Identification of Alzheimer disease-associated variants in genes that regulate retromer function." Neurobiol Aging **33**(9): 2231.e2215-2231.e2230.

Veettil, M. V., B. Kumar, M. A. Ansari, D. Dutta, J. Iqbal, O. Gjyshi, V. Bottero and B. Chandran (2016). "ESCRT-0 Component Hrs Promotes Macropinocytosis of Kaposi's Sarcoma-Associated Herpesvirus in Human Dermal Microvascular Endothelial Cells." J Virol **90**(8): 3860-3872.

Verma, R. and A. Marchese (2015). "The endosomal sorting complex required for transport pathway mediates chemokine receptor CXCR4-promoted lysosomal degradation of the mammalian target of rapamycin antagonist DEPTOR." J Biol Chem **290**(11): 6810-6824.

Vieira, A. V., C. Lamaze and S. L. Schmid (1996). "Control of EGF receptor signaling by clathrin-mediated endocytosis." Science **274**: 2086-2089.

Wallasch, C., J. E. Crabtree, D. Bevec, P. A. Robinson, H. Wagner and A. Ullrich (2002). "Helicobacter pylori-stimulated EGF receptor transactivation requires metalloprotease cleavage of HB-EGF." Biochem Biophys Res Commun **295**(3): 695-701.

Wang, Y., S. Pennock, X. Chen and Z. Wang (2002). "Endosomal signaling of epidermal growth factor receptor stimulates signal transduction pathways leading to cell survival." Mol Cell Biol **22**(20): 7279-7290.

Wang, Y., S. D. Pennock, X. Chen, A. Kazlauskas and Z. Wang (2004). "Platelet-derived growth factor receptor-mediated signal transduction from endosomes." J Biol Chem **279**(9): 8038-8046.

Wang, Z. (2017). ErbB Receptors and Cancer. ErbB Receptor Signaling: Methods and Protocols. Z. Wang. New York, NY, Springer New York**:** 3-35.

Ward, C. W., M. C. Lawrence, V. A. Streltsov, T. E. Adams and N. M. McKern (2007). "The insulin and EGF receptor structures: new insights into ligand-induced receptor activation." Trends Biochem Sci **32**(3): 129-137.

Wassmer, T., N. Attar, M. V. Bujny, J. Oakley, C. J. Traer and P. J. Cullen (2007). "A loss-of-function screen reveals SNX5 and SNX6 as potential components of the mammalian retromer." J Cell Sci **120**(Pt 1): 45-54.

Waterman, H., G. Levkowitz, I. Alroy and Y. Yarden (1999). "The RING finger of c-Cbl mediates desensitization of the epidermal growth factor receptor." J Biol Chem **274**(32): 22151-22154.

Waters, C., B. Sambi, K. C. Kong, D. Thompson, S. M. Pitson, S. Pyne and N. J. Pyne (2003). "Sphingosine 1-phosphate and platelet-derived growth factor (PDGF) act via PDGF beta receptor-sphingosine 1-phosphate receptor complexes in airway smooth muscle cells." J Biol Chem **278**(8): 6282-6290.

Waters, C. M., J. Long, I. Gorshkova, Y. Fujiwara, M. Connell, K. E. Belmonte, G. Tigyi, V. Natarajan, S. Pyne and N. J. Pyne (2006). "Cell migration activated by platelet-derived growth factor receptor is blocked by an inverse agonist of the sphingosine 1-phosphate receptor-1." Faseb j **20**(3): 509-511.

Watson, J. A., B. J. Bhattacharyya, J. H. Vaden, J. A. Wilson, M. Icyuz, A. D. Howard, E. Phillips, T. M. DeSilva, G. P. Siegal, A. J. Bean, G. D. King, S. E. Phillips, R. J. Miller and S. M. Wilson (2015). "Motor and Sensory Deficits in the teetering Mice Result from Mutation of the ESCRT Component HGS." PLoS Genet **11**(6): e1005290.

Wehbi, V. L., H. P. Stevenson, T. N. Feinstein, G. Calero, G. Romero and J. P. Vilardaga (2013). "Noncanonical GPCR signaling arising from a PTH receptor-arrestin-Gbetagamma complex." Proc Natl Acad Sci U S A **110**(4): 1530-1535.

Wehrman, T., X. He, B. Raab, A. Dukipatti, H. Blau and K. C. Garcia (2007). "Structural and mechanistic insights into nerve growth factor interactions with the TrkA and p75 receptors." Neuron **53**(1): 25-38.

Weiss, C. A., E. White, H. Huang and H. Ma (1997). "The G protein alpha subunit (GP alpha1) is associated with the ER and the plasma membrane in meristematic cells of Arabidopsis and cauliflower." FEBS Lett **407**(3): 361-367.

Wenzel, E. M., S. W. Schultz, K. O. Schink, N. M. Pedersen, V. Nahse, A. Carlson, A. Brech, H. Stenmark and C. Raiborg (2018). "Concerted ESCRT and clathrin recruitment waves define the timing and morphology of intraluminal vesicle formation." Nat Commun **9**(1): 2932.

Werthmann, R. C., S. Volpe, M. J. Lohse and D. Calebiro (2012). "Persistent cAMP signaling by internalized TSH receptors occurs in thyroid but not in HEK293 cells." Faseb j **26**(5): 2043-2048.

Wiesmann, C., G. Fuh, H. W. Christinger, C. Eigenbrot, J. A. Wells and A. M. de Vos (1997). "Crystal structure at 1.7 A resolution of VEGF in complex with domain 2 of the Flt-1 receptor." Cell **91**(5): 695-704.

Wiesmann, C., M. H. Ultsch, S. H. Bass and A. M. de Vos (1999). "Crystal structure of nerve growth factor in complex with the ligand-binding domain of the TrkA receptor." Nature **401**(6749): 184-188.

Wilden, U. and H. Kuhn (1982). "Light-dependent phosphorylation of rhodopsin: number of phosphorylation sites." Biochemistry **21**(12): 3014-3022.

Wiley, H. S., W. VanNostrand, D. N. McKinley and D. D. Cunningham (1985). "Intracellular processing of epidermal growth factor and its effect on ligand-receptor interactions." J Biol Chem **260**(9): 5290-5295.

Wilkinson, K. D., M. K. Urban and A. L. Haas (1980). "Ubiquitin is the ATP-dependent proteolysis factor I of rabbit reticulocytes." J Biol Chem **255**(16): 7529-7532.

Woodman, P. G. and C. E. Futter (2008). "Multivesicular bodies: co-ordinated progression to maturity." Curr Opin Cell Biol **20**(4): 408-414.

Wu, C., C. F. Lai and W. C. Mobley (2001). "Nerve growth factor activates persistent Rap1 signaling in endosomes." J Neurosci **21**(15): 5406-5416.

Yamada, M., T. Takeshita, S. Miura, K. Murata, Y. Kimura, N. Ishii, M. Nose, H. Sakagami, H. Kondo, F. Tashiro, J. I. Miyazaki, H. Sasaki and K. Sugamura (2001). "Loss of hippocampal CA3 pyramidal neurons in mice lacking STAM1." Mol Cell Biol **21**(11): 3807-3819.

Yamamura, H. I. and S. H. Snyder (1974). "Muscarinic cholinergic binding in rat brain." Proc Natl Acad Sci U S A **71**(5): 1725-1729.

Yamashita, Y., K. Kojima, T. Tsukahara, H. Agawa, K. Yamada, Y. Amano, N. Kurotori, N. Tanaka, K. Sugamura and T. Takeshita (2008). "Ubiquitin-independent binding of Hrs mediates endosomal sorting of the interleukin-2 receptor beta-chain." J Cell Sci **121**(Pt 10): 1727-1738.

Yarden, Y. and M. X. Sliwkowski (2001). "Untangling the ErbB signalling network." Nat Rev Mol Cell Biol **2**(2): 127-137.

Yokouchi, M., T. Kondo, A. Houghton, M. Bartkiewicz, W. C. Horne, H. Zhang, A. Yoshimura and R. Baron (1999). "Ligand-induced ubiquitination of the epidermal growth factor receptor involves the interaction of the c-Cbl RING finger and UbcH7." J Biol Chem **274**(44): 31707-31712.

Young, P., Q. Deveraux, R. E. Beal, C. M. Pickart and M. Rechsteiner (1998). "Characterization of two polyubiquitin binding sites in the 26 S protease subunit 5a." J Biol Chem **273**(10): 5461-5467.

Yu, J. W. and M. A. Lemmon (2001). "All phox homology (PX) domains from Saccharomyces cerevisiae specifically recognize phosphatidylinositol 3-phosphate." J Biol Chem **276**(47): 44179-44184.

Yu, S. S., R. J. Lefkowitz and W. P. Hausdorff (1993). "b-adrenergic receptor sequestration: a potential mechanism of receptor resensitization." J. Biol. Chem. **268**: 337-341.

Yuzawa, S., Y. Opatowsky, Z. Zhang, V. Mandiyan, I. Lax and J. Schlessinger (2007). "Structural basis for activation of the receptor tyrosine kinase KIT by stem cell factor." Cell **130**(2): 323-334.

Zaccolo, M., P. Magalhaes and T. Pozzan (2002). "Compartmentalisation of cAMP and Ca(2+) signals." Curr Opin Cell Biol **14**(2): 160-166.

Zamborlini, A., Y. Usami, S. R. Radoshitzky, E. Popova, G. Palu and H. Gottlinger (2006). "Release of autoinhibition converts ESCRT-III components into potent inhibitors of HIV-1 budding." Proc Natl Acad Sci U S A **103**(50): 19140-19145.

Zech, T., S. D. Calaminus, P. Caswell, H. J. Spence, M. Carnell, R. H. Insall, J. Norman and L. M. Machesky (2011). "The Arp2/3 activator WASH regulates alpha5beta1-integrin-mediated invasive migration." J Cell Sci **124**(Pt 22): 3753-3759.

Zhang, J., Y. Ma, S. S. Taylor and R. Y. Tsien (2001). "Genetically encoded reporters of protein kinase A activity reveal impact of substrate tethering." Proc Natl Acad Sci U S A **98**(26): 14997-15002.

Zhang, P., Y. Wu, T. Y. Belenkaya and X. Lin (2011). "SNX3 controls Wingless/Wnt secretion through regulating retromer-dependent recycling of Wntless." Cell Res **21**(12): 1677-1690.

Zhang, X., J. Gureasko, K. Shen, P. A. Cole and J. Kuriyan (2006). "An allosteric mechanism for activation of the kinase domain of epidermal growth factor receptor." Cell **125**(6): 1137-1149.